BARK-WATER INTERACTIONS

EDITED BY: Salli F. Dymond, Anna Klamerus-Iwan and John T. Van Stan
PUBLISHED IN: Frontiers in Forests and Global Change

frontiers Research Topics

frontiers

ISSN 1664-8714
ISBN 978-2-88974-077-2
DOI 10.3389/978-2-88974-077-2

About Frontiers

Frontiers is more than just an open-access publisher of scholarly articles: it is a pioneering approach to the world of academia, radically improving the way scholarly research is managed. The grand vision of Frontiers is a world where all people have an equal opportunity to seek, share and generate knowledge. Frontiers provides immediate and permanent online open access to all its publications, but this alone is not enough to realize our grand goals.

Frontiers Journal Series

The Frontiers Journal Series is a multi-tier and interdisciplinary set of open-access, online journals, promising a paradigm shift from the current review, selection and dissemination processes in academic publishing. All Frontiers journals are driven by researchers for researchers; therefore, they constitute a service to the scholarly community. At the same time, the Frontiers Journal Series operates on a revolutionary invention, the tiered publishing system, initially addressing specific communities of scholars, and gradually climbing up to broader public understanding, thus serving the interests of the lay society, too.

Dedication to Quality

Each Frontiers article is a landmark of the highest quality, thanks to genuinely collaborative interactions between authors and review editors, who include some of the world's best academicians. Research must be certified by peers before entering a stream of knowledge that may eventually reach the public - and shape society; therefore, Frontiers only applies the most rigorous and unbiased reviews.
Frontiers revolutionizes research publishing by freely delivering the most outstanding research, evaluated with no bias from both the academic and social point of view. By applying the most advanced information technologies, Frontiers is catapulting scholarly publishing into a new generation.

What are Frontiers Research Topics?

Frontiers Research Topics are very popular trademarks of the Frontiers Journals Series: they are collections of at least ten articles, all centered on a particular subject. With their unique mix of varied contributions from Original Research to Review Articles, Frontiers Research Topics unify the most influential researchers, the latest key findings and historical advances in a hot research area! Find out more on how to host your own Frontiers Research Topic or contribute to one as an author by contacting the Frontiers Editorial Office: frontiersin.org/about/contact

BARK-WATER INTERACTIONS

Topic Editors:
Salli F. Dymond, University of Minnesota Duluth, United States
Anna Klamerus-Iwan, University of Agriculture in Krakow, Poland
John T. Van Stan, Cleveland State University, United States

Citation: Dymond, S. F., Klamerus-Iwan, A., Van Stan, J. T., eds. (2022). Bark-Water Interactions. Lausanne: Frontiers Media SA. doi: 10.3389/978-2-88974-077-2

Table of Contents

frontiers in Forests and Global Change

EDITORIAL
published: 26 November 2021
doi: 10.3389/ffgc.2021.802586

Editorial: Bark-Water Interactions

John T. Van Stan[1]*, *Anna Klamerus-Iwan*[2] *and Salli F. Dymond*[3]

[1] Department of Biological, Geological and Environmental Sciences, Cleveland State University, Cleveland, OH, United States,
[2] Department of Forest Utilization Engineering and Forest Technology, University of Agriculture in Krakow, Kraków, Poland,
[3] Department of Earth and Environmental Sciences, University of Minnesota Duluth, Duluth, MN, United States

Keywords: bark, cortisphere, dermosphere, ecohydrology, ecophysiology, epiphytes

Editorial on the Research Topic

Bark-Water Interactions

In a winter deciduous forest, bark is essentially all one sees aboveground. One sees a few stubborn, marcescent leaves stuck to branches and few people paying much attention to the bark. Yet, those who have given bark some attention, like William Wordsworth, recognize that "what is gained by the exposure of bark and branches compensates, almost, for the loss of foliage[1]" Indeed, the bark cannot "compensate" for the foliage and its essential ecosystem functions, but it certainly protects the physical and physiological support systems undergirding leaves, while providing critical functions itself. As our perspective discusses, bark is an active and passive player in the water cycle in all wooded ecosystems, all year round, on live and dead plants, and in the litter (Van Stan et al.). Given this, a key question for scientists researching wooded ecosystems is how can bark alter water states, fluxes, and the materials it carries? Moreover, do bark-water physicochemical interactions meaningfully affect the plant's ecophysiological functions, or the structure and functioning of related communities (like corticolous fungi or lichens)? This collection of papers provides new insights into these questions and, thereby, charts exciting opportunities for future research on the "bark side" of the water cycle.

OPEN ACCESS

Edited and reviewed by:
Kevin J. McGuire,
Virginia Tech, United States

***Correspondence:**
John T. Van Stan
j.vanstan@csuohio.edu

Specialty section:
This article was submitted to Forest Hydrology, a section of the journal Frontiers in Forests and Global Change

Received: *26 October 2021*
Accepted: *04 November 2021*
Published: *26 November 2021*

Citation:
Van Stan JT, Klamerus-Iwan A and Dymond SF (2021) Editorial: Bark-Water Interactions. Front. For. Glob. Change 4:802586. doi: 10.3389/ffgc.2021.802586

PHYSICAL AND CHEMICAL INTERACTIONS

Walking in the woods, forester Peter Wohlleben noticed something peculiar underneath the branches of his favorite beech tree: "The stones were an unusual shape: they were gently curved with hollowed-out areas. Carefully, I lifted the moss on one of the stones. What I found underneath was tree bark. So, these were not stones, after all, but old wood[2]." In this collection, numerous papers give insight into some of the mysteries of bark, particularly how bark interacts with and transports water and solutes (Ilek et al.; Tonello et al.; Oka et al.; Ponette-González; Zabret and Šraj).

This Research Topic begins with the basic (yet difficult-to-answer) question of how much water bark can store during rainfall. Ilek et al. applied a novel bark wetting experiment, finding that patterns in bark water storage: are linked to the amount of water vapor that bark absorbs between storms (i.e., hygroscopic water); can vary with height; and may impact stemflow and/or communities living on/in bark. Zabret and Šraj analyze a data-rich case study (156 storms with intra-storm time series) to describe four different stemflow responses to rainfall, each corresponding with specific meteorological conditions and/or phenophase. And in the most biodiverse savannah in the world, the Brazilian Cerrado, Tonello et al. links stemflow yield to

[1] *A Guide Through the District of the Lakes in the North of England* (5th ed., 1835). Available online at: https://romantic-circles.org/editions/guide_lakes/editions.2020.guide_lakes.1835.html
[2] *The Hidden Life of Trees: What They Feel, How They Communicate—Discoveries from A Secret World* (2016, Greystone Books).

multiple bark properties rarely measured in ecohydrology, including insoluble lignin content, droplet contact angle and the rate of change as droplets infiltrate into the bark surface. Bark also impacts the quality of draining precipitation water. Focusing on this topic, Ponette-González explores different perspectives and approaches from the past five decades on bark-water interactions. This interdisciplinary synthesis concludes that bark is "an accumulator, transporter, substrate, and reactor." Lastly, Oka et al. (part 1) studied the effects of bark surface structure on stemflow solute concentrations for six tree species in Japanese montane and urban sites. They confirmed some previous findings about bark surface structural influences, showing that current theory on bark structural drivers of stemflow chemistry may be broadly meaningful.

PLANT ECOPHYSIOLOGICAL INTERACTIONS

The bark is "a proud worker" for the plant, as Jean-Henri Fabre notes, "always tirelessly building cells and renewing her foundations from ruins[3]." Contributions to this collection demonstrate the important roles bark-water interactions can play in plant ecophysiology, in the field (Allen and Connor), lab (Oka et al.), and through data and theoretical synthesis (Berry et al.). In the field, Allen and Connor examined the bark-water interactions of wax myrtle shrubs on coastal hummocks, small islands sitting above mesohaline floodwaters in a freshwater swamp. Their observations suggest these shrubs' stemflow can locally augment net precipitation supply to soils, hypothetically increasing freshwater availability in this stressful environment. In the lab, experiments by Oka et al. (part 2) suggest bark anatomy influences stemflow solute concentrations and composition. They describe new potential linkages between bark anatomical traits and the leaching of common macronutrient ions (Mg^{2+}, Ca^{2+}, and K^{+}) by stemflow. These findings have implications for throughfall chemistry, as nutrient leaching from bark occurs along the branchflows that form "drip points." A mini-review by Berry et al. focuses on bark-water-C interactions, discussing how water and C move between the atmosphere and woody stems. This brief review is packed with a synthesis of current theory and novel analyses relying on large-scale datasets. They assess the climate space where woody stem photosynthesis and bark water uptake may be advantageous and how ubiquitous these processes are across plant families. These field, lab, and synthesis studies construct novel hypotheses and theory, whose testing promise interesting insights into the impacts of bark ecophysiology on the water and nutrient cycling of plants.

ECOLOGICAL INTERACTIONS

Bark can host abundant lifeforms within a diversity of microhabitats (see Magyar et al.). Indeed, "when compelled by a shower to take shelter under a tree," Henry David Thoreau employed himself "happily and profitably" by examining these lifeforms, "prying with microscopic eye into the crevices of the bark or the leaves or the fungi[4]" This corticolous community includes microbes, metazoans, and other vegetation, like lichens and bryophytes (Hembre et al.; Magyar et al.; Porada and Giordani). Hembre et al. shows how variable the biomass of nonvascular epiphyte communities can be across a temperate-boreal ecotone, 9–900 kg ha^{-1}, and how much water this biomass can store, 0.003–0.38 mm, while highlighting challenges to estimating epiphyte contributions to canopy hydrology. Porada and Giordani focus on the influence of bark hydrology on corticolous lichens, applying a process-based model (LiBry) with site-level data in Sardinia (Italy). Switching off bark water storage in the model had striking impacts on nutrient cycling (reducing lichen NPP by 21%) and the community structure (changing morphological traits and reducing physiological diversity by 23%). These results suggest bark hydrology can be important to the growth and morphology of lichens (at their site), and provides ample justification for future work to quantify interactions between bark hydrology and epiphytic vegetation elsewhere. The collection also includes work on fungi not engaged in lichen symbiosis. Magyar et al. reviews the past 50 years of literature on fungal spores (conidia) washed down the bark in stemflow. This synthesis of observations were analyzed to discuss emergent hypotheses regarding the roles of stemflow fungi in tree health and to identify a hitherto unnamed paraphyletic group: "dendronatant fungi." Clearly, future research on life-bark-water interactions is merited across scales, from microscopic fungi to regional epiphytic communities.

SUMMARY

Bark-water interactions are understudied processes in wooded ecosystems. This collection of research highlights evidence of the important roles that bark can play in controlling the amount of water that is returned to the atmosphere during storms, or makes it to the soil, groundwater, and streams, as well as the chemical makeup of that water. As bark is an important ecosystem component that can have substantial surface area and water storage, it also exerts controls on the biology of the plants themselves and related organisms, from microbes to metazoans.

AUTHOR CONTRIBUTIONS

All authors listed have made a substantial, direct, and intellectual contribution to the work and approved it for publication.

FUNDING

Support for JTVS during the editing of this collection was provided by US NSF (EAR-1954907).

[3]Translated from: "L'écorce est une fière travailleuse, toujours en fatigue pour faire des cellules et renouveler ses assises en ruines." *Histoire de la Bûche: Récits sur la vie des plantes* (1867).

[4]*A Week on the Concord and Merrimack Rivers* (1849). Available online at: https://gutenberg.org/files/4232/4232-h/4232-h.htm

ACKNOWLEDGMENTS

We are deeply grateful to all of the contributors, reviewers, and editors who made this collection possible. JTVS also would like to thank. Julieta A. Rosell, Doug Aubrey, and Saskia Grootemaat for their insightful and inspiring discussions on various topics related to the "bark side" of the water cycle.

Conflict of Interest: The authors declare that the research was conducted in the absence of any commercial or financial relationships that could be construed as a potential conflict of interest.

Publisher's Note: All claims expressed in this article are solely those of the authors and do not necessarily represent those of their affiliated organizations, or those of the publisher, the editors and the reviewers. Any product that may be evaluated in this article, or claim that may be made by its manufacturer, is not guaranteed or endorsed by the publisher.

frontiers in Forests and Global Change

HYPOTHESIS AND THEORY
published: 25 March 2021
doi: 10.3389/ffgc.2021.623758

Hypothesis and Theory: Fungal Spores in Stemflow and Potential Bark Sources

Donát Magyar[1], John T. Van Stan II[2,3] and Kandikere R. Sridhar[4,5]*

[1] National Public Health Center, Budapest, Hungary, [2] Applied Coastal Research Laboratory, Georgia Southern University, Savannah, GA, United States, [3] Geology and Geography, Georgia Southern University, Savannah, GA, United States, [4] Biosciences, Mangalore University, Mangalore, India, [5] Centre for Environmental Studies, Yenepoya University, Mangalore, India

The study of stemflow fungi began over 50 years ago. Past work has been performed in different climatic regions of the world, with different sampling methods, by mycologists focusing on different taxonomical groups. Therefore, we aim to synthesize this work to delineate major conclusions and emerging hypothesis. Here, we present: (1) a systematic compilation of observations on stemflow conidial concentration, flux, and species composition; (2) an evaluation of the methods underlying these observations; (3) a testable theory to understand spatiotemporal dynamics in stemflow (including honeydews) conidial assemblages, with a focus on their relationship to bark structure and microhabitats; and (4) a discussion of major hypotheses based on past observations and new data. This represents a knowledge gap in our understanding of fungal dispersal mechanisms in forests, in a spatially-concentrated hydrologic flux that interacts with habitats throughout the forest microbiome. The literature synthesis and new data represent observations for 228 fungal species' conidia in stemflow collected from 58 tree species, 6 palm species, and 1 bamboo species. Hypothetical relationships were identified regarding stemflow production and conidial concentration, flux, and species composition. These relationships appear to be driven by bark physico-chemical properties, tree canopy setting, the diversity of in-canopy microenvironments (e.g., tree holes, bark fissures, and epiphytes), and several possible conidia exchange processes (teleomorph aerosols, epi-faunal exchanges, fungal colonization of canopy microhabitats, and droplet impacts, etc.). The review reveals a more complex function of stemflow fungi, having a role in self-cleaning tree surfaces (which play air quality-related ecoservices themselves), and, on the other hand, these fungi may have a role in the protection of the host plant.

Keywords: fungi, conidia, spores, honeydew, bark, cortisphere, phyllosphere

OPEN ACCESS

Edited by:
Daniel Limehouse McLaughlin, Virginia Tech, United States

Reviewed by:
Mark B. Green, Case Western Reserve University, United States
Kasem Soytong, King Mongkut's Institute of Technology Ladkrabang, Thailand

****Correspondence:***
Donát Magyar
magyar.donat@gmail.com

Specialty section:
This article was submitted to Forest Hydrology, a section of the journal Frontiers in Forests and Global Change

Received: *30 October 2020*
Accepted: *04 March 2021*
Published: *25 March 2021*

Citation:
Magyar D, Van Stan JT II and Sridhar KR (2021) Hypothesis and Theory: Fungal Spores in Stemflow and Potential Bark Sources. Front. For. Glob. Change 4:623758. doi: 10.3389/ffgc.2021.623758

INTRODUCTION

During precipitation or condensation, tree canopies capture and drain water down the undersides of branches. These branchflows redirect water from outlying canopy areas to concentrated drip points (Van Stan et al., 2020a), to treeholes [creating isolated aquatic habitats called "dendrotelmata" (Magyar et al., 2017b)], or multiple branchflows may converge at the stem to

create "stemflow" (Sadeghi et al., 2020). Branchflows and stemflow can play important roles within the canopy and in receiving ecosystems. Within tree canopies, branchflows can enable exchanges between the tree's external and internal microbial communities (Aung et al., 2018), or spread pathogens through resident animal communities (e.g., D'Amico and Elkinton, 1995). Branchflows, and their suspended and dissolved constituents, that contribute to dendrotelmata can affect mosquito control and plant health (Carpenter, 1982; Van Stan et al., 2020b). Before stemflow reaches the ground, it may serve as a drinking water source for canopy-dwelling animals, e.g., koalas (Mella et al., 2020). Stemflow that reaches the surface can supply substantial, localized water (Magliano et al., 2019), nutrient (Ponette-González et al., 2020), pollutant (Klučiarová et al., 2008), and organismal fluxes to the litter and soils (Sridhar, 2009; Bittar et al., 2018; Ptatscheck et al., 2018). When stemflow is able to preferentially infiltrate into the subsurface along root channels (Friesen, 2020), it can interact with the rhizosphere (Johnson and Jost, 2011; Rosier et al., 2015), and influence bedrock-soil interactions (Backnäs et al., 2012).

Because stemflow can influence ecohydrological processes throughout the critical zone, the materials carried by stemflow merit research attention regardless of its typically small proportion (<2%) of gross rainfall in natural forests (Van Stan and Gordon, 2018). As stemflow drains through the canopy, it primarily scours the bark surface, dissolving or suspending, and transporting materials on (and within) that surface. Bark surfaces are structurally complex, enabling it to scavenge aerosolized particles (Suzuki, 2006), and some types and sizes of particulates are more effectively scavenged by bark than by leaves (Xu et al., 2019). Bark surfaces are colonized by a wide range of "corticolous" epiphytes, including plants (Mendieta-Leiva et al., 2020), metazoans (Proctor et al., 2002), and microbes (Akinsoji, 1991; Magyar, 2008; Lambais et al., 2014). Waste from phloem-feeding canopy residents, called "honeydews," can be sticky and nutritive (Miller et al., 1994; Shaaban et al., 2020), affecting both aerosol scavenging and the bark residential community (Dhami et al., 2013). Thus, stemflow may encounter a diverse array of organic and inorganic materials and, indeed, a diversity of solutes and particulates have been observed in stemflow in ecologically relevant amounts (Ponette-González et al., 2020). Dissolved organic carbon concentrations in stemflow, for example, represent some of the highest observations to-date in natural waters (Stubbins et al., 2020). The flux of nematodes and tardigrades within stemflow can be 10^5 individuals year^{-1} tree^{-1}, and even larger for rotifers, $\sim 10^6$ individuals year^{-1} tree^{-1} (Ptatscheck et al., 2018). Fungal spores, or conidia, have been observed in stemflow at even higher concentrations, 10^1–10^3 conidia 10-mL^{-1}, resulting in an annualized flux of $\sim 10^9$ conidia ha^{-1} year^{-1} (Gönczöl and Révay, 2004; Sridhar and Karamchand, 2009; Van Stan et al., 2021).

Fungal conidia are non-motile and, therefore, rely on environmental processes, like wind or water flows, for their mobilization. Conidia in stemflow have been observed to be produced, liberated, and dispersed by fungi in synchrony with storms (MacKinnon, 1982). Stemflow-dispersed conidia are branched or filiform; these "staurospores" and "scolecospores" are well-structured for transport in the thin, rivulet-like stemflow pathways (Bandoni and Koske, 1974; Chauvet et al., 2016).

Although more descriptive studies of conidia have been published than any other particulate in stemflow to-date (Ponette-González et al., 2020), there has been no review of these observations in pursuit of a theory to explain, and test hypotheses regarding the spatial and temporal dynamics in the concentration, flux or species composition of stemflow conidial assemblages. Here, we present: (1) a systematic compilation of observations on stemflow conidial concentration, flux and species composition; (2) an evaluation of the methods underlying these observations; (3) a testable theory to understand spatiotemporal dynamics in stemflow (including honeydews) conidial assemblages, with a focus on their relationship to bark structure and microhabitats; and (4) a discussion of major hypotheses based on past observations and new data. This represents a knowledge gap in our understanding of fungal dispersal mechanisms in forests, in a spatially-concentrated hydrologic flux that interacts with habitats throughout the forest microbiome (Van Stan et al., 2021). This effort also addresses recent calls for improved ecological understanding of tree-fungi interactions (Uroz et al., 2016) and fungal spore dispersal within the forest microbiome (Baldrian, 2017).

METHODS

Literature Synthesis

This metaanalysis used data compiled from a synthesis of published studies that reported species of free fungal conidia observed on bark surfaces, in honeydews, and in stemflow (**Supplementary Table 1**). Several databases were searched (Web of Science, BIOSIS, Current Contents Connect, and The Scientific Electronic Library Online) without a date restriction (i.e., 1864-present) for "conidi*" AND "stemflow" OR "bark" OR "honeydew." Search results were pared down to only those studies that reported observations, of at least presence or absence, for conidial assemblages (i.e., studies of a single fungal species were excluded) from intact trees (not logs, stumps, and debris, etc.) that were healthy (i.e., not with studies on phytopathogenic fungi, like *Fusarium* or *Septoria* spp.). We then searched for other woody/rigid plants (woody vines, palms and bamboo) with the same search settings. Digital data on conidial assemblages that were available directly from study authors were compiled into a single database. Digitization of conidia species data in the remaining studies was done using Tabula 1.2.1[1]. To ensure that the Tabula software did not incorrectly digitize the datasets, a random 25% of observations in each table were checked manually. The only Tabula errors encountered were related to mismatched column-row information and these formatting errors were corrected when found. Some studies reported the abundance or frequency of observation for conidia species; in these cases, the data were transformed into presence or absence to enable study inter-comparison. As stemflow, bark and honeydew conidia assemblages are less-researched than for

[1]https://tabula.technology/

FIGURE 1 | Bark types included in studies to-date examining fungal conidia assemblages in stemflow, bark or honeydew: **(a)** scaled or plated bark, e.g., *Picea abies* (Kwiecień, 2005); **(b)** fissured bark, e.g., *Tilia cordata* (Havelaar, 2020); **(c)** ridged bark, e.g., *Quercus cerris* (Lefnaer, 2016); **(d)** flaked or exfoliating bark, e.g., *Metasequoia glyptostroboides* (Salicyna, 2017); **(e)** smooth bark, e.g., *Fagus sylvatica* (Elsner, 2012); **(f)** palm "pseudobark," e.g., *Coccothrinax barbadensis* (Starr and Starr, 2009); and **(g)** bamboo culm, e.g., *Phyllostachys vivax* (Hanfmampf, 2008).

other habitats, several unknown conidia have been found across studies. Microscopic imagery of unknown conidia was compared across studies to determine (1) if the conidia has been identified and (2) if unknown conidia across studies were morphologically similar. Note that bark, stemflow and honeydew data can be from different studies and, thus, may not have been sampled synchronously. However, this is the data available per the authors' knowledge and the literature search described above. The host tree species were recorded for all cases where the information was provided. When the bark texture of sampling tree was described, it was also recorded. Tree species without bark textural descriptions were classed based on taxonomic descriptions or photographic reference materials. The bark textural classes are listed alongside a photographic representation in **Figure 1**. These classes include scaled or plated bark, fissured bark, ridged bark flaked or exfoliating bark, smooth bark, and external plant tissues on tall, non-tree vegetation, analogous to bark: palm "pseudobark," and bamboo culm (**Figure 1**).

Collection and Identification of New Conidia Assemblages

To supplement the database of published conidia assemblages in stemflow, bark and honeydews, additional data from ongoing field studies by the lead author were included in the database. Sampling and conidia identification methods (as described below) were similar to those from previously published studies. These new data include conidial assemblages identified from bark, stemflow and honeydew samples (**Supplementary Table 2**), which were added to the database. Augmentation of published datasets with these new data was done to provide the most comprehensive synthesis available to date for building theory and major hypotheses. These new data permitted better replication of conidial assemblages from existing bark types, honeydew and stemflow. No individual analysis, theoretical discussion, or related hypothesis relied solely on new data.

Stemflow samples were collected directly from the stem by diverting a stemflow rivulet (2–10 mL) into centrifuge tubes. One milliliter of FAA (50% ethanol, 5% glacial acetic acid, 10% formaldehyde) was added to each sample (Ingold, 1975). Water samples were settled; one drop of the sediment was mounted on a microscope slide and allowed to dry. Lactophenol cotton blue was added to the dried sediment to prepare samples for further studies.

Bark samples were collected from living trees in Hungary, then the surface and fissures were analyzed using pressure-sensitive acrylic strips (MACbond B 1200, MACtac Europe S.A., Brussels). The strip consists of a thin (20 μm) polypropylene film coated on

both sides with a rubber-based adhesive, which offers very high adhesion property on wood (Similar methods are widely used in building inspection for molds as well as in clinical mycology). Bark fissures were opened by force using a scalpel put deep into the cracks. A 1.5 cm^2 piece of strip was placed on the opened surface of the fissure, then it was pressed against it and peeled. Lactophenol with cotton blue was added to the sampling side of the strip, which was then covered with a cover slip to prepare semi-permanent slide preparations for further studies. Three-to-four preparations were made from each bark sample.

Honeydew is an extract from piercing and plant-sucking insects, which suck phloem sap, which is rich in nutrients, especially amino acids. To satisfy their protein needs, these insects need large amounts of sap, which contains only 1–2% of proteins, though it is high in water content and sugars. When honeydew production is high on forest trees, honeydew drops fall to the ground or flow down on stems. Animals, mostly birds, ants, wasps and bees (i.e., *Apis mellifera* L.) often feed on honeydew. Honeybees collect and transport it to hives and process it into honeydew honey (often sold and labeled as forest honey). Due to the collecting activities of honeybees the spores trapped in the honeydew will therefore accumulate in honeydew honey. Thus, 10 *g* were sampled from 500 *g* of previously homogenized honey, dissolved in 20 ml of distilled water at 40°C, centrifuged for 10 min at 560 *g* and allowed to settle. The sediment was recovered in 10 ml of distilled water and again centrifuged. The sediment was then collected with a Pasteur pipette and dried onto microscope slides at 40°C. It was then mounted in glycerine-gelatine and covered (Louveaux et al., 1978).

The tapes and slides prepared from all samples were viewed directly under a microscope to identify the types of spores present on the sampled surface. Identification of fungal spores was carried out both from experience and by means of scientific literature and monographs (e.g., Hughes, 1958; Ingold, 1971, 1975; Kendrick, 1990; Ellis and Ellis, 1997; Marvanová, 1997; Gulis et al., 2007). Digital photomicrographs were taken with an Olympus BX-51 microscope at ×800 magnification.

AN EVALUATION OF STEMFLOW CONIDIA SAMPLING METHODS

A description and discussion of the methods used to collect stemflow samples for the quantification and identification of conidial assemblages is necessary to identify any non-trivial limitations surrounding the observations in this synthesis and evaluation. For stemflow, the first samples to be examined for conidia were taken from the foam that can accumulate at the base of some trees (Gönczöl, 1976: **Figure 2a**); however, stemflow sampling has most often been done during storms through the direct transfer of stemflow from the bark surface (e.g., **Figure 2b**) to a collector containing preservative (Gönczöl and Révay, 2004, 2006; Sridhar and Karamchand, 2009; Sudheep and Sridhar, 2010; Ghate and Sridhar, 2015c; Magyar et al., 2018). Rarely have stemflow samples been collected after storms from collection bins (Bandoni, 1981; MacKinnon, 1982). Although sampling from a collection bin after storms has been the norm for stemflow hydrology and solute fieldwork (Levia and Germer, 2015), this post-storm sampling method can introduce species that have colonized the plastic tubing and collection bins between storms. Another limitation of this method is that spores germinate rapidly in water samples and morphological identification and counting can become impossible. Bulk post-storm stemflow sampling allows researchers to collect one sample that integrates the intra-storm variability and all stemflow rivulets around the tree stem (note that many stemflow pathways can travel from the canopy to the surface: **Figures 2b,c**). Conversely, direct sampling of stemflow rivulets into clean or sterilized collectors with preservative during a storm gains a representative snapshot of the conidial assemblage with the least possibility of contamination. This snapshot sampling, however, must be repeated (1) throughout a storm (e.g., Gönczöl and Révay, 2004) to account for the conidial assemblages' intra-storm variability or (2) for all stemflow rivulets around a tree to account for the spatial variability (**Figure 2c**).

To date, the experimental designs for sampling stemflow have not included samples across multiple storm conditions, seasons, or years. Based on theory and past related literature, it may be hypothesized that there is significant intra-storm and seasonal variability in stemflow conidia concentration. Observations of stemflow solutes within storms and among storms of various magnitudes suggest that the timing of any snapshot sampling of stemflow rivulets during the storm can be important (Levia et al., 2011; Van Stan et al., 2020a). Interactions between rainfall intensity and a tree canopy's resistance to stemflow generation (due to high water storage capacity or rough bark, etc.) can result in differing dynamics of materials out-washed by stemflow (**Figure 2d**). For example, typically stemflow rivulets are sampled 15–30 min after stemflow is established (Sridhar and Karamchand, 2009; Sudheep and Sridhar, 2010; Ghate and Sridhar, 2015c)—depending on the storm characteristics and the structure of the tree being sampled, this single sampling event could capture (a) the initial "wash off" pulse of conidia for a moderately intense storm over a canopy which moderately resists flow (**Figure 2d**, magenta), (b) a point along the gradual wetting and washing off period for a low intensity storm over a canopy with high flow resistance (**Figure 2d**, red), or (c) miss the wash off pulse entirely and capture the more dilute, post-wash off period for a high intensity storm over a canopy which permits flow (**Figure 2d**, blue). Some trees with canopies that have very high flow resistance may not have generated stemflow yet, despite all other trees having done so. Thus, these trees would not be able to be sampled by the snapshot approach, for example: see the lack of stemflow data on *Chamaecyparis* or *Taxus* tree species in Gönczöl and Révay (2004, 2006).

Less observational evidence is available to hypothesize on the compositional variability that one may expect among different stemflow rivulets. Still, theoretically, to ensure that spatial variability of conidial transport and assemblage composition around the stem is accounted for, multiple stemflow rivulets (**Figures 2b,c**) should be sampled for conidia. Indeed, it is

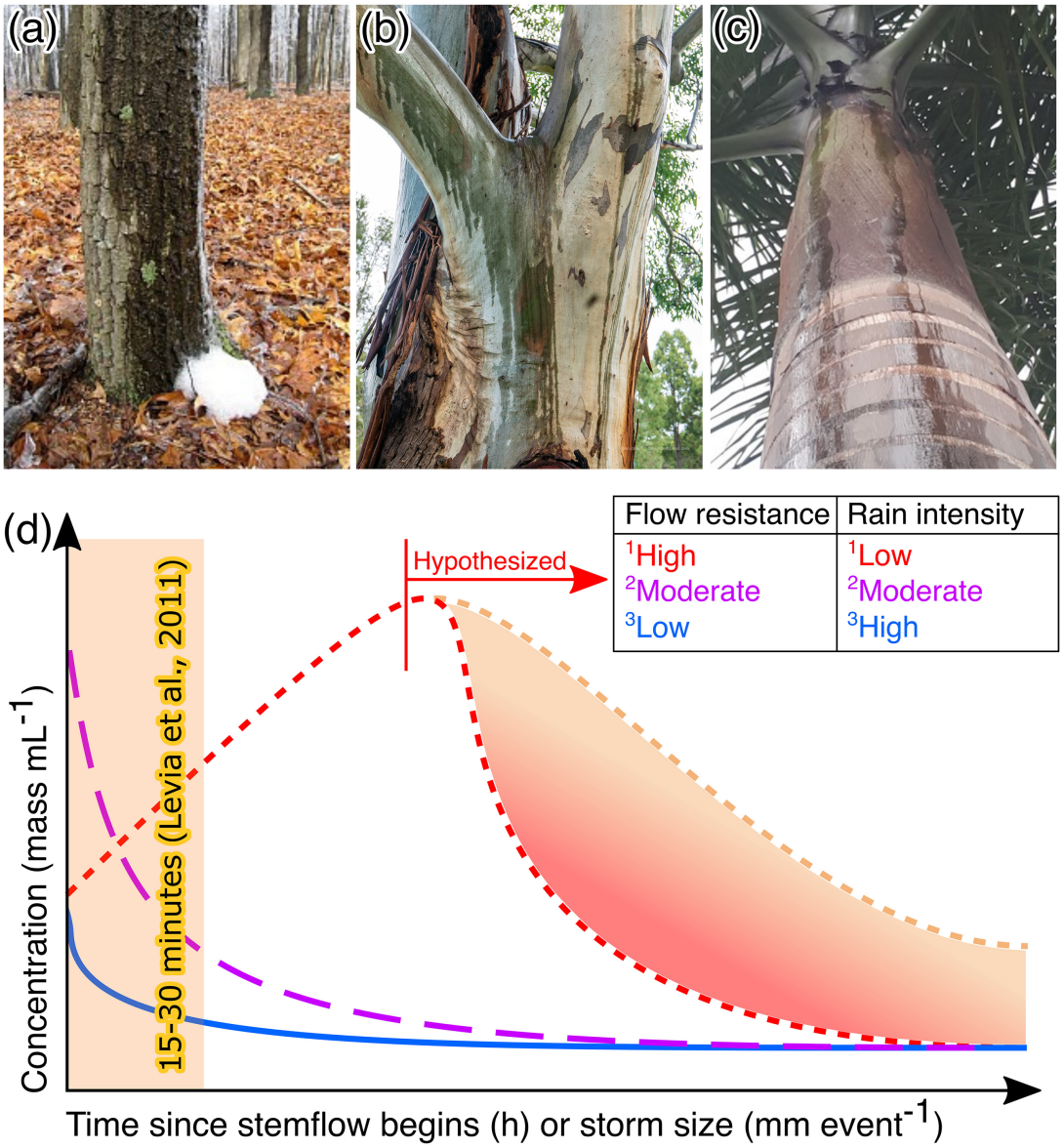

FIGURE 2 | Photographs showing types of stemflow that has been sampled, including **(a)** the foam that can sometimes accumulate at the base of a stemflow rivulet (West, 2010); **(b)** major stemflow rivulets (McPherson, 2018); and **(c)** multiple discrete stemflow rivulets on a single trunk of a palm, *Roystonea regia* [photograph reproduced from Salemi (2019) with permission]. **(d)** Conceptual summary of different temporal dynamics previously observed in stemflow solute concentrations from different combinations of tree species and rain intensities. [1]*Quercus virginiana* hosting a substantial bromeliad-fern-lichen epiphyte assemblage in subtropical maritime forest, Georgia, United States (Van Stan et al., 2017). [2]*Liriodendron tulipifera* and [3]*Fagus grandifolia*, both in a temperate, maritime forest, Delaware, United States (Levia et al., 2011). Note that no new data was used to generate this conceptual summary.

likely that different stemflow rivulets integrate different areas of the canopy—from different aspects, exposures (windward v. leeward), or microenvironments (dendrotelma overflows v. branchflows). The number of discrete stemflow rivulets may change with rainfall intensity—see photographs in Levia et al. (2011)—but dye tests suggest that these rivulets over the bark surface are highly preferential (Imamura et al., 2017) and exhibit non-uniform flow patterns over time (Tischer et al., 2020). The thin sheet-like flow structure of stemflow also makes direct sampling for conidia via syringes challenging, especially during low rainfall intensities. Gönczöl and Révay (2004) commented on this sampling challenge, stating that "during heavy rain when the stemflow was copious the syringe could easily be filled . . . However, during low intensity rain a lesser quantity of water, sometimes 1 or 2 ml, could only be collected." Some studies have addressed the spatial issue by having collected stemflow samples across a trunk area using sterile plastic sheets (Sridhar and Karamchand, 2009; Sudheep and Sridhar, 2010; Ghate and Sridhar, 2015c).

STEMFLOW CONIDIA CONCENTRATIONS AND FLUX ESTIMATES

To the authors' knowledge, few studies report the concentration and flux of stemflow conidia (Gönczöl and Révay, 2006; Sridhar and Karamchand, 2009; Ghate and Sridhar, 2015c) and no studies to date have comprehensively assessed the size of the conidial reservoir on-and-in bark and honeydews, or the temporal variability of these bark conidial sources to stemflow. We also lack an understanding of variability in stemflow conidial concentration, flux and composition across temporal scales as no studies report trends across storms, seasons or years (see previous section). The snapshot data available, however, include several species with disparate bark and canopy structures situated within temperate sites (Germany, Hungary, Romania, and Sweden: Gönczöl and Révay, 2006) and a tropical monsoon site (Mangalore, India: Sridhar and Karamchand, 2009; Ghate and Sridhar, 2015c). No new data was available/added regarding conidia concentrations and fluxes.

The tree species studied across temperate European sites included Fagus sylvatica, Prunus avium, Carpinus betulus, Alnus glutinosa, Quercus cerris, Taxus baccata, Picea abies, and Pinus sylvestris (Gönczöl and Révay, 2006). For these temperate tree species, total conidia concentrations in stemflow ranged from approximately 2,000–16,000 conidia L^{-1}. The maximum stemflow conidia concentration reported for temperate trees was observed from an evergreen needleleaved tree, T. baccata, while the minimum was observed from a deciduous broadleaved tree, Q. cerris (Gönczöl and Révay, 2006). One of the possible drivers of these differences in stemflow conidia concentration may be the amount of stemflow that study trees were able to generate: T. baccata generated very low stemflow volumes compared to Q. cerris (Gönczöl and Révay, 2006). This comparison of the minimum and maximum observations, however, provides a limited insight into differences among major tree types. For example, although an evergreen needleleaved species generated the largest stemflow conidia concentration across temperate sites, the conidia concentration from P. sylvetris, another needleleaved evergreen species, was nearly as low (3,100 conidia L^{-1}) as observed from Q. cerris (Gönczöl and Révay, 2006). Perhaps the larger conidia concentration from T. baccata, specifically, may be due to the bark chemical composition and affinity to store water—this latter may be partially explained by a more complex, exfoliating bark structure compared to the other trees studied. Resins may also play an important role in shaping the stemflow conidia concentration, where, for example, Mycoceros colonization of pine and spruce species (whose bark contains resin droplets that keep the bark dry) was low (Révay and Gönczöl, 2011b; Magyar et al., 2017a). Moreover, a range of growth inhibitory compounds have been reported from the wood of Pinus species (Erdtmann, 1952; Scheffer and Cowling, 1966; Gunasekera and Webster, 1983) that may suppress fungal colonization and sporulation.

An important caveat regarding the Gönczöl and Révay (2006) stemflow conidia concentrations is that, for four of the sampled trees, some spore species were not counted due to being too "numerous." For *A. glutinosa* and *F. sylvatica*, only 1 of the trees had unquantified results and could be ignored due to data being provided from other individual trees of the same species. This was not the case for *Q. cerris*. As a result, conidia concentrations can be considered underestimates for *Q. cerris*. Despite the underestimates for some trees in the Gönczöl and Révay (2006) study, their stemflow conidia concentration results compare well with those from the tropical monsoon studies.

A greater number of species have been investigated at the tropical monsoon site with regards to stemflow conidia concentrations, including trees: *Acacia auriculiformis, Alstonia scholaris, Artocarpus integrifolia, Carallia brachiata, Careya arborea, Eucalyptus tereticornis, Ficus benghalensis, Ficus religiosa, Mangifera indica, Odina wodier, Pongamia glabra, Syzygium cumini, Tectona grandis*, and *Terminalia paniculata* (Sridhar and Karamchand, 2009); and palms: *Areca catechu, Borassus flabellifer, Caryota urens, Cocos nucifera, Livistona rotundifolia*, and *Roystonea regia* (Ghate and Sridhar, 2015c). For the tree species, stemflow conidia concentrations ranged from 4,800–52,600 conidia L^{-1} (Sridhar and Karamchand, 2009). Interestingly, just as observed in Gönczöl and Révay (2006), the highest conidia concentration in stemflow from the tropical monsoon site was observed from a tree species with a complex, exfoliating bark structure: *T. grandis*. The lowest stemflow conidia concentration from any tree sampled by Sridhar and Karamchand (2009) was by the evergreen broadleaved tree, *M. indica*. For the palm species, the range of stemflow conidia concentrations was an order of magnitude lower: 230–5,790 conidia L^{-1} (Ghate and Sridhar, 2015c). Therefore, the lowest observation for stemflow conidia concentrations was reported for a palm species, *Roystonea regia*. To examine whether trends emerge in stemflow conidia concentrations across plant types or with variability in stemflow production, the reported stemflow conidia concentrations were grouped per plant type (**Figure 3A**) and, where possible, plotted against published observations of the species' stemflow fraction (**Figure 3B**).

The median of stemflow conidia concentrations reported to date was highest for evergreen broadleaved trees, 15,750 conidia L^{-1}, followed relatively closed by both evergreen needleleaved trees and deciduous broadleaved trees, 8,134 versus 8,000 conidia L^{-1}, respectively, and was lowest for the palms, 2,665 conidia L^{-1} (**Figure 3A**). One of the two outliers from the deciduous broadleaved trees was discussed earlier (*T. grandis*); the second was *A. integrifolia* (i.e., *Artocarpus heterophyllus*; **Figure 3A**). When available conidia concentration data for plant species are plotted against their stemflow fraction, a general trend emerges where stemflow fraction is inversely related to stemflow conidia concentration (**Figure 3B**). The mechanism behind the hypothetical exponential decay in **Figure 3B** may be related to greater stemflow resulting in the scouring of fungal conidia from bark surfaces and subsequent dilution. Thus, the scouring by high stemflow rates could exhaust the bark conidia available to stemflow and, thus, greater stemflow production would diminish the total conidia per unit volume. This is analogous to the well-known "first flush dynamics" in watersheds (Sansalone and Cristina, 2004).

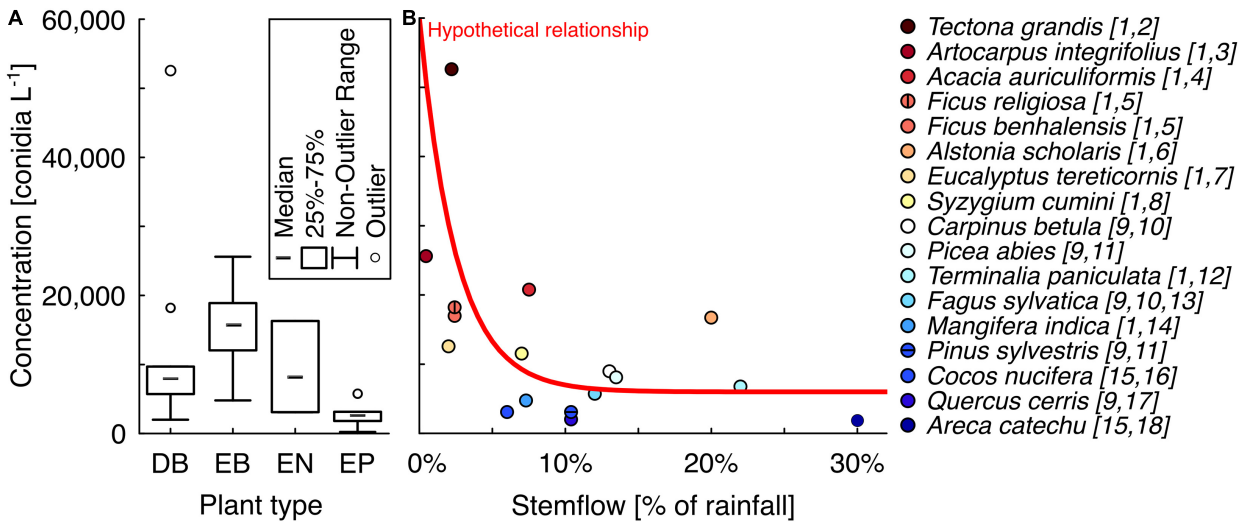

FIGURE 3 | (A) Box and whisker plot comparing the stemflow conidia concentrations measured from different plant types studied to-date: DB, deciduous broadleaved; EB, evergreen broadleaved; EN, evergreen needleleaved; and EP, evergreen palms. **(B)** Plot of available data on stemflow conidia concentration and the mean stemflow (fraction of rainfall). Note that (i) for many species with observations of conidia concentrations (in panel **A**) the authors were unable to find published observations of stemflow fraction and (ii) these datasets (conidia concentration and mean stemflow fraction) were collected using different sampling methods (see methods discussion). However, a relationship between these variables, similar to what has been observed for solute concentrations in past work, may be hypothesized. All data for these plots were from publications: [1] Sridhar and Karamchand (2009), [2] Tanaka et al. (2017), [3] Mali et al. (2020), [4] Bruijnzeel et al. (1987), [5] *Ficus benjamina* from Guevara-Escobar et al. (2007), [6] Ray (1970), [7] Nizinski et al. (2011), [8] Sahu et al. (2006), [9] Gönczöl and Révay (2006), [10] Mitscherlich (1981), [11] Cape et al. (1991), [12] Ndakara (2012), [13] Peck (2004), [14] Ndakara (2016), [15] Ghate and Sridhar [2015c], [16] Serrano (1982), [17] Mosello et al. (2002), and [18] Cheng et al. (2008).

Conidia fluxes from tree species in Sridhar and Karamchand (2009) were recently estimated, ranging from 4–278 $\times$ 10^9 conidia ha^{-1} $year^{-1}$ (Van Stan et al., 2021). Although conidia concentrations in the stemflow of palms were very low (**Figure 3A**), they appear capable of generating fluxes of similar magnitude to trees. This may be a function of the palm species typically having greater stemflow fractions than tree species (Serrano, 1982; Frangi and Lugo, 1985; Cheng et al., 2008; Germer et al., 2010). Stemflow fractions have been reported for two of the palm species investigated by Ghate and Sridhar (2015c): 30 and 6% of annual rainfall for *A. catechu* and *C. nucifera*, respectively, (Serrano, 1982; Cheng et al., 2008). Given these stemflow fractions (of the 3,780 mm $year^{-1}$ mean annual rainfall in Mangalore, India) and assuming the published conidia concentrations are representative, then a hectare of *C. nucifera* or *A. catechu* would theoretically be able to input 7 $\times$ 10^9 and 26 $\times$ 109 conidia ha^{-1} $year^{-1}$, respectively, to the soils near their stems.

CONIDIA SPECIES COMPOSITION IN STEMFLOW

Observations and Hypotheses on the Number and Morphology of Conidia Species

The literature synthesis and new data represent observations for 228 fungal species' conidia in stemflow collected from 58 tree species, 6 palm species, and 1 bamboo species (see dataset, **Supplementary Table 1**). Conidia observed in all canopy habitats included in this study (stemflow, bark and honeydew) consisted of 368 different fungal species (**Supplementary Table 1**). When compared to the bark conidia assemblages synthesized from 63 tree species and 3 vine species, there was a significant portion of overlap between stemflow and bark observations (44%, or 102 shared species), suggesting that stemflow rivulets scour conidia from the bark surfaces over which they drain. Fewer shared species were found for stemflow and honeydews (25%, or 56 shared species). Observing fewer shared conidia species between stemflow and honeydew compared to stemflow and bark is reasonable as the honeydews are seasonal and may not cover all the bark area over which stemflow can drain. Half the conidia species observed in stemflow had not been observed in bark or honeydews (114 spp.); these may originate from bioaerosols, the overflow of tree holes, or any other of the myriad microenvironments within canopies (Sridhar, 2009; Magyar et al., 2016b). Thus, these data suggest that stemflow integrates a diversity of canopy microhabitats for conidia as it drains to the surface.

Stemflow conidia have been observed from taxonomically and ecologically heterogeneous groups of fungi (**Supplementary Table 1**). Several morphologically distinct conidia have been observed in stemflow— many of them have not been identified even to the generic level (Gönczöl and Révay, 2003, 2004, 2006), which confirms the existence of many unknown species in tree canopies. The larger trees seemed to have higher diversity of spores in stemflow, possibly owing to the increased

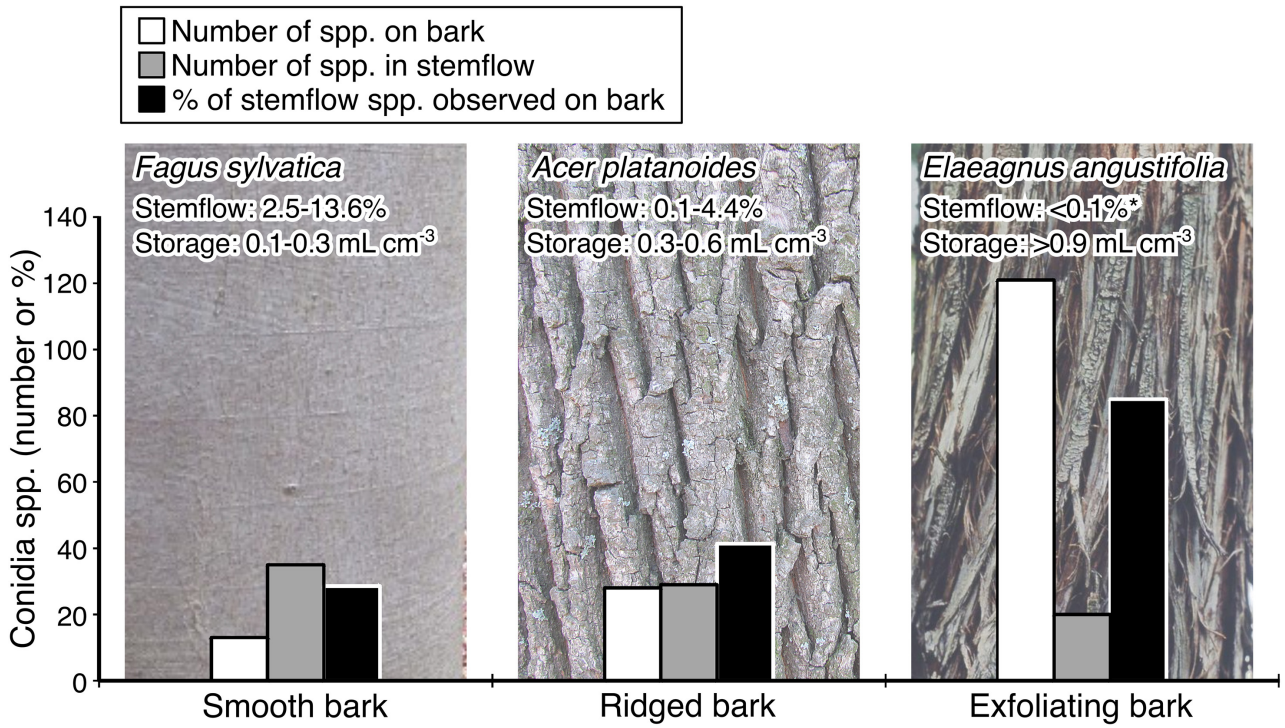

FIGURE 4 | A case study comparison of the number of species of conidia observed in bark (white bar) and stemflow (gray bar) assemblages between species with increasingly complex bark structure. Note that the portion of stemflow conidia species represented by species observed from bark (black bar) samples increases with bark complexity. Conidia data are from published studies (Gönczöl and Révay, 2006; Magyar, 2007, 2008; Révay and Gönczöl, 2011b). Include citations for stemflow and storage estimates. For context, observations of relative stemflow and normative bark water storage capacity are provided: *Fagus grandifolia* (Giacomin and Trucchi, 1992; Krämer and Hölscher, 2009; Van Stan et al., 2016); *Acer platanoides* (Valová and Bieleszová, 2008; Schooling and Carlyle-Moses, 2015; Campellone, 2018); *Elaeagnus angustifolia* (Schooling and Carlyle-Moses, 2015). *Stemflow from *E. angustifolia* reaching this value only occurred for storms ≥ 10 mm event-1 (Schooling and Carlyle-Moses, 2015). Photographs are all under creative commons licenses: *F. sylvatica* (Elsner, 2012), *A. platanoides* bark (Gmihail, 2014), and *E. angustifolia* (T. Davis Sydnor, https://Bugwood.org).

surface area for colonization of bark fissures or the presence of lichens (MacKinnon, 1982). Data available to date indicate that not all tree species are appropriate to develop a high diversity of fungi adapted to stemflow dispersal (**Figure 4**). For example, the number of conidia species observed in the stemflow of tree species that generate relatively high stemflow fractions (>5% of rainfall across their canopy)— like *F. sylvatica*, *Populus tremuloides*, or *C. betulus*— typically exceed 30 spp. (MacKinnon, 1982; Gönczöl and Révay, 2006; Magyar, 2007). On the other hand, tree species which generate relatively low stemflow fractions (<1% of rainfall across their canopy)—like *T. grandis*, *G. dioica* and *E. tereticornis*— are reported to have only 2–20 spp. (Magyar, 2007; Sridhar and Karamchand, 2009; **Supplementary Table 1**). An example comparison of selected tree species with published data on bark and stemflow conidia spp., stemflow fraction, and the bark water storage capacity permits further discussion (**Figure 4**). The more structurally complex, exfoliating bark (*E. angustifolia*) contains more conidia spp. (n = 121), likely because more types of conidia are trapped by the bark and the spongey structure adsorbs and stores water for a long time, allowing the development of thriving fungal colonies (Magyar, 2008). In addition, the trunk structure of this studied *E. angustifolia* tree (being tortuous and steeply inclined) is somewhat unsuitable for trickling of rivulets (Pypker et al., 2011). Likely as a consequence of these features, stemflow from *E. angustifolia* contains the least number of conidia spp. (n = 20) compared to the others, despite its portion of species shared with the bark assemblage is highest (85%). In contrast, beech (*F. sylvatica*) is typically a tall and straight tree. Stemflow from beech trees' comparatively simple bark surface structure not only has the most conidia species, but has a greater number of species than observed on the bark surface (n = 35 spp. in stemflow versus 13 spp. on the bark) and only 29% of the bark conidia species were observed in stemflow. Smooth bark trees with low bark water storage capacities generate more stemflow (André et al., 2008; **Figure 4**), which may wash more bark area clean, integrating a greater amount of canopy microenvironments compared to trees with more complex bark.

Regarding the conidia species found in stemflow, mycological studies on stemflow have focused on morphological species identification, specifically for staurosporous (i.e., radiate or branched), scolecosporous (elongate or thread-like), and helicosporous (spiral-like) taxa. It has long been noted that stauro- and scolecosporous conidia are often water-transported (Ingold, 1966). Later findings suggest that conidia of these fungi are produced, liberated and dispersed synchronously

with rainfall events (MacKinnon, 1982). Thus, the transport of stemflow-specific fungi initiates by the liberation of conidia from their colonies. The complex shape of their branched conidia is advantageous for dispersal as it might be easily torn off from their conidiophores by water tension than a conidium with a smaller surface area. The density of aquatic hyphomycete spores being ∼500 femtogram μm^{-3} (Findlay and Arsuffi, 1989; Bärlocher, 2020), spore dispersal is then followed by a mostly passive drift in the draining stemflow. Additionally, a branched spore occupying several planes can be refloated more easily after settling and moved more freely on water films (MacKinnon, 1982).

Fungal genera on above ground substrates have been found to more likely produce allantoid (curved elongated) spores, to lower the risk of precipitation-related wash out (Calhim et al., 2018). Thus, we note that safe arrival on specific substrates is arguably another important driver of spore morphological evolution in addition to dispersal (Calhim et al., 2018). Still, the branched form of conidia is the product of convergent evolution and secondary adaptation to aquatic mode of life (Ingold, 1975; Belliveau and Bärlocher, 2005; Sudheep and Sridhar, 2010). Ingold (1942, 1953) suggested three selective pressures responsible for branched shapes of conidia: (a) delayed sedimentation for dispersal, (b) settlement on a suitable substrate, and (c) prevention from ingestion by invertebrates. Such conidia are also thought to hold water around the conidium, thereby increasing the possibility of quick germination (Sridhar and Karamchand, 2009). The following subsections will discuss the two different subgroups of these branched, elongated or twisted conidia: "true" aquatic (or Ingoldian) hyphomycetes and a paraphyletic group of conidia currently un-named, which we propose to call "dendronatant fungi" (as discussed in section "Observations and hypotheses on non-Ingoldian, 'dendronatant fungi' in stemflow").

Observations and Hypotheses on Ingoldian Hyphomycetes in Stemflow

The Ingoldian fungi are well-known from streams, but their discovery in stemflow was highly surprising. They are reported from stemflow in both temperate and tropical areas (e.g., Sridhar and Karamchand, 2009; Révay and Gönczöl, 2010). They have been early and regularly reported to occur in a variety of environments other than their preferred habitat. Of all the fungal species identified in the studies synthesized here, 19% (n = 70) of the species are considered Ingoldian fungi (**Supplementary Table 1**). When monitoring stemflow, Bandoni (1981) observed spores of *Gyoerffyella biappendiculata*, a species he considered as an Ingoldian fungus. Later on, the conidia of many other Ingoldian hyphomycetes typical in temperate streams are reported to be common in stemflow and throughfall samples (e.g., *Anguillospora crassa, A. longissima, Alatospora, Articulospora, Flagellospora curvula, Tricladium* spp., and *Varicosporium* spp.; Chauvet et al., 2016). It was also shown that some Ingoldian fungi can actively grow and sporulate in terrestrial litter and soil (Sridhar and Bärlocher, 1993; Sridhar et al., 2020).

Although these fungi have been reported from the phyllosphere of 57 plant species (Chauvet et al., 2016), the growth and sporulation of Ingoldian fungi in tree canopies is only indirectly known by the presence of their conidia in stemflow (Czeczuga and Orłowska, 1999; Sridhar and Karamchand, 2009). It was postulated that there is the existence of a guild of fungi that may "function in canopies much as classical Ingoldian aquatic hyphomycetes in streams" (Carroll, 1981). In addition, a gradient (or zonation) may develop across the canopy owing to stable and unstable niches with macro- and micro-niches (i.e., for tree holes or complex bark structures). Still, many questions exist regarding the ecology of these fungi: Can Ingoldian hyphomycetes adapt to sporulation in free water in canopies? How did these fungi, well-known inhabitants of streams, "climb up" to colonize tree tops? These are amongst the curious open questions in fungal ecology. There are many speculations and hypotheses we may synthesize here (**Figure 5**). Selosse et al. (2008) hypothesized that large numbers of conidia in air bubbles of stream foam may be dispersed through wind or aerosols and onto tree canopies (**Figure 5a**). However, these conidia were almost absent during the air monitoring of spores of two decades (Magyar, unpublished) and were not detected in air samples. Therefore, the hypothesis of airborne dispersal of Ingoldian conidia in large numbers seems to be implausible. Another common mechanism is spore dispersal by rain splash, which is widely known in some plant pathogenic fungi (**Figure 5b**). It occurs when a rain drop falls onto a surface covered by a thin film of water. By this impact, many (100–5,000) secondary droplets produced at its periphery (Madden, 1992). Minute secondary droplets are observed to be blown away by strong wind from stemflow dripping from bark extremities (Magyar, personal field observations, **Figure 5c**). Other types of dispersal mechanisms prevalent during rainfall may also considered, e.g., wet shake-off (**Figure 5d**). It is possible to speculate that some spores transported by stemflow may be aerosolized by secondary splash droplets, stemflow dripping or wet-shake off (**Figures 5b,c$_2$,d**) and transported to longer distances by wind (**Figure 5f**), but further studies dealing with the comparison of spore content of splash or stemflow or fog samples are necessary to confirm this view. Some branched spores are observed on the feet of birds, which may be transported to the tree tops (Vass, 2015; **Figure 5e**). Insects have also been observed drinking regularly from the foam floating on a creek, where Ingoldian fungi are common. It is possibly a way to transport these conidia to the trees too (**Figures 5g**, **6a**). Rainwater containing spores of Ingoldian spores were found to be accumulated in walnut shells. A network of micro-telmata (walnut shells, snail sells, and spots etc.) between trees and a creek may be contribute to a horizontal mesoscale spore dispersal by rainsplash and throughfall (**Figures 5m**, **6b**). Similarly, a network of dendotelmata were found in Őrség, Hungary on *Alnus* and *Carpinus* trees, with many holes per each tree at different heights (**Figure 6c**). Hypothetically such splash from these holes can provide the vertical mesoscale transport of spores, too (**Figure 5n**). However, the above-mentioned transport mechanisms seem to be episodic and unlikely to account for the abundance and diversity of these fungi in stemflow. The most likely explanation involves fungal sexual reproductive structures

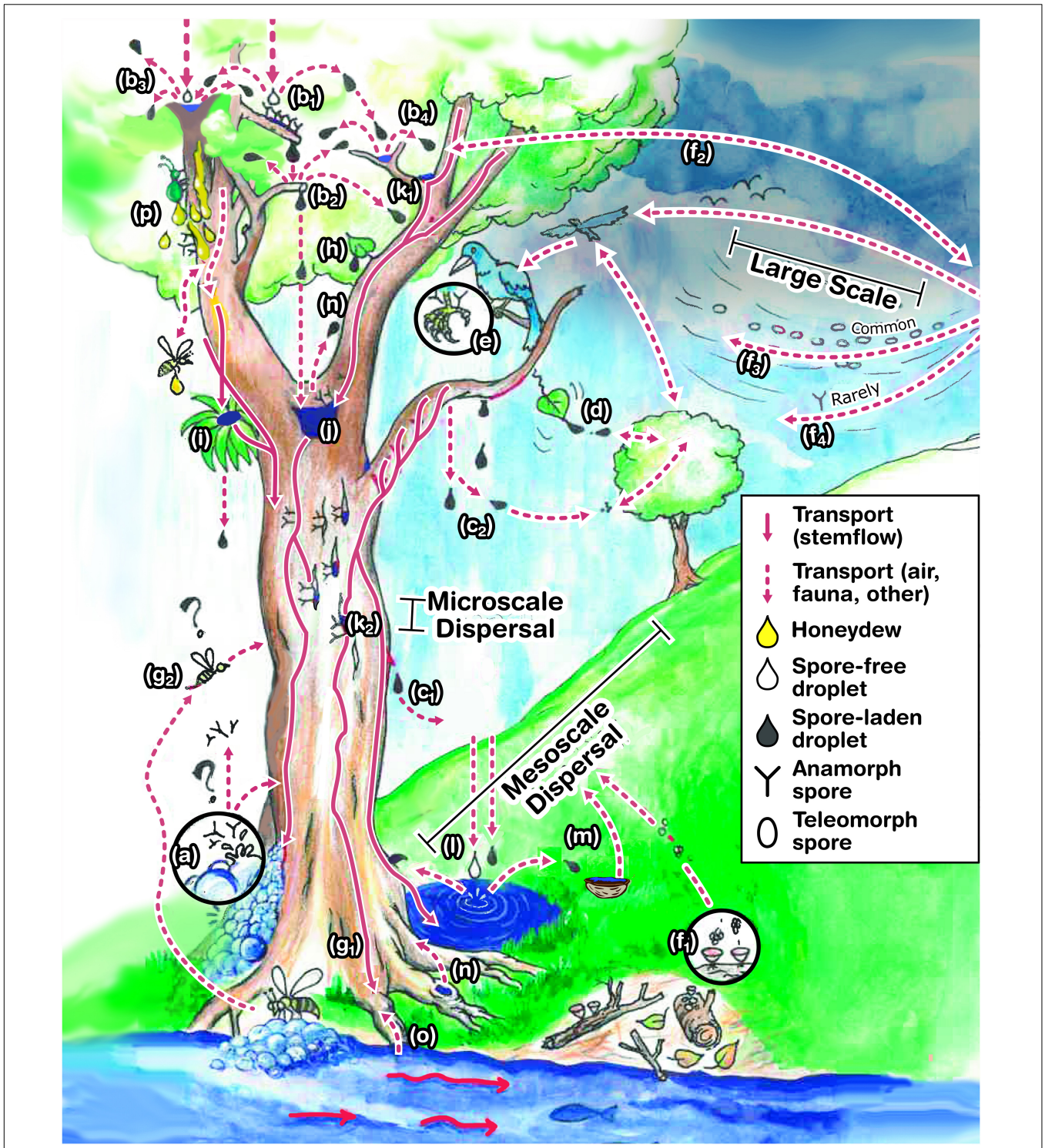

FIGURE 5 | Illustration synthesizing the hypothesized source, fate and transport of Ingoldian and dendronatant conidia found in stemflow, including: **(a)** bubbles; **(b)** splash; **(b_1)** spore-free rain droplet hits a fungal colony; **(b_2)** a spore-laden drop accumulated at the end of twig; **(b_3)** spore-free rain droplet hits spore-laden water film; **(b_4)** spore-laden droplet hits spore-laden water film; **(c)** aerosolized stemflow from **(c_1)** drips from branches and **(c_2)** bark extremities; **(d)** shaking release and dispersal; **(e)** epi-faunal exchange; **(f)** wind dispersal of teleomorph spores **(f_1)** from local or **(f_{2-3})** distant sources; and **(f_4)** while airborne dispersal of anamorphs seems to be rare; **($g_{1,2}$)** exchange by invertebrates visiting streams; phytothelmata in epiphytes; **(h)** throughfall; overflow from **(j)** treeholes, **(k)** aquatic microhabitats in **(k_1)** branch junctions and **(k_2)** bark fissures (note that some is filled with rainwaters while others are out of the way of rivulets and consequently remains dry, some of them of low fungal growth; **(l)** rain and throughfall generates splash transfer between tree, stream and nearby puddles, **(m)** micro-thelmata (e.g., walnut shells) and **(n)** treeholes; **(o)** endophytic colonization and dispersal; and **(p)** spore capture and transport due to honeydew flow and attracted invertebrates.

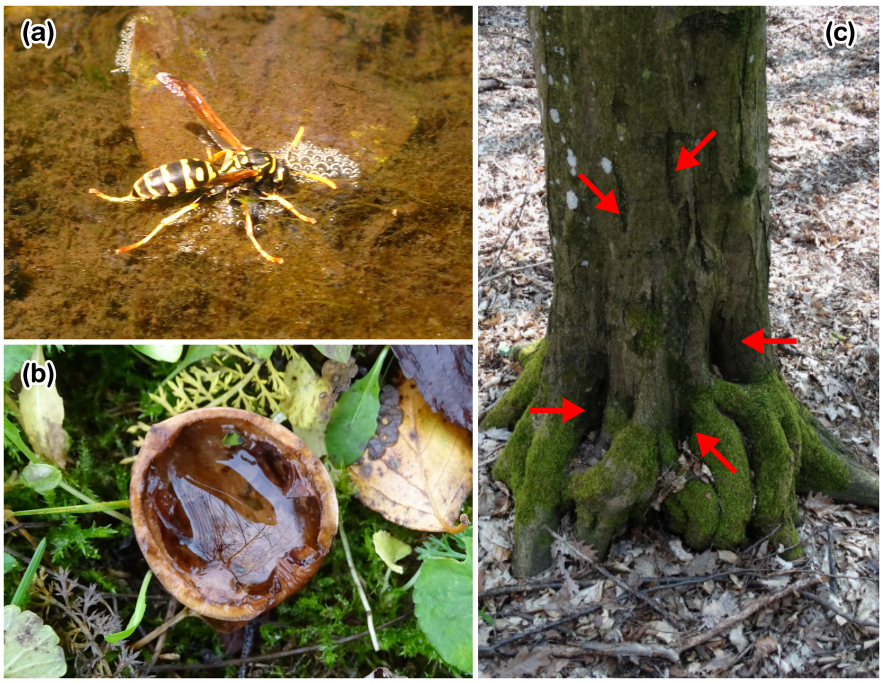

FIGURE 6 | Photographs of potential vectors and microhabitats that may act as sources (or sinks) for stemflow conidia. **(a)** an insect drinking from the foam floating on a creek, where Ingoldian fungi are common. It is possibly a way to transport these conidia from streams to the tree canopy. **(b)** Rainwater accumulated in a walnut shell (i.e., a "micro-phytothelma") between trees and a creek, containing spores of Ingoldian and dendronatant fungi. It may enable a mesoscale spore dispersal by rainsplash and throughfall between a network of such telmata (nutshells, pots, and snail shells, etc.). **(c)** Red arrows point to a network of dendrotelmata found in Őrség, Hungary on *Alnus* and *Carpinus* trees, which can hypothetically provide vertical mesoscale transport of spores (Credit for all photos: D. Magyar).

(teleomorphs) which have non-branched spores adapted to wind dispersal (**Figure 5f**$_{1-3}$) unlike branched ones (**Figure 5f**$_4$). For example, studies on anamorph-teleomorph connections of Ingoldian hyphomycetes showed that the majority of species have evolved from ascomycetes in decaying tree branches in streams (Ranzoni, 1956; Webster and Descals, 1979, Marvanová, 1997; Sivichai and Jones, 2003). To date, however, this remains an untested hypothesis. To test this hypothesis, studies must collect air samples to ascertain the presence of non-branched spores of teleomorphs by a combination of microscopical and molecular techniques.

Sudheep and Sridhar (2010) suggest that the life cycle of these fungi alternates between aquatic and canopy habitats. Tropical areas, like the south-west coast of India, receives substantial rains during monsoon. Thus, occurrence of Ingoldian fungi in tree canopies is not surprising in these regions (Sridhar, 2009). One can speculate that the great quantity of rainfall in the monsoon season may create continuous aquatic habitats in canopies. Bandoni (1981) suspected that the conidia of fungi formed in tree canopies were directly transported to streams through stemflow, throughfall, or invertebrates (**Figure 5g**). Some evidence also suggests that Ingoldian hyphomycetes survive under terrestrial conditions due to their teleomorph states (Chauvet et al., 2016). It is also known that Ingoldian hyphomycetes can survive several of the environmental stresses likely experienced in tree canopies (e.g., pollution or water intermittency; Vass et al., 2013; Ghate and Sridhar, 2015b). Since these fungi are also common in trees of urban environments of polluted areas, further studies should be aimed to study the environmental role of these fungi in such habitats.

Observations and Hypotheses on Non-Ingoldian, "Dendronatant Fungi" in Stemflow

In our data synthesis (including new data), 19% of the total spore species are considered to be Ingoldian fungi (**Supplementary Table 1**). Stemflow is rich in numerous other, morphologically complex conidia that have not been connected to Ingoldian fungi (20% of the total spore species). These spores are hyaline/subhyaline stauro- and scolecospores (and some elongated phragmospores), apparently adapted to dispersal in stemflow. After their discovery, these conidia from non-Ingoldian, canopy-derived fungi were labeled with tentative names like "arboreal aquatic hyphomycetes" (Carroll, 1981) or "terrestrial aquatic hyphomycetes" (Ando, 1992), but these names appear to be inadequate (see Gönczöl and Révay, 2006). Another name, "canopy fungi" were also used for this group, however, this name, too, can be misleading as it may be thought to include foliar fungi non-adapted to stemflow dispersal, like conidia of powdery mildews and smuts. In the following parts, we refer to these fungi as a new paraphyletic group, using a name derived from the Greek "dendro" (for tree) and Latin "natant" (for swimming): "dendronatant fungi." Many studies

have reported the diversity and worldwide presence of conidia from dendronatant fungi in stemflow (MacKinnon, 1982; Ando and Tubaki, 1984a,b; Tubaki et al., 1985; Gönczöl and Révay, 2003, 2004, 2006; Magyar et al., 2005, 2016b; Sridhar et al., 2006; Karamchand and Sridhar, 2008; Sridhar, 2009; Sridhar and Karamchand, 2009; Révay and Gönczöl, 2010, 2011a,b; Sudheep and Sridhar, 2010). Note that some morphologically complex conidia that are not associated with dendronatant fungi have also been reported in stemflow (and bark), like helicosporous fungi, the most common of which include the Helicomyces anamorph of *Tubeufia palmarum*, *Helicomyces* and *Helicosporium* spp.

An intensive search for the source (i.e., sporulating colonies and habitats) of these dendronatant fungi, has resulted in the description of new species, while many others are still unknown, even in metropolitan environment (e.g., Sokolski et al., 2006; Magyar and Révay, 2008, 2009a,b; Magyar et al., 2017b,2018). The ecological role and the source of the conidia of these fungi remain incomplete (Révay and Gönczöl, 2010). Some of them seem to live endophytically in various plant tissues, for example, *Dwayaangam colodena* was proved to be an endophyte in canopy needles of black spruce (*Picea mariana*) needles (Sokolski et al., 2006; **Figure 5o**). Others may live in association with epiphytic ferns, bryophytes and lichens. For example, Sridhar et al. (2006) suggested that water-borne hyphomycetes exist in rhizomes of ferns as endophytes in tropical regions (**Figure 5i**). The majority of these dendronatant fungi species are probably saprotrophs inhabiting senescent or dead leaves trapped in the canopies, where tree holes (**Figure 5j**), junctions of branches (**Figure 5k**$_1$), and fissures of rough cortex of trunks (**Figure 5k**$_2$) serve as ephemeral aqueous microhabitats for these fungi (Magyar, 2008; Magyar et al., 2017b). These accumulation areas support many saprotrophic invertebrates on microliter and canopy soil, their parasites have also appeared here, like predacious fungi of amoebae, nematodes and rotifers. *Dwayaangam heterosporais* known to parasitize eggs of rotifers and nematodes (Barron, 1991). *Lecophagus vermicola* hunts nematodes applying an unusual strategy (Magyar et al., 2016a). Specifically, the fungus captures its nematode victims with adhesive knobs and colonizes its prey with a mycelium of rather broad hyphae on which, again, adhesive knobs are formed which penetrate the nematode's cuticule. As colonized nematodes form a cluster, they become a network enabling the capture of more prey. The fungus lives in the ephemerally aquatic habitat of bark fissures. Stemflow also provides water to the growth of bark-inhabiting fungi colonizing deeper areas of bark fissures, where their spores are present in large number (Magyar, 2008). *Camposporium cambrense* and *C. ontariense* are reported to grow and sporulate heavily on the bark cortex. *Arxiella terrestris, C. japonicum, C. pellucidum, Diplocladiella scalaroides, Endophragmiella taxi, Excipularia fusispora, Oncopodiella,* and *Triadelphia* spp. are primarily known as wood or leaf litter inhabiting fungi may also live on and derived from dead parts of the live trees (Gönczöl and Révay, 2004). It was suggested that many litter inhabiting fungi may colonize their substrates earlier than when the leaves reach the ground (Gönczöl and Révay, 2004).

Massive deposits of pollen grains and spores are found in bark fissures. Consequently, pollen and spore (or myco-) parasitic fungi sporulate here and rely on stemflow-transported spores to colonize new bark fissures. Branched conidia of pollen parasitising fungi (e.g., *Mycoceros* and *Retiarius* spp.) show an adaptation not only for dispersal in stemflow but also trapping pollen grains with specialized arms (Magyar et al., 2018). Most of these dendronatant fungi are little known and hardly studied owing to their sporulating colonies being hidden in bark fissures. Their colonies are tiny, being hardly visible even with the high magnification of stereomicroscopes (Magyar et al., 2018) and lack conidiophores or can be conspicuously micronematous (Ando and Kawamoto, 1986; Ando, 1992). Often identification is difficult or impossible with isolates in pure culture that fail to produce spores or identifiable structures. A special sampling method using adhesive, pressure-sensitive acrylic strips allows observation of sporulation and substrate preference (Magyar and Révay, 2009b) and has led to the discovery of a new habitat in accumulation areas of bark fissures (Magyar, 2008). Similarly, insertion of latex-smeared slides in the canopy junctions may also trap conidia flowing down the stem (Ghate and Sridhar, 2015a). For species that do not sporulate on artificial media, a method of DNA extraction from single conidia was developed as an alternative to perform phylogenetic research (Magyar et al., 2016a).

Finally, these dendronatant fungi seem to be adapted to this habitat, especially in microscale dispersal. Such spores are observed to reach and colonize new accumulation areas, i.e., another bark fissure on the host tree (Magyar, 2008). Since these fissures are found downstream of stemflow, spores tend to have shapes which allow anchoring (**Figure 7**). The K- or Y-shaped species (e.g., *Trinacrium* and *Retiarius*) or multiple, long arms (e.g., *Mycoceros, Dwayaangam*) seem to be a common, effective morphological feature to enable the anchoring of conidia carried by stemflow onto substrates (**Figure 7**)—which also may serve as food for the fungus (commonly microlitter, pollen or other fungi). Another adaptation of stemflow dispersal seems to be the development of protruding hyaline cells, or horns, on pigmented, multi-celled spores (*Excipularia, Oncopodium* and *Oncopodiella* spp., and *Rebentischia unicaudata*; Magyar and Révay, 2009b). Dendronatant fungi appear to have analogous or convergent evolutions as the Ingoldian hyphomycetes of streams, because they experience the same problem in running waters: spores are non-motile, and passive transport is dominated by rainwater flowing toward the soil (Chauvet et al., 2016). Colonization of stationary substrates in streams (litter and wood), and in stemflow (e.g., microlitter in accumulation areas) may help some species to overcome the risks of total removal and extinction due to unidirectional flow of water.

STEMFLOW'S HYPOTHETICAL IMPACT ON BARK FUNGAL COMMUNITY PATTERNS

Stemflow must interact with bark microhabitats as it drains to the surface and, as a result, may not only transport

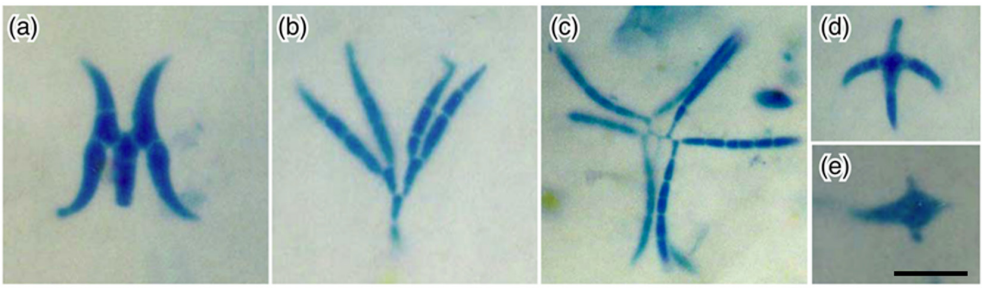

FIGURE 7 | Example conidia of water-borne hyphomycetes recovered from stemflow samples: **(a)** *Dwayangam cornuta*; **(b)** *D. dichotoma*; **(c)** *Dwayangam* sp.; **(d)** *Lemonniera cornuta*; **(e)** *Tumularia tuberculata* collected in India (credit: K. Sridhar). Scale bar = 20 μm.

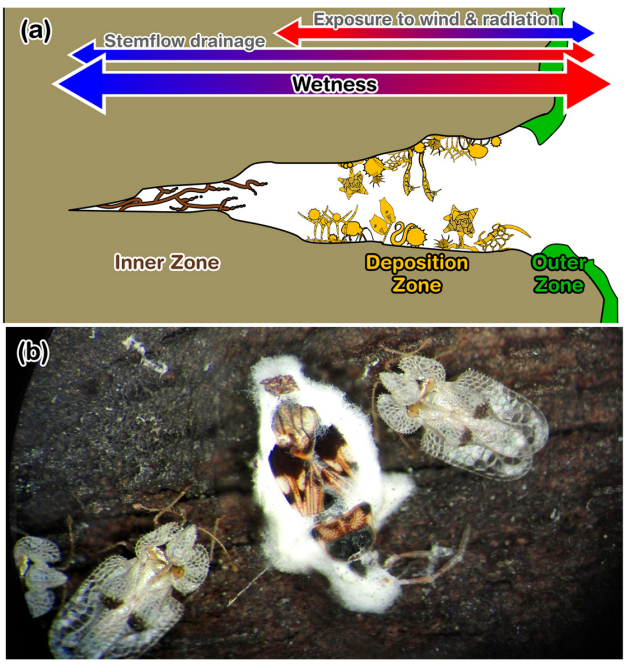

FIGURE 8 | (a) Zones of the bark microhabitat per Magyar (2008), their relative wetness (per stemflow and atmospheric exposure), and their observed microhabitat components. The outer zone consists of lichens, mossed and melanized fungal mycelia. Components of the deposition zone are diverse and abundant, like spores, pollen grains, dust, mites, nematodes and testate amoebae. The inner zone primarily hosted dematiaceous (or "black") fungi colonies. **(b)** Photograph showing example fungal infection of overwintering insects by bark fungi: *Beauveria* sp. on *Heteroptera* sp. and *Corythucha ciliata* on a *Platanus* tree in Budapest, Hungary (credit: D. Magyar).

conidia, but may hypothetically affect the bark reservoir's fungal community composition. Patterns of bark microhabitats and stemflow-related water processes hypothetically align (**Figure 8a**). Stemflow rivulets drain along the bark microrelief, tending to follow furrows (Tucker et al., 2020), especially if the bark is not particularly spongey (Brown and Barker, 1970; Van Stan and Levia, 2010). Stemflow water that saturates bark furrows may be better sheltered from evaporative drivers, like wind and radiation, than waters draining along bark ridges (**Figure 8a**), allowing bark moisture to persist for longer periods of time in bark furrows than on ridges (Young, 1937). These bark microhabitats collect substantial particulates, including conidia, as several hundreds of kilograms of dust per year may be captured from a canopy capable of scavenging 66–80% of atmospheric aerosols (Steubing and Kirschbaum, 1976). The total amount of dust ($PM_{2.5}$) removed annually by trees is enormous, varied from 4.7 tonnes in Syracuse (NY, United States) to 64.5 tonnes in Atlanta (GA, United States; Nowak et al., 2013).

There are many anemophilous fungal species (Ingold, 1971) which may be deposited on bark surfaces, whereafter their survival and reproduction may depend on microclimatological conditions, especially moisture conditions (Chauvet et al., 2016). Evidence that many scavenged aerosol fungi are unable to thrive on bark surfaces can be found through comparisons of conidia assemblages simultaneously collected from air and bark samples, which differ markedly (Magyar, 2008). In fact, common airborne fungi are rarely seen in stemflow (or throughfall; Gönczöl and Révay, 2004, 2006; Magyar et al., 2005). Thus, fungi community patterns throughout the bark microhabitat may be significantly influenced by interactions between the bark microclimate and its major moisture source, stemflow.

Along this hypothetical bark moisture gradient (**Figure 8a**), microhabitats have been previously described by Magyar (2008), where lichens, mosses and melanized fungal mycelia dominate the "outer zone" on the ridge, which transitions into a "deposition zone" hosting a large variety of captured aerosol particulates (including aerially-transported conidia and pollen) and small metazoans, until reaching an "inner zone" at the base of bark furrows dominated by large "black" (i.e., dematiaceous) fungi colonies (**Figure 8a**). Many of the fungal community members that reside among these bark microhabitats are rarely observed, as they cannot be detected using standard "washing and plating" techniques; however, understanding their ecological roles and environmental controls may yield insights into these communities' function. For example, are they pathogenic or do they support a healthy bark microbiome? Do fungal community members of the bark microbiome control invertebrate pests? Fungal epidemics of overwintering insects and nematodes by bark fungi are often observed (*Lecophagus, Dactylaria, Dactylellina,* and *Beauveria* spp.; e.g., **Figure 8b**). Are deep, moist bark fissure microhabitats shelters for many fungal species,

enabling survival during unfavorable conditions? Theoretically, stemflow not only has multiple fungal microhabitats with which it may interact, but stemflow dynamics themselves may influence bark fungal communities and their patterns.

CONCLUSION

Hypotheses Based on Available Data and Theory

The following hypotheses regarding stemflow conidia assemblages emerged from our analysis of published observations to date:

H1. Stemflow conidia concentrations are inversely related to the amount of rainfall that a tree drains as stemflow. This suggests that stemflow conidia concentrations are limited by the conidia "reservoir" on the bark surfaces over which stemflow drains. Future work may be merited on quantifying the size and dynamics of the bark conidia reservoir.

H2. Stemflow transports an ecologically and biogeochemically relevant amount of conidia ($>10^9$ ha^{-1} y^{-1}) to the localized soil areas at the base of individual trees. This suggests that stemflow conidia fluxes may represent "hot spots and moments" of fungal dispersal to litter, soil, and potentially root areas. Stemflow infiltration areas range from 10^{-1}–10^1 m^2 $tree^{-1}$ (Van Stan and Allen, 2020) and stemflow pulses have been found to influence litter layers (Tanaka et al., 1991; Iida et al., 2005; Rashid and Askari, 2014) and drain throughout habitats of the plant microbiome, including the rhizosphere and pedosphere (Van Stan et al., 2020b).

H3. Diversity of stemflow conidia assemblages increases with increasing stemflow generation. Available observations suggest that tree canopies which generally produce large amounts of stemflow, may host a greater diversity of fungal species adapted to stemflow dispersal. Such high conidial diversity in stemflow, however, may be time-dependent, as concentrations tend to be higher at the early minutes of the rain event for canopies with low flow resistance.

H4. Origins of conidia from Ingoldian and dendronatant fungi in stemflow can vary depending on multiple site-specific, species-specific and/or canopy structural properties, e.g.: (i) presence of aerosolized teleomorphs (Ranzoni, 1956; Webster and Descals, 1979, Marvanová, 1997; Sivichai and Jones, 2003), (ii) endophytes of leaves or epiphytes (Sokolski et al., 2006; Sridhar et al., 2006), (iii) birds that interact with marine and canopy environments (e.g., Vass, 2015), and (iv) saprotrophs inhabiting senescent or dead leaves trapped in the canopies (Magyar, 2008; Magyar et al., 2017a).

H5. Many dendronatant fungal species found in stemflow appear to be adapted to stemflow dispersal. Observations suggest that conidia of some species are produced, liberated and dispersed synchronously with rainfall events (MacKinnon, 1982). Some conidia also have unique structures (for example: K- and Y-forms; multiple long arms; protruding horn-like hyaline cells) that assist in film (i.e., stemflow) dispersal and anchoring in other canopy habitats (Bandoni and Koske, 1974; Magyar and Révay, 2009b; Chauvet et al., 2016).

H6. Stemflow-bark interactions may influence patterns in bark fungal community structure. This is based on comparing patterns of bark microhabitats (Magyar, 2008) and stemflow-related moisture/microclimatological processes (Tucker et al., 2020), which hypothetically align.

We reiterate that these are hypotheses based on the data available to date and remain to be tested. The available data underlying these hypotheses have several caveats (discussed throughout the preceding sections); however, we hope that these hypotheses will provide a framework for future work at the intersection of mycology and critical zone science in forests, especially during storms.

Frontiers at the Intersection of Bark, Stemflow and Fungi

Surprisingly, trees showing high fungal diversity were found in urban environments. It can be hypothesized that the canopy of urban trees are rich in different pollutants, used as nutrient source of fungi. Organic particles deposited on the canopy are washed off to the fissures, where bark inhabiting fungi digest them. Unlike trees, most fungi are not sensitive to urban stress (especially extremotolerant species). Traffic-related wounds, as well as air and soil pollution are major challenges to urban trees, but it is positive to opportunistic fungal pathogens. Low biodiversity of urban tree lines increases the risk of plant epidemics. As a result of globalization, new pests are introduced frequently. Some invasive insects produce honeydew on urban trees, where sooty molds develop in high quantities. Plant pathogenic fungi on trees, like *Schizophyllum commune* threaten susceptible tree taxa in the parks and streets (Vulinoviæ et al., 2019). On the other hand, non-pathogenic fungi form a protective layer on their aerial surfaces. Mycoparasitic, nematode-destroying and entomopathogenic fungi are common on the bark. A two-step self-cleaning mechanism may be functioning on trees. First, a physical clearing by water-repellent characteristic of leaf cuticle and the covering waxes. Surface particles are picked up by rolling water droplets and are thus easily cleaned off the surface. If a water droplet rolls across a contaminated leaf surface the adhesion between the particle, irrespective of its chemistry, and the droplet is higher than between the particle and the surface. Self-cleaning is the well-known prevention of contamination of the area of the phylloplane exposed to light resulting in reduced photosynthesis (Koch et al., 2008). The second step of self-cleaning is the "digestion" of organic particles by the fungus layer on the large surface area of the bark. It was observed that a mixed vegetation of *Pinus*, *Elaeagnus* and *Platanus* tree species results in the appearance of pollen-consuming microfungi. Pines provide nutrient-rich

pollen grains while *Elaeagnus* and *Platanus* bark offer suitable physical environment for fungal development (Magyar et al., 2017a). Airborne pollen therefore can may be reduced by planning green areas. Fungal diversity of urban trees may have many other unexplored uses. Stemflow-dispersed spores are also reported to be effective in biological control of insects. *Beauveria bassiana* is a common entomopathogenic hyphomycete that, when the aqueous suspension of this fungus (as a bioprotectant) sprayed onto trees to form stemflow, the treatment was as effective similar to chemical insecticides (Jakus and Blazenec, 2011). Thus, fundamental research on stemflow and its conidia may not only yield theoretical insights regarding ecohydrological and biogeochemical processes, it may yield practical insights and "myco-solutions" regarding tree health and management.

DATA AVAILABILITY STATEMENT

The original contributions presented in the study are included in the article/**Supplementary Material**, further inquiries can be directed to the corresponding author/s.

AUTHOR CONTRIBUTIONS

DM: conceptualization, supervision, writing—original draft preparation, photos, and spore identification. JV: conceptualization, statistical analysis, and writing—original draft preparation. KS: review, photos, and spore identification. All authors contributed to the article and approved the submitted version.

ACKNOWLEDGMENTS

The authors would like to thank János Gönczöl for his valuable comments.

SUPPLEMENTARY MATERIAL

The Supplementary Material for this article can be found online at: https://www.frontiersin.org/articles/10.3389/ffgc.2021.623758/full#supplementary-material

REFERENCES

Akinsoji, A. (1991). Studies on epiphytic flora of a tropical rain forest in southwestern Nigeria: II: bark microflora. *Vegetatio* 92, 181–185. doi: 10.1007/BF00032605

Ando, K. (1992). A study of terrestrial aquatic hyphomycetes. *Trans. Mycol. Soc. Jpn.* 33, 415–425.

Ando, K., and Kawamoto, I. (1986). Arborispora, a new genus of hyphomycetes. *Trans. Mycol. Soc. Jpn.* 27, 119–128.

Ando, K., and Tubaki, K. (1984a). Some undescribed hyphomycetes in the rain drops from intact leaf-surface. *Trans. Mycol. Soc. Jpn.* 25, 21–37.

Ando, K., and Tubaki, K. (1984b). Some undescribed hyphomycetes in the rain water draining from intact trees. *Trans. Mycol. Soc. Jpn.* 25, 39–47.

André, F., Jonard, M., and Ponette, Q. (2008). Influence of species and rain event characteristics on stemflow volume in a temperate mixed oak–beech stand. *Hydrol. Process. Int. J.* 22, 4455–4466. doi: 10.1002/hyp.7048

Aung, K., Jiang, Y., and He, S. Y. (2018). The role of water in plant–microbe interactions. *Plant J.* 93, 771–780. doi: 10.1111/tpj.13795

Backnäs, S., Laine-Kaulio, H., and Kløve, B. (2012). Phosphorus forms and related soil chemistry in preferential flowpaths and the soil matrix of a forested podzolic till soil profile. *Geoderma* 189, 50–64. doi: 10.1016/j.geoderma.2012.04.016

Baldrian, P. (2017). Forest microbiome: diversity, complexity and dynamics. *FEMS Microbiol. Rev.* 41, 109–130.

Bandoni, R. J. (1981). "Aquatic hyphomycetes from terrestrial litter," in *The Fungal Community, Its Organization and Role in The Ecosystem*, eds D. T. Wicklow and G. C. Carroll (New York, NY: Marcel Dekker), 693–708.

Bandoni, R. J., and Koske, R. E. (1974). Monolayers and microbial dispersal. *Science* 183, 1079–1081. doi: 10.1126/science.183.4129.1079

Bärlocher, F. (2020). "Sporulation by aquatic hyphomycetes," in *Methods to Study Litter Decomposition*, eds F. Bärlocher, M. Gessner, and M. Graça (Cham: Springer). doi: 10.1007/978-3-030-30515-4

Barron, G. L. (1991). A new species of Dwayaangam parasitic on eggs of rotifers and nematodes. *Can. J. Bot.* 69, 1402–1406. doi: 10.1139/b91-180

Belliveau, M. J.-R., and Bärlocher, F. (2005). Molecular evidence confirms multiple origins of aquatic hyphomycetes. *Mycol. Res.* 109, 1407–1417. doi: 10.1017/s0953756205004119

Bittar, T. B., Pound, P., Whitetree, A., Moore, L. D., and Van Stan, J. T. (2018). Estimation of throughfall and stemflow bacterial flux in a subtropical oak-cedar forest. *Geophys. Res. Lett.* 45, 1410–1418. doi: 10.1002/2017gl075827

Brown, J. H. Jr., and Barker, A. C. Jr. (1970). An analysis of throughfall and stemflow in mixed oak stands. *Water Resourc. Res.* 6, 316–323. doi: 10.1029/wr006i001p00316

Bruijnzeel, L. A., Sampurno, S. P., and Wiersum, K. F. (1987). Rainfall interception by a young *Acacia auriculiformis* (A. Cunn) plantation forest in West Java, Indonesia: application of Gash's analytical model. *Hydrol. Process.* 1, 309–319. doi: 10.1002/hyp.3360010402

Calhim, S., Halme, P., Petersen, J. H., Læssøe, T., Bässler, C., and Heilmann-Clausen, J. (2018). Fungal spore diversity reflects substrate-specific deposition challenges. *Sci. Rep.* 8:5356. doi: 10.1038/s41598-018-23292-8

Campellone, S. V. (2018). *An Investigation into the Factors Affecting Street Tree Rainfall Interception*. Masters Thesis. Philadelphia, PA: Drexel University.

Cape, J. N., Brown, A. H. F., Robertson, S. M. C., Howson, G., and Paterson, I. S. (1991). Interspecies comparisons of throughfall and stemflow at three sites in northern Britain. *For. Ecol. Manag.* 46, 165–177. doi: 10.1016/0378-1127(91)90229-o

Carpenter, S. R. (1982). Stemflow chemistry: effects on population dynamics of detritivorous mosquitoes in tree-hole ecosystems. *Oecologia* 53, 1–6. doi: 10.1007/bf00377128

Carroll, G. C. (1981). *Mycological Inputs to Ecosystems Analysis. The Fungal Community: Its Organization and Role in the Ecosystem*. New York, NY: Marcel Dekker, 557–580.

Chauvet, E., Cornut, J., Sridhar, K. R., Selosse, M. A., and Bärlocher, F. (2016). Beyond the water column: aquatic hyphomycetes outside their preferred habitat. *Fungal Ecol.* 19, 112–127. doi: 10.1016/j.funeco.2015.05.014

Cheng, J. D., Lin, J. P., Lu, S. Y., Huang, L. S., and Wu, H. L. (2008). Hydrological characteristics of betel nut plantations on slopelands in central Taiwan. *Hydrol. Sci. J.* 53, 1208–1220. doi: 10.1623/hysj.53.6.1208

Czeczuga, B., and Orłowska, M. (1999). Hyphomycetes in rainwater, melting snow and ice. *Acta Mycol.* 34, 181–200. doi: 10.5586/am.1999.014

D'Amico, V., and Elkinton, J. S. (1995). Rainfall effects on transmission of gypsy moth (Lepidopter a: Lymantriidae) nuclear polyhedrosis virus. *Environ. Entomol.* 24, 1144–1149. doi: 10.1093/ee/24.5.1144

Dhami, M. K., Weir, B. S., Taylor, M. W., and Beggs, J. R. (2013). Diverse honeydew-consuming fungal communities associated with scale insects. *PLoS One* 8:e70316. doi: 10.1371/journal.pone.0070316

Ellis, M. B., and Ellis, J. P. (1997). *Microfungi on Land Plants – An Identification Handbook*. London: Croom Helm.

Elsner, G. (2012). *Wimmerwuchs an Buche (Fagus sylvatica)*. Available online at: https://commons.wikimedia.org/wiki/File:Wimmerwuchs.jpg (accessed on 26 May 2020).

Erdtmann, H. (1952). "Phenolic and other extraneous components of coniferous heartwoods; their relation to taxonomy," in *Wood Chemistry*, Vol. 1, eds L. E. Wise and E. C. Jahn (New York, NY: Reinhold), 661–688.

Findlay, S. E. G., and Arsuffi, T. L. (1989). Microbial growth and detritus transformations during decomposition of leaf litter in a stream. *Freshw. Biol.* 21, 261–269. doi: 10.1111/j.1365-2427.1989.tb01364.x

Frangi, J. L., and Lugo, A. E. (1985). Ecosystem dynamics of a subtropical floodplain forest. *Ecol. Monogr.* 55, 351–369. doi: 10.2307/1942582

Friesen, J. (2020). "Flow pathways of throughfall and stemflow through the subsurface," in *Precipitation Partitioning by Vegetation*, eds J. T. Van Stan, E. Gutmann, and J. Friesen (Cham: Springer), 215–228. doi: 10.1007/978-3-030-29702-2_13

Germer, S., Werther, L., and Elsenbeer, H. (2010). Have we underestimated stemflow? Lessons from an open tropical rainforest. *J. Hydrol.* 395, 169–179. doi: 10.1016/j.jhydrol.2010.10.022

Ghate, S. D., and Sridhar, K. R. (2015a). A new technique to monitor conidia of aquatic hyphomycetes in streams using latex-coated slides. *Mycology* 6, 161–167. doi: 10.1080/21501203.2015.1110209

Ghate, S. D., and Sridhar, K. R. (2015b). Diversity of aquatic hyphomycetes in sediments of temporary streamlets of Southwest India. *Fungal Ecol.* 14, 53–61. doi: 10.1016/j.funeco.2014.11.005

Ghate, S. D., and Sridhar, K. R. (2015c). Rain-borne fungi in stemflow and throughfall of six tropical palm species. *Czech Mycol.* 67, 45–58.

Giacomin, A., and Trucchi, P. (1992). Rainfall interception in a beech coppice (Acquerino, Italy). *J. Hydrol.* 137, 141–147. doi: 10.1016/0022-1694(92)90052-w

Gmihail. (2014). *Acer Platanoides Bark*. Available online at: https://commons.wikimedia.org/wiki/File:Acer_platanoides_bark_Bgd.jpg (accessed on 1 October 2020).

Gönczöl, J. (1976). Ecological observations on the aquatic hyphomycetes of Hungary II. *Acta Bot. Acad. Scient. Hungar.* 22, 51–60.

Gönczöl, J., and Révay, Á (2003). Treehole fungal communities: aquatic, aero-aquatic and dematiaceous hyphomycetes. *Fungal Divers.* 12, 19–34. doi: 10.1016/j.fbr.2007.02.003

Gönczöl, J., and Révay, Á (2004). Fungal spores in rainwater: stemflow, throughfall and gutter conidial assemblages. *Fungal Divers.* 16, 67–86.

Gönczöl, J., and Révay, Á (2006). Species diversity of rainborne hyphomycete conidia from living trees. *Fungal Divers.* 22, 37–54.

Guevara-Escobar, A., González-Sosa, E., Véliz-Chávez, C., Ventura-Ramos, E., and Ramos-Salinas, M. (2007). Rainfall interception and distribution patterns of gross precipitation around an isolated *Ficus benjamina* tree in an urban area. *J. Hydrol.* 333, 532–541. doi: 10.1016/j.jhydrol.2006.09.017

Gulis, V., Marvanová, L., and Descals, E. (2007). "An illustrated key to the common temperate species of aquatic hyphomycetes," in *Methods to Study Litter Decomposition: A Practical Guide*, eds M. A. S. Graça, F. Bärlocher, and M. O. Gessner (Dordrecht: Springer), 153–168. doi: 10.1007/1-4020-3466-0_21

Gunasekera, S. A., and Webster, J. (1983). Inhibitors of aquatic and aero-aquatic hyphomycetes in pine and oak wood. *Trans. Br. Mycol. Soc.* 80, 121–125. doi: 10.1016/s0007-1536(83)80172-7

Hanfmampf. (2008). *Culm of Phyllostachys vivax f. Aureocaulis*. Available online at: https://commons.wikimedia.org/wiki/File:Phyllostachys_vivax_Aureocaulis_culm.JPG (accessed on 26 May 2020).

Havelaar, A. (2020). *Stock Photo - Abstract Pattern of Bark on Tiliacordata or Small Leaved Linden*. Malaysia: 123RF.

Hughes, S. J. (1958). Revisiones Hyphomycetum aliquot cum appendice de nominibus rejiciendis. *Can. J. Bot.* 36, 727–836. doi: 10.1139/b58-067

Iida, S., Kakubari, J., and Tanaka, T. (2005). "Litter marks" indicating infiltration area of stemflow-induced water. *Tsukuba Geoenviron. Sci* 1, 27–31.

Imamura, N., Levia, D. F., Toriyama, J., Kobayashi, M., and Nanko, K. (2017). Stemflow-induced spatial heterogeneity of radiocesium concentrations and stocks in the soil of a broadleaved deciduous forest. *Sci. Total Environ.* 599, 1013–1021. doi: 10.1016/j.scitotenv.2017.05.017

Ingold, C. T. (1942). Aquatic hyphomycetes of decaying alder leaves. *Trans. Br. Mycol. Soc.* 25, 339–417. doi: 10.1016/s0007-1536(42)80001-7

Ingold, C. T. (1953). *Dispersal in Fungi*. Oxford: Claredon Press. doi: 10.1097/00010694-195311000-00014

Ingold, C. T. (1966). The tetraradiate aquatic fungal spore. *Mycologia* 58, 43–56. doi: 10.2307/3756987

Ingold, C. T. (1971). *Fungal Spores, Their Liberation and Dispersal*. Oxford: Clarendon Press.

Ingold, C. T. (1975). An illustrated guide to aquatic and water-borne hyphomycetes (Fungi Imperfecti) with notes on their biology. *Freshw. Biol. Assoc. Sci. Publ.* 30, 1–96.

Jakus, R., and Blazenec, M. (2011). Treatment of bark beetle attacked trees with entomopathogenic fungus *Beauveria bassiana* (Balsamo) Vuillemin. *Folia For. Polon. Ser. A For.* 53, 150–155.

Johnson, M. S., and Jost, G. (2011). "Ecohydrology and biogeochemistry of the rhizosphere in forested ecosystems," in *Forest hydrology and Biogeochemistry*, eds D. Levia, D. Carlyle-Moses, and T. Tanaka (Dordrecht: Springer), 483–498. doi: 10.1007/978-94-007-1363-5_24

Karamchand, K. S., and Sridhar, K. R. (2008). Water-borne conidial fungi inhabiting tree holes of the west coast and Western Ghats of India. *Czech Mycol.* 60, 63–74. doi: 10.33585/cmy.60105

Kendrick, B. (1990). "Fungal allergens," in *Sampling and Identifying Allergenic Pollens and Moulds*, ed. E. G. Smith (San Antonio, TX: Blewstone Press), 41–165.

Klučiarová, D., Márton, P., Pichler, V., Márton, E., and Túnyi, I. (2008). Pollution detection by magnetic susceptibility measurements aided by the stemflow effect. *Water Air Soil Pollut.* 189, 213–223. doi: 10.1007/s11270-007-9569-8

Koch, K., Bhushan, B., and Barthlott, W. (2008). Diversity of structure, morphology and wetting of plant surfaces. *Soft Matter* 4, 1943–1963. doi: 10.1039/b804854a

Krämer, I., and Hölscher, D. (2009). Rainfall partitioning along a tree diversity gradient in a deciduous old-growth forest in Central Germany. *Ecohydrology* 2, 102–114. doi: 10.1002/eco.44

Kwiecień, A. (2005). *Piceaabies Bark, Poland, Near Wrocław*. Available online at: https://commons.wikimedia.org/wiki/File:Picea_abies_bark.jpg (accessed on 26 May 2020).

Lambais, M. R., Lucheta, A. R., and Crowley, D. E. (2014). Bacterial community assemblages associated with the phyllosphere, dermosphere, and rhizosphere of tree species of the Atlantic forest are host taxon dependent. *Microb. Ecol.* 68, 567–574. doi: 10.1007/s00248-014-0433-2

Lefnaer, S. (2016). *Quercus cerris SL2*. Available online at: https://commons.wikimedia.org/wiki/File:Quercus_cerris_sl2.jpg (accessed on 26 May 2020).

Levia, D. F., and Germer, S. (2015). A review of stemflow generation dynamics and stemflow-environment interactions in forests and shrublands. *Rev. Geophys.* 53, 673–714. doi: 10.1002/2015rg000479

Levia, D. F., Van Stan, J. T., Siegert, C. M., Inamdar, S. P., Mitchell, M. J., Mage, S. M., et al. (2011). Atmospheric deposition and corresponding variability of stemflow chemistry across temporal scales in a mid-Atlantic broadleaved deciduous forest. *Atmos. Environ.* 45, 3046–3054. doi: 10.1016/j.atmosenv.2011.03.022

Louveaux, J., Maurizio, A., and Vorwohl, G. (1978). Methods of melissopalynology. *Bee World* 59, 139–157. doi: 10.1080/0005772x.1978.11097714

MacKinnon, J. A. (1982). *Stemflow and Throughfall Mycobiota of a Trembling Aspen-Red Alder Forest*. Doctoral dissertation. Vancouver, BC: University of British Columbia.

Madden, L. V. (1992). Rainfall and the dispersal of fungal spores. *Adv. Plant Pathol.* 8, 39–79.

Magliano, P. N., Whitworth-Hulse, J. I., and Baldi, G. (2019). Interception, throughfall and stemflow partition in drylands: global synthesis and meta-analysis. *J. Hydrol.* 568, 638–645. doi: 10.1016/j.jhydrol.2018.10.042

Magyar, D. (2007). "Aeromycological aspects of mycotechnology," in *Mycotechnology: Current Trends and Future Prospects*, ed. M. K. Rai (New Delhi: I.K. International Publishing House), 226–263.

Magyar, D. (2008). The tree bark: a natural spore trap. *Asp. Appl. Biol.* 89, 7–16.

Magyar, D., and Révay, Á (2008). *Trinaciumtothii* spec. nov. (Hyphomycetes) from the cortex of living tree. *Nova Hedwigia* 87, 513–519. doi: 10.1127/0029-5035/2008/0087-0513

Magyar, D., and Révay, Á (2009a). New species of Oncopodiella (Hyphomycetes) from living trees. *Nova Hedwigia* 88, 169–182. doi: 10.1127/0029-5035/2009/0088-0169

Magyar, D., and Révay, Á (2009b). *Oncopodium elaeagni*, a new hyphomycete from Hungary. *Nova Hedwigia* 88, 475–481. doi: 10.1127/0029-5035/2009/0088-0475

Magyar, D., Gönczöl, J., Révay, Á, Grillenzoni, F., and Seijo-Coello, M. D. C. (2005). Stauro- and scolecoconidia in floral and honeydew honeys. *Fungal Divers.* 20, 103–120.

Magyar, D., Merényi, Z., Bratek, Z., Baral, H.-O., and Marson, G. (2016a). *Lecophagus vermicola* sp. nov., a nematophagous hyphomycete with an unusual hunting strategy. *Mycol. Progress* 15, 1137–1144. doi: 10.1007/s11557-016-1235-3

Magyar, D., Merényi, Z., Körmöczi, P., Bratek, Z., and Kredics, L. (2017a). Phylogenetic analysis and description of two new species of pollen-parasitic Retiarius (anamorphic Orbiliomycetes). *Nova Hedwigia* 105, 411–423. doi: 10.1127/nova_hedwigia/2017/0420

Magyar, D., Merényi, Z., Udvardy, O., Kajtor-Apatini, D., Körmöczi, P., Fülöp, A., et al. (2018). *Mycoceros antennatissimus* gen. et sp. nov.: a mitosporic fungus capturing pollen grains. *Mycol. Progress* 17, 33–43. doi: 10.1007/s11557-017-1275-3

Magyar, D., Mura-Mészáros, A., and Grillenzoni, F. (2016b). Fungal diversity in floral and honeydew honeys. *Acta Bot. Hungar.* 58, 145–166. doi: 10.1556/034.58.2016.1-2.6

Magyar, D., Vass, M., and Oros, G. (2017b). Dendrotelmata (water-filled tree holes) as fungal hotspots-a long term study. *Crypt. Mycol.* 38, 55–66. doi: 10.7872/crym/v38.iss1.2017.55

Mali, S. S., Sarkar, P. K., Naik, S. K., Singh, A. K., and Bhatt, B. P. (2020). Predictive models for stemflow and throughfall estimation in four fruit tree species under hot and sub-humid climatic region. *Hydrol. Res.* 51, 47–64. doi: 10.2166/nh.2019.052

Marvanová, L. (1997). "Freshwater hyphomycetes: a survey with remarks on tropical taxa," in *Tropical Mycology*, eds K. K. Janardhanan, C. Rajendran, K. Natarajan, and D. L. Hawksworth (New York, NY: Science Publishers), 169–226.

McPherson, J. R. (2018). *Eucalyptus grandis, The Flooded Gum or Rose Gum, Has a Few Ornamentally Planted Specimens in 7th Brigade Park*. Available online at: https://commons.wikimedia.org/wiki/File:Eucalyptus_grandis_stem_flow_lines_7th_Brigade_Park_Chermside_L1100312.jpg (accessed on 1 October 2020).

Mella, V. S., Orr, C., Hall, L., Velasco, S., and Madani, G. (2020). An insight into natural koala drinking behaviour. *Ethology* 126, 858–863. doi: 10.1111/eth.13032

Mendieta-Leiva, G., Porada, P., and Bader, M. Y. (2020). "Interactions of epiphytes with precipitation partitioning," in *Precipitation Partitioning by Vegetation*, eds J. Van Stan II, E. Gutmann, and J. Friesen (Cham: Springer), 133–146. doi: 10.1007/978-3-030-29702-2_9

Miller, W. B., Peralta, E., Ellis, D. R., and Perkins, H. H. Jr. (1994). Stickiness potential of individual insect honeydew carbohydrates on cotton lint. *Text. Res. J.* 64, 344–350. doi: 10.1177/004051759406400606

Mitscherlich, G. (1981). *Wald, Wachstum und Umwelt. 2. Band: Waldklima und Wasserhaushalt*. Frankfurt am Main: Sauerländer's Verlag.

Mosello, R., Brizzio, C. R., Kotzias, D., Marchetto, A., Rembges, D., and Tartari, G. (2002). The chemistry of atmospheric deposition in Italy in the framework of the National Programme for Forest Ecosystems Control (CONECOFOR). *J. Limnol.* 61, 77–92. doi: 10.4081/jlimnol.2002.s1.77

Ndakara, O. E. (2012). Biogeochemical consequences of hydrologic conditions in isolated stands of terminalia cattapa in the rainforest zone of Southern Nigeria. *Spec. Publ. Niger. Assoc. Hydrol. Sci.* 1, 134–144. doi: 10.4314/ejesm.v5i1.1

Ndakara, O. E. (2016). Hydrological nutrient flux in isolated exotic stands of *Mangifera Indica* Linn: implications for sustainable rainforest ecosystem management in South-Southern Nigeria. *Niger. J. Sci. Environ.* 14, 125–131.

Nizinski, J. J., Galat, G., and Galat-Luong, A. (2011). Water balance and sustainability of eucalyptus plantations in the Kouilou basin (Congo-Brazzaville). *Russ. J. Ecol.* 42, 305–314. doi: 10.1134/s1067413611040126

Nowak, D. J., Hirabayashi, S., Bodine, A., and Hoehn, R. (2013). Modeled PM2. 5 removal by trees in ten US cities and associated health effects. *Environ. Pollut.* 178, 395–402. doi: 10.1016/j.envpol.2013.03.050

Peck, A. K. (2004). *Hydrometeorologische und Mikroklimatische Kennzeichen von Buchenwäldern*. PhD thesis. Freiburg im Breisgau: University of Freiburg.

Ponette-González, A. G., Van Stan, J. T., and Magyar, D. (2020). "Things seen and unseen in throughfall and stemflow," in *Precipitation Partitioning by Vegetation*, eds J. Van Stan II, E. Gutmann, and J. Friesen (Cham: Springer), 71–88. doi: 10.1007/978-3-030-29702-2_5

Proctor, H. C., Montgomery, K. M., Rosen, K. E., and Kitching, R. L. (2002). Are tree trunks habitats or highways? A comparison of oribatid mite assemblages from hoop-pine bark and litter. *Austr. J. Entomol.* 41, 294–299. doi: 10.1046/j.1440-6055.2002.00309.x

Ptatscheck, C., Milne, P. C., and Traunspurger, W. (2018). Is stemflow a vector for the transport of small metazoans from tree surfaces down to soil? *BMC Ecol.* 18:43. doi: 10.1186/s12898-018-0198-4

Pypker, T. G., Levia, D. F., Staelens, J., and Van Stan, J. T. (2011). "Canopy structure in relation to hydrological and biogeochemical fluxes," in *Forest Hydrology and Biogeochemistry*, eds D. Levia, D. Carlyle-Moses, and T. Tanaka (Dordrecht: Springer), 371–388. doi: 10.1007/978-94-007-1363-5_18

Ranzoni, F. V. (1956). The perfect state of Flagellosporapenicillioides. *Am. J. Bot.* 43, 13–17. doi: 10.1002/j.1537-2197.1956.tb10456.x

Rashid, N. S. A., and Askari, M. (2014). ""Litter marks" around oil palm tree base indicating infiltration area of stemflow-induced water," in *Proceedings of the National Seminar on Civil Engineering Research*, Johor Bahru.

Ray, M. P. (1970). Preliminary observations on stem-flow, etc., in *Alstonia scholaris* and *Shorea robusta* plantations at Arabari, West Bengal. *Indian For.* 96, 482–493.

Révay, Á, and Gönczöl, J. (2010). Rainborne hyphomycete conidia from evergreen trees. *Nova Hedwigia* 91, 151–163. doi: 10.1127/0029-5035/2010/0091-0151

Révay, Á, and Gönczöl, J. (2011a). Aquatic hyphomycetes and other water-borne fungi in Hungary. *Czech Mycol.* 63, 133–151. doi: 10.33585/cmy.63203

Révay, Á, and Gönczöl, J. (2011b). Canopy fungi ("terrestrial aquatic hyphomycetes") from twigs of living evergreen and deciduous trees in Hungary. *Nova Hedwigia* 92, 303–316. doi: 10.1127/0029-5035/2011/0092-0303

Rosier, C. L., Moore, L. D., Wu, T., and Van Stan, J. T. (2015). Forest canopy precipitation partitioning: an important plant trait Influencing the spatial structure of the symbiotic soil microbial community. *Adv. Bot. Res.* 75, 215–240. doi: 10.1016/bs.abr.2015.09.005

Sadeghi, S. M. M., Gordon, D. A., and Van Stan, J. T. II (2020). "A global synthesis of throughfall and stemflow hydrometeorology," in *Precipitation Partitioning by Vegetation*, eds J. Van Stan II, E. Gutmann, and J. Friesen (Cham: Springer), 49–70. doi: 10.1007/978-3-030-29702-2_4

Sahu, M. L., Seth, N. K., and Upadhyaya, D. (2006). Exploratory studies on rainfall partitioning in block plantations of social forestry trees in central India. *J. Trop. For.* 22, 12–15.

Salemi, L. F. (2019). Turning rain into internal precipitation and stemflow: observations of palm trees in a urban environment. *Cerrado Agroc. Rev. Centre Univ. Pato de Minas* 10, 45–50. doi: 10.33585/cmy.67106

Salicyna. (2017). *Metasequoia Glyptostroboides, Marszewo Forest*. Available online at: https://commons.wikimedia.org/wiki/File:Metasequoia_glyptostroboides_2017-05-16_0376.jpg (accessed on 26 May 2020).

Sansalone, J. J., and Cristina, C. M. (2004). First flush concepts for suspended and dissolved solids in small impervious watersheds. *J. Environ. Eng.* 130, 1301–1314. doi: 10.1061/(asce)0733-9372(2004)130:11(1301)

Scheffer, T. C., and Cowling, E. B. (1966). Natural resistance of wood to microbial deterioration. *Ann. Rev. Phytopathol.* 4, 147–170. doi: 10.1146/annurev.py.04.090166.001051

Schooling, J. T., and Carlyle-Moses, D. E. (2015). The influence of rainfall depth class and deciduous tree traits on stemflow production in an urban park. *Urban Ecosyst.* 18, 1261–1284. doi: 10.1007/s11252-015-0441-0

Selosse, M., Vohník, M., and Chauvet, E. (2008). Out of the rivers: are some aquatic hyphomycetes plant endophytes? *New Phytol.* 178, 3–7. doi: 10.1111/j.1469-8137.2008.02390.x

Serrano, R. C. (1982). *Hydrology of Different Coconut (Cocos nucifera L.)-based agroecosystems*. Los Baños: University of the Philippines.

Shaaban, B., Seeburger, V., Schroeder, A., and Lohaus, G. (2020). Sugar, amino acid and inorganic ion profiling of the honeydew from different hemipteran species feeding on Abies alba and Piceaabies. *PLoS One* 15:e0228171. doi: 10.1371/journal.pone.0228171

Sivichai, S., and Jones, E. B. G. (2003). "Teleomorphic-anamorphic connections of freshwater fungi," in *Freshwater Mycology. Fungal Diversity Series*, eds C. K. M. Tsui and K. D. Hyde (Ottawa: National Museum of Sciences), 259–274.

Sokolski, S., Piché, Y., Chauvet, E., and Bérubé, J. A. (2006). A fungal endophyte of black spruce (*Picea mariana*) needles is also an aquatic hyphomycete. *Mol. Ecol.* 15, 1955–1962. doi: 10.1111/j.1365-294x.2006.02909.x

Sridhar, K. R. (2009). *Fungi in the Tree Canopy–An Appraisal. Applied Mycology*. Wallingford: CAB International, 73–91. doi: 10.1079/9781845935344.0073

Sridhar, K. R., and Bärlocher, F. (1993). Aquatic hyphomycetes on leaf litter in and near a stream in Nova Scotia, Canada. *Mycol. Res.* 97, 1530–1535. doi: 10.1016/s0953-7562(09)80229-3

Sridhar, K. R., and Karamchand, K. S. (2009). Diversity of water-borne fungi in stemflow and throughfall of tree canopies in India. *Sydowia* 61, 327–344.

Sridhar, K. R., Karamchand, K. S., and Bhat, R. (2006). Arboreal water-borne hyphomycetes on oak-leaf basket fern *Drynaria quercifolia*. *Sydowia-Horn-* 58, 309–320.

Sridhar, K. R., Nagesh, H., and Sharathchandra, K. (2020). Assemblage and diversity of asexual fungi in 10 terrestrial damp leaf litters: comparison of two incubation techniques. *Asian J. Mycol.* 3, 362–375. doi: 10.5943/ajom/3/1/10

Starr, K., and Starr, F. (2009). *Coccothrinaxbarbadensis Bark at Kahului, Maui, Hawaii*. Available online at: https://commons.wikimedia.org/wiki/File:Starr-090806-4046-Coccothrinax_barbadensis-bark-Kahului-Maui_(24344960903).jpg (accessed on 26 May 26 2020).

Steubing, L., and Kirschbaum, U. (1976). Immissionsbelastung der Strassenrandvegetation. *Nat. Landschaft.* 51, 239–244.

Stubbins, A., Guillemette, F., and Van Stan, J. T. (2020). "Throughfall and stemflow: the crowning headwaters of the aquatic carbon cycle," in *Precipitation Partitioning by Vegetation*, eds J. Van Stan II, E. Gutmann, and J. Friesen (Cham: Springer), 121–132. doi: 10.1007/978-3-030-29702-2_8

Sudheep, N. M., and Sridhar, K. R. (2010). Water-borne hyphomycetes in tree canopies of Kaiga (Western Ghats), India. *Acta Mycol.* 45, 185–195. doi: 10.5586/am.2010.024

Suzuki, K. (2006). Characterisation of airborne particulates and associated trace metals deposited on tree bark by ICP-OES, ICP-MS, SEM-EDX and laser ablation ICP-MS. *Atmos. Environ.* 40, 2626–2634. doi: 10.1016/j.atmosenv.2005.12.022

Tanaka, N., Levia, D., Igarashi, Y., Yoshifuji, N., Tanaka, K., Tantasirin, C., et al. (2017). What factors are most influential in governing stemflow production from plantation-grown teak trees? *J. Hydrol.* 544, 10–20. doi: 10.1016/j.jhydrol.2016.11.010

Tanaka, T., Tsujimura, M., and Taniguchi, M. (1991). "Infiltration area of stemflow-induced water," in *Annual Report-Institute of Geoscience* (Tsukuba: University of Tsukuba), 30–32.

Tischer, A., Michalzik, B., and Lotze, R. (2020). Nonuniform but highly preferential stemflow routing along bark surfaces and actual smaller infiltration areas than previously assumed: a case study on European beech (*Fagus sylvatica* L.) and sycamore maple (*Acer pseudoplatanus* L.). *Ecohydrology* 13:e2230. doi: 10.1002/eco.2230

Tubaki, K., Tokumasu, S., and Anclo, K. (1985). Morning dew and Tripospermum (Hyphomycetes). *Bot. J. Linnean Soc.* 91, 45–50. doi: 10.1111/j.1095-8339.1985.tb01133.x

Tucker, A., Levia, D. F., Katul, G. G., Nanko, K., and Rossi, L. F. (2020). A network model for stemflow solute transport. *Appl. Math. Model.* 88, 266–282. doi: 10.1016/j.apm.2020.06.047

Uroz, S., Buee, M., Deveau, A., Mieszkin, S., and Martin, F. (2016). Ecology of the forest microbiome: highlights of temperate and boreal ecosystems. *Soil Biol. Biochem.* 103, 471–488. doi: 10.1016/j.soilbio.2016.09.006

Valová, M., and Bieleszová, S. (2008). Interspecific variations of bark's water storage capacity of chosen types of trees and the dependence on occurrence of epiphytic mosses. *GeoSci. Eng.* 54, 45–51.

Van Stan, J. T., and Allen, S. T. (2020). What we know about stemflow's infiltration area. *Front. For. Glob. Change* 3:61. doi: 10.3389/ffgc.2020.00061

Van Stan, J. T., and Gordon, D. A. (2018). Mini-review: stemflow as a resource limitation to near-stem soils. *Front. Plant Sci.* 9:248. doi: 10.3389/fpls.2018.00248

Van Stan, J. T., and Levia, D. F. (2010). Inter-and intraspecific variation of stemflow production from Fagus grandifoliaEhrh.(American beech) and *Liriodendron tulipifera* L.(yellow poplar) in relation to bark microrelief in the eastern United States. *Ecohydrology* 3, 11–19. doi: 10.1002/eco.83

Van Stan, J. T., Hildebrandt, A., Friesen, J., Metzger, J. C., and Yankine, S. A. (2020a). "Spatial variability and temporal stability of local net precipitation patterns," in *Precipitation Partitioning by Vegetation*, eds J. Van Stan II, E. Gutmann, and J. Friesen (Cham: Springer), 89–104. doi: 10.1007/978-3-030-29702-2_6

Van Stan, J. T., Lewis, E. S., Hildebrandt, A., Rebmann, C., and Friesen, J. (2016). Impact of interacting bark structure and rainfall conditions on stemflow variability in a temperate beech-oak forest, central Germany. *Hydrol. Sci. J.* 61, 2071–2083. doi: 10.1080/02626667.2015.1083104

Van Stan, J. T., Morris, C. E., Aung, K., Kuzyakov, Y., Magyar, D., Rebollar, E. A., et al. (2020b). "Precipitation partitioning—hydrologic highways between microbial communities of the plant microbiome?," in *Precipitation Partitioning by Vegetation*, eds J. Van Stan II, E. Gutmann, and J. Friesen (Cham: Springer), 229–252. doi: 10.1007/978-3-030-29702-2_14

Van Stan, J. T., Ponette-Gonzalez, A. G., Swanson, T., and Weathers, K. C. (2021). Concepts and questions: throughfall and stemflow are major hydrologic highways for particulate traffic through tree canopies. *Front. Ecol. Environ.* (in press).

Van Stan, J. T., Wagner, S., Guillemette, F., Whitetree, A., Lewis, J., Silva, L., et al. (2017). Temporal dynamics in the concentration, flux, and optical properties of tree-derived dissolved organic matter in an epiphyte-laden oak-cedar forest. *J. Geophys. Res. Biogeosci.* 122, 2982–2997. doi: 10.1002/2017jg004111

Vass, M. (2015). *Hydrobiological Properties and Ecology of Fungal Consortia of Dendrotelmata*. Ms.C. thesis. Veszprém: Pannon University.

Vass, M., Révay, Á, Kucserka, T., Hubai, K., Üveges, V., Kovács, K., et al. (2013). Aquatic hyphomycetes as survivors and/or first colonizers after a red sludge disaster in the Torna stream, Hungary. *Int. Rev. Hydrobiol.* 98, 217–224. doi: 10.1002/iroh.201301540

Vulinoviæ, J. N., Loliæ, S. B., Vujèiæ, S. B., and Matavulj, M. N. (2019). *Schizophyllum commune*–the dominant cause of trees decay in alleys and parks in the City of Novi Sad (Serbia). *Biol. Serb.* 40, 26–33.

Webster, J., and Descals, E. (1979). "The teleomorphs of water-borne hyphomycetes from freshwater," in *The Whole Fungus*, ed. B. Kendrick (Ottawa: National Museums of Canada), 419–447.

West, J. (2010). *Nature Notes: Tree Foam*. Available online at: http://ramblinghemlock.blogspot.com/2010/09/first-website.html (accessed 1 October 2020)

Xu, X., Yu, X., Mo, L., Xu, Y., Bao, L., and Lun, X. (2019). Atmospheric particulate matter accumulation on trees: a comparison of boles, branches and leaves. *J. Clean. Prod.* 226, 349–356. doi: 10.1016/j.jclepro.2019.04.072

Young, C. (1937). Acidity and moisture in tree bark. *Proc. Indiana Acad. Sci.* 47, 106–114.

Conflict of Interest: The authors declare that the research was conducted in the absence of any commercial or financial relationships that could be construed as a potential conflict of interest.

frontiers in Forests and Global Change

PERSPECTIVE
published: 09 April 2021
doi: 10.3389/ffgc.2021.660662

Bark-Water Interactions Across Ecosystem States and Fluxes

John T. Van Stan[1,2], Salli F. Dymond[3] and Anna Klamerus-Iwan[4]*

[1] Applied Coastal Research Laboratory, Georgia Southern University, Savannah, GA, United States, [2] Department of Geology and Geography, Georgia Southern University, Savannah, GA, United States, [3] Department of Earth and Environmental Sciences, University of Minnesota Duluth, Duluth, MN, United States, [4] Department of Forest Utilization Engineering and Forest Technology, University of Agriculture in Krakow, Kraków, Poland

To date, the perspective of forest ecohydrologists has heavily focused on leaf-water interactions – leaving the ecohydrological roles of bark under-studied, oversimplified, or omitted from the forest water cycle. Of course, the lack of study, oversimplification, or omission of processes is not inherently problematic to advancing ecohydrological theory or operational practice. Thus, this perspective outlines the relevance of bark-water interactions to advancing ecohydrological theory and practice: (i) across scales (by briefly examining the geography of bark); (ii) across ecosystem compartments (i.e., living and dead bark on canopies, stems, and in litter layers); and, thereby, (iii) across all major hydrologic states and fluxes in forests (providing estimates and contexts where available in the scant literature). The relevance of bark-water interactions to biogeochemical aspects of forest ecosystems is also highlighted, like canopy-soil nutrient exchanges and soil properties. We conclude that a broad ecohydrological perspective of bark-water interactions is currently merited.

Keywords: hydrology, precipitation, transpiration, evaporation, water uptake, biogeochemistry, bark, forest

OPEN ACCESS

Edited by:
Tom Grant Pypker, Thompson Rivers University, Canada

Reviewed by:
Julieta A. Rosell, National Autonomous University of Mexico, Mexico
Taehee Hwang, Indiana University Bloomington, United States

****Correspondence:***
John T. Van Stan
professor.vanstan@gmail.com

Specialty section:
This article was submitted to Forest Hydrology, a section of the journal Frontiers in Forests and Global Change

Received: *29 January 2021*
Accepted: *18 March 2021*
Published: *09 April 2021*

Citation:
Van Stan JT, Dymond SF and Klamerus-Iwan A (2021) Bark-Water Interactions Across Ecosystem States and Fluxes. Front. For. Glob. Change 4:660662. doi: 10.3389/ffgc.2021.660662

INTRODUCTION

Woody plants are some of Earth's tallest, largest (in terms of mass), and longest-lived organisms. Materials derived from woody plants literally provided the structural support for human development worldwide (Fernow, 1913), continue to do so (Westoby, 1989; Wiersum, 1995), and are critical variables in plans to combat and cope with climate change (Pinkard et al., 2015). Woody plants owe their ecological achievements and societal importance, in part, to an anatomical interface between the external world and their internal stem tissues, called "bark." Despite generally being <15% of total stem volume (c.f., Rosell et al., 2017), bark protects plants from disturbances like fire (Pausas, 2015) and insects (Ferrenberg and Mitton, 2014), can contribute significantly to stem mechanics (Rosell and Olson, 2014), and plays key roles in stem damage recovery (Romero et al., 2009).

Besides these plant physiological roles, bark surfaces engage in profound passive interactions with other biotic and abiotic variables. The porous outer bark layer can host a diverse microbial community (Magyar, 2008; Lambais et al., 2014) as well as an abundant epiphyte assemblage (Van Stan and Pypker, 2015) which is capable of hosting its own extensive microbial community (Anderson, 2014). Bark surface structure also impacts invertebrate communities, for example: affecting resource discovery time for arboreal ants (Yanoviak et al., 2017) and acting as an environmental filter for total invertebrate communities on dead trees (Zuo et al., 2016). These

passive biotic roles of bark, to some extent, hinge on bark's hydrologic functions. Indeed, the water dynamics that support and control life on bark surfaces are a product of that surface's hygroscopic interactions with water vapor (Kapur and Narayanamurti, 1934; Ilek et al., 2017, 2021), absorption and chemical exchange with liquid precipitation (Voigt and Zwolinski, 1964; Levia and Herwitz, 2005), evaporation response to micrometeorological conditions (Van Stan et al., 2017a), and its melt-related (e.g., albedo) and adhesive properties with regard to ice precipitation (Levia and Underwood, 2004; Roesch and Roeckner, 2006). Of these processes, particularly little research has focused on the ability of bark to absorb and retain water vapor (hygroscopic) despite its strong interconnection to the other bark biogeochemical functions.

Generally, the forest ecohydrological research community has focused on leaf-water interactions to date (e.g., Novick et al., 2019; Holder, 2020). As a result, hydrologic processes operating in and on bark are currently underrepresented (both in magnitude and in parametrization) by land surface models. This may be due to the lack of experimental work on the subject to date, since little-to-no data exist regarding many apparent bark surface and internal properties hypothesized to influence its water storage states, as well as its drainage and evaporative fluxes. The breadth of unobserved properties and unexamined processes within bark-water interactions yield a diversity of research opportunities that may improve land surface and climate models and their applications. To initiate a broader discussion of these opportunities, here we describe a perspective of bark-water interactions that illustrates the broad geographic (spatiotemporal) extent of bark and discuss its connections to ecohydrological processes across forest ecosystem states and fluxes.

A BRIEF LOOK AT THE GEOGRAPHY OF BARK

Bark is both spatially expansive and temporally persistent and, therefore, its interactions with the hydrologic cycle may be as well. Regarding the spatial extent, if we estimate bark's global surface area from the same type of land surface model input data used to estimate global leaf surface area (i.e., Vorholt, 2012), then the bark surface is nearly as large as the Asian continent, ∼41 million km^2 (Van Stan et al., 2020). The surface area of this "bark continent" is likely an underestimate as it is based on stem area index (SAI) of standing plants (**Figures 1a,b**), which does not include the added surface area due to bark surface structural complexity or due to bark on fallen woody debris – see Fang et al. (2019), and references therein, regarding SAI estimation methods. These different bark compartments (standing live, standing dead, and fallen debris) would likely have different effects on ecosystem water fluxes. Across these compartments, the additional surface area due to bark microrelief will hypothetically vary across species. For example, an embryonic step toward estimating the additional surface area due to bark microrelief on live stems is achievable using LaserBark scans (a high-resolution stem lidar system: Van Stan et al., 2010; see **Supplementary Section 1**). This analysis suggests that there is negligible additional bark surface area in the case of smooth-barked trees, like *Fagus sylvatica*; however, moderately rough bark (e.g., *Pinus contorta*) and deeply furrowed bark (e.g., *Quercus robur*) can add ∼10% and ∼16% to bark surface area, respectively, when compared with a fitted circular circumference (**Supplementary Figure 1**). Although only supported by a relatively small set of high-resolution lidar scans, woody surface area approximations that do not account for bark microrelief may meaningfully underestimate the surface area of this continent of bark.

This estimate of global bark surface area appears small compared to the ∼1 billion km^2 estimate of global leaf surface area (Vorholt, 2012); however, unlike many leaf surfaces, the bark surface is present across all seasons. Plant phenology can include bark shedding events (Borger, 1973); however, these events differ meaningfully from leaf shedding events. Most notably, bark shedding temporarily increases surface area for external bark-water interactions (due to the flaking; **Figures 1c,d**) and it results in bark becoming present not just in the tree canopy (i.e., new bark), but in the understory (i.e., trapped sheddings; **Figure 1e**) and litter layer (i.e., bark litter; **Figures 1f,g**). Based on the few measurements to date, bark litter decomposes much slower than leaf litter (Grootemaat et al., 2017) – with decomposition half-lives ranging from 4.9 to 9.4 years in the litter layer (Johnson et al., 2014). Thus, a brief look at the geography of bark reveals that it can be present in wooded watersheds all year round, on live and dead plants, from the canopy top to the litter below.

THE ANATOMY OF BARK-WATER INTERACTIONS

"Bark" is anatomically defined as all stem tissues outside of the vascular cambium (**Figure 1f**). More specifically, bark consists of the functional and non-functional phloem (produced by the vascular cambium), and either a single periderm (for some species) or alternating layers of old periderm and phloem [for species that have successive periderms, called the rhytidome (Evert, 2006; **Figure 1f**)]. The periderm is made up of three types of tissues – the phellogen, or cork cambium, is a radial meristem that produces phelloderm to the inside, and phellem, or cork, to the outside. These bark anatomical layers are often grouped into "inner" and "outer" bark functional layers; however, the distinction between these functional layers can change across studies. A useful distinction for ecologists and hydrologists is clearly one which separates the metabolically active and inactive (i.e., living vs. dead) tissues into the inner bark and outer bark, respectively. Using this distinction, the collection of tissues between the most recent layers of phloem and the most recently produced phelloderm may be classified as the living "inner bark," while the phellem (in species with one periderm) or the rhytidome (in species with multiple periderms) is the "outer bark" (Kramer and Kozlowski, 1960). Although the ontogeny of bark is poorly understood (Rosell and Olson, 2007, 2014), in general, the living part of a plant's periderm, its cellular structure, and its relationship with environmental and growth

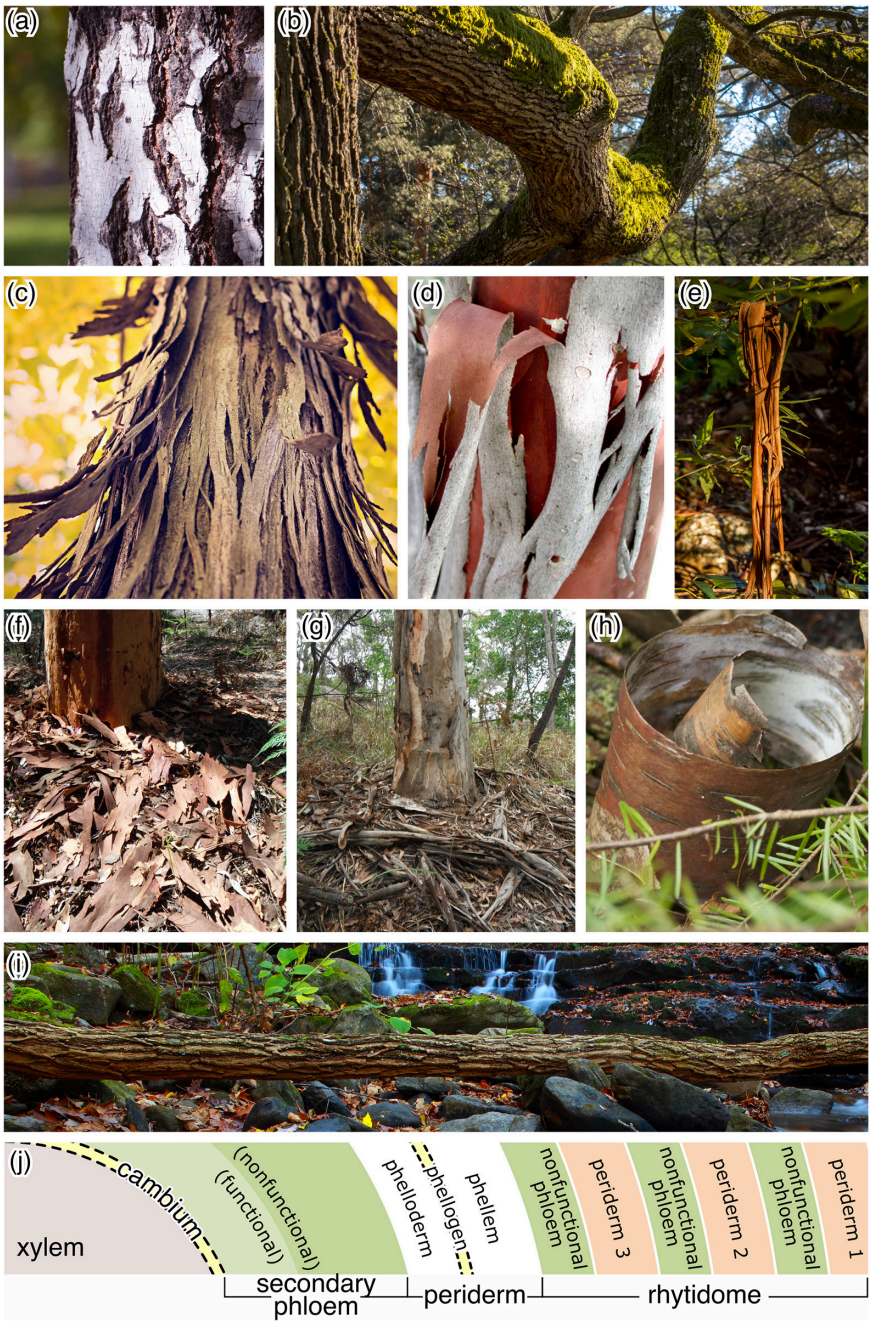

FIGURE 1 | Bark is present throughout a forest – beyond tree **(a)** stems and **(b)** branches. Bark shedding can **(c,d)** temporarily increase on-stem bark surface area, **(e)** release peelings that become trapped in understory canopies, and **(f–h)** cover the forest floor. Bark must also be broken down on **(i)** fallen dead trees. **(j)** Anatomy of the inner and outer bark. All photographs from open source databases (e.g., Pixabay, Wikimedia Commons) unless credited otherwise. Credits: **(a)** Tatyana Fyodorova; **(b)** Thomas B. Didgeman; **(c)** Ryan McGuire; **(d)** Niel Sperry; **(e)** Sandid (Pixabay); **(f,g)** permission from Saskia Grootemaat; **(h)** Justin Leonard; **(i)** Troy Lilly.

factors interact to control the outer characteristics of a tree's bark and can result in a wide array of bark structural properties (see examples in **Figure 1**). For smooth-barked trees such as *Fagus grandifolia* or *Populus tremuloides*, a single periderm may persist without rupturing for long periods of time or the entirety of the plant's life. For rough-barked trees, species with a single periderm can rupture as the plant grows, or the first (of successive) periderm can rupture as the plant grows and significant tangential tensile stress is placed on the bark. These ruptured, successive periderms may exfoliate over time for some species; for others, they may persist and develop rough and thick bark. The physical structure of the inner and outer bark layers

contain biochemical components (e.g., resin and suberin) that can interact to alter these interfaces' interactions with internal and external waters. Since bark is present in and below the forest canopy, it theoretically could interact with the forest water and energy budget at several points (**Figure 2**). Additionally, because bark can exist in litter, on coarse debris, and in the canopy, it has multiple opportunities to interact (both internally and externally) with different hydrological fluxes.

Of course, each bark functional layer can interact with the water cycle. Starting from the outside-in, the outer bark passively intercepts water during storms. The interception of rainfall by the outer bark can be significant, accounting for 50–80% of the forest canopy's total water storage capacity (depending on storm conditions) at an Australian tropical rainforest, even for smooth-barked trees (Herwitz, 1985). The evaporation of intercepted precipitation from the outer bark is rarely quantified, and generally has been assumed to be trivial: <2% of total canopy interception-related evaporation (Linhoss and Siegert, 2016). However, in an urban tree row, evaporation from the outer bark represented a non-trivial portion of canopy evaporation: up to 40% (Van Stan et al., 2017a). For solid precipitation, outer bark microrelief has long been known to enable the adhesion of large ice deposits to branches, stems, and exposed tree roots (Klamerus-Iwan et al., 2020a) – even creating "champignons de neige" (snow mushrooms) on the bark of stumps (see photographs 2–6 in Salamin, 1959). Interestingly, Salamin (1959) discusses the effect of outer bark roughness on the mode of snow interception, saying that "on the trunks of trees with smooth bark, it is deposited *in a narrow band* [whereas] on trunks with very rough bark, it is stored *in a heap* with great adhesive power[1]." Intercepted snow may remain on the bark until air temperatures warm (inducing melt) or a mechanical force (like wind) redistributes it; however, the outer bark's albedo can play a role in initiating snowmelt in the canopy even under freezing conditions (Levia and Underwood, 2004). These same bark structures interact with draining precipitation waters, affecting the timing and spatial distribution of throughfall and stemflow fluxes (Pypker et al., 2011).

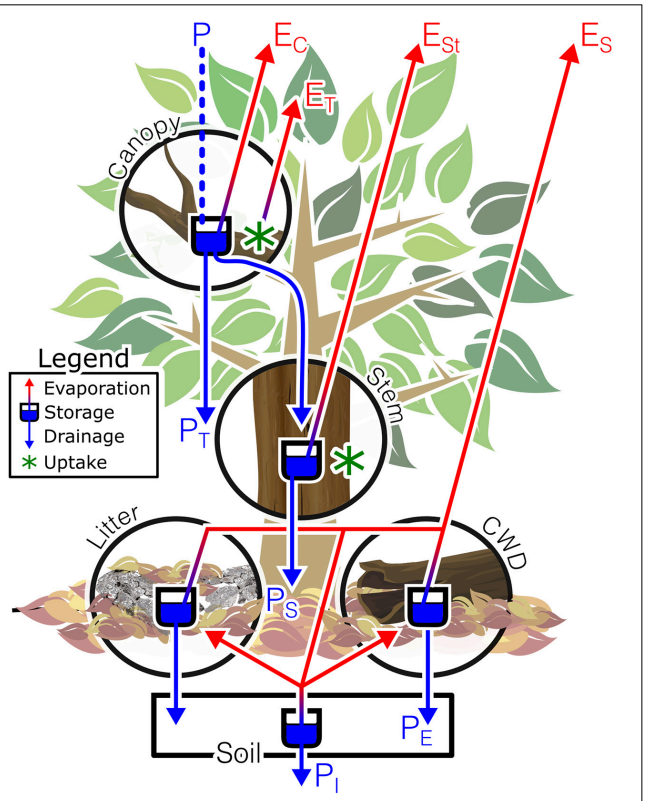

FIGURE 2 | The forest water cycle and opportunities for bark-water interactions. Incoming precipitation (P) can be stored and evaporated at various points, from the bark on the canopy (E_C), stem (E_{St}) and in the litter (including coarse woody debris, CWD), and soil surface (E_S). In the canopy and on the stem, bark-water interactions can result in uptake and a portion of this uptaken water may be transpired (E_T). Precipitation will also interact with canopy bark as it drains as throughfall (P_T), stemflow (P_S); litter bark and CWD before becoming effective precipitation (P_E) and infiltration (P_I).

Between storms, the outer bark passively exchanges water vapor with the atmosphere (i.e., hygroscopically). The hygroscopic response of the outer bark can be observable daily, and has fascinated scientists since its first reported observation by Gregor Kraus in 1877 (Haasis, 1934). This hygroscopic response can vary widely across tree species (0.5–1.5 mm per 1 cm of thickness), depending on the outer bark's bulk density and porosity (Ilek et al., 2017, 2021). How physicochemical properties affect hygroscopicity of the outer bark remains little researched, especially under natural conditions; however, Ilek et al. (2017) found that 10–30% of the outer bark's water storage capacity could be filled hygroscopically for several species representing a range of common European coniferous and deciduous trees in a temperate continental climate – but, this contribution exceeded 60%, at times, for a humid forest site (Ilek et al., 2021). Hypothetically, the hygroscopic (partial) filling of outer bark pore space may explain some of the variability in canopy water storage capacity between storms. If the outer bark is wet enough, some tree species have been observed to uptake rhytidome-stored water internally (e.g., Katz et al., 1989; Mayr et al., 2014; Earles et al., 2016). While bark is not typically considered in estimates of plant water-use or water redistribution, it has been shown that bark can both take up and lose water across a variety of species (Wittmann and Pfanz, 2008; Earles et al., 2016; Wolfe, 2020). The physical path that intercepted (or hygroscopic) rhytidome water follows into the inner bark may be through non-suberized areas of the phellem cell walls, which can be hydrophilic (Earles et al., 2016). From there, a strong osmotic gradient may draw this intercepted water into the xylem (Zwieniecki and Holbrook, 2009). Water can also move from bark rays into the xylem – a route previously called an "undervalued route of water transport" (e.g., van Bel, 1990; Pfautsch et al., 2015).

As a result of these processes, the inner bark also hosts a dynamic reservoir of water storage (Srivastava, 1964). A study of 90 species across a range of woody ecosystems found that inner bark water storage can account for a non-trivial portion,

[1]Translated from French on page 53 of Salamin (1959): "sur le tronc des arbres à écorce lisse, elle se dépose *en bande étroite*. sur les troncs dont l'écorce est fortement rugueuse, elle se conserve *en tas* ayant un grand pouvoir adhésif. . ."

17–76%, of the total stem water storage (Rosell et al., 2014). For coastal redwood trees (*Sequoia sempervirens*), the saturated bark is thought to increase xylem hydraulic conductivity through refilling of tracheid cells (Earles et al., 2016). Similar movement of water between the bark and inner xylem cells has been observed for white spruce (*Picea glauca*) as well (Katz et al., 1989). While the percent contribution of bark water to total tree transpiration may be relatively small compared to the supply from soils during stress-free periods, this contribution may become significant during periods of drought. For woody species in dryland or seasonally dry ecosystems, bark water storage could represent a crucial buffer against daily-to-seasonal scale changes in water availability (Scholz et al., 2007; Rosell and Olson, 2014), where phloem rays could transport water from the inner bark to the xylem (Pfautsch et al., 2015). Bark water vapor conductance in eight tropical tree species was correlated with higher degrees of stem water deficit and mortality in both natural and greenhouse conditions (Wolfe, 2020). Bark-water interactions (i.e., bark hydraulics) such as these may be scaled via parametrization into tree-scale water flow-storage models (e.g., Steppe and Lemeur, 2007; Mencuccini et al., 2013; Chan et al., 2016) – a future effort along this vein could provide a pathway for first-order estimates of impacts on water states and fluxes at the regional and watershed scales. Altogether, such findings indicate that there is hydrologic connectivity between bark and xylem, the area of stems that carry out water transportation, and that more research is needed to quantify bark-water-uptake contributions to overall plant water use.

AFTER THE BARK DEPARTS: OFF-THE-TREE OPPORTUNITIES TO INFLUENCE FOREST HYDROLOGY

The bark can depart from the canopy and enter the litter layer during seasonal shedding events or episodic disturbances, like branch breakage or tree throw. In forests where seasonal bark shedding occurs (**Figure 1**), it can compose ∼20–50% of the litter layer (McColl, 1966; Woods and Raison, 1983; Lamb, 1985; Van Stan et al., 2017b). Scant data exist to estimate the contribution of bark sheddings to litter water storage and evaporation. The thin bark sheddings of *Pinus elliottii*, composing 18% of the litter layer, could account for ∼10–30% of the litter water storage capacity, reducing throughfall reaching soils (Van Stan et al., 2017b). Recent work finds that the litter layer's water storage dynamics can also be considerably influenced from below, by intercepting soil vapor flux during wet-to-dry transitions (Zhao et al., 2021). Hypothetically, the unique structure of bark sheddings (i.e., hydrophobic strips that cover wide areas relative to a leaf; **Figures 1f,g**) could aid the litter layer to intercept soil vapor fluxes. Of course, there are much larger bark-covered impediments to inputs from above (throughfall) and below (soil vapor) in forest litter: coarse woody debris (CWD). The specific influence of bark on the water balance of CWD has not, to the authors' knowledge, been assessed; however, recent work on deadwood found that the least decomposed wood samples (those with "fragmented bark") had the lowest initial water absorbability, highest water repellency and, as a result, the lowest storage capacity compared to samples without bark (Błońska et al., 2018; Klamerus-Iwan et al., 2020b). This is not to say that the localized water storage capacity of CWD is negligible. For example, logs with in-tact bark from four common tree species in the H.J. Andrews Experimental Forest (OR, United States), were observed to store and evaporate up to 60% of throughfall (Sexton and Harmon, 2009). Sexton and Harmon (2009) noted that the bark surface could repel 3–29% of rainfall as runoff from the logs. Clearly there are many open, fundamental questions related to bark's hydrological interactions after its departure from the canopy. Perhaps most fundamentally, how do bark hydrological traits significantly differ when on a living tree vs. coarse woody debris vs. shed bark flakes? And, if bark hydrological traits do differ between these states, is it relevant to hydrological processes?

BARK-WATER INTERACTIONS AND BIOGEOCHEMISTRY

The bark-water interactions discussed above have biogeochemical impacts, both external and internal to the plant. Externally, bark can exchange both inorganic and organic solutes with the comparatively dilute precipitation waters as they drain to the surface as throughfall and, even more so, as stemflow. Solute uptake, leaching, wash-off and transformation during bark-water interactions have all been reported (Katz et al., 1989; Tobón et al., 2004; Gaige et al., 2007; Hofhansl et al., 2012). Leaching of ionic solutes, especially K^+, Mg^{2+}, and Ca^{2+}, from bark to draining precipitation waters has been reported in past work (Levia and Herwitz, 2005; Hofhansl et al., 2012). Bark uptake of NH_4^+ and NO_3^- from net precipitation fluxes has also been reported (Parker, 1983; Crockford et al., 1996; André et al., 2008). Biochemical transformations have also been reported for water-bark interactions, for example, the optical characteristics of dissolved organic matter in stemflow appears to change with increasing bark residence time (Van Stan et al., 2017c). Bark surfaces can also be excellent traps for coarse particles (Xu et al., 2019), including fungal spores (Magyar, 2008), nutrient-rich pollen (Groenman-van Waateringe, 1998), and pollutants (Catinon et al., 2009) – all of which can be scoured and transported to the surface by branchflow and stemflow (Ponette-González et al., 2020). For vegetation residing on bark – corticolous lichen and bryophytes, for example – studies have found strong relationships with bark water storage and the nutrient content of bark leachates (i.e., stemflow) (Farmer et al., 1991; McGee et al., 2019). Internally, bark water uptake and carbohydrate storage may interact to enable embolism repair (Nardini et al., 2011; Pfautsch et al., 2015; Rosell, 2019). Indeed, recent research finds that (non-structural) carbohydrate storage in the inner bark (for 45 woody, tropical species) can be substantial, accounting for 17–36% of total storage (Rosell et al., 2020). For deadwood, recent work has found that the dissolved organic matter leached into soils during storms can alter soil properties, increasing the retention of soil water beneath (Piaszczyk et al., 2020). For bark alone,

its decomposition effects on soil properties has also received renewed attention. At the Shale Hills Critical Zone Observatory (PA, United States), for example, bark decomposition strongly influenced the composition of nearby soil microbial communities and this influence varied by bark type (Malik et al., 2020). Thus, bark-water interactions are connected to biogeochemical processes, from solute and particulate cycling and transport to soil physicochemistry and microbial properties.

CONCLUSION

Given the expansive and temporally persistent geography of bark, as well as the diversity of its anatomical structures and water-related functions, we conclude that a broad ecohydrological perspective of bark-water interactions is currently merited. Observations available to date, especially recent observations, suggest that bark-water interactions play relevant roles in most major water (mass and energy) states and fluxes in a forest ecosystem. Moreover, bark – whether alive or dead – appears to couple water to other biogeochemical aspects of forest ecosystems, from canopy-to-soil nutrient exchanges to soil physicochemistry and microbial community structure. This perspective therefore urges ecohydrology research to more comprehensively consider the roles of bark across ecosystem compartments (as dead wood, sheddings, and on standing trees), as well as its structure and properties, to test the conditions under which bark-water interactions may be relevant (or may be ignored) in ecological and hydrological processes. Recent insights regarding bark's possible hydrological importance to distressed plants (e.g., as a water source during drought or as an agent of embolism repair) are especially of interest. Thus, future work on the ecohydrological roles of bark (whether thick or thin) may provide key insights to forest ecohydrological functions (through thick and thin).

DATA AVAILABILITY STATEMENT

The original contributions presented in the study are included in the article/**Supplementary Material**, further inquiries can be directed to the corresponding author.

AUTHOR CONTRIBUTIONS

JV conceived the study, then structured the manuscript in collaboration with SD and AK-I. **Figure 1** was initially designed by JV, **Figure 2** was initially designed by SD, then both figures were finalized after comment by JV, SD, and AK-I. Writing tasks were split among the authors, so that all contributed draft text and reviewed each other's draft text. All authors contributed to the article and approved the submitted version.

FUNDING

JV acknowledges the support from the United States-NSF (EAR-1954907).

ACKNOWLEDGMENTS

We would like to thank the peer reviewers, and Travis Swanson for his discussion and programming assistance with the bark surface area analyses.

SUPPLEMENTARY MATERIAL

The Supplementary Material for this article can be found online at: https://www.frontiersin.org/articles/10.3389/ffgc.2021.660662/full#supplementary-material

REFERENCES

Anderson, O. R. (2014). Microbial communities associated with tree bark foliose lichens: a perspective on their microecology. *J. Eukaryot. Microbiol.* 61, 364–370. doi: 10.1111/jeu.12116

André, F., Jonard, M., and Ponette, Q. (2008). Effects of biological and meteorological factors on stemflow chemistry within a temperate mixed oak–beech stand. *Sci. Total Environ.* 393, 72–83. doi: 10.1016/j.scitotenv.2007.12.002

Błońska, E., Klamerus-Iwan, A., Łagan, S., and Lasota, J. (2018). Changes to the water repellency and storage of different species of deadwood based on decomposition rate in a temperate climate. *Ecohydrology* 11:e2023. doi: 10.1002/eco.2023

Borger, G. A. (1973). *Development and Shedding of Bark. In Shedding of plant parts*. New York: Academic Press, 205–236.

Catinon, M., Ayrault, S., Clocchiatti, R., Boudouma, O., Asta, J., Tissut, M., et al. (2009). The anthropogenic atmospheric elements fraction: a new interpretation of elemental deposits on tree barks. *Atmospheric Environ.* 43, 1124–1130. doi: 10.1016/j.atmosenv.2008.11.004

Chan, T., Hölttä, T., Berninger, F., Mäkinen, H., Nöjd, P., Mencuccini, M., et al. (2016). Separating water-potential induced swelling and shrinking from measured radial stem variations reveals a cambial growth and osmotic concentration signal. *Plant Cell Environ.* 39, 233–244. doi: 10.1111/pce.12541

Crockford, R. H., Richardson, D. P., and Sageman, R. (1996). Chemistry of rainfall, throughfall and stemflow in a eucalypt forest and a pine plantation in south-eastern australia: 3. Stemflow and total inputs. *Hydrol. Proc.* 10, 25–42. doi: 10.1002/(sici)1099-1085(199601)10:1<25::aid-hyp297>3.0.co;2-w

Earles, J. M., Sperling, O., Silva, L. C., McElrone, A. J., Brodersen, C. R., North, M. P., et al. (2016). Bark water uptake promotes localized hydraulic recovery in coastal redwood crown. *Plant Cell. Environ.* 39, 320–328. doi: 10.1111/pce.12612

Evert, R. F. (2006). *Esau's Plant Anatomy: Meristems, Cells, and Tissues of the Plant Body: Their Structure, Function, and Development*. New Jersey: John Wiley & Sons, Inc.

Fang, H., Baret, F., Plummer, S., and Schaepman-Strub, G. (2019). An overview of global leaf area index (LAI): methods, products, validation, and applications. *Rev. Geophys.* 57, 739–799. doi: 10.1029/2018rg000608

Farmer, A. M., Bates, J. W., and Bell, J. N. B. (1991). Seasonal variations in acidic pollutant inputs and their effects on the chemistry of stemflow, bark and epiphyte tissues in three oak* woodlands in NW Britain. *New Phytol.* 118, 441–451. doi: 10.1111/j.1469-8137.1991.tb00026.x

Fernow, B. E. (1913). *A brief history of forestry in Europe, the United States and other countries*, 3rd Edn. Canada: University Press Toronto.

Ferrenberg, S., and Mitton, J. B. (2014). Smooth bark surfaces can defend trees against insect attack: resurrecting a 'slippery' hypothesis. *Funct. Ecol.* 28, 837–845. doi: 10.1111/1365-2435.12228

Gaige, E., Dail, D. B., Hollinger, D. Y., Davidson, E. A., Fernandez, I. J., Sievering, H., et al. (2007). Changes in canopy processes following whole-forest canopy nitrogen fertilization of a mature spruce-hemlock forest. *Ecosystems* 10, 1133–1147. doi: 10.1007/s10021-007-9081-4

Groenman-van Waateringe, W. (1998). Bark as a natural pollen trap. *Rev. Palaeobot. Palynol.* 103, 289–294. doi: 10.1016/s0034-6667(98)00040-2

Grootemaat, S., Wright, I. J., Van Bodegom, P. M., Cornelissen, J. H., and Shaw, V. (2017). Bark traits, decomposition and flammability of australian forest trees. *Aus. J. Bot.* 65, 327–338. doi: 10.1071/bt16258

Haasis, F. W. (1934). *Diametral changes in tree trunks (No. 581.134 H112)*. Washington, DC (EUA): Carnegie Institution of Washington.

Herwitz, S. R. (1985). Interception storage capacities of tropical rainforest canopy trees. *J. Hydrol.* 77, 237–252. doi: 10.1016/0022-1694(85)90209-4

Hofhansl, F., Wanek, W., Drage, S., Huber, W., Weissenhofer, A., and Richter, A. (2012). Controls of hydrochemical fluxes via stemflow in tropical lowland rainforests: effects of meteorology and vegetation characteristics. *J. Hydrol.* 452, 247–258. doi: 10.1016/j.jhydrol.2012.05.057

Holder, C. D. (2020). *Advances and Future Research Directions in the Study of Leaf Water Repellency. In Forest-Water Interactions*. Cham: Springer, 261–278.

Ilek, A., Kucza, J., and Morkisz, K. (2017). Hygroscopicity of the bark of selected forest tree species. *iForest Biogeosci. For.* 10, 220–226. doi: 10.3832/ifor1979-009

Ilek, A., Siegert, C. M., and Wade, A. (2021). Hygroscopic contributions to bark water storage and controls exerted by internal bark structure over water vapor absorption. *Trees* 24, 1–13. doi: 10.1007/s00468-021-02084-0

Johnson, C. E., Siccama, T. G., Denny, E. G., Koppers, M. M., and Vogt, D. J. (2014). In situ decomposition of northern hardwood tree boles: decay rates and nutrient dynamics in wood and bark. *Can. J. Forest Res.* 44, 1515–1524. doi: 10.1139/cjfr-2014-0221

Kapur, S., and Narayanamurti, D. (1934). Hygroscopicity of tree barks. *Indian For.* 60, 702–707.

Katz, C., Oren, R., Schulze, E. D., and Milburn, J. A. (1989). Uptake of water and solutes through twigs of Picea abies (L.) Karst. *Trees* 3, 33–37.

Klamerus-Iwan, A., Link, T. E., Keim, R. F., and Van Stan, J. T. (2020a). "Storage and routing of precipitation through canopies," in *Precipitation Partitioning by Vegetation: A Global Synthesis*, eds J. T. Van Stan, E. D. Gutmann, and J. Friesen (Cham, Switzerland: Springer Nature), 17–34. doi: 10.1007/978-3-030-29702-2_2

Klamerus-Iwan, A., Lasota, J., and Błońska, E. (2020b). Interspecific variability of water storage capacity and absorbability of deadwood. *Forests* 11:575. doi: 10.3390/f11050575

Kramer, P., and Kozlowski, T. (1960). *Physiology of Trees*. New York, NY: McGraw-Hill, Inc.

Lamb, R. (1985). Litter fall and nutrient turnover in two eucalypt woodlands. *Aus. J. Bot.* 33, 1–14. doi: 10.1071/bt9850001

Lambais, M. R., Lucheta, A. R., and Crowley, D. E. (2014). Bacterial community assemblages associated with the phyllosphere, dermosphere, and rhizosphere of tree species of the atlantic forest are host taxon dependent. *Microb. Ecol.* 68, 567–574. doi: 10.1007/s00248-014-0433-2

Levia, D. F., and Herwitz, S. R. (2005). Interspecific variation of bark water storage capacity of three deciduous tree species in relation to stemflow yield and solute flux to forest soils. *Catena* 64, 117–137. doi: 10.1016/j.catena.2005.08.001

Levia, D. F., and Underwood, S. J. (2004). Snowmelt induced stemflow in northern hardwood forests: a theoretical explanation on the causation of a neglected hydrological process. *Adv. Water Res.* 27, 121–128. doi: 10.1016/j.advwatres.2003.12.001

Linhoss, A. C., and Siegert, C. M. (2016). A comparison of five forest interception models using global sensitivity and uncertainty analysis. *J. Hydrol.* 538, 109–116. doi: 10.1016/j.jhydrol.2016.04.011

Magyar, D. (2008). The tree bark: a natural spore trap. *Asp Appl Biol* 89, 7–16.

Malik, R. J., Trexler, R. V., Eissenstat, D. M., and Bell, T. H. (2020). Bark decomposition in white oak soil outperforms eastern hemlock soil, while bark type leads to consistent changes in soil microbial composition. *Biogeochemistry* 150, 329–343. doi: 10.1007/s10533-020-00701-7

Mayr, S., Schmid, P., Laur, J., Rosner, S., Charra-Vaskou, K., Dämon, B., et al. (2014). Uptake of water via branches helps timberline conifers refill embolized xylem in late winter. *Plant Physiol.* 164, 1731–1740. doi: 10.1104/pp.114.236646

McColl, J. G. (1966). Accession and decomposition of litter in spotted gum forests. *Aus. Forestry* 30, 191–198. doi: 10.1080/00049158.1966.10675413

McGee, G. G., Cardon, M. E., and Kiernan, D. H. (2019). Variation in acer saccharum marshall (sugar maple) bark and stemflow characteristics: implications for epiphytic bryophyte communities. *Northeastern Nat.* 26, 214–235. doi: 10.1656/045.026.0118

Mencuccini, M., Hölttä, T., Sevanto, S., and Nikinmaa, E. (2013). Concurrent measurements of change in the bark and xylem diameters of trees reveal a phloem-generated turgor signal. *New Phytol.* 198, 1143–1154. doi: 10.1111/nph.12224

Nardini, A., Gullo, M. A. L., and Salleo, S. (2011). Refilling embolized xylem conduits: is it a matter of phloem unloading? *Plant Sci.* 180, 604–611. doi: 10.1016/j.plantsci.2010.12.011

Novick, K. A., Konings, A. G., and Gentine, P. (2019). Beyond soil water potential: an expanded view on isohydricity including land–atmosphere interactions and phenology. *Plant Cell. Environ.* 42, 1802–1815. doi: 10.1111/pce.13517

Parker, G. G. (1983). Throughfall and stemflow in the forest nutrient cycle. *Adv. Ecol. Res.* 13, 57–133. doi: 10.1016/s0065-2504(08)60108-7

Pausas, J. G. (2015). Bark thickness and fire regime. *Funct. Ecol.* 29, 315–327. doi: 10.1111/1365-2435.12372

Pfautsch, S., Renard, J., Tjoelker, M. G., and Salih, A. (2015). Phloem as capacitor: radial transfer of water into xylem of tree stems occurs via symplastic transport in ray parenchyma. *Plant Physiol.* 167, 963–971. doi: 10.1104/pp.114.254581

Piaszczyk, W., Lasota, J., and Błońska, E. (2020). Effect of organic matter released from deadwood at different decomposition stages on physical properties of forest soil. *Forests* 11:24. doi: 10.3390/f11010024

Pinkard, E., Battaglia, M., Bruce, J., Matthews, S., Callister, A. N., Hetherington, S., et al. (2015). A history of forestry management responses to climatic variability and their current relevance for developing climate change adaptation strategies. *For. An. Int. J. For. Res.* 88, 155–171. doi: 10.1093/forestry/cpu040

Ponette-González, A. G., Van Stan, J. T., and Magyar, D. (2020). *Things Seen and Unseen in Throughfall and Stemflow. In Precipitation Partitioning by Vegetation*. Cham: Springer, 71–88.

Pypker, T. G., Levia, D. F., Staelens, J., and Van Stan, J. T. (2011). *"Canopy structure in relation to hydrological and biogeochemical fluxes," in Forest hydrology and biogeochemistry*. Cham: Springer, 371–388.

Roesch, A., and Roeckner, E. (2006). Assessment of snow cover and surface albedo in the ECHAM5 general circulation model. *J. Clim.* 19, 3828–3843. doi: 10.1175/jcli3825.1

Romero, C., Bolker, B., and Edwards, C. E. (2009). Stem responses to damage: the evolutionary ecology of *Quercus* species in contrasting fire regimes. *New Phytol.* 182, 261–271. doi: 10.1111/j.1469-8137.2008.02733.x

Rosell, J. A. (2019). Bark in woody plants: understanding the diversity of a multifunctional structure. *Integr. Compar. Biol.* 59, 535–547. doi: 10.1093/icb/icz057

Rosell, J. A., Gleason, S., Méndez-Alonzo, R., Chang, Y., and Westoby, M. (2014). Bark functional ecology: evidence for tradeoffs, functional coordination, and environment producing bark diversity. *New Phytol.* 201, 486–497. doi: 10.1111/nph.12541

Rosell, J. A., and Olson, M. E. (2007). Testing implicit assumptions regarding the age vs. size dependence of stem biomechanics using pittocaulon (senecio) praecox (asteraceae). *Am. J. Bot.* 94, 161–172. doi: 10.3732/ajb.94.2.161

Rosell, J. A., and Olson, M. E. (2014). The evolution of bark mechanics and storage across habitats in a clade of tropical trees. *Am. J. Bot.* 101, 764–777. doi: 10.3732/ajb.1400109

Rosell, J. A., Piper, F. I, Jiménez-Vera, C., Vergílio, P. C., Marcati, C. R., Castorena, M., et al. (2020). Inner bark as a crucial tissue for non-structural carbohydrate storage across three tropical woody plant communities. *Plant Cell. Environ.* 44, 156–170. doi: 10.1111/pce.13903

Rosell, J. A., Wehenkel, C., Pérez-Martínez, A., Arreola Palacios, J. A., García-Jácome, S. P., and Olguín, M. (2017). Updating bark proportions for the estimation of tropical timber volumes by indigenous community-based forest enterprises in quintana roo, mexico. *Forests* 8:338. doi: 10.3390/f8090338

Salamin, P. (1959). Le manteau de neige dans les forêts de Hongrie. *Hydrol. Sci. J.* 4, 47–79. doi: 10.1080/02626665909493143

Scholz, F. G., Bucci, S. J., Goldstein, G., Meinzer, F. C., Franco, A. C., and & Miralles-Wilhelm, F. (2007). Biophysical properties and functional significance of stem water storage tissues in neotropical savanna trees. *Plant Cell. Environ.* 30, 236–248. doi: 10.1111/j.1365-3040.2006.01623.x

Sexton, J. M., and Harmon, M. E. (2009). Water dynamics in conifer logs in early stages of decay in the pacific northwest, USA. *Northwest Sci.* 83, 131–139. doi: 10.3955/046.083.0204

Srivastava, L. M. (1964). *Anatomy, chemistry, and physiology of bark. In International review of forestry research*, Vol. 1. Amsterdam: Elsevier, 203–277.

Steppe, K., and Lemeur, R. (2007). Effects of ring-porous and diffuse-porous stem wood anatomy on the hydraulic parameters used in a water flow and storage model. *Tree Physiol.* 27, 43–52. doi: 10.1093/treephys/27.1.43

Tobón, C., Sevink, J., and Verstraten, J. M. (2004). Solute fluxes in throughfall and stemflow in four forest ecosystems in northwest Amazonia. *Biogeochemistry* 70, 1–25. doi: 10.1023/b:biog.0000049334.10381.f8

van Bel, A. J. E. (1990). Xylem-phloem exchange via the rays: the undervalued route of transport. *J. Exp. Bot.* 41, 631–644. doi: 10.1093/jxb/41.6.631

Van Stan, J. T., Jarvis, M. T., and Levia, D. F. (2010). An automated instrument for the measurement of bark microrelief. *IEEE Trans. Instrumen. Measur.* 59, 491–493. doi: 10.1109/tim.2009.2031338

Van Stan, J. T., Morris, C. E., Aung, K., Kuzyakov, Y., Magyar, D., Rebollar, E. A., et al. (2020). *Precipitation Partitioning—Hydrologic Highways Between Microbial Communities of the Plant Microbiome? In Precipitation Partitioning by Vegetation*. Cham: Springer, 229–252.

Van Stan, J. T., Norman, Z., Meghoo, A., Friesen, J., Hildebrandt, A., Côté, J.-F., et al. (2017a). Edge-to-stem variability in wet-canopy evaporation from an urban tree row. *Boundary-Layer Meteorol.* 165, 295–310. doi: 10.1007/s10546-017-0277-7

Van Stan, J. T., Coenders-Gerrits, M., Dibble, M., Bogeholz, P., and Norman, Z. (2017b). Effects of phenology and meteorological disturbance on litter rainfall interception for a *Pinus elliottii* stand in the southeastern united states. *Hydrol. Proc.* 31, 3719–3728. doi: 10.1002/hyp.11292

Van Stan, J. T., Wagner, S., Guillemette, F., Whitetree, A., Lewis, J., Silva, L., et al. (2017c). Temporal dynamics in the concentration, flux, and optical properties of tree-derived dissolved organic matter in an epiphyte-laden oak-cedar forest. *J. Geophys. Res. Biogeosci.* 122, 2982–2997. doi: 10.1002/2017jg004111

Van Stan, J. T., and Pypker, T. G. (2015). A review and evaluation of forest canopy epiphyte roles in the partitioning and chemical alteration of precipitation. *Sci. Total Env.* 536, 813–824. doi: 10.1016/j.scitotenv.2015.07.134

Voigt, G. K., and Zwolinski, M. J. (1964). Absorption of stemflow by bark of young red and white pines. *For. Sci.* 10, 277–282.

Vorholt, J. A. (2012). Microbial life in the phyllosphere. *Nat. Rev. Microbiol.* 10, 828–840. doi: 10.1038/nrmicro2910

Westoby, J. (1989). *Introduction to world forestry: people and their trees*. Oxford: Basil Blackwell.

Wiersum, K. F. (1995). 200 years of sustainability in forestry: lessons from history. *Environ. Manage.* 19, 321–329. doi: 10.1007/bf02471975

Wittmann, C., and Pfanz, H. (2008). Antitranspirant functions of stem periderms and their influence on corticular photosynthesis under drought stress. *Trees* 22, 187–196. doi: 10.1007/s00468-007-0194-3

Wolfe, B. T. (2020). Bark water vapour conductance is associated with drought performance in tropical trees. *Biol. Lett.* 16:20200263. doi: 10.1098/rsbl.2020.0263

Woods, P. V., and Raison, R. J. (1983). Decomposition of litter in sub-alpine forests of *Eucalyptus delegatensis, E. pauciflora* and *E. dives*. *Aus. J. Ecol.* 8, 287–299. doi: 10.1111/j.1442-9993.1983.tb01326.x

Xu, X., Yu, X., Mo, L., Xu, Y., Bao, L., and Lun, X. (2019). Atmospheric particulate matter accumulation on trees: a comparison of boles, branches and leaves. *J. Cleaner Produc.* 226, 349–356. doi: 10.1016/j.jclepro.2019.04.072

Yanoviak, S. P., Silveri, C., Stark, A. Y., Van Stan, J. T., and Levia, D. F. (2017). Surface roughness affects the running speed of tropical canopy ants. *Biotropica* 49, 92–100. doi: 10.1111/btp.12349

Zhao, L., Yebra, M., van Dijk, A. I., Cary, G. J., Matthews, S., and Sheridan, G. (2021). The influence of soil moisture on surface and sub-surface litter fuel moisture simulation at five australian sites. *Agric. Forest Meteorol.* 298:108282. doi: 10.1016/j.agrformet.2020.108282

Zuo, J., Berg, M. P., Klein, R., Nusselder, J., Neurink, G., Decker, O., et al. (2016). Faunal community consequence of interspecific bark trait dissimilarity in early-stage decomposing logs. *Funct. Ecol.* 30, 1957–1966. doi: 10.1111/1365-2435.12676

Zwieniecki, M. A., and Holbrook, N. M. (2009). Confronting maxwell's demon: biophysics of xylem embolism repair. *Trends Plant Sci.* 14, 530–534. doi: 10.1016/j.tplants.2009.07.002

Conflict of Interest: The authors declare that the research was conducted in the absence of any commercial or financial relationships that could be construed as a potential conflict of interest.

frontiers in Forests and Global Change

ORIGINAL RESEARCH
published: 15 April 2021
doi: 10.3389/ffgc.2021.654375

Bark Effects on Stemflow Chemistry in a Japanese Temperate Forest I. The Role of Bark Surface Morphology

Ayano Oka[1], Junko Takahashi[2], Yoshikazu Endoh[3] and Tatsuyuki Seino[2,3†]*

[1] Graduate School of Life and Environmental Sciences, University of Tsukuba, Tsukuba, Japan, [2] Faculty of Life and Environmental Sciences, University of Tsukuba, Tsukuba, Japan, [3] Ikawa Forest Station, Mountain Science Center, University of Tsukuba, Ikawa, Japan

OPEN ACCESS

Edited by:
John T. Van Stan, Georgia Southern University, United States

Reviewed by:
Juan Whitworth-Hulse, CONICET Institute of Applied Mathematics San Luis (IMASL), Argentina
Seyed Mohammad Moein Sadeghi, University of Tehran, Iran

***Correspondence:**
Ayano Oka
sbtn.notchi@gmail.com

†Present address:
Tatsuyuki Seino, Yatsugatake Forest Station, Mountain Science Center, University of Tsukuba, Minamimaki, Japan

Specialty section:
This article was submitted to Forest Hydrology, a section of the journal Frontiers in Forests and Global Change

Received: *16 January 2021*
Accepted: *22 March 2021*
Published: *15 April 2021*

Citation:
Oka A, Takahashi J, Endoh Y and Seino T (2021) Bark Effects on Stemflow Chemistry in a Japanese Temperate Forest I. The Role of Bark Surface Morphology. Front. For. Glob. Change 4:654375. doi: 10.3389/ffgc.2021.654375

Stemflow can be an important pathway for the drainage of precipitation and related solutes through tree canopies to forest soils. As stemflow must drain along bark surfaces, the effects of bark structure on stemflow chemical composition is merited. This study examines the relationship between stemflow chemistry and bark surface structure for six species of varying bark morphology (four deciduous broadleaf trees and two evergreen coniferous trees) at a montane and an urban site in Japan. Stemflow from smooth-barked species contained greater concentrations of solutes that appear to be rinsed from the stem surface (i.e., sea salt aerosols); while, rougher-barked tree species contained greater or less concentrations of solutes that appear to be leached (e.g., Ca^{2+}) or taken-up (e.g., inorganic N) by the bark, respectively. Site-specific atmospheric environments also influenced thee bark-stemflow chemistry relationships—where the greater elemental deposition in the urban plot generally resulted in greater stemflow chemistry than observed in the lower-deposition montane plot. Our results therefore suggest that the dynamics of dry deposition wash-off by stemflow, and the exchange of dissolved solutes between stemflow and the bark surface, are influenced by the surface structure of the bark and the site's atmospheric environment. Therefore, the interactions between bark surface structure and its surrounding atmospheric environment are important factors in the stemflow-related elemental cycling between the tree and precipitation.

Keywords: bark morphology, direct rainfall, inorganic carbon, mineral cycling, stemflow, throughfall

INTRODUCTION

As rainfall drains through tree canopies, it becomes an important nutrient input to the forest floor. This is because a portion of the rainwater contacts the leaves, branches, and epiphytes of the tree canopy, becoming throughfall (droplets that pass through, and drip from the canopy), and stemflow (a portion that travels over the bark surface to the base of the tree stem). Throughfall and stemflow become chemically altered as solutes are leached from the tree canopy surfaces, dry-deposited components are washed away by the draining rainwaters, and these

surfaces (and/or their resident flora and fauna) uptake or transform solutes within the rainwater (Ponette-González et al., 2020). In forests, compared to other vegetated landscapes, throughfall accounts for the majority of the rainfall (Lin et al., 2020), while stemflow from trees rarely exceeds 2% of total rainfall (Van Stan and Gordon, 2018). Stemflow's small proportion of the canopy rainwater balance, however, does not prevent it from contributing significantly to the net rainfall nutrient flux (Levia and Germer, 2015). Because stemflow can collect water from a large area of the tree canopy and spatially concentrate this water to a small area at the base of the tree, 10^{-2}–10^{1} m^2 $tree^{-1}$ (Van Stan and Allen, 2020), it can be a concentrated nutrient flux worthy of investigation in ecosystem ecology and hydrology disciplines (Levia and Germer, 2015; Van Stan and Gordon, 2018). In fact, several studies in various forest systems have found stemflow to be able to contribute 10–51% of various dissolved inorganic N fluxes per hectare, despite being <10% of gross rainfall (Liu et al., 2003; Pilegaard et al., 2003; Oziegbe et al., 2011; Germer et al., 2012). Thus, it is necessary to incorporate stemflow in investigations of forest water and nutrient cycling processes.

Stemflow can be highly enriched in a variety of solutes, including inorganic cations (e.g., K^+, Na^+, Ca^{2+}, Mg^{2+}, NH_4^+), anions (e.g., Cl^-, SO^{2-}, NO_3^-) (Parker, 1983), and dissolved organic C (DOC: Stubbins et al., 2020). The chemical composition of stemflow can differ substantially among tree species and across forest settings (e.g., Limpert and Siegert, 2019; Liu et al., 2019; Su et al., 2019). Variability in stemflow chemistry across forest settings may be related to differences in surrounding landscape properties (Rodrigo et al., 2003), and storm synoptic patterns (Siegert et al., 2017). Stemflow chemical variability across species at the same site, may be due to interspecific differences in canopy structures that alter the canopies' ability to capture and accumulate aerosols or change the solute leaching and uptake properties of canopy surfaces (Levia et al., 2011). As stemflow drains primarily down bark-covered canopy elements (like branches and stems), some past research examining interspecific differences in stemflow chemistry has focused on differences in bark external structure (Levia and Herwitz, 2005; McGee et al., 2019).

The structure of the bark surface can affect stemflow chemistry by altering the amount and type of dry deposited materials capture on bark (Xu et al., 2019), the corticolous epiphytic vegetation and microbes (Magyar, 2008; McDonald et al., 2017), the bark surface area for solute exchange (Whittaker and Woodwell, 1967), and the water storage and residence time in the canopy (Levia and Herwitz, 2005). Few studies explicitly examine the interaction between bark surface structure and stemflow chemistry. Levia and Herwitz (2005) conducted a comparative study of the chemical composition and water retention of stemflow in three broad-leaved trees with different bark morphologies (*Betula lenta* L., *Carya glabra* Mill., and *Quercus rubra* L.) with a purpose similar to that of the present study, and reported that capacity of bark water storage and stemflow chemistry were different among bark surface morphology. Limpert and Siegert (2019) examined stemflow for a wider suite of solutes, including macronutrient ions and dissolved organic matter, and reported that thicker-barked (fire-tolerant) oaks produced more enriched stemflow than thinner-bark species, theoretically due to greater residence time. Su et al. (2019) reported the flux of inorganic ions in forests by stemflow analysis for deciduous trees with deeply furrowed bark and evergreen trees with smoother bark, finding that the stemflow from the deciduous trees was more chemically enriched due to greater surface area, contact time, and more dead materials in the rougher bark.

These studies show that the dynamics of bark surface-mediated solute exchange with stemflow can play a part in the nutrient cycle of forests. Thus, this study aims to build on these previous findings by conducting comparative evaluations of the impact of tree bark surface structure on stemflow chemistry (pH, dissolved organic carbon (DOC), dissolved inorganic carbon (DIC), Cl^-, NO_3^-, SO_4^{2-}, Na^+, NH_4^+, Mg^{2+}, Ca^{2+}, and K^+) across multiple tree species situated within study sites that represent pristine (the Minami Alps mountains) and suburban (Tokyo) sites in Japan. Seven tree species representing a range of bark surface structure, from smooth-to-rough, were selected for the study (**Figure 1**). We expect to reject the null hypothesis: stemflow chemistry will not differ among species of differing bark surface structure. Results are expected to show that, for stemflow from smoother-to-rougher bark: (i) solutes predominantly originating from wash-off (like Na^+, Cl^-, and DOC) and leaching (like Mg^{2+}, Ca^{2+}, and K^+) will become more concentrated; but (ii) solutes susceptible to being taken up or transformed by the bark surface (like NO_3^- and NH_4^+) will become less concentrated. The relationships between stemflow solute concentrations and bark surface structure are also expected to (iii) differ between sites due to the influence of human activities and differences in rainfall itself.

MATERIALS AND METHODS

Study Sites

The study sites included a montane, temperate forest in Tashiro of Shizuoka City, central Japan (the Shizuoka site, **Figure 1**); and, a suburban, temperate forest at the Tsukuba Experimental Forest, Mountain Research Center, University of Tsukuba, Japan (the Tsukuba site, **Figure 1**). For the Shizuoka site (35.307672 N, 138.199925 E), the elevation is 966 m a.s.l., the annual rainfall is 3110.1 mm, and the annual mean temperature is 11.4°C; the Tsukuba site (36.115326 N, 140.101504 E) has an elevation of 25 m a.s.l. and an annual rainfall of 1282.9 mm and an annual average temperature of 13.8°C (1981–2010 statistical period per AMeDAS: Japan Meteorological Agency, 2019). Canopy height of the study site at the Shizuoka site was approx. 20 m (Seino and Endoh, 2019), and at the Tsukuba site was almost the same as at the Shizuoka site (Seino, personal observations). The Shizuoka site is approx. 48 km far from the nearest coast, and the Tsukuba site is approx. 45 km away.

Study Species and Their Bark Structure

The tree species selected for this study included deciduous broadleaved and evergreen conifer species (**Figure 1**). The

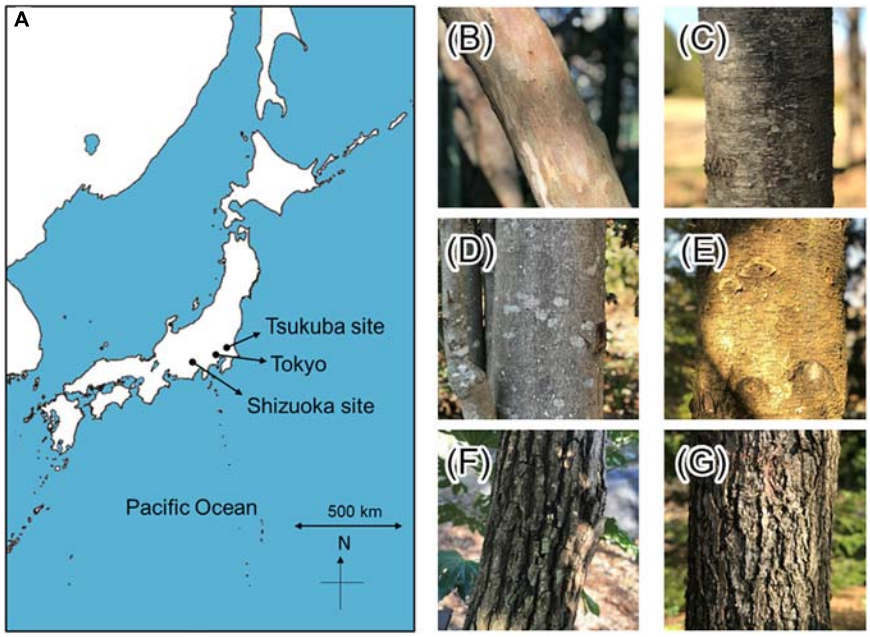

FIGURE 1 | (A) The study sites. The map scale is 1:5,164,000. The bark morphology of target species. **(B)** *Clethra barbinervis*, **(C)** *Padus grayana*, **(D)** *Magnolia obovata*, **(F)** *Abies firma*, **(G)** *Castanea crenata*, and **(H)** *Tsuga diversifolia.* The bark morphology of *Tsuga sieboldii* is the same as *T. diversifolia*.

selected deciduous broadleaved trees were found at both the montane and the suburban forest sites, and included *Clethra barbinervis* Siebold. & Zucc. (Japanese Clethra), *Padus grayana* Maxim. (Japanese bird cherry), *Magnolia obovata* Thunb. (Japanese whitebark magnolia), and *Castanea crenata* Siebold. & Zucc. (Japanese chestnut). The selected evergreen conifers included *Abies firma* Siebold. & Zucc. (momi fir) at both sites, *Tsuga sieboldii* Carr. (Japanese hemlock) only at Shizuoka site, and *Tsuga diversifolia* (Maxim.) Mast. (kometsuga) only at Tsukuba site. The bark types were categorized and photos showing the bark surface structure are provided in **Figure 1**. Both of the *Tsuga* species have a coarse, thick, exfoliating bark with fissures, where *T. diversifolia* has a vertically peeling bark structure while *T. sieboldii* has a square-like cracked and flaky bark structure. The bark of *A. firma* is scaley and has resinous blisters, which is smoother than the *Tsuga* species but rougher and thicker than many of the broadleaved species. *Clethra barbinervis* also has exfoliating bark, but it is the thinnest bark of all the study species—although the exfoliating bark flakes add a "mottling" to the surface. The bark of *P. grayana* is also quite smooth and thin; however, it is laterally marked by shallow lenticels. *Magnolia obovata* presents a stippled, gray bark that is moderately rough and thick, yet *C. crenata* has the thickest bark of all the study species and is deeply furrowed.

Rainfall and Stemflow Sampling

The study period ran from May to December 2018 with tree selection and equipment installation from May to August 2018. Sound individual trees with low inclination of the stem and little influence by other canopy cover or vine plants were selected as target trees. Rain and stemflow water samples were collected and chemically analyzed for four storms. Sampling dates for the Shizuoka site were September 11, September 26, October 17, and November 29 2018; and, for the Tsukuba site were September 12, September 23, October 10, and December 9 2018 (**Figure 2**). We recognize that sampling only four storms limits the power of our analyses due to under-replication. These storms represent a range of their rainfall amount and duration.

Rainfall was collected by drilling a hole in the lid of a 5 L polyethylene tank and attaching a 9 cm diameter funnel. To prevent litter and insects from entering the funnel, a ping-pong ball was placed in the funnel, and the entire funnel was covered with a net (**Figure 3**). One gauge each was installed at the Shizuoka and Tsukuba site. Stemflow was collected by installing collars to capture waters draining down the outside of the stem which drained these waters to polyethylene collection bins using the following methods. First, to prevent rainwater from seeping out of the collar, the lichen on the stems where the collar was to be installed was removed, and paraffin wax was applied. Second, a 5 cm wide, 5 mm thick rubber roll was placed beneath and fixed to the tree stem to divert the water draining down the bark surface into a 25 cm wide, 3 mm thick rubber sheet with a water intake valve at the bottom (which was wrapped around the stem). Instant adhesive and silicone for caulking were used to bond the rubber to the tree stem. One end of a vinyl hose, with water pipe sealing tape wrapped around both ends, was inserted into the outer rubber collar where the water outlet was located, and the other end was connected to a 5 L polyethylene tank with a hole drilled in the lid. Finally, rubber bands were used to secure the poly tank to the stem (**Figure 3**). In total, 148 water samples were obtained during the study period for the six target species with three replicate trees per species (Shizuoka

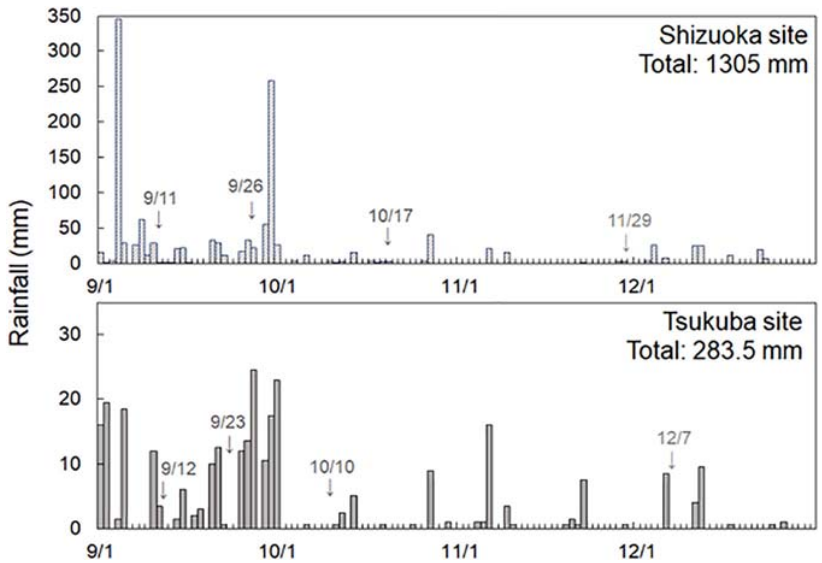

FIGURE 2 | Rainfall and sampling date from 1 September to 31 December 2018 at the Shizuoka and Tsukuba sites. Rainfall data at the Shizuoka site is from the Water Information System of the Ministry of Land, Infrastructure, Transport and Tourism (http://www1.river.go.jp/cgi-bin/SrchRainData.exe?ID=105031285523010&KIND=1&PAGE=0, last viewed 3 December 2019), and at Tsukuba site is measured by the meteorological station of the Tsukuba Experimental Forest, Mountain Science Center, University of Tsukuba.

site: rainfall (n = 4), stemflow (n = 72); Tsukuba site: rainfall (n = 4), stemflow (n = 68)). Between storms, rainfall and stemflow samplers were rinsed by DW after every sampling. Gauges were sampled within 24 h of the end of a storm event.

Chemical Analysis

Each water sample was filtered through a 0.45 μm filter (GLCTD-MCE2545, Shimadzu GLC, Tokyo), then the following chemical parameters were measured: pH, dissolved organic carbon (DOC), inorganic carbon (DIC), and inorganic ion concentrations (Cl^-, NO_3^-, SO_4^{2-}, Na^+, NH_4^+, Mg^{2+}, Ca^{2+}, and K^+). A total organic carbon analyzer (TOC-V CSH, Shimadzu, Kyoto) was used to measure DOC and DIC. Inorganic ion concentrations were measured using ion chromatography (Prominence series, Shimadzu, Kyoto). Calibration curves were prepared using five mixed standard solution for the peak area of each ion, and quantification was performed after confirming their correlation coefficients.

Statistical Analysis

Statistical analyses were performed using R version 3.4.2 (R Core Team, 2017) with a multiple-way analysis of variance (ANOVA) for comparing effects between sites and tree species, and differences among species were compared by one-way ANOVA and Tukey's multiple comparisons for chemistries of rainfall and stemflow. Heteroscedasticity of each values was checked by Bartlett's test before ANOVA. To evaluate patterns within the several stemflow chemical parameters, altogether, we applied a Principal Components Analysis on a matrix of log-transformed solute concentration data using the online ClustVis application[1] by Metsalu and Vilo (2015). ClustVis was chosen, not only due to its simplicity, but due to its ease of reproducibility.

RESULTS

Rainfall Solute Concentrations

Rainwater solute concentrations were all lower for the montane site (Shizuoka) compared to the urban site (Tsukuba) (**Figure 4**). Mean (±SD) of rainwater concentrations in DOC, Cl^-, SO_4^{2-}, Na^+, Mg^{2+}, Ca^{2+}, and K^+ for Shizuoka were 1.4 ± 0.6 mg L^{-1}, 6.3 ± 4.1 μmol L^{-1}, 2.2 ± 1.6 μmol L^{-1}, 7.7 ± 2.9 μmol L^{-1}, 1.3 ± 0.9 μmol L^{-1}, 0.1 ± 0.2 μmol L^{-1}, and 1.3 ± 2.2 μmol L^{-1}, respectively. For the Tsukuba site, rainwater concentrations of the same solutes were larger and more variable, being 4.4 ± 3.8 mg L^{-1}, 46.7 ± 31.9 μmol L^{-1}, 9.0 ± 3.4 μmol L^{-1}, 40.5 ± 27.6 μmol L^{-1}, 6.7 ± 3.0 μmol L^{-1}, 9.2 ± 4.0 μmol L^{-1}, and 7.4 ± 4.9 μmol L^{-1}, respectively. For the N solutes, all observations were below observation limits in rain samples from the montane Shizuoka site; while mean (±SD) NO_3^- and NH_4^+ concentrations for the urban site were 13.4 ± 9.1 μmol L^{-1} and 16.8 ± 15.3 μmol L^{-1}, respectively. Thus, all chemical parameters measured in rainfall, barring pH, were statistically significant between sites (unpaired t-test, $p > 0.05$) for pH, $p < 0.05$ for excepted pH).

Stemflow Chemical Variability Across Species of Differing Bark Roughness

Across the study species, there was a general trend of decreasing stemflow pH with increasing bark roughness, from 6.0 ± 0.4

[1]https://biit.cs.ut.ee/clustvis/

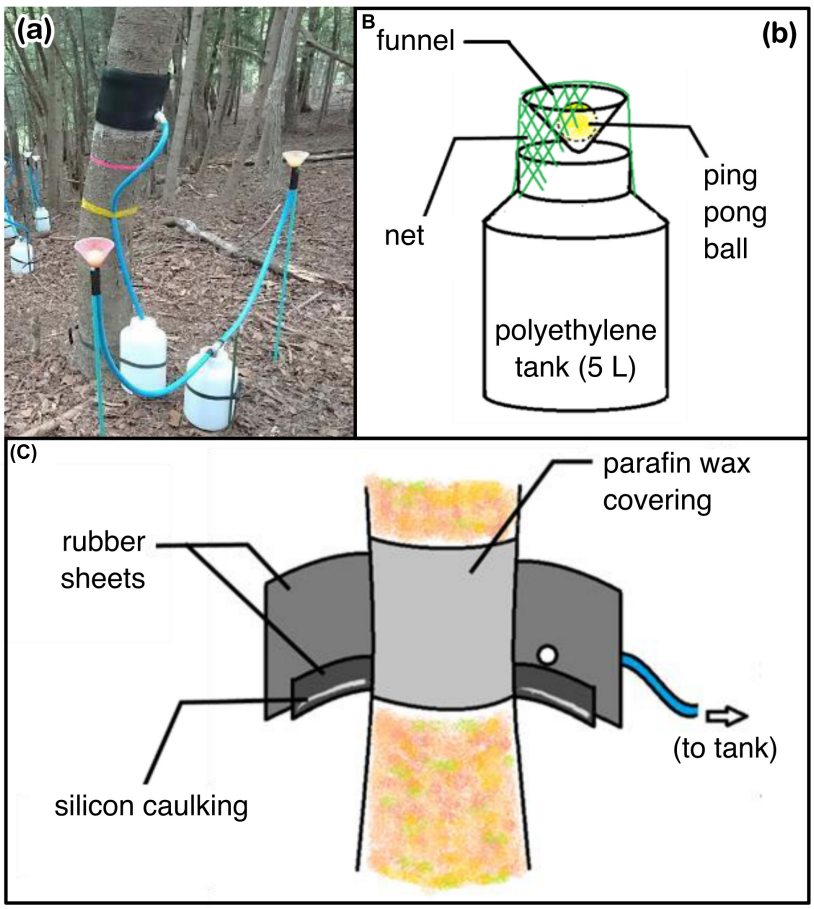

FIGURE 3 | Photograph and diagrams of the water sampling system. **(a)** Photograph of the implementation on *Abies firma* at the Shizuoka site, **(b)** diagram of water collector for direct rainfall, **(c)** water collection system for stemflow.

for smooth-barked (broadleaved) species like *C. barbinervis* and *P. grayana* to 5.5 ± 0.4 for rough-barked (evergreen) species like *T. sieboldii* and *T. diversifolia* (**Figure 4**). Na^+, SO_4^{2-}, Cl^-, and Ca^{2+} also showed the same trend as pH, and species and site effects were detected for Na^+ and Ca^{2+} [Two-way ANOVA, $F_{(5,\ 132)} = 3.07$, $p < 0.001$ for Na^+; $F_{(0.129)} = 2.81$, $p < 0.001$ for Ca^{2+}], while only site effects were detected for SO_4^{2-} [Two-way ANOVA, $F_{(1,\ 132)} = 3.07$, $p < 0.001$]. Deep teared bark type as *C. crenata* especially high in Ca^{2+}. Patterns of NH_4^+ were low in *C. barbinervis* and coniferous species. In broad-leaved trees, the concentration in *C. crenata* stemflow tended to be higher at both the Shizuoka and Tsukuba sites, while for conifers, the stemflow of *T. sieboldii* was higher than that of *A. firma* at the Shizuoka site, whereas that of *T. diversifolia* was lower than that of *A. firma* at the Tsukuba site (**Figure 4**).

Principal Components Analysis: Stemflow Chemical Variability Across Species and Sites

Further exploration of the several stemflow chemical parameters across species and sites was done by applying a principal components analysis (**Figure 5**). Two principal components were selected that represented 76% of the variability in the stemflow chemistry dataset [64% in component 1 (PC1) and 12% in component 2 (PC2)]. Individual stemflow observations per species at each site (faded-color symbols) were widely distributed across the principal components space (**Figure 5**). The mean principal component scores for each species' stemflow chemistry at each site (represented by solid-colored symbols) show more distinctly how these observations amalgamated into two broad clusters, based primarily on site-specific differences (rather than species- or bark-related differences). The loadings plot (lower right of **Figure 5**) indicates that primarily "washed off" solutes (i.e., Na^+, Cl^-, SO_4^{2-}) may explain the site-related clustering. This major site-related clustering based on solutes that were likely washed-off agrees with the rainfall data showing that the urban (Tsukuba) site had significantly higher rainwater solute concentrations compared to the montane (Shizuoka) site (**Figure 4**).

Secondarily, the loadings plot indicates that interspecies variability within these site-specific PCA clusters spread out in relation to their primarily "exchanged" solute concentrations (i.e., DOC, Ca^{2+}, K^+, and Mg^{2+}). The ordering of species

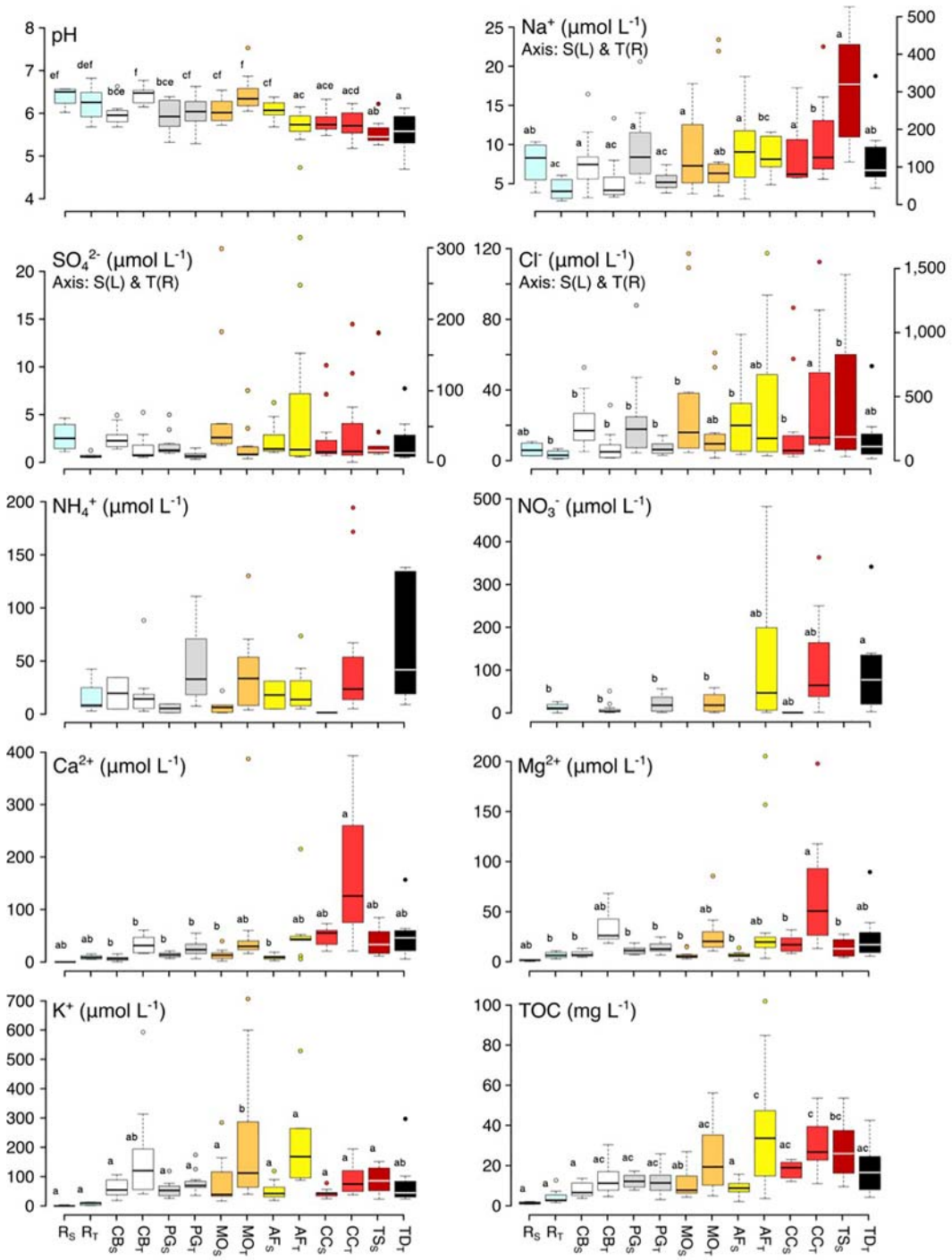

FIGURE 4 | Box-plot of TOC, pH, Cl^-, NO_3^-, SO_4^{2-}, Na^+, NH_4^+, Mg^{2+}, Ca^{2+}, and K^+concentrations of stemflow by species at foliated and defoliated periods. Species abbreviations are Clethra barbinervis (CB), Padus grayana (PG), Magnolia obovate (MO), Abies firma (AF), Castanea crenata (CC), Tsuga diversifolia (TD), and Tsuga sieboldii (TS). Different letters should indicate significant differences between factor levels. Bars in figure are SD. The letters in the figure mean that there is no difference according to Tukey's comparison.

with differing bark structure along the PCA plot's representation of solute "exchange" differs between sites. For the montane site, where solute deposition contributions were lower, the roughest-barked tree species, both broadleaved and needeleaved (*C. crenata*, *T. sieboldii*) plotted high on PC2 (**Figure 5**). A cluster of smoother-barked tree species at Shizuoka, also both broadleaved and needleleaved (*C. barbinervis, A. firma, M. obovata*) is observed in the negative domain of PC2. The

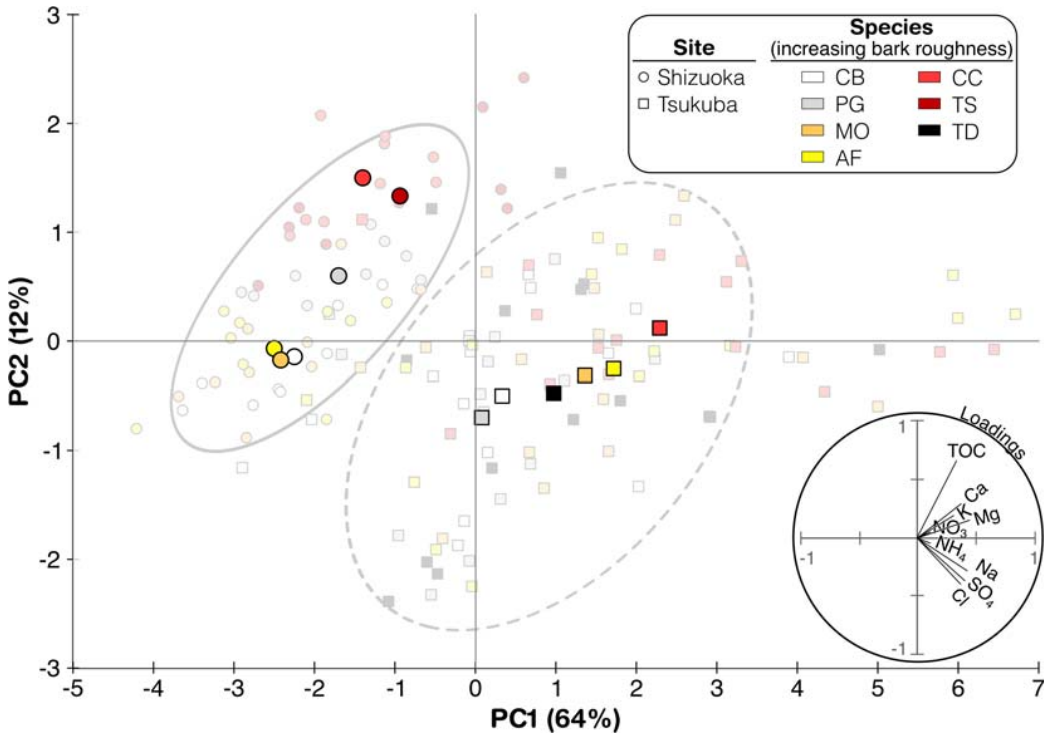

FIGURE 5 | Principal component analysis with TOC, pH, Cl^-, NO_3^-, SO_4^{2-}, Na^+, NH_4^+, Mg^{2+}, Ca^{2+}, and K^+ concentrations measured in the Shizuoka site (solid line) and the Tsukuba site (dotted line). The arrows represent variable eigenvectors in the space plotted by the first two PCA axes. The projection of the lines along each axis indicates their relative importance.

smooth-barked tree with deep lenticels, *P. grayana*, however, plotted intermediately between these other Shizuoka clusters on PC2. Interestingly, at the high-deposition urban site, Tsukuba, the interspecies variability within the PCA cluster is more evenly spaced along a continuum of smooth-to-rough bark (**Figure 5**). Although *T. diversifolia* is a rougher bark, it's peeling bark structure is qualitatively smoother than *T. sieboldii* (see **Figure 1**), which may explain its location within the PCA space, nearby to the other more moderately rough barked species (*A. firma, M. obovata*). Thus, this PCA plot suggests that deposition chemistry is the principal driver of stemflow chemistry in this study; moreover, the site with higher deposition chemistry (Tsukuba) also produced a more evenly spaced solute "exchange" continuum along bark roughness (**Figure 5**).

DISCUSSION

Stemflow Chemical Variability Across Bark Roughness

Stemflow solute concentration and composition varied significantly across the bark roughness continuum represented by our seven study tree species, including both broadleaved and evergreen species (**Figure 1**). Thus, these results reject the null hypothesis that stemflow chemistry will not differ among species of differing bark surface structure. Relationships along the smoother-to-rougher bark continuum for stemflow chemistry were consistent across sites, where solutes predominantly originating from atmospheric deposition and wash-off (like Na^+, Cl^-, and DOC) and leaching (like Mg^{2+}, Ca^{2+}, and K^+) generally increased with increasing bark roughness (**Figure 4**). Indeed, the PCA plot for stemflow data from the site with higher deposition, the urban Tsukuba site, showed this continuum relatively clearly (**Figure 5**). Reported solute concentrations fall within the range of those reported in previous stemflow literature (Parker, 1983; Levia and Germer, 2015; Van Stan and Stubbins, 2018). The higher stemflow solute concentrations from rough-barked trees, like *C. crenata* and *T. sieboldii*, also agree with the highly enriched stemflow solutions observed from similarly rough barked tree species, like *Quercus* species (Levia and Herwitz, 2005; Van Stan et al., 2017), *Cyclobalanopsis* species (Su et al., 2019), *Fraxinus pennsylvanica* (Schooling et al., 2017), *Liriodendron tulipifera* (Levia et al., 2011). Therefore, in combination with previous results, our study supports the conceptual model that bark structure may decrease bulk stemflow solute concentration by influencing both (a) the amount of materials captured by bark and (b) the amount of stemflow available to dilute those washed off (and exchanged) materials (Van Stan and Gordon, 2018).

On the other hand, stemflow solutes susceptible to being taken up or transformed by the bark surface (like NO_3^- and NH_4^+) displayed more complex responses across the species with changing bark roughness. In some cases, concentrations increased for smoother-barked trees, like mean NH_4^+ was higher

for *P. grayana* than (the very rough-barked) *C. crenata* at the Tsukuba site (**Figure 4**). We note that concentrations of NO_3^- and NH_4^+ were low or almost undetectable for stemflow from many species and many storms (**Figure 4**). And that the loadings plot in the PCA shows a very small effect of N ion concentrations on overall patterns of stemflow chemistry (**Figure 5**). The generally low concentrations of these solutes may be due to strong uptake, as several studies have reported net uptake of both NH_4^+ and NO_3^- across forest sites, for throughfall as well as stemflow (Parker, 1983; Kloeti et al., 1989; Crockford et al., 1996; Cavalier et al., 1997; André et al., 2008). The instances of high inorganic N concentrations (higher than rainfall N concentrations) for some species at the urban Tsukuba site—especially those with moderate-to-rough bark—may reflect the amount of N build-up within these barks due to the urban deposition of particulates (i.e., Xu et al., 2019) rather than increased leaching. Although, we acknowledge the possibility of canopy N losses due to urban impacts on its nutrient intrasystem cycling (i.e., Decina et al., 2018). There was no difference in pH between the bark types. In the case of broad-leaved species, the pH of the stemflow of *C. crenata* was low, while that of *B. grossa*, which has the same coarse longitudinally split bark, was higher in Takenaka et al. (1998) (*C. crenata*, 5.61; *Quercus crispula* Blume, 5.79 at Aichi, central Japan) and Tsukahara (1994) (*C. crenata*, 5.6; *Q. crispula*, 6.2; at Yamagata, northern Japan), suggesting species specificity due to another factors (regional differences and so on) than the bark characters.

Comparison of Stemflow Chemistry Across Sites

For stemflow, the Shizuoka (montane) and Tsukuba (urban) sites showed very different trends in solute concentrations and solute composition. NO_3^- concentrations at the Shizuoka site were not sufficiently high to be considered, while at the Tsukuba site, concentrations were high in most samples (**Figure 4**). This difference may be due to the urban atmospheric deposition at Tsukuba compared to Shizuoka (Lovett et al., 2000). The stemflow of *C. crenata*, *A. firma,* and *T. sieboldii* tended to be relatively high, and the stemflow of *A. firma* in particular increased rapidly. The concentration of Na^+ was 10–20 times higher at the Tsukuba site than at the Shizuoka site. In contrast to the Shizuoka site, there was no difference between species at the Tsukuba site. NH_4^+ was hardly detected in samples at the Shizuoka site but was detected in many samples at the Tsukuba site. Although the concentrations of Mg^{2+} and Ca^{2+} were remarkably higher at the Tsukuba site than at the Shizuoka site, the trends at each site were similar (**Figure 4**). There was a common tendency for lower concentrations of direct rainfall and higher concentrations of *C. crenata* in stemflow relative to that of *C. barbinervis, P. grayana,* and *M. obovata.* In the stemflow of conifers at the Shizuoka site, *A. firma* was higher, while *A. firma* was higher at the Tsukuba site. For K^+, the results were similar to those of Mg^{2+} and Ca^{2+}, while bark type had no effect, except for stemflow in *M. obovata,* and stemflow in *C. barbinervis*. Katagiri (1977) reported high Mg^{2+} and Ca^{2+} content in the trunk of *C. crenata* and high K^+ content in the leaves of *C. barbinervis*, suggesting that the nutrient content in each layer of the tree is involved in the dynamics of leaching substances.

Overall, the major differences between the Shizuoka and Tsukuba sites are thought to be differences in component concentrations due to differences in rainfall (**Figure 4**), and the presence or absence of nitrogen components due to differences in human activities such as traffic volume. The concentrations of Mg^{2+}, Ca^{2+}, and K^+ for TOC and inorganic ions in Oka et al. (2019) suggested that organic acids are leaching along with these base cations, while the current results suggest that the counterparts to organic acids are mainly Mg^{2+} and Ca^{2+}, which are influenced by bark. Besides, the concentrations of nitrogen and K^+ obtained from the Tsukuba site suggest that NH_4^+ and K^+ moving in conjunction. One reason for this is that the Tsukuba site is close to a farm, so components from the application of fertilizer were dispersed and detected in the stem stream. Besides, a comparison of the leaf-dressing and leaf-declining seasons showed a tendency for higher concentrations in the leaf-declining season, which may be due to the greater precipitation in summer than in winter (Eaton et al., 1973; Su et al., 2019).

An interesting cross-site finding, from the PCA plot, was that the solutes generally considered as exchangeable (DOC, K^+, etc.), showed little trend across the species of varying bark roughness at the montane site. However, there was a clear "lining up" of the species' stemflow chemistry (with regard to highly exchangeable solutes) along a general bark roughness continuum for the urban site, where deposition was much higher (**Figure 5**). We believe that this finding is interesting, because one would expect that higher deposition of soluble elements to these tree canopies would "mask" any potential trends in bark solute exchange—yet, the alignment along these loadings for PC2 is apparent (**Figure 5**). Is this an indication that high-deposition environments impact, not only the capture and washoff of solutes, but the exchange of related solutes? This is a reasonable question as urban atmospheric deposition is known to impact canopy physiology (Calfapietra et al., 2015). Alternatively, the trend observed in the PCA related to bark roughness and exchangeable solutes may have little-to-do with increased bark-water-solute exchange, and more-to-do with the increased capture of soluble aerosols by the more effective (rougher) "bark traps" for particulates (Magyar, 2008; Xu et al., 2019).

Comparison Between Conifers and Broad-Leaved Trees

Many studies have found a tendency of low pH in coniferous stemflows (Sassa et al., 1990; Levia and Germer, 2015). The results also showed a tendency to lower stemflow, especially in two *Tsuga* species. The pH of *C. crenata* and *A. firma* also tends to decrease in response to stemflow. It has been reported that stemflow in broad-leaved trees inhibits the acidification of soil during the process of rainfall reaching the soil (Sassa and Hasegawa, 1992; Neary and Gizyn, 1994). This may explain why this effect is lower in *C. crenata* and conifer leaves, which are less able to repel rainfall and stay in the tree canopy due to their hard and well-developed cuticle, and why it tends to be

different in coarse-barked *Q. crispula* and *J. mandshurica,* as mentioned in the comparison with previous studies (Shibata and Sakuma, 1996; Levia and Herwitz, 2005; Oka et al., 2019). In terms of TOC, SO_4^{2-}, Mg^{2+}, and Ca^{2+}, the relationship between *M. obovata* and *C. crenata* at the Shizuoka site corresponded to the relationship between *A. firma* and two *Tsuga* species, suggesting that there is also a bark influence between conifers and broad-leaved trees. On the other hand, in stemflow at the Shizuoka site, Cl^- was higher in *M. obovata* than in *C. crenata,* and that in *A. firma* was lower than in *T. sieboldii*; however, at the Tsukuba site, Cl^- was lower in *M. obovata* than in *C. crenata,* and that in *A. firma* was higher than that in *T. diversifolia*, which was the complete opposite of the trend for conifers and broad-leaved trees. This is because the amount of stock of dry deposition on trees differs due to the difference in rainfall between sites, and the amount of stock is low in *M. obovata* and easy to retain in *C. crenata.* Rainfall capture by canopy leaves were different broad-leaved trees and confers, and this was affected to stemflow chemistry (Shibata and Sakuma, 1996; Abbasian et al., 2015; Su et al., 2019). Besides, the leaf area of *Magnolia* and *Castanea* is relatively large, even as compared to other broad-leaved trees (White, 1983), and conifers have small needle leaves.

CONCLUSION

The results of this study agree with research at other sites that bark surface structure is related to stemflow chemistry. Additionally, this relationship between bark surface structure and stemflow chemistry at our sites depended on the tree canopies external environment (specifically, whether the atmospheric deposition environment was montane or urban). Site-specific differences appear to be driven by increased wet deposition (more concentrated rainfall chemistry) at the urban site compared to the montane site. The retention capacity of (assumed) dry deposited elements was different between study trees with smooth and rough barks—and their mobilization by stemflow depended on the rainfall amount at each site. At the Shizuoka site, where there is more (chemically dilute) rainfall, the smooth bark type, with its thin bark structure without grooves, appears to immediately rinse the bark of soluble minerals. On the other hand, the coarse bark type, with multi-layered and wavy surface structures, permitted the bark to store substantial amounts of soluble materials that became available during the stemflow process in the Shizuoka site. Our results support a growing body of literature that suggest bark surface structure can affect the dynamics of elemental cycling in the forest ecosystem by influencing stemflow chemistry.

DATA AVAILABILITY STATEMENT

The original contributions presented in the study are included in the article/supplementary material, further inquiries can be directed to the corresponding author/s.

AUTHOR CONTRIBUTIONS

AO, YE, and TS collected samples. AO and JT carried out chemical analyses. All authors contributed to the writing of the manuscript, conceived and designed the research plan.

FUNDING

This study was partly supported by a Grant-in-Aid from the Mountain Research Center, University of Tsukuba.

ACKNOWLEDGMENTS

We are grateful to Yoshihiko Tsumura, Takashi Kamijo, and laboratory members of Ikurinken for their helpful advice; JV and the two reviewers for manuscript improvements; Shozo Kato of Kato Limited Partnership Company and staff members of the Ikawa Forest Station, Mountain Research Center, University of Tsukuba, for their kind support at the Shizuoka site; and Junya Tamaoki and Miho Sato of the Tsukuba Experimental Forest, Mountain Research Center, University of Tsukuba, for their kind support at the Tsukuba site. This research is part of a Master thesis of the University of Tsukuba by AO.

REFERENCES

Abbasian, P., Attarod, P., Sadeghi, S. M. M., Van Stan, J. T., and Hojjati, S. M. (2015). Throughfall nutrients in a degraded indigenous forest and a plantation in the of North of Iran. *Forest Systems* 24:e035. doi: 10.5424/fs/2015243-06764

André, F., Jonard, M., and Ponette, Q. (2008). Effects of biological and meteorological factors on stemflow chemistry within a temperate mixed oak–beech stand. *Sci. Total Environ.* 393, 72–83.

Calfapietra, C., Peñuelas, J., and Niinemets, Ü (2015). Urban plant physiology: adaptation-mitigation strategies under permanent stress. *Trends Plant Sci.* 20, 72–75. doi: 10.1016/j.tplants.2014.11.001

Cavalier, J., Jaramillo, M., Solis, D., and de León, D. (1997). Water balance and nutrient inputs in bulk precipitation in tropical montane cloud forest in Panama. *J. Hydrol.* 193, 83–96. doi: 10.1016/S0022-1694(96)03151-4

Crockford, R. H., Richardson, D. P., and Sageman, R. (1996). Chemistry of rainfall, throughfall and stemflow in a Eucalypt forest and a Pine plantation in south-eastern Australia: 3. *Stemflow Total Inputs* 10, 25–42.

Decina, S. M., Templer, P. H., and Hutyra, L. R. (2018). Atmospheric inputs of nitrogen, carbon, and phosphorus across an urban area: unaccounted fluxes and canopy influences. *Earth's Future* 6, 134–148. doi: 10.1002/2017ef000653

Eaton, J. S., Likens, G. E., and Bormann, H. (1973). Throughfall and stemflow chemistry in a northern hardwood forest. *J. Ecol.* 61, 495–508. doi: 10.2307/2259041

Germer, S., Zimmermann, A., Neill, C., Krusche, A. V., and Elsenbeer, H. (2012). Disproportionate single-species contribution to canopy-soil nutrient flux in an Amazonian rainforest, For. *Ecol. Manage* 267, 40–49. doi: 10.1016/j.foreco.2011.11.041

Japan Meteorological Agency (2019). *AMeDAS: 1981–2010, Ministry of Land, Infrastructure, Transport, and Tourism Meteorological Agency HP*. Tokyo: Japan Meteorological Agency.

Katagiri, S. (1977). *Studies on Mineral Cycling in a Deciduous Broad-leaved Forest at Sanbe Forest of Shimane University (IV): Concentration of Nutrient Elements of Trees*. Rome: FAO.

Kloeti, P., Keller, H. M., and Guecheva, M. (1989). *Effects of Forest Canopy on Throughfall Precipitation Chemistry*. Baltimore: Baltimore Symposium.

Levia, D. F., and Germer, S. (2015). A review of stemflow generation dynamics and stemflow-environment interactions in forests and shrublands. *Rev. Geophys.* 53, 673–714. doi: 10.1002/2015RG000479

Levia, D. F., and Herwitz, S. R. (2005). Interspecific variation of bark water storage capacity of three deciduous tree species in relation to stemflow yield and solute flux to forest soils. *Catena* 64, 117–137. doi: 10.1016/j.catena.2005.08.001

Levia, D. F., Van Stan, J. T., Siegert, C. M., Inamdar, S. P., Mitchell, M. J., Mage, S. M., et al. (2011). Atmospheric deposition and corresponding variability of stemflow chemistry across temporal scales in a mid-Atlantic broadleaved deciduous forest. *Atmospheric Environ.* 45, 3046–3054.

Limpert, K., and Siegert, C. (2019). Interspecific differences in canopy-derived water, carbon, and nitrogen in upland oak-hickory forest. *Forests* 10:1121.

Lin, M., Sadeghi, S. M. M., and Van Stan, J. T. (2020). Partitioning of rainfall and sprinkler-irrigation by crop canopies: a global review and evaluation of available research. *Hydrology* 7:76. doi: 10.3390/hydrology7040076

Liu, W., Fox, J. E. D., and Xu, Z. (2003). Nutrient budget of a montane evergreen broad-leaved forest at ailao mountain national nature reserve, yunnan, southwest China. *Hydrol. Processes* 17, 1119–1134.

Liu, Y., Jiang, L., You, C., Li, H., Tan, S., Tan, B., et al. (2019). Base cation fluxes from the stemflow in three mixed plantations in the rainy zone of western China. *Forests* 10:1101. doi: 10.3390/f10121101

Lovett, G. M., Traynor, M. M., Pouyat, R. V., Carreiro, M. M., Zhu, W. X., and Baxter, J. W. (2000). Atmospheric deposition to oak forests along an urban–rural gradient. *Environ. Sci. Technol.* 34, 4294–4300. doi: 10.1021/es001077q

Magyar, D. (2008). The tree bark: a natural spore trap. *Asp Appl. Biol.* 89, 7–16.

McDonald, L., Van Woudenberg, M., Dorin, B., Adcock, A. M., McMullin, R. T., and Cottenie, K. (2017). The effects of bark quality on corticolous lichen community composition in urban parks of southern Ontario. *Botany* 95, 1141–1149. doi: 10.1139/cjb-2017-0113

McGee, G. G., Cardon, M. E., and Kiernan, D. H. (2019). Variation in Acer saccharum Marshall (sugar maple) bark and stemflow characteristics: implications for epiphytic bryophyte communities. *Northeastern Nat.* 26, 214–235. doi: 10.1656/045.026.0118

Metsalu, T., and Vilo, J. (2015). ClustVis: a web tool for visualizing clustering of multivariate data using principal component analysis and heatmap. *Nucleic Acids Res.* 43, W566–W570.

Neary, A. J., and Gizyn, W. I. (1994). Throughfall and stemflow chemistry under deciduous and coniferous forest canopies in south-central Ontario. *Canadian J. Forest Res.* 24, 1089–1100. doi: 10.1139/x94-145

Oka, A., Takahashi, J., Endoh, Y., and Seino, T. (2019). Effect of bark characteristics on stemflow and its chemical components. *Nagoya Repositary.* 67, 29–34.

Oziegbe, M. B., Muoghalu, J. I., and Oke, S. O. (2011). Litterfall, precipitation and nutrient fluxes in a secondary lowland rain forest in Ile-Ife, Nigeria. *Acta Bot. Brasil.* 25, 664–671. doi: 10.1590/S0102-33062011000300020

Parker, G. G. (1983). Throughfall and stemflow in the forest nutrient cycle. *Adv. Ecol. Res.* 13, 57–133. doi: 10.1016/s0065-2504(08)60108-7

Pilegaard, K., Mikkelsen, T. N., Beier, C., Jensen, N. O., Ambus, P., and Ro-Poulsen, H. (2003). Field measurements of atmosphere-biosphere interactions in a Danish beech forest. *Boreal Environ. Res.* 8, 315–333.

Ponette-González, A. G., Van Stan, J. T., and Magyar, D. (2020). "Things seen and unseen in throughfall and stemflow," in *Precipitation Partitioning by Vegetation*, eds J. T. Van Stan, E. Gutmann, and J. Friesen (Cham: Springer), 71–88. doi: 10.1007/978-3-030-29702-2_5

R Core Team (2017). *R: A Language and Environment for Statistical Computing*. Vienna: R Core Team.

Rodrigo, A., Avila, A., and Roda, F. (2003). The chemistry of precipitation, throughfall and stemflow in two holm oak (Quercus ilex L.) forests under a contrasted pollution environment in NE Spain. *Sci. Total Environ.* 305, 195–205. doi: 10.1016/s0048-9697(02)00470-9

Sassa, T., Goto, K., Hasegawa, K., and Ikeda, S. (1990). *Acidity and Nutrient Elements of the Rainfal1, Throughfall and Stemflow in the Typical Forests Around Morioka City, Iwate Pref., Japan. Characteristic pH Value of the Stemflow in Several Tree Species*. Rome: FAO, doi: 10.18922/jjfe.32.2_43

Sassa, T., and Hasegawa, K. (1992). *Suppression of Soil Acidification by the Stemflow of Some Tree Species. The Case of Yellow-poplar (tulip tree)*. Rome: FAO, doi: 10.11519/jjfs1953.74.5_437

Schooling, J. T., Levia, D. F., Carlyle-Moses, D. E., Dowtin, A. L., Brewer, S. E., Donkor, K. K., et al. (2017). Stemflow chemistry in relation to tree size: A preliminary investigation of eleven urban park trees in British Columbia, Canada. *Urban Forestry Urban Green.* 21, 129–133. doi: 10.1016/j.ufug.2016.11.013

Seino, T., and Endoh, Y. (2019). Ecological positions of conifers on the stand structure of the temperate forest in central Japan. *Chubu Forestry Res.* 67, 25–28. doi: 10.18999/chufr.67.25

Shibata, H., and Sakuma, T. (1996). Canopy modification of precipitation chemistry in deciduous and coniferous forests affected by acidic deposition. *Soil Sci. Plant Nutrit.* 42, 1–10. doi: 10.1080/00380768.1996.10414683

Siegert, C. M., Levia, D. F., Leathers, D. J., Van Stan, J. T., and Mitchell, M. J. (2017). Do storm synoptic patterns affect biogeochemical fluxes from temperate deciduous forest canopies? *Biogeochemistry* 132, 273–292.

Stubbins, A., Guillemette, F., and Van Stan, J. T. II (2020). "Throughfall and stemflow: the crowning headwaters of the aquatic carbon cycle," in *In Precipitation Partitioning by Vegetation*, eds J. T. Van Stan, E. Gutmann, and J. Friesen (Cham: Springer), 121–132. doi: 10.1007/978-3-030-29702-2_8

Su, L., Zhao, C., Xu, W., and Xie, Z. (2019). Hydrochemical fluxes in bulk precipitation, throughfall, and stemflow in a mixed evergreen and deciduous broadleaved forest. *Forests* 10:507. doi: 10.3390/f10060507

Takenaka, C., Suzuki, M., Yamaguchi, N., and Shibata, E. (1998). Chemical characteristics of stem flow collected from deciduous trees. *Nagoya University Forest Sci.* 17, 11–17.

Tsukahara, H. (1994). Studies on the chemical properties of stemflow (I) differences in EC, pH, and major ion concentrations among tree species. *Trans. Japanese For. Society* 105, 407–410. (in Japanese)

Van Stan, J. T., and Allen, S. T. (2020). What we know about stemflow's infiltration area. *Front. For. Glob. Chang.* 3, 1–7. doi: 10.3389/ffgc.2020.00061

Van Stan, J. T., and Gordon, D. A. (2018). Mini-Review: stemflow as a resource limitation to near-stem soils. *Front. Plant Sci.* 9:248. doi: 10.3389/fpls.2018.00248

Van Stan, J. T., and Stubbins, A. (2018). Tree-DOM: dissolved organic matter in throughfall and stemflow. *Limnol. Oceanography Lett.* 3, 199–214. doi: 10.1002/lol2.10059

Van Stan, J. T., Wagner, S., Guillemette, F., Whitetree, A., Lewis, J., Silva, L., et al. (2017). Temporal dynamics in the concentration, flux, and optical properties of tree-derived dissolved organic matter in an epiphyte-laden oak-cedar forest. *J. Geophys. Res.: Biogeosci.* 122, 2982–2997. doi: 10.1002/2017jg004111

White, P. S. (1983). Corner's rules in eastern deciduous trees: allometry and its implications for the adaptive architecture of trees. *Bull. Torrey Botan. Club.* 110, 203–212. doi: 10.2307/2996342

Whittaker, R. H., and Woodwell, G. M. (1967). Surface area relations of woody plants and forest communities. *Am. J. Botany* 54, 931–939. doi: 10.1002/j.1537-2197.1967.tb10717.x

Xu, X., Yu, X., Mo, L., Xu, Y., Bao, L., and Lun, X. (2019). Atmospheric particulate matter accumulation on trees: a comparison of boles, branches and leaves. *J. Clean. Product.* 226, 349–356. doi: 10.1016/j.jclepro.2019.04.072

Conflict of Interest: The authors declare that the research was conducted in the absence of any commercial or financial relationships that could be construed as a potential conflict of interest.

frontiers in Forests and Global Change

ORIGINAL RESEARCH
published: 20 April 2021
doi: 10.3389/ffgc.2021.668682

Bark Water Storage Plays Key Role for Growth of Mediterranean Epiphytic Lichens

Philipp Porada[1]* *and Paolo Giordani*[2]

[1] Ecological Modeling, Department of Biology, University of Hamburg, Hamburg, Germany, [2] DIFAR - Università di Genova, Genova, Italy

Epiphytic lichens are a characteristic feature of many forests around the world, where they often cover large areas on stems and branches. Recently, it has been found that lichens may contribute substantially to carbon and nutrient uptake in forests. Moreover, they have a large influence on interception of rainfall at the global scale, which leads to a shift of the water balance toward evaporation and a cooling of near-surface air temperature. It is thus crucial to understand which environmental factors are relevant for their growth and survival, and which potential risks may result from climate change. Water supply is a key factor which controls active time and, consequently, the carbon balance of the epiphytes. However, it is largely unclear, to what extent different modes of water uptake, which include bark water, may affect active time and growth under varying environmental conditions. Quantitative estimates on the relevance of bark water storage and its interspecific variation are, however, missing. Here, we apply the process-based, dynamic non-vascular vegetation model LiBry to assess the relevance of bark water for epiphytic lichens. LiBry not only accounts for the main physiological processes of mosses and lichens, it also represents explicitly the diversity of the organisms, by simulating a large number of possible physiological strategies. We run the model for a site in Sardinia, where epiphytic lichens are abundant. Moreover, the Mediterranean region is of interest due to likely substantial effects of global warming on local epiphytes. For current climatic conditions, the LiBry model predicts net primary production (NPP) of 32 $g\,C\,m^{-2}a^{-1}$ per stem area and biomass of 48 $g\,C\,m^{-2}$ for the study region. In a second run, where uptake of bark water is switched off in the model, estimated NPP is reduced by 21%. Moreover, the simulated number of surviving strategies, representing physiological diversity, decreases by 23%. This is accompanied by changes in the simulated community composition, where strategies which have a more compact thallus increase their share on the total cover. Hence, our model simulation suggests a substantial role of bark water for growth and morphology of epiphytic lichens in Sardinia.

Keywords: vegetation model, ecophysiology, functional diversity, epiphytic lichen, Mediterranean vegetation, DGVM, non-vascular plants, precipitation partitioning

OPEN ACCESS

Edited by:
Anna Klamerus-Iwan, University of Agriculture in Krakow, Poland

Reviewed by:
Ewa Papierowska, Warsaw University of Life Sciences, Poland
Marcin Dyderski, Institute of Dendrology (PAN), Poland

***Correspondence:**
Philipp Porada
philipp.porada@uni-hamburg.de

Specialty section:
This article was submitted to Forest Hydrology, a section of the journal Frontiers in Forests and Global Change

Received: *17 February 2021*
Accepted: *22 March 2021*
Published: *20 April 2021*

Citation:
Porada P and Giordani P (2021) Bark Water Storage Plays Key Role for Growth of Mediterranean Epiphytic Lichens. Front. For. Glob. Change 4:668682. doi: 10.3389/ffgc.2021.668682

1. INTRODUCTION

Non-vascular (NV) epiphytes, such as lichens or mosses, are a characteristic feature of many tropical, temperate, and boreal forests around the world. Their epiphytic life style makes them largely dependent on water supply from the atmosphere, which is available in the canopy in form of throughfall, stemflow, dew, or fog, and which usually shows high temporal variability (Hargis et al., 2019). Moreover, NV epiphytes have no means of actively controlling water loss, in contrast to the stomata of vascular plants. The organisms are, however, adapted to these conditions through poikilohydry, the ability to deactivate their metabolism when they dry out, and reactivate when water becomes available again (e.g., Proctor et al., 2007; Kranner et al., 2008).

Due to the substantial amount of NV epiphytic biomass in many forests around the world (Van Stan and Pypker, 2015), their water storage may significantly affect interception of rainfall and increase evaporation at the global scale (Porada et al., 2018). Furthermore, due to this larger amount of water vapor transported from the land surface to the atmosphere, the heat flux due to convection of warm air is reduced, which may lead to cooling of the land surface (Davies-Barnard et al., 2014). Another impact of NV epiphytes on ecosystems is the alteration of throughfall and stemflow chemistry, resulting from biotic nitrogen fixation, capturing of nutrients from wet and dry deposition, or bioaccumulation of elements. Moreover, these properties make the organisms suitable bioindicators. The collected compounds may then be leached during rainfall events, depending on their chemical state and the capability of the NV epiphytes to retain them (Klos et al., 2005). Furthermore, the organisms recycle nutrients leached from vascular plant biomass or derived from decaying leaf litter (Van Stan and Pypker, 2015).

The various ecosystem functions carried out by NV epiphytes may be significantly affected by climate change. NV epiphytes adapted to warmer climatic conditions in temperate or boreal-montane climates may benefit from climatic change (Aptroot and van Herk, 2007). However, multiple studies expect negative impacts of climate change on NV epiphytes in the course of global warming in different regions of the world. Reductions in the distribution range of epiphytic lichens already occur in Southern Europe, for instance (Nascimbene et al., 2016). Furthermore, experiments suggest that tropical epiphytic bryophytes may suffer from prolonged drought periods (Metcalfe and Ahlstrand, 2019), same as cold-adapted epiphytic lichens in boreal regions (Smith et al., 2018). Also statistical modeling approaches, such as species distribution models, predict that NV epiphytes will be often negatively affected by climate change (Ellis et al., 2007; Rubio-Salcedo et al., 2017; Ellis and Eaton, 2021).

Impacts of changing climatic conditions will likely be modulated, and often amplified, by management practices, such as intensified forest management. The lack of old trees and increased dryness due to edge effects, for instance, may have additional negative effects on NV epiphytes (Johansson, 2008). In addition to general habitat loss, the disappearance of certain forest types and host tree species may have detrimental effects for NV epiphyte communities (Nascimbene and Marini, 2010; Wierzcholska et al., 2020). Thereby, loss of host trees may not only be caused by management, but also result from invasive species, such as the black locust (Nascimbene et al., 2020). Furthermore, also changes in atmospheric deposition of nutrients or pollutants may, in combination with host tree species, have stronger impacts on NV community composition than climate (Łubek et al., 2018).

Hence, both climatic and non-climatic factors, such as the substrate, will most probably play a crucial role in future abundance of NV epiphytes. Changes in these factors may not only affect amount and timing of water supply, but also lead to shifts in water source, which may affect community composition and abundance of NV epiphytes (Rodríguez-Quiel et al., 2019). Impacts on community composition may result from physiological adaptation of the organisms to the predominant mode of water supply, both at the inter-specific and also at the intra-specific level (Gauslaa, 2014).

For many NV epiphyte species, water flow along the bark, so-called stemflow, may represent a substantial contribution to their water supply. While stemflow is generally small compared to throughfall, in some forests it may account for up to a third of precipitation (Van Stan and Gordon, 2018). Since stemflow is a relatively fast process, NV epiphytes may require adaptations for an efficient uptake of water, such as rhizinomorphs, for instance (Valladares et al., 1998; Gauslaa, 2014; Merinero et al., 2014). Thereby, the utilization of stemflow by the organisms as a water source may be facilitated by temporary storage of water in the bark. The bark water reservoir usually has a size of a few millimeters of water or less, and it differs both within and between tree species (Klamerus-Iwan et al., 2020). It has been shown that bark properties, which also vary between tree species, may have a significant impact on the community composition of NV epiphytes (Kenkel and Bradfield, 1981; Bates, 1992). In particular, tree-specific bark water storage capacity may explain a part of the variation in NV epiphyte species richness between tree species (Jagodziński et al., 2018).

Although the potential importance of bark water storage for NV epiphytes has been recognized (e.g., Franks and Bergstrom, 2000), it is largely unclear how relevant the uptake of water from bark is for the water supply, and, consequently, the carbon balance of NV epiphytes in general. Furthermore, it is poorly known which factors control intra- and inter-specific variation of NV epiphytes regarding the ability to take up water from the bark reservoir. It is likely that physiological trade-offs exist between the capacity to utilize bark water and other properties associated with the water balance of the organisms, such as pore size distribution or specific thallus mass (Valladares et al., 1993; Porada et al., 2013).

The aim of this study is to assess the role of the bark water reservoir for the water balance and growth of NV epiphytes in a quantitative way. To this end, we formulate the following hypotheses:

1. The bark water reservoir represents a relevant source of water supply for NV epiphytes,
2. NV epiphytes are able to remain active for longer periods of time due to the bark water reservoir, and show thus a higher productivity,

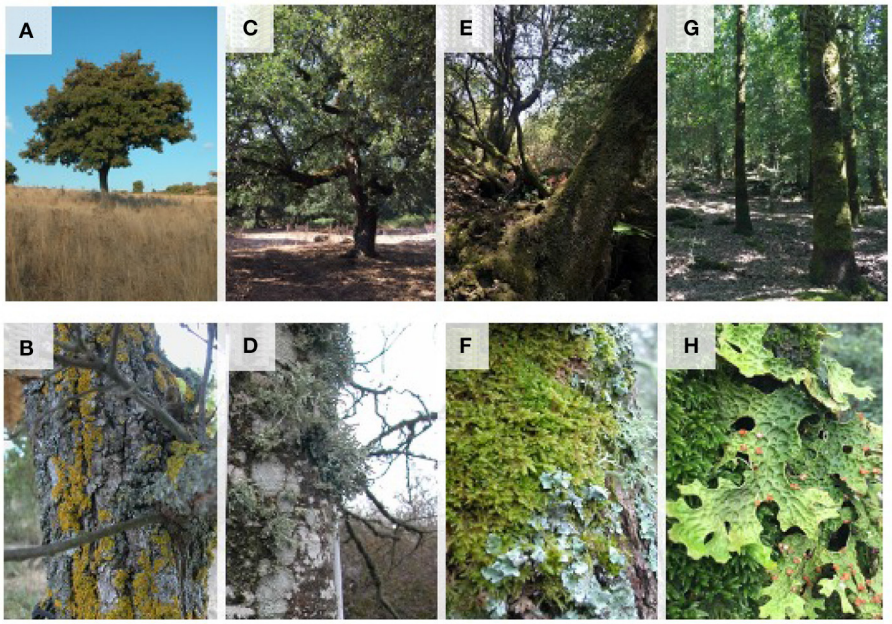

FIGURE 1 | Epiphytic NV vegetation in different habitats of the study area: isolated trees in open grassland areas **(A)** mainly colonized by xerophilous species of narrow-lobed foliose and crustose lichens **(B)**; agroforestry areas with thermophilous oak woodlands **(C)** with species-rich communities of foliose, crustose, and fruticose lichens **(D)**; open holm-oak forests in mountainous areas **(E)** with epiphytic communities of bryophytes and hygrophilous foliose lichens **(F)**; mature holm-oak and downy oak forests **(G)** colonized by extensive mossy mats and large foliose lichens of the genus Lobaria **(H)**.

3. The bark water reservoir affects the community composition of NV epiphytes.

We examine these hypotheses using the process-based non-vascular vegetation model LiBry (e.g., Porada et al., 2013, 2018). The LiBry model computes the main physiological functions of non-vascular vegetation which are connected to carbon, water and energy balances, based on climatic input data and other environmental conditions. Through variation of the bark water storage capacity in LiBry, we are able to quantify the relative importance of water uptake from bark compared to other sources, and the associated effects on productivity and growth. Furthermore, LiBry accounts explicitly for diversity of the organisms by simulating a large number of different physiological strategies. This makes the model ideal to study potential trade-offs connected to bark water uptake, and to elucidate the impacts of the mode of water supply on community composition of NV epiphytes.

We apply LiBry at the local scale for a field site in Sardinia. The site constitutes a good model for the study in question because it comprises a considerable set of Mediterranean ecosystems, both forest and open wooded areas. Despite the fact that the area is subject to strong water deficits for many months of the year, it hosts a remarkable diversity and morpho-functional variety of NV epiphytes (Giordani et al., 2019, see also **Figure 1**) adapted to the different available water sources. Finally, we discuss the implications of our findings for potential shifts in abundance and community composition of NV epiphytes under climate change, and for the feedback of the organisms on precipitation partitioning.

2. METHODS

2.1. Model Description

The process-based Lichen and Bryophyte model (LiBry) which is applied in this study was developed to estimate carbon uptake by non-vascular vegetation at the global scale, based on climatic conditions, in order to quantify the contribution of the organisms to the global carbon balance, and, furthermore, to other global biogeochemical cycles (Porada et al., 2013, 2014, 2017). The model version used here builds on the latest developments, published in Porada et al. (2018), Porada et al. (2019), and Baldauf et al. (2020).

LiBry is a dynamic global vegetation model (DGVM), which focuses on non-vascular organisms, such as lichens and bryophytes, but also simulates terrestrial algae and cyanobacteria. Vascular vegetation, such as trees and grasses, is represented only in a simplified way, to provide boundary conditions for the non-vascular organisms, such as area for growth of epiphytes, for example. The main basic physiological functions, which lichens and bryophytes share with vascular plants, such as photosynthesis or respiration, and their climatic drivers, such as radiation, temperature, or precipitation, are simulated in LiBry similarly to other, vascular, DGVMs. The same is true for biophysical processes connected to the energy and water balance. Beyond these, however, LiBry includes various processes

which are specific to non-vascular vegetation. In particular, the organisms' lack of active control over water loss is represented in the model (poikilohydry), which distinguishes them from the homoiohydric vascular plants that regulate their water loss via stomata. This is compensated, also in the model, by the ability of non-vascular organisms to deactivate their metabolism upon drying, which allows them to survive long periods without water supply (e.g., Proctor, 2000).

Moreover, the LiBry model explicitly takes into account physiological trade-offs with regard to the interactions of vegetation and environment. The concept of trade-offs is central to the functioning of modern DGVMs, and allows to connect the modeled carbon budget of plants to the adaptation to different climatic conditions. Vascular plants in DGVMs, for instance, may allocate assimilated carbon either to roots or to shoots, while ambient climate determines which allocation pattern is advantageous. The LiBry model considers multiple trade-offs which are key to the ecophysiology of non-vascular vegetation, such as the trade-off between metabolic activity and CO_2-uptake from the atmosphere. The water, which the organisms accumulate in their bodies to be active and to assimilate carbon, partly leads to blocking of the diffusion pathways for CO_2 from the atmosphere to the chloroplasts. Consequently, a species-specific optimum water saturation exists where metabolic activity is sufficient, but photosynthesis is not yet substantially limited by CO_2 diffusion (Lange et al., 1999). The extent of the reduction in CO_2-diffusivity with increasing water content depends largely on the pore size distribution of the non-vascular tissue (Valladares et al., 1993). Organisms which have a large fraction of small pores experience diffusion limitation more strongly than organisms which have, on average, larger pores. However, at low water content, small pores can be of advantage, since they retain water more efficiently due to capillary forces. Moreover, the low water potential inside the organism, resulting from small pore sizes, allows for uptake of water from unsaturated air. It has been shown that activation from air humidity alone may be relevant for the annual carbon gains of NV epiphytes (Jonsson Čabrajić et al., 2010). In a similar way, uptake of water from the bark water reservoir may be driven by a gradient in water potential between the unsaturated tissue of NV epiphytes and the saturated bark. The physiological trade-offs connected to the ability of bark water uptake may thus determine the ecological success of NV epiphytes growing on bark. In addition to trade-offs associated with water relations, LiBry takes into account the dependence of photosynthetic capacity on respiration costs, resulting from turnover of the Rubisco-Enzyme. This trade-off, which is illustrated through correlations between photosynthetic capacity, tissue nitrogen content, and specific respiration rate, has been studied in detail in vascular plants (Kattge et al., 2009). Also for non-vascular vegetation, it has been shown that photosynthetic capacity correlates with nitrogen content (Wang et al., 2017), and high nitrogen concentration is linked to high respiration rates (Palmqvist et al., 2002).

The main physiological trade-offs of non-vascular vegetation have a strong impact on the set of physiological strategies which are successful under certain given climatic conditions. In LiBry, success is defined through a positive carbon balance (gains minus losses) of non-vascular organisms in the long-term. A simulated physiological strategy gains carbon via photosynthesis, which is computed based on the established Farquhar-scheme (Farquhar and von Caemmerer, 1982). Carbon loss results from respiration and tissue turnover in the model, which both depend on photosynthetic capacity of the simulated organism, due to enzyme turnover. Furthermore, the temperature dependence of respiration is calculated via a Q_{10}-relationship. Net Primary Production (NPP) is then computed as photosynthesis minus respiration, accumulated on a monthly basis. NPP is used in the model to increase the biomass of the simulated organisms, and to extend the surface fraction they cover. In case of NV epiphytes, this is the fraction of occupied total bark area. Biomass and cover are reduced through tissue turnover, and also disturbance, such as fire, which is represented in LiBry via fixed, ecosystem-specific intervals.

To represent physiological diversity of non-vascular organisms, the LiBry model simulates a large number, meaning several thousand, of different physiological strategies. A strategy is defined by a set of 11 physiological parameters in the model version used here, such as specific area, growth height, specific water storage capacity, optimum temperature, or photosynthetic capacity. The ranges of possible values for each parameter are determined from the literature (see Porada et al., 2013), and the strategies are created at the start of a model run by randomly sampling these literature-based ranges. Thereby, the physiological trade-offs which are relevant for non-vascular vegetation are taken into account. A high photosynthetic capacity, for instance, results in a high specific respiration rate. For any given location where the model is run under defined climatic conditions, usually only a fraction of the initial strategies are successful and show a positive carbon balance in the long-term. Through weighting of these strategies by their relative growth rate, average values of non-vascular vegetation properties can be estimated by the LiBry model, such as productivity or biomass at a given site.

2.2. New Processes and Parametrizations

For this study, we extended the representation of hydrological processes in the LiBry model with regard to the uptake of water from bark by NV epiphytes. Otherwise, the hydrological scheme used here corresponds largely to the model version published in Porada et al. (2018). In the model, water enters the canopy via rainfall, dew or snow. Depending on the leaf area index of the vascular vegetation, a certain fraction Φ_R of the rainfall is intercepted by the canopy, while the remainder is directly routed to the ground as throughfall (see **Figure 2**). Thereby, the interception fraction is calculated as:

$$\Phi_R = \left(\frac{LAI}{LAImax}\right)^{p_{Icpt}} \quad (1)$$

where LAI is the leaf area index of the location where the model is run, $LAImax$ is the maximum LAI in a global data set (Porada et al., 2013) and $p_{Icpt} = 0.5$ is a parameter, which changes the shape of the relation between the relative LAI value ($LAI/LAImax$) and the interception fraction Φ_R. For $p_{Icpt} = 1.0$,

Φ_R is assumed to increase linearly with increasing values of LAI, while for p_{Icpt} <1.0, Φ_R has a concave shape, which means that rainfall is intercepted faster than linearly with increasing LAI, and vice versa, for p_{Icpt} >1.0, Φ_R is convex, and high LAI values are required for efficient interception. Snowfall is assumed to directly add to throughfall. Depending on the surface type, a certain fraction Φ_W of intercepted rainfall enters the interception reservoir (leaf or bark surface without NV epiphytes) or adds to the water content of the organisms, until their storage capacity is reached. The remainder of intercepted rainfall, $1 - \Phi_W$, cannot be taken up quickly enough by the different surfaces in the canopy, and, together with surplus water from the reservoirs, is directed downwards. It either enters the bark reservoir, or adds to throughfall, depending on the fraction Φ_B. Subsequently, surplus water from the bark reservoir is directed to the ground as stemflow. Dew is assumed to completely add to the interception reservoir or the NV epiphyte reservoir. Evaporation from the NV epiphytes' water reservoir is calculated based on a modified Penman-Monteith approach (Monteith, 1981), as a function of net radiation, relative humidity, and wind speed. Also the surface temperature of the organisms is calculated by this approach, as a result of the coupled energy and water balance. The canopy area which is available for growth of NV epiphytes is represented in the LiBry model by the sum of leaf area index (LAI) and stem area index (SAI), and the vertical distribution of this area is approximated by a single layer, which is located at medium height in the canopy. Consequently, the NV epiphytes receive an average intensity of radiation, which is less than the intensity at the top of the canopy, and also the intensity of rainfall is reduced, so that the product of canopy area and rainfall per area is equal to the total rainfall flux, and the mass balance for water is conserved. In LiBry, the forest type, defined by a biome classification, determines which parts of the canopy are suitable for the growth of NV epiphytes (Porada et al., 2013). In this study, we consider only NV epiphytes growing on stems (and, occasionally, branches) of trees at the study site, growth on leaves is not included, since it does not occur at the study site.

To account for water supply from the bark, we extended the hydrological scheme of the LiBry model as follows: Below the NV epiphytes, an additional water reservoir is introduced, which has a storage capacity of 1.4 [mm] of water, based on measurements at the study site (see below). The water balance of the bark reservoir is calculated as follows:

$$W_{NEW} = W_{OLD} + Q_{NV}\Delta_t - Q_{UP}\Delta_t \quad (2)$$

where W_{NEW} [mm] is the new water content of the bark reservoir computed at the current time step of the model, W_{OLD} is the water content of the previous time step, Q_{NV} [mm s^{-1}] is overflow of water from NV epiphytes growing on bark, Q_{UP} [mm s^{-1}] is the flux of water from the bark to the NV epiphytes, and Δ_t [s] is the length of the time step of the model. Additionally, W_{NEW} is limited to the storage capacity, and the resulting surplus water is assigned to throughfall. Uptake of water from bark is possible in the model, when the water potential inside the NV epiphytes is lower than the water potential in the bark. It is calculated based on the standard approach for a diffusive flux:

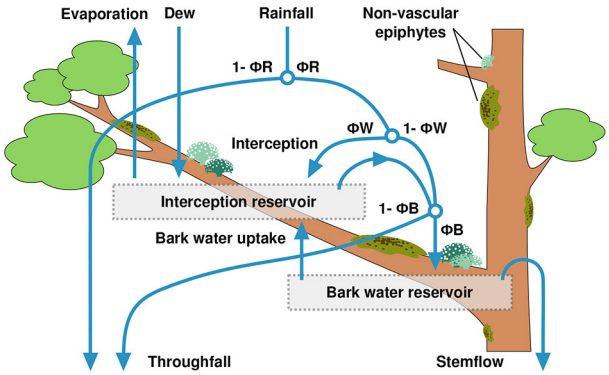

FIGURE 2 | Scheme of precipitation partitioning in the LiBry model, including the newly introduced bark water reservoir. The model parameters Φ_R, Φ_W, and Φ_B control the fractions of rainfall which are directed to throughfall, either directly or via drip from the canopy, into the interception reservoir, the bark water reservoir, or to stemflow.

$$Q_{UP} = max\left(0.0, \frac{X_{BARK} - X_{NV}}{X_{minNV}} p_{kB}\right) \quad (3)$$

where X_{BARK} [MPa] is the bark water potential, X_{NV} [MPa] is the water potential inside the NV epiphytes, and X_{minNV} = −50.0 [MPa] is the minimum water potential which the organisms are able to create. The latter is used to normalize the gradient in water potential between bark and NV epiphytes to a value of 1.0 in case the bark reservoir is saturated, and the NV epiphytes have reached their minimum potential due to desiccation at the same time. We furthermore assume that the diffusive flux of water from NV epiphytes back to the bark reservoir is negligible, and that the bark reservoir is mainly supplied by overflow from the NV epiphytes or other canopy surfaces (see **Figure 2**), which have a water potential of zero under this condition. The parameter p_{kB} = 1.5E-3 [mm s^{-1}] is an average hydraulic conductivity at the bark-epiphyte interface, which translates the gradient in water potential into a water flux. p_{kB} was chosen to correspond roughly to the saturated hydraulic conductivity of loam (Carsel and Parrish, 1988), since appropriate values for bark could not be found in the literature. In the current version of the model (Baldauf et al., 2020), the water potential of non-vascular vegetation is computed by the following equation:

$$X_{NV} = min\left(0.0, max\left(X_{minNV}, p_{X1}\left(1.0 - \frac{p_{SatX}}{S_{NV}}\right)\right)\right) \quad (4)$$

where p_{X1} = 15.0 [ ] is a parameter which determines the slope of the decrease in water potential with increasing desiccation, S_{NV} [ ] is the water saturation of the organisms, and p_{SatX} [ ] is a parameter which denotes the value of saturation, at which the water potential becomes negative. It should be mentioned that the LiBry model considers only water which is extractable under natural conditions for computing the saturation. Thus, a saturation of 0.0 does not mean that no water is left in the thallus.

The value of p_{SatX} may vary between different physiological strategies in the model. The potential of water stored in the bark is written as:

$$X_{BARK} = min\left(0.0, max\left(X_{minB}, p_{X2}\left(1.0 - \frac{1.0}{S_{BARK}}\right)\right)\right) \quad (5)$$

where X_{minB} = −45.0 [MPa] is the minimum water potential in bark, p_{X2} = 5.0 [ ] is a slope parameter, and S_{BARK} is the water saturation of the bark, in analogy to Equation (4). X_{minB} and p_{X2} are chosen according to the assumption that NV epiphytes are able to take up water from the bark if both reservoirs have a similar water saturation.

In the LiBry version developed for this study, uptake from the bark is only possible when the simulated NV epiphytes create a sufficiently negative water potential upon drying. The value of the water potential of a physiological strategy simulated in LiBry at a given water saturation depends on its pore size distribution, which is not described directly in the model, but which is expressed through the parameter p_{SatX}. The maximum value of p_{SatX} = 1.0 means that the water potential of the simulated strategy becomes negative as soon as water is extracted from the tissue, due to evaporation. At a saturation of around 23%, the water potential reaches its prescribed minimum value of −50 MPa [see Baldauf et al. (2020) for details]. Thus, a value of S_{NV} = 1.0 means that the strategy has a relatively dense tissue structure and a high ability to take up water from the bark reservoir. This is linked, however, to a relatively low diffusivity for CO_2 under high water saturation, which reduces productivity. The minimum value of p_{SatX} = 0.0 means that the water in the tissue of a physiological strategy is only weakly bound, and can be extracted almost completely without decreasing the water potential. In many moss species and also certain lichens, for instance, a substantial fraction of the water which can be stored on total is located externally on top of the thallus, where it can freely evaporate. Due to this open structure, however, these species usually show only a slight decrease in CO_2-diffusivity and a high potential productivity under high water saturation (e.g., Wang and Bader, 2018).

2.3. Description of Study Site

The study area was selected in the western part of the island of Sardinia (Italy), located in the center of the Mediterranean Sea. The area stretches from the rocky coasts, to the coastal plains, up to the first mountain reliefs of Montiferru and the Marghine chain, which reach altitudes of about 1,000–1,200 m. The climate is typically Mediterranean, with dry and hot summers and relatively rainy and mild winters. In particular, due to the proximity of the sea and frequent humid atmospheric currents from the west, the area is included within the Mediterranean pluviseasonal oceanic macrobioclimate, ranging from the Upper Thermo- to the Lower Meso-Mediterranean thermotypic horizons, and from the Upper dry to the Lower humid ombrothermic horizons with Euoceanic characteristics (Canu et al., 2015).

Although the study area is considered to be in a semi-natural condition, it is subject to some sources of anthropogenic disturbance that nevertheless have low to moderate impacts on the region's ecosystems. Among these, the most relevant are grazing by sheep and goats, which, although not intensive, is widespread over large areas; forest management in wooded areas is rather limited and generally compatible with the maintenance of epiphytic communities. Fires of low intensity and extension are frequent, while major events may affect each area with an interval of several decades.

We selected 64 sites based on a stratified random sampling design (**Figure 3**). At each site, we installed a 20 x 20 m plot within which 1 to 6 trees were selected in proportion to the tree cover of the plot. The occurrence of NV epiphyte species was recorded in each 10x10 cm quadrat of a sampling grid, which consisted of a 10 x 50 cm ladder that was divided into five quadrats and systematically placed on the N, E, S, and W sides of each tree bole, with the top edge 1.5 m above ground level; More details are given in Giordani et al. (2014, 2019). Each sampling grid was photographed in order to derive the coverage value of each growth form at tree level (see below).

2.3.1. Leaf and Stem Area Index, Bark Water Storage Capacity

In each plot, we measured the circumferences of all trees with a tape measure and the height of a representative sample of trees, obtained by triangulation with a hypsometer (Leica DISTO A5 Laser Distance Meter). These data were then used to calculate the Stem Area Index (SAI), as follows:

$$SAI = \sum_{n=1}^{t} \frac{c_{TRUNK}(n) h_{TREE}(n)}{A_{PLOT}} \quad (6)$$

where t is the number of trees in a plot, c_{TRUNK} is the circumference of a tree trunk, h_{TREE} is the height of a tree, and A_{PLOT} is the area of a plot.

We calculated data of Leaf Area Index (LAI) for the study area, taking into account both the annual and the seasonal mean and variability derived from a set of satellite images. For broadleaf canopies, LAI is defined as the one-sided green leaf area per unit ground area. Data were retrieved from MODIS satellite images in the period 2002-2011. The MOD15A2H Version 6 Moderate Resolution Imaging Spectroradiometer (MODIS) LAI product is an 8-day composite dataset with 500 meters (m) pixel size. The algorithm chooses the "best" pixel available from all the acquisitions of the Terra sensor from within the 8-day period (Myneni et al., 2015).

The determination of the maximum bark water storage was carried out following Hauck et al. (2006). Three bark samples of 1 x 2 cm and 2 mm thickness were selected for each tree. The samples were previously cleaned with tweezers and a cutter to remove any lichen or bryophyte layer that might be present. The samples were then dried in an oven at 80° C for 24 h and weighed, obtaining the dry weights. They were then immersed in distilled water for 24 h and weighed after removing excess water by draining them, thus obtaining the weight at the state of maximum hydration. The Bark Water Storage WSC_{BARK} was

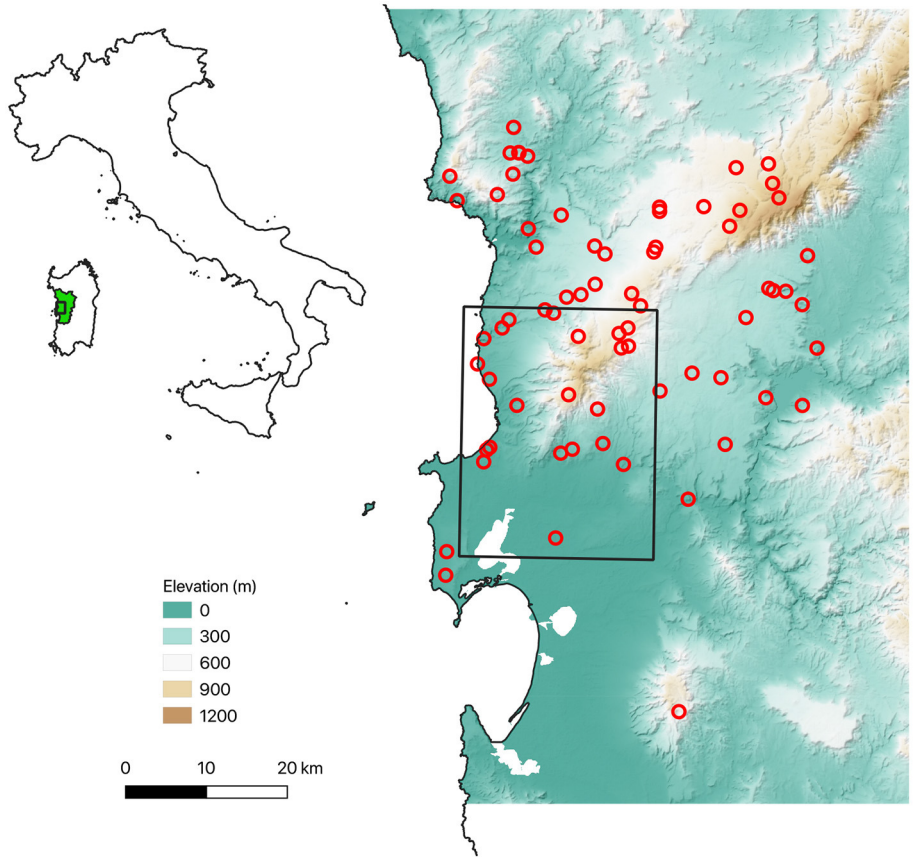

FIGURE 3 | Overview of the sampling plots. The black rectangle marks the grid cell selected from the global ERA5 climate data set, which was used to run the LiBry model (see "Model setup" below).

calculated according to the formula:

$$WSC_{\mathrm{BARK}} = \frac{fw - dw}{dw} \quad (7)$$

Where *fw* is the fresh weight of a sample and *dw* is its dry weight.

2.3.2. Morphological Properties

We sampled a total of 214 lichen species which, for the purposes of this work, were subsequently assigned to 8 groups identified on the basis of growth forms, following and partially modifying the scheme suggested by Nimis (2016): fruticose (Frut), foliose large (FolL), broad lobed foliose (FolB), narrow-lobed foliose (FolN), foliose gelatinose (FolG), squamulose (Squa), conspicuous crustose (CruCo), inconspicuous crustose (CruIn), and bryophytes (Bryo). Examples of each growth form are shown in **Figure 1**, and the relative cover fractions of the growth forms are shown in **Figure 4**.

While observational data on the relative abundances of NV epiphytes at the level of growth forms are available for the study site (**Figure 4**), data on their morphological properties had to be taken from literature (Gauslaa and Ustvedt, 2003; Hurtado et al., 2020a,b). We thus computed the median values of the literature-based morphological properties specific thallus mass (STM) and water storage capacity (WSC) for each growth form, and then used the observed abundances to compute weighted average values of STM and WSC for the study site (**Table 1**). In the same way, we also computed weighted minimum and maximum STM and WSC. For several growth forms, STM and WSC were not available. These were not included in the calculation of the average STM and WSC values.

2.4. Model Setup

For this study, we drive the LiBry model with climate variables based on the global ERA5 reanalysis data set (Hersbach et al., 2020). This data set contains time series of climate variables from 1979 to 2019 in hourly temporal resolution, on a global grid with a spatial resolution of 0.28125° x 0.28125°. The climate variables used as input by the LiBry model include: down-welling short-wave (400–700 nm) solar radiation [W m^{-2}], down-welling long-wave (near infrared,700–2,500 nm) radiation [W m^{-2}], air temperature at 2 m height [K], relative humidity [fraction], rainfall [mm s^{-1}], snowfall [mm s^{-1}], and near-surface (10 m) wind speed [m s^{-1}].

For the study site, we selected a grid cell of the ERA5 data which has the south-west corner at 8° 26' 15" E, 39° 56' 15" N, and thus includes the north-western part of the province of Oristano

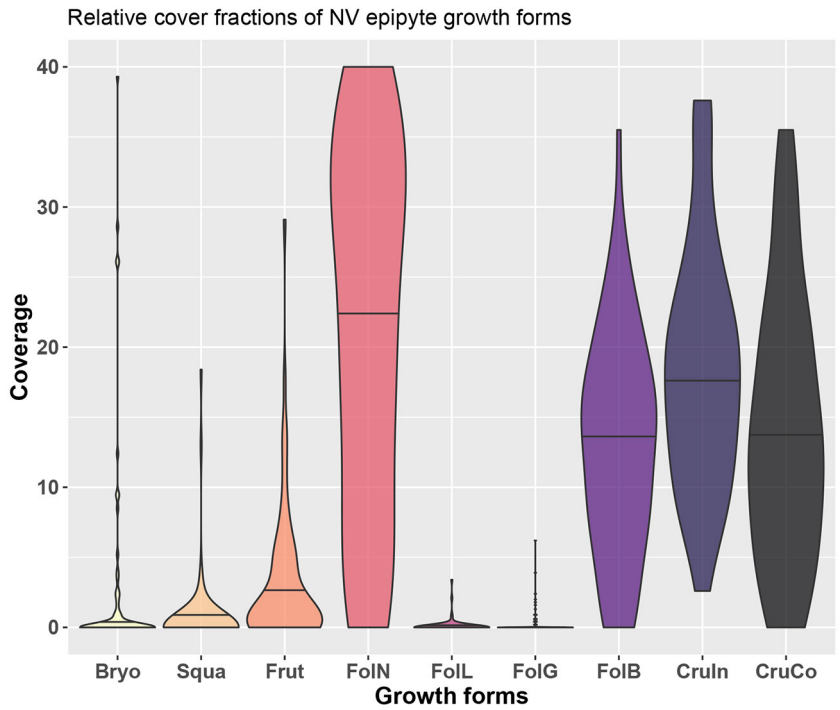

FIGURE 4 | Overview of growth forms at the study site and the distribution of their relative cover across different trees.

TABLE 1 | Minimum, median, and maximum values of specific thallus mass (STM, [kg m^{-2}]) and water storage capacity (WSC, [kg m^{-2}]) for different growth forms of NV epiphytes which are found in the study region.

Growth form	Bryo	Squa	Frut	FolN	FolL	FolG	FolB	CruIn	CruCo	weighted
STM min	–	–	0.92	0.96	0.89	0.34	0.57	–	–	0.85
median	–	–	1.18	1.74	1.22	0.64	0.91	–	–	1.47
max	–	–	1.51	3.22	1.69	0.95	1.39	–	–	2.59
WSC min	–	–	1.30	1.73	2.11	1.44	0.93	–	–	1.49
median	–	–	1.75	3.24	2.50	6.34	1.42	–	–	2.67
max	–	–	2.54	11.4	2.86	11.3	2.12	–	–	8.31
Weights	0.04	0.007	0.03	0.34	0.001	0.004	0.14	0.24	0.20	
Weights adapted	0	0	0.07	0.66	0.002	0.007	0.27	0	0	

The "–" means that STM and WSC were not available for the respective growth forms. The last two row show the weights based on the observed abundances of the growth forms in the study region, and the adapted weights excluding the growth forms where no STM and WSC data were found.

in Sardinia, where the field plots shown in **Figure 3** are located. To assess, if the global climate data are a good approximation of the local climatic conditions, we compared ERA5 rainfall and temperature to estimates based on 19 local weather stations in the study region for the period of 1979 to 2019. The multi-year monthly distributions (**Figure 5**) show a very good agreement between ERA5 and local data. Only the annual temperature amplitude of the ERA5 data seems to be slightly smaller, and the interannual variability of the rainfall slightly larger compared to the station data.

Further environmental conditions which are necessary to drive the LiBry model are the disturbance interval of the ecosystem where the NV epiphytes are located, and the LAI and SAI of the vascular vegetation. The disturbance interval is set to 30 years. LAI data from the study region are included in LiBry as multi-year monthly average values, ranging from 2.5 m^2 m^{-2} in spring to 0.5 m^2 m^{-2} in autumn and winter, and SAI is set to a constant value of 0.1 m^2 m^{-2}, based on the median value of 64 field plots. Bark water storage capacity in LiBry is based on the median value of 217 sampled trees in the study region and is set to 1.4 mm.

We run two LiBry simulations using the same input data, to quantify the impact of bark water storage on the growth of NV epiphytes at the study site. The first simulation includes a

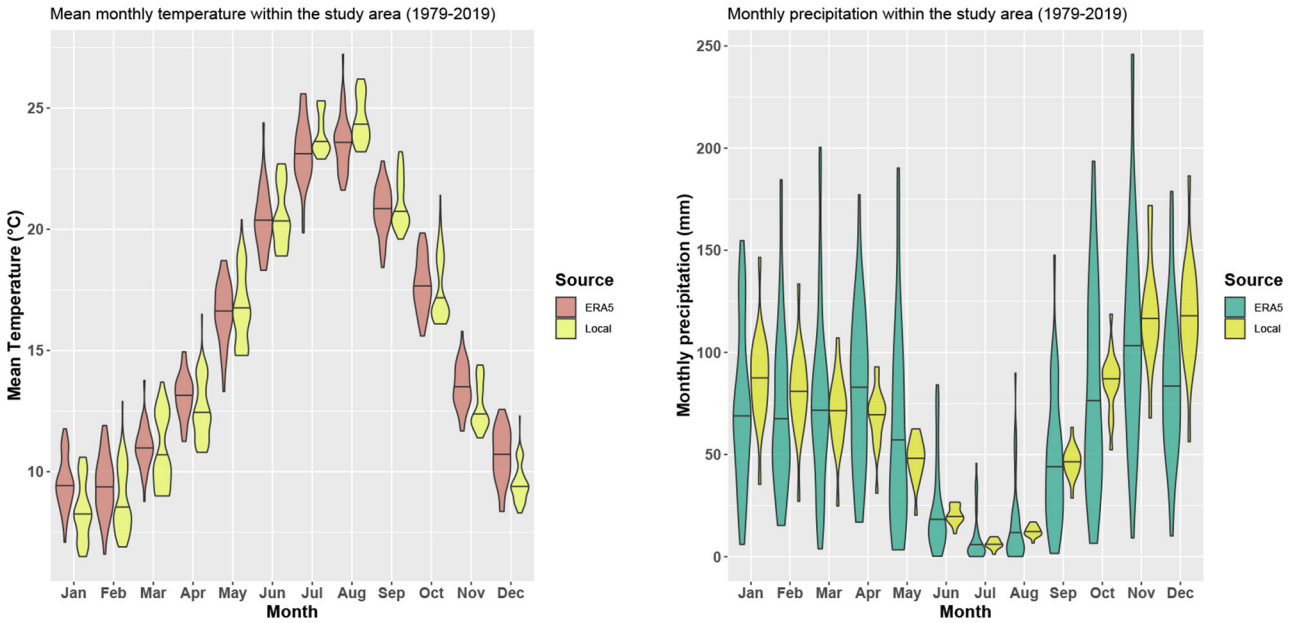

FIGURE 5 | Comparison of ERA5 2 m air temperature and rainfall to local weather station data from the study region.

bark water reservoir of 1.4 mm, which represents an additional water supply for the organisms. In the second simulation, uptake of water from the bark reservoir is set to zero. By comparing the two runs with regard to the properties of the simulated NV epiphytes, we can estimate the relevance of the bark water reservoir for their physiological functioning and also their community composition.

The LiBry model is run for 600 years, repeating the full ERA5 data set (41 years), to drive the carbon balances of the simulated strategies into a steady state and ensure that the remaining strategies are able to survive in the long-term. Thereby, survival means that the strategies maintain a positive biomass for at least 600 model years. Hence, although NPP may be negative for certain periods during the simulation, it is necessary that the long-term average NPP is positive. In LiBry even inactive organisms have a small turnover of biomass, so they cannot survive with zero NPP for 600 years. The initial number of strategies is set to 3000, to cover sufficiently the multi-dimensional parameter space of physiological properties (see also Porada et al., 2013).

2.5. Model Validation and Sensitivity Analysis

To validate the LiBry model for this study, we compare the simulated properties of NV epiphytes to observations from the site in Sardinia, complemented by data from the literature. Thereby, we focus on the dominant growth forms and average morphological properties across species, such as specific thallus mass (STM) and water storage capacity (WSC). Based on the surviving strategies of a simulation, the LiBry model computes average STM and WSC for the study region. These estimates are then compared to the observation-based STM and WSC shown in **Table 1**. Moreover, we assess the plausibility of precipitation partitioning and the canopy energy balance simulated by LiBry.

In addition to the model validation, we carry out a sensitivity analysis of our simulated results, to quantify the impacts of uncertainties in the input data and the chosen parameter values on our findings. We vary the following model parameters by a factor of 2 and 0.5, respectively, since the properties are likely to have a broad range of possible values, and may be positively skewed:

- bark water storage capacity
- hydraulic conductivity at bark-epiphyte interface
- bark water potential
- shape parameter for the interception fraction of rainfall (p_{Icpt}, Equation 1)
- disturbance interval

Furthermore, we vary the following properties by ± 20%:

- fraction of rainfall uptake into the interception reservoirs (Φ_{W}, **Figure 2**)
- fraction of water on bark which is taken up by bark reservoir (Φ_{B}, **Figure 2**)
- Leaf area index (LAI)
- rainfall rate

The reason for varying LAI is that time-series data at plot scale were not available for our site. However, we expect that the resolution of the data is still sufficiently fine to provide a realistic average estimate for the study region. Finally, we vary air temperature by ± 2° C, and we also test an alternative scheme for interactions between the physiological strategies in LiBry, While

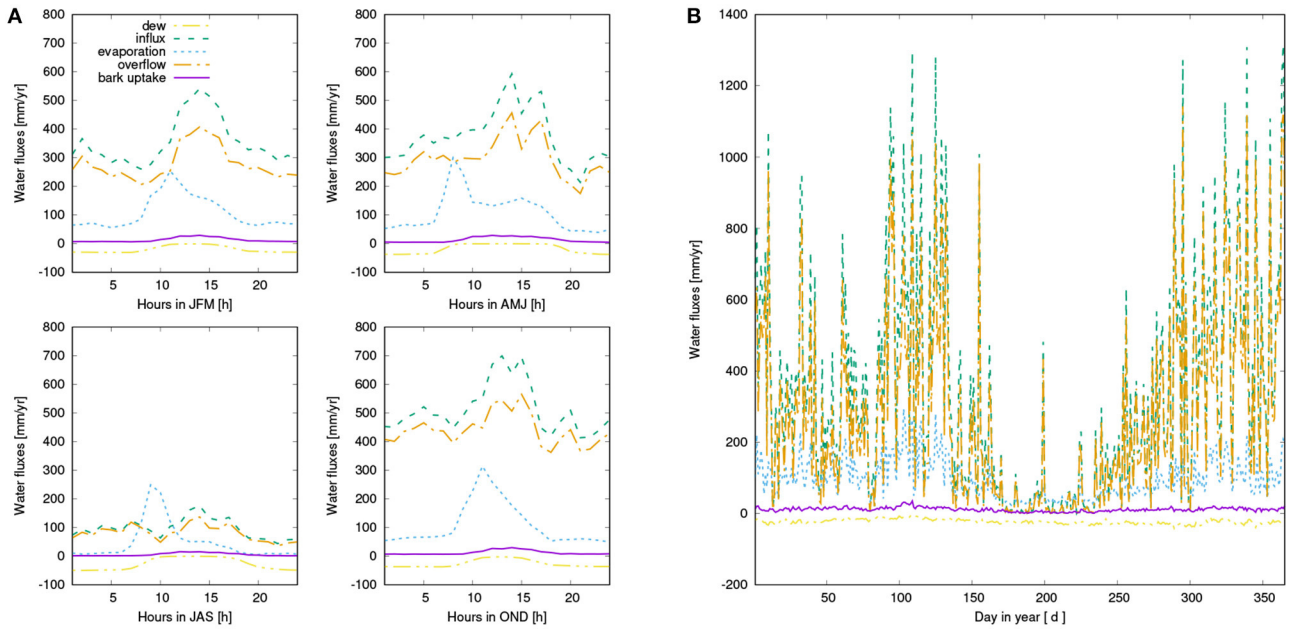

FIGURE 6 | (A) Mean diurnal water balance of the simulated canopy for four seasons: Dew input (purple), rainfall (green), overflow from the canopy due to saturation of the interception reservoir or the NV epiphytes (orange), which is directed either to throughfall or to the bark reservoir, evaporation from the interception reservoir or the NV epiphytes (blue), and bark water uptake (yellow). **(B)** Seasonal pattern of water fluxes, same color coding as in **(A)**.

they are weighted in the default model setup by their relative growth rates, here we assume that all strategies have equal weights (neutral model), which means that the (averaged) model results, such as NPP, are more influenced by "rare" strategies.

3. RESULTS

3.1. Simulated Water and Carbon Balance

For the study region in Sardinia, the LiBry model predicts high abundance and cover fraction of NV epiphytes (238 surviving physiological strategies out of 3000 initial ones; 77 % of total stem surface area covered by the organisms). The net primary production (NPP) of the organisms per stem area amounts to 32 g C m^{-2} a^{-1}. At the ecosystem level, however, simulated NPP has a value of only 1.9 g C m^{-2} a^{-1}, which is low compared to other regions of the world. Average NPP values of NV epiphytes in tropical rainforests or temperate forests, for instance, have been estimated to range from 6 to 10 g C m^{-2} a^{-1} (Elbert et al., 2012). Low simulated ecosystem NPP mainly results from the low stem area index in the study region. Simulated biomass of NV epiphytes is consistent with NPP and amounts to 48 g C m^{-2} per stem area and 3.1 g C m^{-2} of ground surface at the ecosystem level, respectively.

Water input into the canopy in form of rainfall and dew is partitioned by LiBry into throughfall, stemflow, and evaporation of intercepted water (see also **Figure 2**). For the study region, annual rainfall amounts to 667 mm a^{-1}. The largest part of rainfall is directed to throughfall (71 %), while 11 % are intercepted and evaporate, and 18 % leave the canopy as stemflow. Bark water uptake represents a relevant source of water supply according to our model estimates, and amounts to 11 mm a^{-1}, while dew and rainfall contribute 23 and 335 mm a^{-1}, respectively (see also **Figure 6**).

When bark water uptake is switched off in the model, NPP is reduced substantially by 21%. This difference mainly results from reduced NPP in spring and early summer (see **Figure 7**). Throughout the year, NPP of the organisms in the control simulation is lowest in summer, while fall and spring show highest rates of NPP. While NPP and respiration have a similar magnitude in spring, NPP exceeds respiration in winter, and is in turn lower than respiration in late summer, fall, and early winter. However, average daily NPP is still positive throughout the year.

The number of surviving strategies in the run without bark water uptake is reduced from 238 to 183, and the average physiological properties of the surviving strategies are shifted, albeit to a relatively small extent. Compared to the control run, the strategies have a slightly lower fraction of permanently air-filled thallus space and a higher fraction of small pores (**Table 2**). This means that they show increased water storage capacity and increased uptake of water from unsaturated air, and also a faster activation at low thallus water content, at the cost of a lower CO_2-diffusivity at increasing thallus water content. Other physiological properties do not show substantial changes in their average values, such as growth height, porosity, photosynthetic capacity, optimum temperature, or albedo; also hydrophobicity of the thallus changes only slightly. Thereby, photosynthetic capacity refers to the parameter $V_{C,MAX}$ of the Farquhar photosynthesis scheme (Farquhar and von Caemmerer, 1982), which is used in LiBry, and hydrophobicity corresponds to a certain value of water saturation, below which potential water

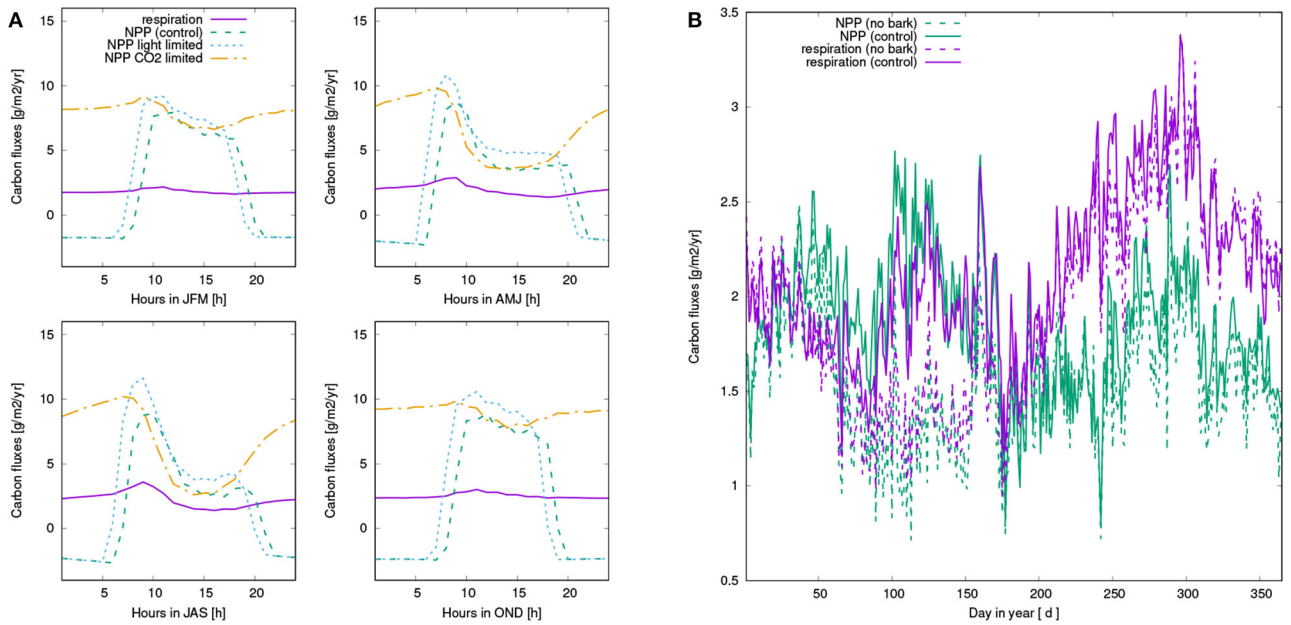

FIGURE 7 | (A) Mean diurnal pattern of simulated carbon fluxes for four seasons, averaged over all surviving strategies of the control run: Net photosynthesis (green), Respiration (purple), light-limited rate of net photosynthesis (blue), and CO_2-limited rate (orange). Net photosynthesis is computed as the minimum of the two rates. **(B)** Seasonal pattern of carbon balance of NV epiphytes: NPP (green) and respiration (purple) of the control run (solid lines) and the run without bark water uptake (dashed lines). All values are based on averaging over the last 10 years of the simulation.

TABLE 2 | Physiological parameters used in the LiBry model to define a physiological strategy.

Parameter	Control run	No bark reservoir
Height	0.11	0.12
Porosity	0.92	0.92
Air-filled thallus space	0.65	0.60
Fraction of small pores	0.71	0.76
Photosynthetic capacity	0.63	0.62
Optimum temperature	0.81	0.81
Albedo	0.50	0.50
Hydrophobicity	0.39	0.37

*Average values of all surviving strategies are shown, weighted by their share on the total cover, for the control run and also for the run without a bark water reservoir (see **Figure A1** in the appendix for the full distributions). The parameter values are normalized to the ranges of their possible values, which are based on literature (Porada et al., 2013).*

uptake is limited to a fixed rate. A higher value of hydrophobicity, meaning the threshold saturation, thus means that the maximum rate of water uptake of the thallus stays reduced for a longer time.

While the average composition of the simulated NV epiphyte community remains relatively stable when the bark water reservoir is switched off, the individual strategies experience changes in their share on the total cover. This is shown in **Figure 8** for the five strategies with the largest share on the cover in the control simulation, which make up together almost 50% of the total cover. Some parameters seem to be related to the change in cover. The two strategies which have the lowest total porosity and highest optimum temperature consistently show gains in cover, and vice versa. Furthermore, these two strategies also have a lower fraction of the thallus which remains air-filled at saturation, compared to the other strategies, and a lower fraction of small pores. The implications of these parameter shifts are discussed below. Please note that the parameter ranges in **Figure 8** are normalized. Other parameters do not show a clear tendency in cover change, such as photosynthetic capacity, or height, for instance.

3.2. Comparison to Observations

LiBry estimates an interception fraction of 11% for the study area, which matches well with large-scale estimates for Sardinia (Miralles et al., 2010). The simulated share of stemflow on the water balance (18%) is relatively high, but still only half as high as observed maximum values (Van Stan and Gordon, 2018). The diurnal and seasonal patterns of surface temperature of the NV epiphytes simulated by LiBry are in a realistic range for the study site (P.Giordani, pers. commun.).

The successful physiological strategies simulated by LiBry for the study region are characterized by a low to intermediate height (0.5 – 2.5 cm, 1.7 cm on average), a high total porosity, a relatively high fraction of small pores, which is associated with a stronger attraction of water in the thallus and more efficient uptake of water from humid air, an intermediate to high photosynthetic capacity and respiration rate, and a high optimum temperature of photosynthesis (see **Table 2**, **Figure 8** and **Figure A1**). The simulated morphological characteristics are largely consistent with the growth forms which can be found at the study site.

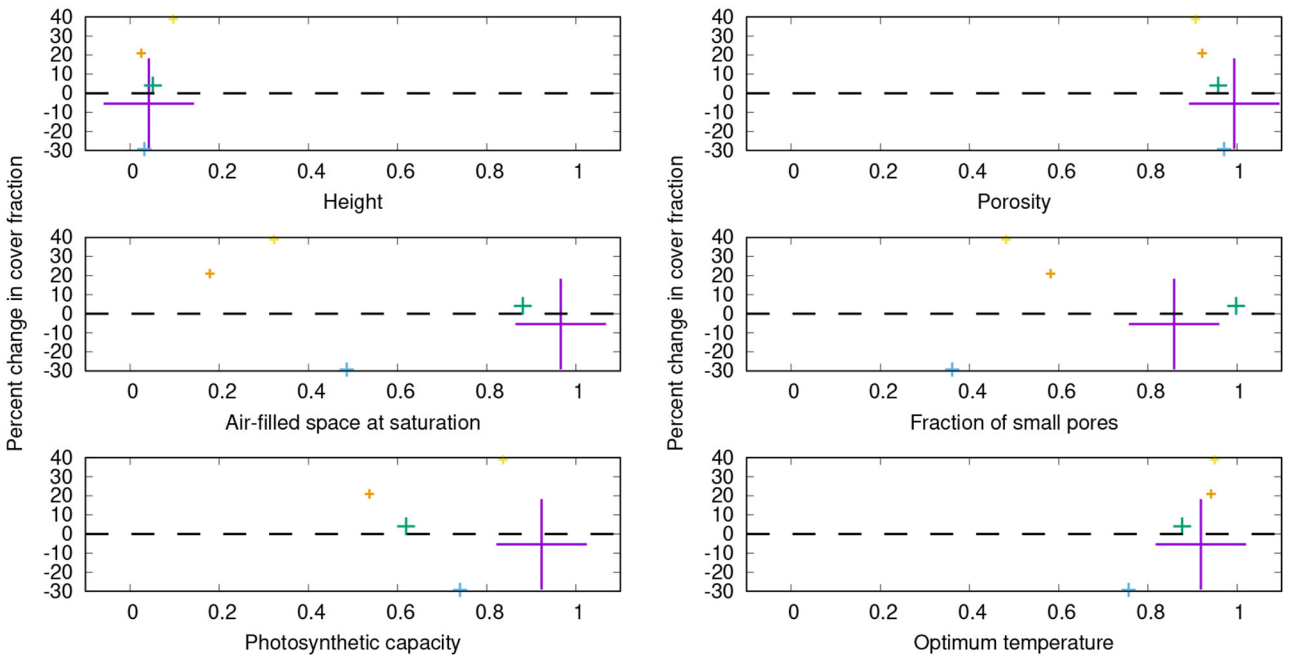

FIGURE 8 | Percent changes in share on the total cover for the five physiological strategies which have the largest relative cover values in the control simulation, resulting from switching off the bark reservoir in LiBry. The color denotes the individual strategies, and the size of the crosses is proportional to the share of the strategy on the total cover. The dominant strategy (purple) has a share of 31% on the total cover in the control simulation. On the x-axes, a subset of the physiological parameters is shown which define a strategy in the LiBry model. The values of these parameters are normalized to the range between 0 and 1, where 0 corresponds to the lowest value and 1 to the highest value used in LiBry, based on the literature (Porada et al., 2013).

The LiBry model predicts average community values of specific thallus mass (STM) of 1.1 kg m^{-2} and water storage capacity (WSC) of 3.7 kg m^{-2}. This compares well to the values, which were derived from observed abundance of growth forms at the study site, combined with estimated STM and WSC form the literature (**Table 1**). Simulated STM is slightly lower than observed, and WSC slightly higher. However, the observation-based range is relatively narrow, and the associated uncertainty is high.

3.3. Sensitivity Analysis

Our simulated estimates show an overall low sensitivity to variation in model parameter values (**Table 3**). The highest impacts on NPP at the ecosystem scale are due to reducing the disturbance interval by half, or doubling it. However, the associated changes in NPP are almost entirely due to changes in total surface cover of NV epiphytes, which result from more or less area which is lost to disturbance each year. The NPP per bark area does not change significantly. The second largest effects result from changes in LAI and air temperature. Thereby, a 20% lower LAI increases the NPP per area by 10%, and a likewise higher LAI decreases it by 5 %, which can be explained by the canopy scheme used in LiBry. Although lower LAI decreases the total amount of light and water captured by the canopy in the model, the concentration of these fluxes may increase due to the smaller canopy area, resulting in higher per-area productivity. Reduction of temperature by 2° C results in an 8% increase in NPP, also per bark area, while warmer temperature results in reduced NPP by 7%. Switching the scheme for interactions between strategies in LiBry to a neutral model (equal weights for all strategies) only slightly reduces NPP by 2%. However, the average morphological properties of the strategies shift substantially, resulting in increases of STM to 5.8 kg m^{-2} and WSC to 8.2 kg m^{-2}. These values are outside the ranges which are derived from observations at the study site. Also the average height of the simulated NV epiphytes, which increases to 3.7 cm, seems to be too high.

4. DISCUSSION

We simulated net primary production (NPP), cover, and the distribution of physiological properties of a community of NV epiphytes for a study region in Western Sardinia, using the process-based non-vascular vegetation model LiBry. Based on the model simulations, we quantified the importance of the bark water reservoir for the organisms.

Our main finding is a substantial reduction of NPP when water supply from the bark reservoir is switched off in the model. Based on the seasonal pattern of NPP (**Figure 7**), it is likely that the lower annual NPP results from reduced activity in spring due to decreased water availability in this time of the year (see also **Figure A2**). Furthermore, **Figures 6A**, **7A** show that dew is a relevant source of water for the simulated organisms, as photosynthesis exhibits a characteristic peak in the

TABLE 3 | Change in the simulated NPP of NV epiphytes, compared to the control run, resulting from variation of model parameters or climate input data.

Parameter/input	Type of variation	Response to decrease	Response to increase
Bark water storage	x 0.5 / 2.0	− 5 %	+ 7 %
Bark conductivity	x 0.5 / 2.0	+ 1 %	− 1 %
Bark water potential	x 0.5 / 2.0	+ 1 %	− 4 %
Interception fraction	x 0.5 / 2.0	+ 2 %	− 3 %
Disturbance interval	x 0.5 / 2.0	− 17 %	+ 11 %
Canopy uptake fraction	± 20 %	0 %	0 %
Bark uptake fraction	± 20 %	− 1 %	+ 1 %
Leaf area index (LAI)	± 20 %	+ 10 %*	− 5 %*
Rainfall rate	± 20 %	− 1 %	+ 1 %
Air temperature	± 2° C	+ 8 %	− 7 %

*A * means per-area NPP instead of ecosystem scale NPP.*

morning hours after the thallus has been saturated during the night. This is consistent with observations (Lange et al., 1985; Baruffo and Tretiach, 2007; Tretiach et al., 2012). In fall and winter, however, photosynthesis is then in the afternoon hours only slightly limited by lack of water (**Figure 7A**). This means that water does not seem to be a strongly limiting factor. Since respiration is increased relative to NPP from late summer to early winter, a combination of high water saturation and warm temperature may limit NPP instead of active time. In summer, in turn, **Figures 6**, **7** show a strong decline in available water, associated with a substantial reduction in NPP in the afternoon. Hence, in summer the strong evaporative demand might overrule the positive effect of the bark water reservoir on NPP of the simulated NV epiphytes. This effect may be less pronounced in spring, which explains the important role of bark water supply for the simulated organisms during this time of the year. These findings confirm our hypotheses (1) and (2), the bark reservoir is a relevant source of water for the organisms and it allows for higher productivity of NV epiphytes, although the effect is most pronounced in spring.

It should be mentioned that carbon costs due to the short period of high respiration following reactivation (Palmqvist, 2000) are not yet considered in the LiBry model. This means that we can quantify impacts of the length of activity on the carbon balance of NV epiphytes, but may not capture all gains /losses of carbon due to a lower /higher number of active intervals throughout the year. However, the LiBry model accounts for turnover of biomass in the inactive state. Negative effects of longer periods of inactivity in spring on the carbon balance of NV epiphytes are thus captured by the model.

Another key result of our study is that the role of bark water supply for NV epiphytes may be species-specific. When bark water uptake is switched off in the model, not all physiological strategies are affected to an equal extent (**Figure 8**). Furthermore, gains and losses in cover do not seem to be distributed randomly between the strategies, but some tendencies can be recognized. Strategies which have (1) a lower total porosity and (2) a higher optimum temperature increase their share on the total cover compared to the control run. They are furthermore characterized by (3) low fractions of small pores and (4) air-filled thallus space at saturation. It is, however, not straightforward to interpret this outcome, due to the complex dependencies between physiological parameters, dynamic water content, and carbon balance in the model. In LiBry, reduced total porosity is associated with increased resistance to water loss at the cost of water storage capacity, assuming an increase of resistance with the volume of cell walls and gelatinous substances (Valladares et al., 1998). A lower fraction of air-filled space, in turn, increases water storage capacity, at the cost of a lower diffusivity for CO_2 at full saturation (Cowan et al., 1992). A low fraction of small pores, however, increases diffusivity of CO_2 at intermediate values of saturation, at the cost of a reduced ability to attract water in the thallus by capillary forces (Valladares et al., 1993). This leads to slower activation from humid air and decreased bark water uptake in the model. Considering these physiological trade-offs, the simulated changes in cover may be explained by selection pressure toward longer water retention when bark water is not available anymore. The higher surface resistance associated with lower porosity may prolong active time. The resulting reduced WSC may be compensated by a reduction of the air-filled space, leading to lower CO_2-diffusivity. This would then be compensated by a reduced fraction of small pores, which may counteract the decreased CO_2-diffusivity to some extent. The following reduced capacity for bark water uptake would have no negative effect on the carbon balance in the simulation where the bark reservoir is switched off. Except for the morning hours, simulated NPP is limited by the CO_2-limited rate of photosynthesis (**Figure 7A**). This means that CO_2 diffusion limitation may prevent strategies which have an even more compact thallus than those shown in **Figure 8** from being successful in the simulation without bark reservoir. Thus, limited ability of adaptation to changed environmental conditions due to physiological trade-offs (Merinero et al., 2015) may be an additional reason for the reduced NPP compared to the control run. Overall, the model results confirm our hypothesis (3), the bark water reservoir plays an important role for the community composition of NV epiphytes.

A further consequence of reduced water supply may be elevated surface temperature caused by lack of evaporative cooling (Davies-Barnard et al., 2014), which would explain the selection of strategies which have a higher optimum temperature in the simulation without bark reservoir. However, the difference in surface temperature is small compared to the control run, less than 0.1°C on average. An alternative explanation is the consequence of reduced active time and potentially increased CO_2 limitation for the carbon balance of the simulated organisms. At a given surface temperature, a higher optimum temperature not only leads to lower photosynthesis in the model, but also to lower respiration. Since respiration shows a stronger response to temperature under warm climate, it may be more beneficial for the carbon balance of the simulated NV epiphytes to have a markedly reduced respiration rate, at the cost of a less reduced photosynthesis rate.

Although we find a species-specific effect of the bark water reservoir on the carbon balance of NV epiphytes, the average

physiological parameter values show no strong trends (**Table 2**). This is due to the fact that the strategies which have the largest shares on the total cover are the same in both the control simulation and the one without bark water uptake, even though their relative shares on the cover change, as discussed above. However, the reduction of the number of surviving species from 238 to 183 shows that strategies which have a small share on the total cover, resulting from little NPP, would be significantly affected by the decrease in bark water reservoir. Although this process would not lead to a significant quantitative change in the overall contribution of NV epiphytic communities at the landscape level, the effect would be far from negligible on ecosystem functionality at the microscale. These underrepresented strategies contribute to increasing the range of possible ecological adaptations to particular microclimatic conditions determined by the micromorphological variability of the trunks. The loss of these unique characteristics as a result of the decrease in bark water reservoir would lead to an imbalance in the relationship between functional vulnerability and functional over-redundancy and, ultimately, to the impoverishment and trivialization of epiphytic NV communities.

The validation of our simulated estimates is challenging, since we lack detailed information of the hydrological pathways in the canopy at the study site, and also field measurements of the carbon balance of the NV epiphytes. However, we find a general consistency of our results with characteristic values for this type of ecosystem. Another source of uncertainty is the estimation of the physiological properties of the NV epiphyte community in the study region. While we are able to constrain the range of possible values of morphological parameters to some extent, it is difficult to obtain exact estimates of average properties at the community level, which would require an extensive field campaign combined with laboratory analysis. Hence, to address the uncertainties associated with our modeling approach, we carried out a sensitivity analysis which included hydrological properties of the canopy, newly introduced model processes, and environmental conditions, such as climate. Since we did not find strong sensitivity of our estimates to variation in model parameters and inputs, we believe that our findings are valid in spite of the relatively large uncertainties in the approach.

Our estimates have several implications for the potential impacts of climate change on the community composition of NV epiphytes and the associated feedbacks on precipitation partitioning and the hydrological cycle. Firstly, the bark water reservoir may provide a relevant additional water supply for NV epiphytes, which makes possible increased NPP under sub-optimal environmental conditions, such as global warming and increased dryness. The reduction in NPP and the lower number of strategies in the simulation without bark water uptake indicate potential negative consequences of climate change on diversity of NV epiphytes, due to decreased active time. This may also occur indirectly, in case host trees are replaced by other tree species which have a reduced bark water storage capacity, for instance. Regarding potential feedbacks on local climate, our estimates suggest limited effects on surface temperature due to the low total bark area in the study region. In ecosystems which exhibit a larger coverage and biomass of NV epiphytes, a substantial feedback on surface temperature may occur.

From an application perspective, our results highlight the importance of adopting correct forest management strategies that reconcile the economic use of resources with the sustainability of fragile epiphytic communities. As demonstrated by our temporal simulation, this approach, generally valid, is even more critical in a Mediterranean environment where the prolonged summer water deficit makes the bark a fundamental reservoir for the survival of poikilohydric species. The quantification of the water requirements of epiphytic communities and of the water potentially available in the forest environment will allow to detail targeted forestry interventions compatible with the maintenance of the communities within their physiological optimum (Bianchi et al., 2020).

Future research can be developed to further modulate the results obtained from predictive models. Among the various aspects that could contribute to this, we draw attention to (i) the collection of more field data to obtain detailed information both on the water retention capacity of the different barks and on the physiological response of the NV epiphytes that colonize them, and (ii) greater attention to microclimatic characteristics so as to be able to increase the degree of spatial detail of the models and make them more aligned with the scale of actual biological activity of the NV epiphytes. To conclude, we found that the bark water reservoir in Sardinia is an important factor for increased productivity of NV epiphytes due to prolongation of active time. Moreover, it may sustain rare species in the ecosystem, which may otherwise not be sufficiently productive to survive in the long-term, and may thus increase potential diversity of NV epiphytes.

DATA AVAILABILITY STATEMENT

The raw data supporting the conclusions of this article will be made available by the authors, without undue reservation.

AUTHOR CONTRIBUTIONS

PP and PG designed the study concept together. PP developed the model code and ran the simulations. PG provided data for model evaluation. PP wrote the manuscript, with substantial input by PG. Both authors contributed to the article and approved the submitted version.

FUNDING

PP appreciates funding by the Deutsche Forschungsgemeinschaft (DFG, German Research Foundation) - 408092731, which made possible a part of the model development work.

ACKNOWLEDGMENTS

PP thanks Annika Jahnke-Bornemann (University of Hamburg, CEN) for support regarding the preparation of model input data.

REFERENCES

Aptroot, A., and van Herk, C. (2007). Further evidence of the effects of global warming on lichens, particularly those with trentepohlia phycobionts. *Environ. Pollut.* 146, 293–298. doi: 10.1016/j.envpol.2006.03.018

Baldauf, S., Porada, P., Raggio, J., Maestre, F. T., and Tietjen, B. (2020). Relative humidity predominantly determines long-term biocrust-forming lichen cover in drylands under climate change. *J. Ecol.* 109, 1370–1385. doi: 10.1101/2020.06.09.141564

Baruffo, L., and Tretiach, M. (2007). Seasonal variations of fo, fm, and fv/fm in an epiphytic population of the lichen *Punctelia subrudecta* (Nyl.) Krog. *Lichenologist* 39, 555–566. doi: 10.1017/S0024282907006846

Bates, J. (1992). Influence of chemical and physical factors on *Quercus* and *Fraxinus* epiphytes at Loch Sunart, Western Scotland: a multivariate analysis. *J. Ecol.* 80, 163–179. doi: 10.2307/2261073

Bianchi, E., Benesperi, R., Brunialti, G., Di Nuzzo, L., Fackovcová, Z., Frati, L., et al. (2020). Vitality and growth of the threatened lichen *Lobaria pulmonaria* (L.) Hoffm. in response to logging and implications for its conservation in Mediterranean oak forests. *Forests* 11:995. doi: 10.3390/f11090995

Canu, S., Rosati, L., Fiori, M., Motroni, A., Filigheddu, R., and Farris, E. (2015). Bioclimate map of Sardinia (Italy). *J. Maps* 11, 711–718. doi: 10.1080/17445647.2014.988187

Carsel, R. F., and Parrish, R. S. (1988). Developing joint probability distributions of soil water retention characteristics. *Water Resour. Res.* 24, 755–769. doi: 10.1029/WR024i005p00755

Cowan, I., Lange, O., and Green, T. (1992). Carbon-dioxide exchange in lichens: determination of transport and carboxylation characteristics. *Planta* 187, 282–294. doi: 10.1007/BF00201952

Davies-Barnard, T., Valdes, P. J., Jones, C. D., and Singarayer, J. S. (2014). Sensitivity of a coupled climate model to canopy interception capacity. *Clim. Dynam.* 42, 1715–1732. doi: 10.1007/s00382-014-2100-1

Elbert, W., Weber, B., Burrows, S., Steinkamp, J., Büdel, B., Andreae, M., et al. (2012). Contribution of cryptogamic covers to the global cycles of carbon and nitrogen. *Nat. Geosci.* 5, 459–462. doi: 10.1038/ngeo1486

Ellis, C., Coppins, B., Dawson, T., and Seaward, M. (2007). Response of british lichens to climate change scenarios: trends and uncertainties in the projected impact for contrasting biogeographic groups. *Biol. Conserv.* 140, 217–235. doi: 10.1016/j.biocon.2007.08.016

Ellis, C. J., and Eaton, S. (2021). Microclimates hold the key to spatial forest planning under climate change: cyanolichens in temperate rainforest. *Glob. Change Biol.* doi: 10.1111/gcb.15514. [Epub ahead of print].

Farquhar, G., and von Caemmerer, S. (1982). "Modelling of photosynthetic response to environmental conditions," in *Encyclopedia of Plant Physiology*, Vol. 12B, eds O. Lange, P. Nobel, C. Osmond, and H. Ziegler (Heidelberg: Springer). p. 549–587.

Franks, A. J., and Bergstrom, D. M. (2000). Corticolous bryophytes in microphyll fern forests of south-east queensland: distribution on Antarctic beech *(Nothofagus moorei)*. *Aust. Ecol.* 25, 386–393. doi: 10.1046/j.1442-9993.2000.01048.x

Gauslaa, Y. (2014). Rain, dew, and humid air as drivers of morphology, function and spatial distribution in epiphytic lichens. *Lichenologist* 46, 1–16. doi: 10.1017/S0024282913000753

Gauslaa, Y., and Ustvedt, E. (2003). Is parietin a UV-B or a blue-light screening pigment in the lichen *Xanthoria parietina*? *Photochem. Photobiol. Sci.* 2, 424–432. doi: 10.1039/b212532c

Giordani, P., Incerti, G., Rizzi, G., Rellini, I., Nimis, P. L., and Modenesi, P. (2014). Functional traits of cryptogams in Mediterranean ecosystems are driven by water, light and substrate interactions. *J. Veg. Sci.* 25, 778–792. doi: 10.1111/jvs.12119

Giordani, P., Malaspina, P., Benesperi, R., Incerti, G., and Nascimbene, J. (2019). Functional over-redundancy and vulnerability of lichen communities decouple across spatial scales and environmental severity. *Sci. Total Environ.* 666, 22–30. doi: 10.1016/j.scitotenv.2019.02.187

Hargis, H., S.G., G., Porada, P., Moore, G., Ferguson, B., and Van Stan II, J. (2019). Arboreal epiphytes in the soil-atmosphere interface: how often are the biggest "buckets" in the canopy empty? *Geosciences* 9, 1–17. doi: 10.3390/geosciences9080342

Hauck, M., Hofmann, E., and Schmull, M. (2006). Site factors determining epiphytic lichen distribution in a dieback-affected spruce–fir forest on Whiteface Mountain, New York: microclimate. *Ann. Bot. Fennici* 43, 1–12. Available online at: https://www.jstor.org/stable/23727271

Hersbach, H., Bell, B., Berrisford, P., Hirahara, S., Horányi, A., Munoz-Sabater, J., et al. (2020). The era5 global reanalysis. *Q. J. R. Meteorol. Soc.* 146, 1999–2049. doi: 10.1002/qj.3803

Hurtado, P., Prieto, M., de Bello, F., Aragón, G., López-Angulo, J., Giordani, P., et al. (2020a). Contrasting environmental drivers determine biodiversity patterns in epiphytic lichen communities along a European gradient. *Microorganisms* 8:1913. doi: 10.3390/microorganisms8121913

Hurtado, P., Prieto, M., Martínez-Vilalta, J., Giordani, P., Aragón, G., López-Angulo, J., et al. (2020b). Disentangling functional trait variation and covariation in epiphytic lichens along a continent-wide latitudinal gradient. *Proc. R. Soc. B Biol. Sci.* 287:20192862. doi: 10.1098/rspb.2019.2862

Jagodziński, A., Wierzcholska, S., Dyderski, M., Horodecki, P., Rusińska, A., Gdula, A., et al. (2018). Tree species effects on bryophyte guilds on a reclaimed post-mining site. *Ecol. Eng.* 110, 117–127. doi: 10.1016/j.ecoleng.2017.10.015

Johansson, P. (2008). Consequences of disturbance on epiphytic lichens in boreal and near boreal forests. *Biol. Conserv.* 141, 1933–1944. doi: 10.1016/j.biocon.2008.05.013

Jonsson Čabrajić, A., Lidén, M., Lundmark, T., Ottosson-Löfvenius, M., and Palmqvist, K. (2010). Modelling hydration and photosystem II activation in relation to *in situ* rain and humidity patterns: a tool to compare performance of rare and generalist epiphytic lichens. *Plant Cell Environ.* 33, 840–850. doi: 10.1111/j.1365-3040.2009.02110.x

Kattge, J., Knorr, W., Raddatz, T., and Wirth, C. (2009). Quantifying photosynthetic capacity and its relationship to leaf nitrogen content for global-scale terrestrial biosphere models. *Glob. Change Biol.* 15, 976–991. doi: 10.1111/j.1365-2486.2008.01744.x

Kenkel, N., and Bradfield, G. (1981). Ordination of epiphytic bryophyte communities in a wet-temperate coniferous forest, South-Coastal British Columbia. *Vegetatio* 45, 147–154. doi: 10.1007/BF00054669

Klamerus-Iwan, A., Link, T. E., Keim, R., and Van Stan II, J. (2020). "Storage and routing of precipitation through canopies," in *Precipitation Partitioning by Vegetation - A Global Synthesis*, eds J. Van Stan II, E. Gutmann, and J. Friesen (Cham: Springer Nature Switzerland AG).

Klos, A., Rajfur, M., and Waclawek, W. (2005). Ion equilibrium in lichen surrounding. *Bioelectrochemistry* 66, 95–103. doi: 10.1016/j.bioelechem.2004.04.006

Kranner, I., Beckett, R., Hochman, A., and Nash, T. H. (2008). Desiccation-tolerance in lichens: a review. *Bryologist* 111, 576–593. doi: 10.1639/0007-2745-111.4.576

Lange, O., Green, T., and Reichenberger, H. (1999). The response of lichen photosynthesis to external CO_2 concentration and its interaction with thallus water-status. *J. Plant Physiol.* 154, 157–166. doi: 10.1016/S0176-1617(99)80204-1

Lange, O., Tenhunen, J., Harley, P., and Walz, H. (1985). "Method for field measurements of CO_2-Exchange. The diurnal changes in net photosynthesis and photosynthetic capacity of lichens under Mediterranean climatic conditions," in *Lichen Physiology and Cell Biology,* ed D. Brown (Boston, MA: Springer). p. 23–39.

Łubek, A., Kukwa, M., Jaroszewicz, B., and Czortek, P. (2018). Changes in the epiphytic lichen biota of Białowieża Primeval Forest are not explained by climate warming. *Sci. Total Environ.* 643, 468–478. doi: 10.1016/j.scitotenv.2018.06.222

Merinero, S., Hilmo, O., and Gauslaa, Y. (2014). Size is a main driver for hydration traits in cyano- and cephalolichens of boreal rainforest canopies. *Fungal Ecol.* 7, 59–66. doi: 10.1016/j.funeco.2013.12.001

Merinero, S., Martínez, I., Rubio-Salcedo, M., and Gauslaa, Y. (2015). Epiphytic lichen growth in Mediterranean forests: effects of proximity to the ground and reproductive stage. *Basic Appl. Ecol.* 16, 220–230. doi: 10.1016/j.baae.2015.01.007

Metcalfe, D. B., and Ahlstrand, J. C. M. (2019). Effects of moisture dynamics on bryophyte carbon fluxes in a tropical cloud forest. *New Phytol.* 222, 1766–1777. doi: 10.1111/nph.15727

Miralles, D. G., Gash, J. H., Holmes, T. R. H., de Jeu, R. A. M., and Dolman, A. J. (2010). Global canopy interception from satellite

observations. *J. Geophys. Res. Atmos.* 115, 1–8. doi: 10.1029/2009JD013530

Monteith, J. (1981). Evaporation and surface temperature. *Quart. J. R. Met. Soc.* 107, 1–27.

Myneni, R., Knyazikhin, Y., and Park, T. (2015). *MOD15A2H MODIS/Terra Leaf Area Index/FPAR 8-Day L4 Global 500m SIN Grid V006 [Data set]*. NASA EOSDIS Land Processes DAAC.

Nascimbene, J., Benesperi, R., Casazza, G., Chiarucci, A., and Giordani, P. (2020). Range shifts of native and invasive trees exacerbate the impact of climate change on epiphyte distribution: the case of lung lichen and black locust in Italy. *Sci. Total Environ.* 735:139537. doi: 10.1016/j.scitotenv.2020.139537

Nascimbene, J., Casazza, G., Benesperi, R., Catalano, I., Cataldo, D., Grillo, M., et al. (2016). Climate change fosters the decline of epiphytic *Lobaria* species in italy. *Biol. Conserv.* 201, 377–384. doi: 10.1016/j.biocon.2016.08.003

Nascimbene, J., and Marini, L. (2010). Oak forest exploitation and black-locust invasion caused severe shifts in epiphytic lichen communities in Northern Italy. *Sci. Total Environ.* 408, 5506–5512. doi: 10.1016/j.scitotenv.2010.07.056

Nimis, P. L. (2016). *The Lichens of Italy. A Second Annotated Catalogue*. EUT Edizioni Università di Trieste. (Trieste).

Palmqvist, K. (2000). Tansley review no. 117. Carbon economy in lichens. *New Phytol.* 148, 11–36. doi: 10.1046/j.1469-8137.2000.00732.x

Palmqvist, K., Dahlman, L., Valladares, F., Tehler, A., Sancho, L., and Mattsson, J. (2002). CO_2 exchange and thallus nitrogen across 75 contrasting lichen associations from different climate zones. *Oecologia* 133, 295–306. doi: 10.1007/s00442-002-1019-0

Porada, P., Pöschl, U., Kleidon, A., Beer, C., and Weber, B. (2017). Estimating global nitrous oxide emissions by lichens and bryophytes with a process-based productivity model. *Biogeosciences* 14, 1593–1602. doi: 10.5194/bg-2016-420

Porada, P., Tamm, A., Raggio, J., Cheng, Y., Kleidon, A., Pöschl, U., et al. (2019). Global NO and HONO emissions of biological soil crusts estimated by a process-based non-vascular vegetation model. *Biogeosciences* 16, 2003–2031. doi: 10.5194/bg-16-2003-2019

Porada, P., Van Stan, J., and Kleidon, A. (2018). Significant contribution of non-vascular vegetation to global rainfall interception. *Nat. Geosci.* 11, 563–567. doi: 10.1038/s41561-018-0176-7

Porada, P., Weber, B., Elbert, W., Pöschl, U., and Kleidon, A. (2013). Estimating global carbon uptake by lichens and bryophytes with a process-based model. *Biogeosciences* 10, 6989–7033. doi: 10.5194/bg-10-6989-2013

Porada, P., Weber, B., Elbert, W., Pöschl, U., and Kleidon, A. (2014). Estimating impacts of lichens and bryophytes on global biogeochemical cycles of nitrogen and phosphorus and on chemical weathering. *Global Biogeochem. Cycles* 28, 71–85. doi: 10.1002/2013GB004705

Proctor, M. (2000). The bryophyte paradox: tolerance of desiccation, evasion of drought. *Plant Ecol.* 151, 41–49. doi: 10.1023/A:1026517920852

Proctor, M., Oliver, M., Wood, A., Alpert, P., Stark, L., Cleavitt, N., et al. (2007). Desiccation-tolerance in bryophytes: a review. *Bryologist* 110, 595–621. doi: 10.1639/0007-2745(2007)110[595:DIBAR]2.0.CO;2

Rodríguez-Quiel, E., Mendieta-Leiva, G., and Bader, M. (2019). Elevational patterns of bryophyte and lichen biomass differ among substrates in the tropical montane forest of Baru volcano, Panama. *J. Bryol.* 41, 95–106. doi: 10.1080/03736687.2019.1584433

Rubio-Salcedo, M., Psomas, A., Prieto, M., Zimmermann, N. E., and Martínez, I. (2017). Case study of the implications of climate change for lichen diversity and distributions. *Biodivers. Conserv.* 26, 1121–1141. doi: 10.1007/s10531-016-1289-1

Smith, R. J., Nelson, P. R., Jovan, S., Hanson, P. J., and McCune, B. (2018). Novel climates reverse carbon uptake of atmospherically dependent epiphytes: Climatic constraints on the iconic boreal forest lichen evernia mesomorpha. *Am. J. Bot.* 105, 266–274. doi: 10.1002/ajb2.1022

Tretiach, M., Baruffo, L., and Piccotto, M. (2012). Effects of Mediterranean summer conditions on chlorophyll a fluorescence emission in the epiphytic lichen *Flavoparmelia soredians*: a field study. *Plant Biosyst.* 146, 171–180. doi: 10.1080/11263504.2012.727881

Valladares, F., Sancho, L., and Ascaso, C. (1998). Water storage in the lichen family *Umbilicariaceae*. *Bot. Acta* 111, 99–107.

Valladares, F., Wierzchos, J., and Ascaso, C. (1993). Porosimetric study of the lichen family *Umbilicariaceae*: anatomical interpretation and implications for water storage capacity of the thallus. *Am. J. Bot.* 80, 263–272.

Van Stan, J. II., and Gordon, D. A. (2018). Mini-review: stemflow as a resource limitation to near-stem soils. *Front. Plant Sci.* 9:248. doi: 10.3389/fpls.2018.00248

Van Stan, J. II., and Pypker, T. (2015). A review and evaluation of forest canopy epiphyte roles in the partitioning and chemical alteration of precipitation. *Sci. Total Environ.* 536, 813–824. doi: 10.1016/j.scitotenv.2015.07.134

Wang, Z., and Bader, M. (2018). Associations between shoot-level water relations and photosynthetic responses to water and light in 12 moss species. *AoB Plants* 10:ply034. doi: 10.1093/aobpla/ply034

Wang, Z., Liu, X., Bader, M., Feng, D., and Bao, W. (2017). The 'plant economic spectrum' in bryophytes, a comparative study in subalpine forest. *Am. J. Bot.* 104, 261–270. doi: 10.3732/ajb.1600335

Wierzcholska, S., Dyderski, M., and Jagodziński, A. (2020). Potential distribution of an epiphytic bryophyte depends on climate and forest continuity. *Global Planet. Change* 193:103270. doi: 10.1016/j.gloplacha.2020.103270

Conflict of Interest: The authors declare that the research was conducted in the absence of any commercial or financial relationships that could be construed as a potential conflict of interest.

APPENDIX

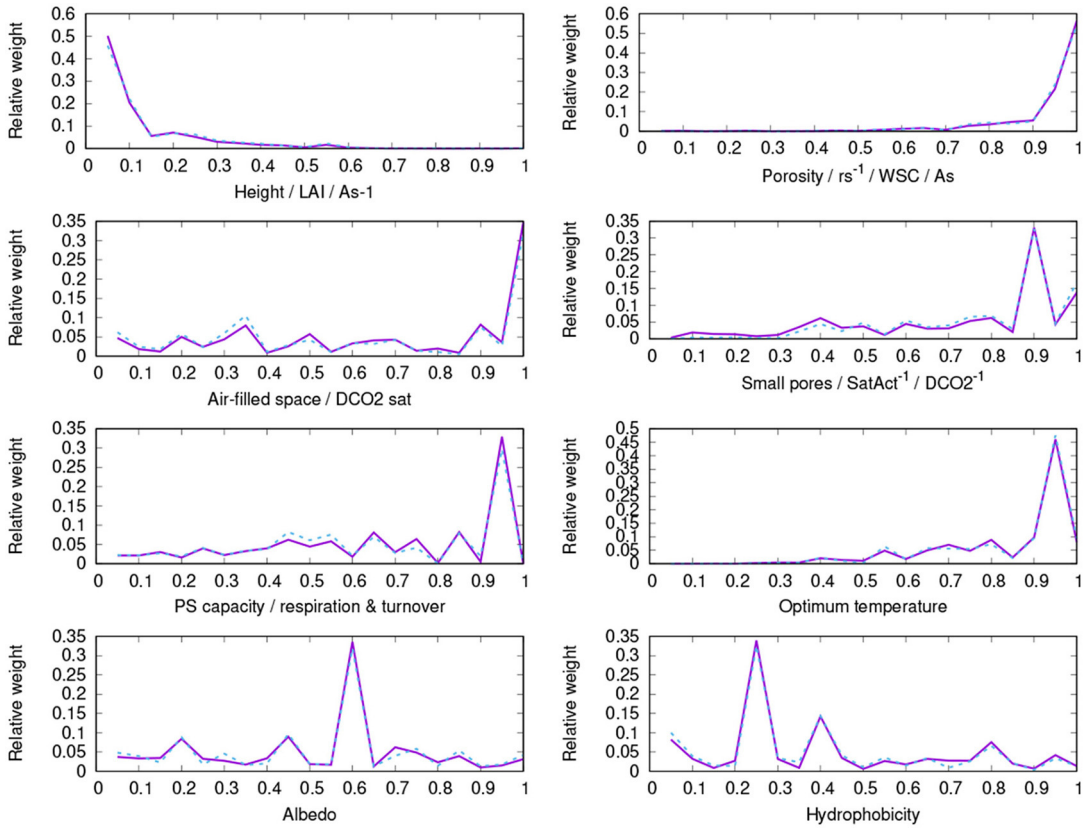

FIGURE A1 | Parameter distribution of surviving strategies of the control run (purple, solid) and the run without bark water reservoir (blue, dashed).

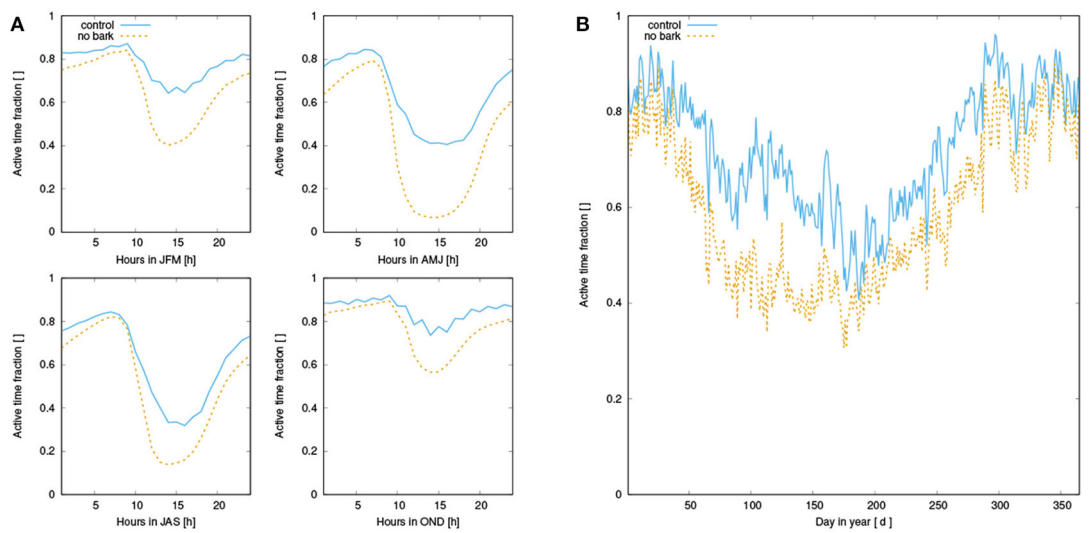

FIGURE A2 | (A) Mean diurnal activity pattern of simulated NV epiphytes for four seasons, averaged over all surviving strategies of the control run (blue, solid) and the run without bark reservoir (orange, dashed); **(B)** Seasonal pattern of activity.

frontiers in Forests and Global Change

ORIGINAL RESEARCH
published: 11 May 2021
doi: 10.3389/ffgc.2021.663100

How Characteristics of a Rainfall Event and the Meteorological Conditions Determine the Development of Stemflow: A Case Study of a Birch Tree

*Katarina Zabret and Mojca Šraj**

Department of Environmental Civil Engineering, Faculty of Civil and Geodetic Engineering, University of Ljubljana, Ljubljana, Slovenia

OPEN ACCESS

Edited by:
John T. Van Stan, Georgia Southern University, United States

Reviewed by:
Yafeng Zhang, Northwest Institute of Eco-Environment and Resources, Chinese Academy of Sciences (CAS), China
Tom Grant Pypker, Thompson Rivers University, Canada

***Correspondence:**
Mojca Šraj
mojca.sraj@fgg.uni-lj.si

Specialty section:
This article was submitted to Forest Hydrology, a section of the journal Frontiers in Forests and Global Change

Received: *02 February 2021*
Accepted: *19 April 2021*
Published: *11 May 2021*

Citation:
Zabret K and Šraj M (2021) How Characteristics of a Rainfall Event and the Meteorological Conditions Determine the Development of Stemflow: A Case Study of a Birch Tree. Front. For. Glob. Change 4:663100. doi: 10.3389/ffgc.2021.663100

The process of rainfall partitioning is usually addressed by three components: rainfall interception, throughfall and stemflow. The occurrence and proportion of stemflow depends on many complexly interconnected factors. To contribute to the interpretation of these interdependencies, the influence of rainfall event characteristics and phenoseasons on stemflow development was analyzed with a new approach. In this study we have focused on the development of stemflow during 156 rainfall events with complete time series records for a single birch tree (*Betula pendula* Roth.) at a study plot in the city of Ljubljana, Slovenia. For each one of the selected events, diagrams of rainfall and stemflow development during the event were prepared and grouped according to their visual similarities using hierarchical clustering. Additionally, significant meteorological characteristics were determined for each group of events. Four characteristic types of stemflow response were identified and connected to the corresponding event characteristics. Events showing negligible stemflow response to rainfall increase were characterized with rainfall amounts lower than 5 mm, high rainfall intensities, and occurrence in the leafed phenophase. A slow stemflow increase, independent of the increase of the rainfall volume in the open, was recognized for rainfall events delivering less than 20 mm of rainfall during a 5-h duration on average. The majority of these events were observed in the leafed phenophase, corresponding to higher air temperature and vapor pressure deficit. The occurrence of stemflow events, whose development followed the increase of the rainfall amount, was not dependent on the phenophase. However, during these events the average air temperature and vapor pressure deficit were lower, the rainfall amount was larger and the rainfall duration longer in comparison to the events showing independent increase with rainfall. The fourth type of response of stemflow was defined by a strong stemflow response in connection to large rainfall amounts and the longest rainfall duration, as observed for events in the leafless period. The four characteristic types of stemflow response provide additional information on the possible proportion of the rainfall reaching the ground as stemflow.

Keywords: stemflow, stemflow response, rainfall characteristics, phenophase, hierarchical clustering

INTRODUCTION

Trees are an important part of vegetation in our environment, contributing to air quality, biodiversity, energy conservation, atmospheric CO_2 reduction, aesthetics and quality of living environment (McPherson et al., 2005; Zabret and Šraj, 2019). However, trees also influence the hydrological cycle as they redistribute precipitation. Precipitation partitioning by trees is defined by three components, i.e., interception, throughfall, and stemflow. Interception is the precipitation amount that is retained on leaves and branches, eventually evaporating to the atmosphere and not reaching the ground. Throughfall is the portion of the precipitation reaching the ground underneath the tree due to dripping from the leaves or falling through the openings in the canopy, while stemflow describes the flow of the precipitation down the tree branches and stem. However, in comparison to the amount and proportions of throughfall to gross rainfall, stemflow values are minor (Šraj et al., 2008; Staelens et al., 2008; Mużyło et al., 2012; Swaffer et al., 2014; Zabret et al., 2018; Sadeghi et al., 2020).

Stemflow is the component of rainfall partitioning that contributes the lowest amounts of water to the ground. Due to its close contact with the tree surface, it is also the most challenging to measure (Levia and Germer, 2015; Sadeghi et al., 2020). Therefore, it is quite often neglected and not measured in analysis of the rainfall partitioning process (Carlyle-Moses et al., 2004; Asadian and Weiler, 2009; Sadeghi et al., 2015; Kermavnar and Vilhar, 2017). However, some studies showed that stemflow contribution is not as negligible as it seems (Xiao et al., 2000; Staelens et al., 2008; Germer et al., 2010; Schooling and Carlyle-Moses, 2015). Under certain conditions, stemflow is an important component of the water cycle and as such it should be taken into account. However, it is a very challenging task to identify the conditions under which stemflow should be treated with additional attention.

The amount of stemflow and its proportion to gross rainfall depends on various variables (Crockford and Richardson, 2000; Zabret, 2013; Levia and Germer, 2015; Zabret et al., 2018; Sadeghi et al., 2020), which are mainly characterized as biotic (tree properties) and abiotic (precipitation event characteristics or meteorological conditions). The response of stemflow depends on the combination of all the factors for which the complex interaction has been addressed by multiple researchers. A study performed by Siegert and Levia (2014) was based on long-term observations which covered a wide variety of storm events as well as two tree species with a significantly different bark morphology. It showed that meteorological conditions in combination with tree traits play a complex role in influencing the stemflow amount. The influence of rainfall characteristics according to the phenoseasons was analyzed by Mużyło et al. (2012). They showed that in the leafless period longer rainfall events resulted in larger stemflow amounts while in the leafed period the interaction between stemflow and rain event characteristics was not that explicit. A significantly higher stemflow during the leafless rather than in the leafed period was observed also in other studies (André et al., 2008; Šraj et al., 2008; Zabret et al., 2017; Zabret and Šraj, 2019). However, leaf wettability and water storage capacity are also varying with seasons (Klamareus-Iwan and Witek, 2018). Additionally, Iida et al. (2017) showed that not only the phenophase but also the length of the event and its period (i.e., the first and the second half of the event development) influenced the response of stemflow. During the first half of the event, the observed stemflow values were lower and expressed a higher correlation with rainfall than during the second half. Schooling and Carlyle-Moses (2015) carried out an extensive study measuring stemflow for multiple isolated deciduous trees and concluded that in addition to a distinctive combination of tree characteristics, inducing larger stemflow volumes, also meteorological properties of the events play a significant role. Cayuela et al. (2018) observed different stemflow dynamics between the tree species due to a complex interaction of biotic and abiotic factors, while it was more influenced by abiotic than biotic factors. The research of short-time step development of stemflow as a function of tree species and tree size was performed by Levia et al. (2010), suggesting that all three parameters, namely tree species, tree size, and meteorological conditions, have detectable effects on stemflow yield. Similarly, van Stan et al. (2014) compared the influence of rainfall event characteristics for stemflow by differently sized trees and observed that the tree size was a factor altering the relationship between stemflow and meteorological conditions. The focus on the wind characteristics influencing stemflow was done by van Stan et al. (2011), comparing stemflow generation by trees with differing crown characteristics. The fact that stemflow response cannot be solely explained by the rainfall amount was also confirmed by Park and Cameron (2008), who analyzed stemflow response according to the canopy characteristics. The largest stemflow amounts were observed for a tree species with the highest live canopy length, the largest leaf area index, and the smallest canopy openness. Additionally, smooth bark was observed not to play a significant role in this case as bark absorptivity, leaf arrangement and branch angle seem to have a larger impact. Also, Schooling and Carlyle-Moses (2015) observed the variable effect of bark relief, as it depends also on the rainfall amount and single or multi leader form of the tree stem. However, other researchers in general reported that larger values of stemflow were observed for trees with smoother bark in comparison to those with the rougher one (André et al., 2008; Šraj et al., 2008; Cayuela et al., 2018; Zabret et al., 2018; Zhang et al., 2020).

Stemflow occurrence, its amount, dynamics of flow, and response to rainfall in the open are subject to multiple factors. The influence of biotic and abiotic factors is convoluted. In addition, the factors are also interdependent. These complex interactions were addressed in multiple previous studies, taking into account different combinations of factors and presenting different viewpoints. To contribute to the understanding of this complicated process, we took advantage of the long-term and high-resolution time-step measurements of stemflow, which were analyzed applying a new approach. The development of the amount of stemflow and rainfall in the open was presented graphically as the sum of the detected amounts per event. The figures were then automatically grouped based solely on their visual similarity using the hierarchical clustering approach. Only then we identified the characteristics of the events grouped in

the same cluster. With this method we aimed to provide new insight into how the stemflow is expected to develop under certain rainfall event conditions. Furthermore, we also tried to determine when it is necessary to consider stemflow in the rainfall partitioning analysis.

MATERIALS AND METHODS

Study Site

The study plot is part of a small urban park in the city of Ljubljana, Slovenia. The park is located in the city's suburb (46.04 °N, 14.49 °E) and is surrounded by a few single-story residential and public buildings. The study plot extends across a lawn with some individual trees and covers an area of approximately 600 m^2. On the southern side of the plot there is a two-story building. Additional measurements of rainfall on two locations at the study plot (near the building and in the open at the northern edge of the park, 18 m apart) for a shorter time period were performed to exclude the influence of the building on rainfall. Pearson correlation coefficient for the rainfall amounts measured at both locations was equal to 0.991 and there were no statistically significant differences between the means of the two datasets (p = 0.830). However, the slope of the regression line (0.911) was statistically different than 1 ($p < 0.001$). This indicates that the rainfall measured at the rain gauge may be up to 9 % higher. This error may be attributed mainly to the wind conditions. Therefore, more detailed measurements focusing on wind conditions and rain distribution at the study plot should be performed to confirm this observation.

Ljubljana is located in central Slovenia, characterized by sub-alpine climate with well-defined seasons. The Köppen Climate Classification subtype for this climate is "Cfb." The average temperature in winter is around −3°C and in summer 24°C. According to the long-term average (1986–2016), the total annual rainfall in Ljubljana is approximately 1,380 mm. The most rainfall is delivered in autumn, while the driest season is winter (ARSO, 2020).

For this study we focused on the birch tree (*Betula pendula* Roth.) located in the south western part of the plot. West to the studied tree there is another birch growing; however, the trees' canopies do not overlap. The observed birch tree is 16.2 m high, it has an 18.3 cm diameter at breast height, the projected area of the tree's canopy is 20.3 m^2, and the average branch inclination is upward and equals 53.3°. The bark is smooth and quite thin (3 mm) with a storage capacity of 0.7 mm. For the birch tree, four phenoseasons are significant: leafed, leaf-fall, leafless, and leafing. During the season with a fully leafed canopy, the storage capacity of the observed tree is equal to 3.5 mm, the canopy coverage is 78.3%, and the leaf area index is 2.6.

Data

The tree's height, the area of the projected canopy, and the branch inclination were determined from the photographs, taken at a required distance to avoid deformation of proportions. The diameter at breast height was calculated from the measured perimeter of the stem. The bark samples were extracted using a steel hole puncher. For the collected samples, the thickness and weight were measured. To determine the bark storage capacity, the samples were soaked in water for 24 h and then dried at 40°C until the weight of the samples, which was checked at half-hour intervals, stopped to decrease (Pérez-Harguindeguy et al., 2013). Phenoseasons were determined according to our observations of the numerosity of the leaves in the canopy, supported with the leaf area measurements, which were extensively performed during leafing and leaf-fall periods. The leaf area index was measured using LAI-2200c Plant Canopy Analyzer (LI-COR) following the protocol for isolated trees (Li-COR, 2015). Canopy coverage was estimated from the ratio of black to white areas on the pre-processed photographs of the tree canopy, taken vertically 1 m above the ground.

At the study plot we measured all the components of rainfall partitioning; however, only rainfall and stemflow are used in this study. These measurements have been performed since the beginning of 2014 (e.g., Zabret et al., 2017; Zabret et al., 2018; Zabret and Šraj, 2018; Zabret and Šraj, 2019). The period from 1 January 2014 to 30 September 2018 was selected for the analysis. The selected time period covers all seasons and corresponding phenoseasons, which occurred multiple times. We have selected 590 events for further analysis, excluding snow and sleet events as well as events during which the clogging of the tipping buckets was observed.

Rainfall in the open was measured using a tipping bucket rain gage with an automatic data logger (0.2 mm/tip, ONSET RG2-M, Onset HOBO Event data logger). The recorded rainfall series were divided into rainfall events, separated with at least 4-h dry periods. The length of the dry period between the events was determined according to the observations during field and previous measurements. From the recorded time series, the rainfall event duration, rainfall event intensity and the length of the dry period between the two events were calculated. For the rainfall events, which delivered less than 5 mm of rainfall in less than 2 h, additional verification of the duration and the intensity was performed using data, collected with a disdrometer (OTT Parsivel), positioned on the rooftop of a nearby building (Zabret et al., 2017).

Stemflow was collected using a rubber collar, spirally wrapped around the stem, attached with nails and packed with silicon (**Figure 1**). Collected water was transferred to a tipping bucket equipped with an automatic data logger (0.2 mm/tip, ONSET RG2-M, Onset HOBO Event data logger). The time series of the stemflow data was split according to the predefined rainfall events. The stemflow amount was corrected according to the canopy contribution area (Livesley et al., 2014; Siegert and Levia, 2014). The sum of stemflow (Σ SF) and rainfall amount (Σ R) per events were additionally calculated and used to determine the proportion of stemflow according to the rainfall in the open:

$$SF\ [\%] = \frac{\sum SF\ [mm]}{\sum R\ [mm]}$$

Additional meteorological data were included in the analysis to describe the microclimatic conditions during the event. Data on wind speed, wind direction, air temperature, and

FIGURE 1 | Study plot **(left)** and measurements of the stemflow at the selected birch tree **(right)**.

air humidity were obtained from the meteorological station Ljubljana Bežigrad, operated by the Slovenian Environmental Agency (ARSO, 2020). According to its location in the Ljubljana basin, its data are representative for the observed location (Nadbath, 2008). Using half-hour records of the observed variables their average values during the selected rainfall events were calculated.

Methods

The influence of meteorological variables on stemflow development by birch tree was investigated using a different approach than usual. Instead of first analyzing the characteristics of the events, we graphically presented the development of rainfall and stemflow per event. Therefore, in the first step the graphical presentation of the measured rainfall and stemflow data was prepared. In the second step, we grouped the figures into clusters using hierarchical clustering, and in the third step, we analyzed the meteorological variables per events, grouped in individual cluster.

The graphical representation of the rainfall and stemflow development per event was based on the complete time series of the measured rainfall and stemflow. The raw measured time series were divided by rainfall events, separated with dry period of at least 4 h. Data were summarized in 5-min intervals and the values were plotted on the graphs, with the x-axis indicating the duration of the rainfall event in 5-min intervals and the y-axis indicating the summarized amount of rainfall or stemflow in mm (**Figures 2**, **4**). The graphs of rainfall and stemflow development were generated using the function ggplot (Wickham et al., 2020) in R, a software environment for statistical computing and graphics (R Core Team, 2020). The values of stemflow were increased by a factor of 10 to be able to demonstrate the increase in stemflow due to its low values in comparison to rainfall. These graphs were all prepared using the same algorithm regardless of the rainfall event duration, the total amount of rainfall or stemflow. The unprocessed graphs were then used for hierarchical clustering.

Hierarchical clustering of figures was performed in the Orange software (Demšar et al., 2013). First, the figures were transformed into a numerical format using the image embedding algorithm. Then, the Cosine metrics was applied to calculate the distances among the figures, describing their similarity (**Figure 2**). The figures, named by the date of the event, were grouped into the clusters according to their visual similarity, which was also taken into account in their numerical transformation and calculated using a distances metrics. According to the splitting of the dendrogram, the division of the data set into four clusters was selected, corresponding to the third row of the dendrogram or the height ratio of 64% (**Figure 2**).

According to the results of hierarchical clustering, the events were divided into four clusters. For each cluster, the typical response of stemflow was observed between the grouped figures (**Figure 4**). However, the common meteorological characteristics associated with such a response were analyzed in the third step. For the events of each cluster we determined the total rainfall amount and duration, the average rainfall intensity, the average wind speed and direction, air temperature and vapor pressure deficit, as well as the dry period duration before the event and the phenoseason in which the event was observed (**Figure 5**). A comparison of these characteristics per cluster was performed.

RESULTS

General Stemflow and Rainfall Event Characteristics

In the observed period from 1 January 2014 to 30 September 2018, the 590 registered rainfall events in total delivered 6,203 mm of rainfall. Stemflow was detected during 250 rainfall events, for which the complete time series of rainfall in the open, throughfall, and stemflow were compared. Some data were recognized as clearly incorrect due to fouling of the collectors (e.g., ant infestation, clogging of inflow with leaves) and were removed from the considered data set. Therefore, 156 events with complete time series records of rainfall and stemflow were selected for the further analysis. Stemflow was detected for the events with at least 0.8 mm, while 8 mm of rainfall was needed to initiate continuous flow of stemflow.

The 156 analyzed rainfall events in total delivered 3,066.5 mm of rainfall, from 0.8 to 102 mm of rainfall per single event

(**Table 1**). The shortest rainfall event lasted for 13 min, delivering 2 mm of rainfall, while the longest rainfall event, observed in November 2016, lasted for more than 2 days (67 h) and delivered 84 mm of rainfall. The average rainfall intensity of the analyzed events was equal to 2.4 mm/h (± 2.6 mm/h), reaching up to 13 mm/h, observed during an hour long event in the beginning of June 2016. The average air temperature was equal to 12.4°C (± 5.3°C) and the average vapor pressure deficit was equal to 0.17 kPa (± 0.16 kPa) per event. Approximately half of the events were observed during the leafed period from mid-April to mid-September, one third of the events was observed during leafless period from the late October to the end of March and the rest of the events were detected either during leafing or leaf-fall periods (**Table 1**).

Stemflow by birch tree during the analyzed events averaged to 3.0% of rainfall in the open, ranging between 0.02 and 15.57%. The stemflow data were not normally distributed as indicated by the results of histogram (skewness = 1.5 and kurtosis = 2.1) and the Shapiro-Wilk normality test (p = 9.94e-13) (van Stan and Gordon, 2018). For almost half of the considered events (45%) the observed stemflow was less than 1% of rainfall in the open, while for majority of the events (80%) stemflow accounted for less than 5% (**Figure 3**). Therefore, the median value of stemflow for analyzed events was equal to 1.6% of rainfall in the open.

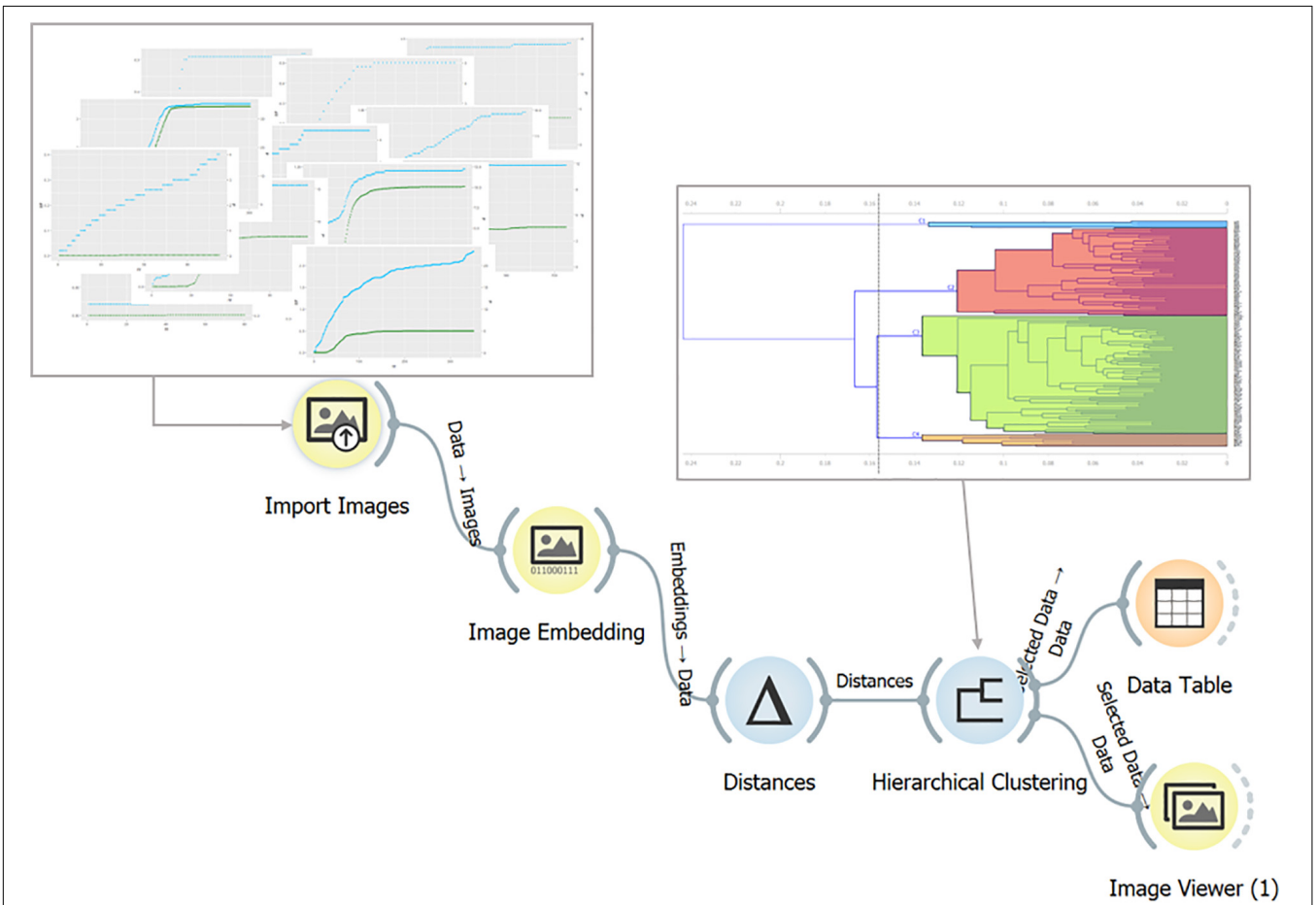

FIGURE 2 | A flowchart of the steps for hierarchical clustering in Orange software with examples of imported images and final dendrogram with division into four clusters.

TABLE 1 | The total rainfall and stemflow (SF) amounts and average event-based values of rainfall duration (Rd), intensity (Ri), wind speed (Ws), air temperature (T) and vapor pressure deficit (VPD) for the events during the individual phenoseasons.

Phenoseason	No of events	Rainfall (mm)	SF (mm)	Rd (h)	Ri (mm/h)	Ws (m/s)	T (°C)	VPD (kPa)
Leafed	85	1424.4	53.6	9.5 (±9.3)	2.7 (±2.8)	1.3 (±0.6)	15.5 (±4.0)	0.23 (±0.20)
Leaf-fall	12	208.8	6.3	7.4 (±5.3)	3.4 (±3.2)	1.2 (±0.5)	14.2 (± 3.0)	0.12 (±0.07)
Leafless	52	1258.1	78.9	16.7 (±14.8)	1.7 (±1.8)	1.4 (±0.5)	7.0 (±3.2)	0.10 (±0.06)
Leafing	7	175.2	5.7	11.5 (±6.3)	2.6 (±1.6)	1.4 (±0.5)	11.2 (±2.7)	0.13 (±0.03)
All	156	3066.5	144.5	11.9 (±11.7)	2.4 (±2.6)	1.3 (±0.5)	12.4 (±5.3)	0.17 (±0.16)

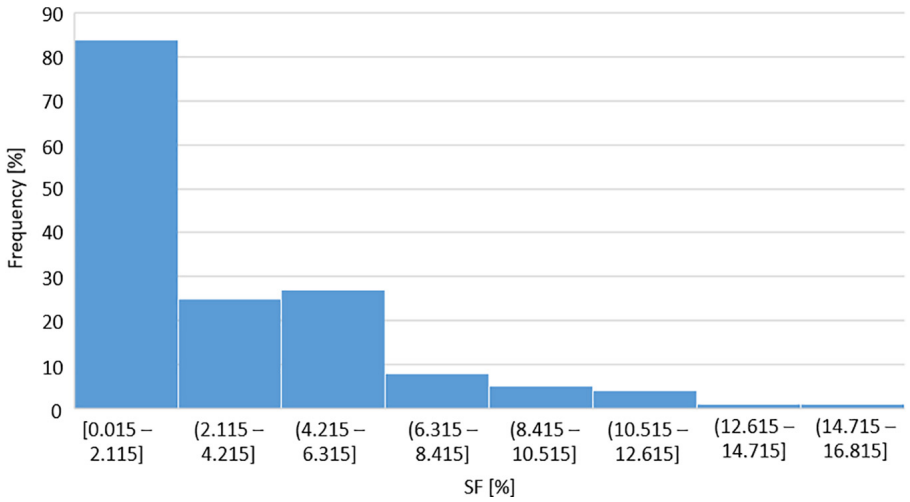

FIGURE 3 | Histogram of measured stemflow values for birch tree.

The highest values of stemflow were observed during the leafless period, 4.3% on average per event and with a median of 4.2%, resulting in total of 78.9 mm of rainfall in the open during 52 events (**Table 1**). During the leafing period the average stemflow per event was a bit smaller than in the leafless period, as its median was equal to 2.2%. Stemflow was on average the lowest during the leaf-fall and the leafed period, when its median was equal to 0.3 and 0.6%, respectively. In the leafed period stemflow in total contributed 53.6 mm during 85 events (**Table 1**). The difference between the stemflow values in leafed and leafless periods was statistically significant with p-value less than 0.001.

Hierarchical Clustering

The results of hierarchical clustering are presented on a dendrogram (**Figure 2**, top right). Based on the structure of dendrogram's branches, four clusters were selected. The figures, grouped in each cluster were reviewed and accordingly four types of stemflow response were determined (**Figure 4**), namely the group of no response, the group of slow and independent increase, the group of moderate increase and the group of strong response of stemflow.

Events, showing no response of stemflow according to the increasing total amount of rainfall in the open, were grouped in cluster 1. 5 events were grouped in this cluster with stemflow reaching between 0.07 and 0.23% of rainfall per event, on average 0.11% (**Figure 5**). Four of them were detected in the leafed and one at the end of the leafless period. The rainfall amount per event was on average quite low (2.8 mm) and the events were short (27 min on average). As the majority of the events were observed in the leafed period, corresponding to the warmer months of the year, a fairly high average air temperature (18.1°C) and vapor pressure deficit (0.6 kPa) were also observed.

For the events, merged in cluster 2, the grouped figures indicated slow increase of stemflow, which was independent to the increase of the rainfall totals in the open (**Figure 4**). Cluster 2 merges 61 events with a median value of stemflow equal to 0.18% of rainfall (**Figure 5**). The majority of the events (40 events) were observed during the leafed phenoseason. Analysis of the grouped figures shows that stemflow responded to the increase in rainfall amount. However, the line representing the stemflow volume increases slower and independently of the rainfall volume line (**Figure 4**). Rainfall events, grouped in cluster 2, were also quite small as the rainfall amount per event was on average 6.1 mm and did not exceed 18.5 mm (**Figure 5**). The rainfall event duration was on average 5.3 h, resulting in a fairly average rainfall event intensity of 2.12 mm/h, similar to the average intensities of the rainfall events grouped in clusters 3 and 4 (**Figure 5**). However, events with observed minimum and maximum values of rainfall intensity were assigned to cluster 2. Air temperature during the selected events was quite high, i.e., 13.9°C on average, while the average value of vapor pressure deficit of the events accounted for 0.2 kPa. The length of the dry period between the events ranged from 4.9 h to more than 11 days.

Moderate increase of stemflow amount was observed during the events grouped in cluster 3. This cluster was also the largest, combining 81 events with stemflow proportion averaging 3.8% of rainfall per event. The development of the stemflow followed in most cases the development of rainfall during the event (**Figure 4**). The amount of stemflow reaching the ground was significantly smaller than the amount of rainfall in the open, however, the increase in its amount with the development of the event followed the shape of the curve, formed by the increase in the rainfall amount. Characteristics of the rainfall events, assigned to cluster 3, show larger rainfall amounts and longer duration of the events comparing to the events grouped in clusters 1 and 2 (**Figure 5**). The average amount of rainfall was 28.1 mm and the average duration of the rainfall events was 16.6 h. This results in similar rainfall intensities as those for the events grouped in cluster 2 (**Figure 5**). Air temperature during the events was slightly lower, ranging from 0.8 to 20.3°C, while vapor pressure deficit values ranged from 0.01 to 0.42 kPa. Half of the events (40 events) were observed during the leafed period,

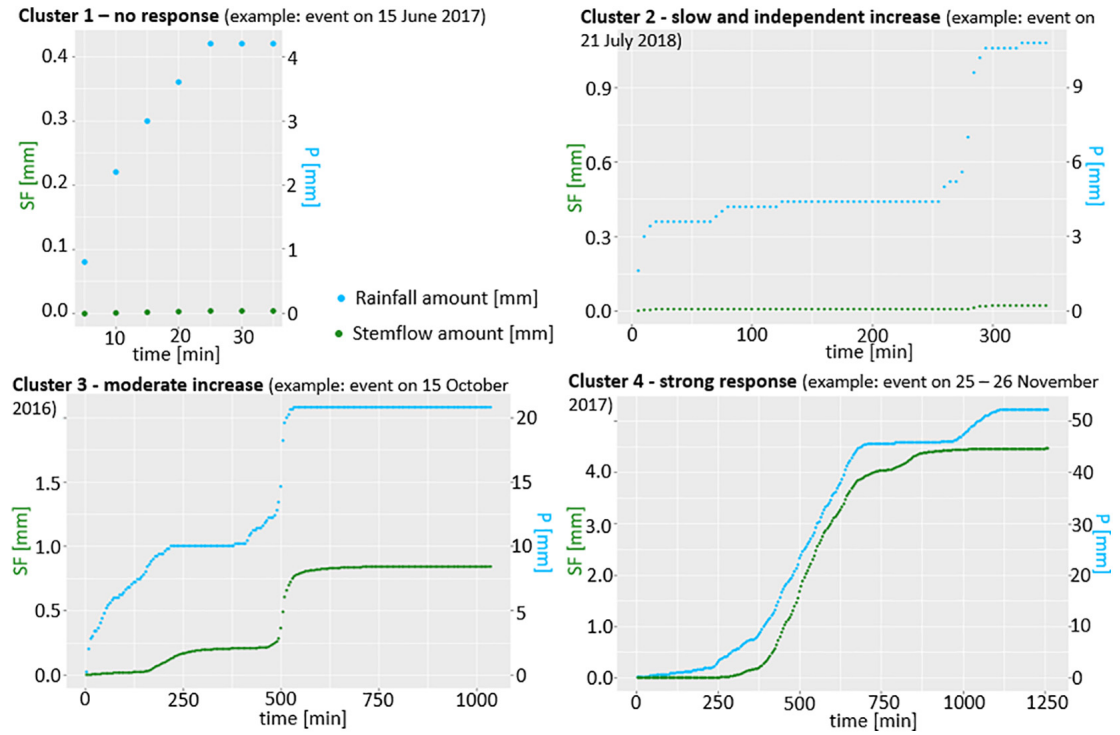

FIGURE 4 | Examples of figures showing typical development of stemflow and rainfall grouped in individual clusters (amounts of stemflow and rainfall are plotted as the sum of the detected amounts at 5-min time intervals; the left y-axis shows values of stemflow increased by a factor of 10, the right y-axis shows values of rainfall in the open).

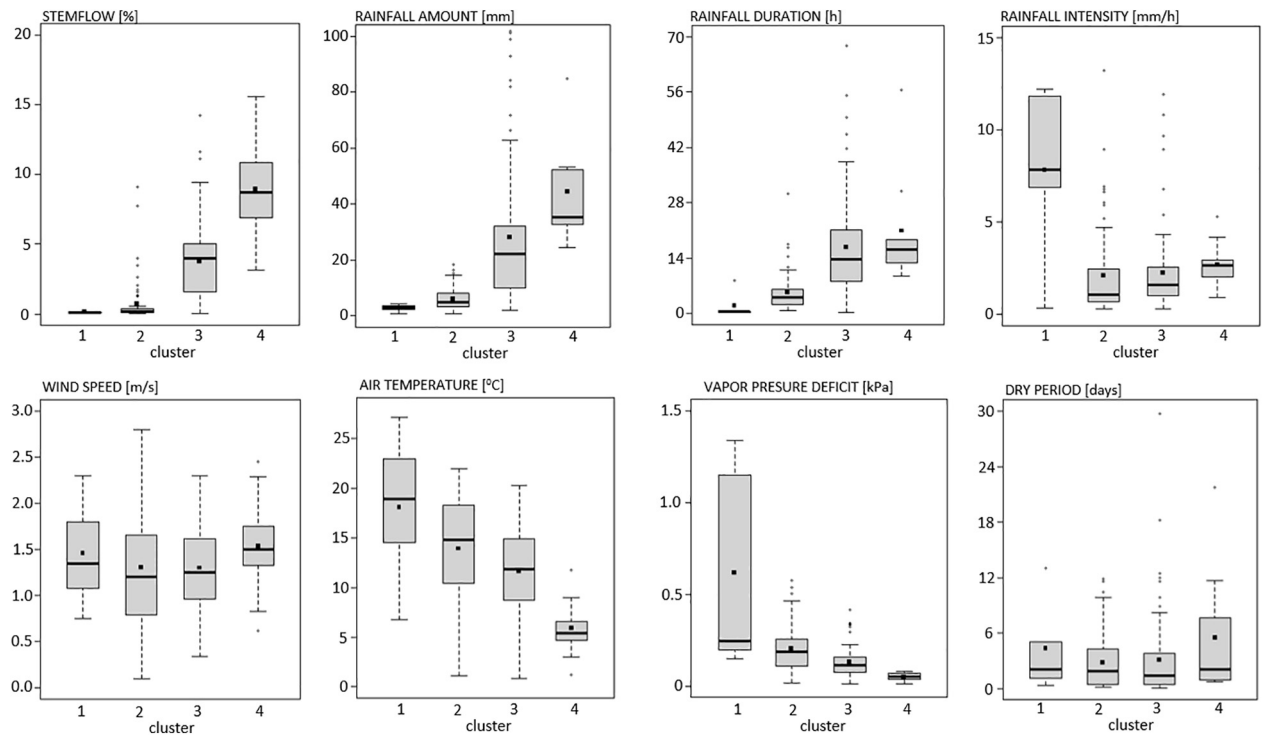

FIGURE 5 | Comparison of rain event characteristics for the events grouped in each cluster.

while the rest of the events associate with the transitional or the leafless period.

Events with the strongest response of stemflow to the amount of rainfall in the open were assigned to cluster 4. 9 events grouped in cluster 4 were characterized with a stemflow proportion between 3.1 and 15.6% of rainfall per event, on average 9.0% of rainfall (**Figure 5**). They were mainly detected in the leafless period, only one event was observed in the leafed and one in the leafing period. All of the events delivered a substantial amount of rainfall (on average 44.5 mm per event), which resulted in a high proportion of stemflow and its strong response to the increase of rainfall amount during the progress of the event (**Figure 4**). The line of the magnified stemflow volume (multiplied by 10 for a clearer comparison) actually exceeded the volume of the plotted rainfall line in some cases. In addition to the large rainfall amounts, these events were also among the longest, averaging 20.8 h, but still quite intense (on average 2.7 mm/h; **Figure 5**). According to the corresponding phenoseasons and the time of the year in which the events occurred, the average air temperature during the events was the lowest, between 1 and 9°C and on average 5.9°C, with the exception of one event observed during the leafed period (11.8°C). The average vapor pressure deficit was the lowest among the four clusters, on average equal to 0.05 kPa. For the events in cluster 4 the longest dry periods were observed prior to the events, lasting more than 5 days on average.

DISCUSSION

For monitoring of stemflow and data analysis only one birch tree was selected. Although the considerable intra-specific variations in stemflow are expected and the data of the presented analysis cannot be generalized to the other tree species, the main contribution of this research is in the data set itself and in the analysis that is enabled by such a dataset. The collection of a long term data with a short-time step is very time consuming, requires long-term presence of qualified staff and financial resources to maintain the equipment as well as ensuring the presence of the researchers, maintaining the plot and equipment, regularly collecting and analyzing the data. Therefore, the data sets covering several years and providing measurements in real time during the events are scarce. However, such data are needed to enable understanding of the influence of changing meteorological conditions during seasons on stemflow and its temporal development. Therefore, such a data set is crucial for supporting the implementation of new methods of analysis and understanding the development of stemflow.

Stemflow Characteristics

On average per event stemflow by birch tree accounted for 3.0% of rainfall in the open. Significant difference ($p < 0.001$) in stemflow values was observed between the leafed and the leafless period, as the difference in average stemflow per the period was equal to 2.6%. The average amount of stemflow is similar to the values observed for other deciduous tree species considered as having a smooth bark surface and growing in urban areas. Livesley et al. (2014) reported an average stemflow of 1.7% for *Eucaliptus saligna* tree in Melbourne, Australia, Xiao and McPherson (2011) observed 2.1% of stemflow under *Citrus limon* and 4.1% of stemflow under *Liquidambar styraciflua* tree in Oakland, California, and Guevara-Escobar et al. (2007) reported 2.2% of stemflow under *Ficus benjamina* tree in Queretaro city, Mexico.

Additionally, differences in the stemflow values for the deciduous trees among the leafed and leafless period were observed also in other studies. The difference reported for the two phenoseasons was similar to 1.7% detected in a deciduous forest plot in Eastern Pyrenees Mountains in Spain (Mużyło et al., 2012) and in a deciduous north-faced forest in Slovenia (Šraj et al., 2008). Furthermore, 1.6 % difference was observed for beech and 2.0% for oak tree, located in a mixed oak-beech stand in Belgium (André et al., 2008), 1.2% was monitored in a dry tropical forest in Northeast Brazil (Brasil et al., 2020) and a 3.1% difference was measured for a single beech tree in Belgium (Staelens et al., 2008). In all of the mentioned studies larger stemflow values were observed during the leafless period. In general, some differences in rainfall partitioning by deciduous trees are expected between the phenoseasons due to the substantial changes of the canopy characteristics (Zabret, 2013). During the leafless period the absence of leaves and consequently the bare branches regulate the retention and the redistribution of the rainfall water differently than during the fully leafed canopy, influencing also the paths of flow of the intercepted rainfall. In the leafed period significant amount of water is retained on the leaves and when the surface water droplet retention is fulfilled, rainfall start to drip to the ground as throughfall instead of running down the branches and stem as stemflow. Namely, due to the leaves hydrophobicity and the angle, raindrops stored on the leaves are mainly directed to the ground as dripping (Holder and Gibbes, 2016). However, during the leafless period rainfall is intercepted only by branches. When the bark storage capacity of the branches is reached, water starts to gather on the surface of the branches. Some drops fall toward the ground, however, the substantial amount is also following the flow path created by the branches toward the stem and the ground as stemflow (Sadeghi et al., 2020).

The analysis of stemflow amount and its development under birch tree indicated, that there were 0.8 mm of rainfall needed to initiate stemflow, while continuous flow was observed during the events with more than 8 mm of rainfall. The value needed to initiate the stemflow is similar to 0.6 mm, observed in a deciduous forest in Slovenia (Šraj et al., 2008) and to 1 mm reported for a single *Eucalyptus saligna* tree in Melbourne, Australia (Livesley et al., 2014). All of the mentioned tree species have smooth bark and all of the locations are categorized by "Cfb" climate according to the Köppen climate classification. Therefore, this simple comparison indicates that for the trees with similar bark characteristics and in similar climate zones stemflow initiate in a comparable manner. However, further information on other tree characteristics such as orientation of the branches or canopy size may offer an additional explanation, but such data are seldom available in the published research (Levia and Herwitz, 2005).

On the other hand, the comparison of values needed for continuous observation of stemflow show different responses of the compared trees. In the case of *E. saligna* tree only 2 mm

was needed (Livesley et al., 2014), whereas for the birch tree, 8 mm of rainfall was required to initiate continuous stemflow. Furthermore, a value of 5 mm was reported to initiate continuous stemflow in case of *Fagus gradifolia* tree, growing in a forest located in Maryland, United States (Siegert and Levia, 2014), 8.5 mm was needed in case of tanoaks in Caspar Creek watershed in California (Reid and Lewis, 2009), and Su et al. (2016) reported values between 6.9 mm and 14.8 mm for trees in a subtropical forest of Daba Mountains in Central China. All of the mentioned tree species have smooth bark surface, however, the locations of these study plots belong to various climates. This comparison indicates that the rainfall amount and the tree characteristics (i.e., bark structure, surface and absorptiveness, canopy coverage) are not the most influencing parameters, regulating the stemflow. According to the presented values of the studies from all over the world, also the micro-climatic conditions may substantially influence the occurrence and the development of stemflow (Inkiläinen et al., 2013; van Stan et al., 2016).

The Development of Stemflow

According to the collected data we have produced graphs representing the rainfall and stemflow development during the rainfall event. The hierarchical clustering of the figures resulted in four groups, describing different levels of stemflow response. We were not able to find any similar study with such a short time data step for larger number of events. However, a few studies were identified, providing sufficient data for comparison of stemflow response per a single event to the one observed in our analysis (**Figure 4**).

Iida et al. (2017) analyzed the intra-storm scale rainfall interception dynamics, using hourly data. The analysis was performed for one selected event, which delivered 30.1 mm of rainfall during more than 2 days. A graph of stemflow and rainfall development for the considered event would be assigned to cluster 3 of the presented analysis. The characteristics of the considered event also correspond to the values, significant for the events grouped in cluster 3 (**Figure 5**). Additionally, Levia et al. (2010) performed 5-min time step measurements of stemflow production for different tree species with various characteristics. In the analysis, the synchronicity between the timing of rainfall and stemflow yield was also presented. The data collected during an ∼8-h long event, delivering 7.6 mm of rainfall, show a slight response of the stemflow volume to the rainfall volume increase. According to the response of stemflow, this event would be assigned to cluster 2, corresponding also to its meteorological characteristics (**Figure 5**).

The results, presented by Levia et al. (2010) and Iida et al. (2017) correspond well to the observations of the stemflow response, presented in this study (**Figures 4**, **5**). The measurements, performed by Iida et al. (2017) focused on coniferous Japanese cedar tree, located in Tsukuba, Japan, which is classified as "Cfa" according to the Köppen Climate Classification. Levia et al. (2010) presented results for deciduous *F. grandifolia* tree, located in Maryland, United States, also characterized by "Cfa" climate subtype. Thus, the climate characteristics of both mentioned locations are similar to the one at the observed study plot in Ljubljana ("Cfb" by Köppen Climate Classification). Additionally, *F. grandifolia* is quite similar tree species to observed birch tree, as both are deciduous trees with smoother bark surface. However, the observed *F. grandifolia* tree had much larger diameter at breast height (74.9 cm) than our birch tree (18.3 cm). In addition, Japanese cedar tree is coniferous tree species with bark that peels off in long strips. Therefore, the comparison of the results suggests, that under similar climate the development of stemflow with the rainfall event progress is independent to the tree species. However, comparison with multiple measurements for a larger number of tree species is necessary to verify this observation.

The Influence of Meteorological Variables

For the considered rainfall events, the general characteristics of the influential variables per cluster were analyzed to characterize how the meteorological conditions during the event regulate the development of stemflow. The range of the values per individual cluster indicate the dependence on the rainfall amount, duration and intensity, the phenoseason in which the event was observed, as well as the average air temperature and vapor pressure deficit during the event. However, no characteristic values per cluster were observed for the average wind speed and its direction during the event (**Figure 5**).

The studies, focused on the variables, influencing the stemflow amount, usually reported the total rainfall amount per event as the most influencing variable (Xiao et al., 2000; Staelens et al., 2008; Germer et al., 2010; Siegert and Levia, 2014; van Stan et al., 2014; Su et al., 2016; Zabret et al., 2018; Zhang et al., 2020). This is expected, as the tree canopy and the bark storage capacity are becoming saturated during the initial phase of the event. When the rainfall amount reaches the threshold, saturating the canopy and the bark, stemflow can fully initiate. This process was confirmed by Xiao et al. (2000) during the high frequency measurements of rainfall, throughfall and stemflow. They demonstrated that in the case of the small rainfall events stemflow was controlled by the antecedent moisture of the tree surface, while for saturated tree conditions the magnitude of stemflow was dependent on the amount of rainfall. Also, Germer et al. (2010) reported that the time between the maximum rainfall intensity and the maximum stemflow depends on the rainfall amount saturating canopy storage capacity. Additionally, higher storage capacity of the trunk and branches of the oak in comparison to the beech tree species was recognized as a crucial variable influencing rainfall thresholds for stemflow occurrence (André et al., 2008). Considerable influence of rainfall amount on the stemflow development and its total value was also observed in this study. Values of total rainfall amount per event, grouped in individual cluster, were significantly different ($p < 0.05$). Additionally, significant difference was observed also between the stemflow values per cluster ($p < 0.001$), except between clusters 1 and 2 ($p = 0.21$). Also the correlation coefficient of 0.992 between the median values of stemflow and rainfall amount per cluster indicate significant interdependence between the rainfall and stemflow amount, as well as the response of stemflow.

Rainfall amount per events, grouped in clusters 1 and 2, were quite similar as the median value for cluster 1 was equal to 3.0 mm and for cluster 2 was 5.0 mm. Additionally, all rainfall events delivering less than 5 mm of rainfall were assigned either to cluster 1 or cluster 2. Further comparison of rainfall characteristics for only these small rainfall events (<5 mm) showed, that events assigned to cluster 1 were significantly shorter ($p < 0.05$) and their rainfall intensity was significantly higher ($p < 0.001$) in comparison to the events in cluster 2. Air temperature and vapor pressure deficit during the small rainfall events, grouped in cluster 1, were also significantly higher. As all of these events were observed in the leafed period, these differences are not related to the season. Although stemflow values for the events, grouped in clusters 1 and 2 were not that different, the stemflow response was (**Figure 4**). Therefore, it seems that the stemflow response during the rainfall events delivering less than 5 mm is related to the intensity and duration of the rainfall, as well as to the meteorological conditions during the event. For similar amounts of rainfall, stemflow will increase during the events with longer and less intense precipitation, while short and intense events will not produce any noticeable flow down the stem. This observation corresponds to the finding of Xiao et al. (2000), who reported that for the rainfall intensity greater than 1.5 mm/h stemflow for oak and pear trees was decreasing. Similarly, in a laboratory experiment Keim et al. (2006) showed that branches generally retain more water at a high rainfall intensity until some incremental storage is reached.

Although rainfall intensity was recognized as a variable, regulating stemflow response for the small rainfall events, its values were not significantly different among clusters. Furthermore, the average values of the rainfall intensity per clusters 2, 3, and 4 were equal to 2.4, 2.3 and 2.7 mm/h, respectively, while the median values show a slight deviations of values for cluster 4, as median rainfall intensity values were equal to 1.2, 1.6, and 2.6 mm/h, respectively. As the mean and median values of rainfall intensity for clusters 2 and 3 were similar, the distinct response of stemflow may be assigned to statistically significantly different ($p < 0.0001$) rainfall amounts and duration of the events, assigned to clusters 2 and 3. This might be connected to the observations by Mużyło et al. (2012), who pointed out the influence of rainfall duration on stemflow in the leafless period and the influence of rainfall intensity in the leafed period. Namely, the notable influence of rainfall intensity was detected for the events, assigned to cluster 1, which were observed mainly in the leafed period. Regardless of the complex interaction between the variables, the results might also be different taking into account the inter-event rainfall intensity values of shorter time steps. For example, Staelens et al. (2008) observed that the maximum hourly and 10-min rainfall intensity had a higher correlation with the stemflow values than the average rainfall intensity, while Cayuela et al. (2018) showed a significant response of stemflow to 5-min rainfall intensity.

The difference in the stemflow development during the events, grouped in clusters 2, 3, and 4 is not correlated to the intensity of the rainfall during the event. However, in addition to an increase in the rainfall amount and duration, a significant decrease of average air temperature and vapor pressure deficit (VPD) among the events in a single cluster were observed ($p < 0.005$). The average air temperature and VPD during the events correspond to the season/phenoseason in which the event was observed. In addition, rainfall characteristics are dependent on the season to some extent (Mużyło et al., 2012; Levia and Germer, 2015; Brasil et al., 2020). However, the size of clusters 2 and 3 is quite large (corresponding to 61 and 81 events, respectively) and the events are not characterized only by one prevailing phenoseason. The majority of the rainfall events, grouped in cluster 2, were observed between April and October (leafed period), while 13 out of 61 events occurred from November to March (leafless period). This is also reflected in the on average high air temperatures and VPD (**Figure 5**). Events, which delivered the most rainfall and lasted for the longest time, were grouped in clusters 3 and 4. Although no phenoseason prevailed among the events grouped in cluster 3 (40 events were observed in leafed, 29 in leafless and 12 in transitional period), the air temperature and VPD were significantly lower than during the events assigned to clusters 1 or 2.

The comparison of the rainfall event characteristics with the corresponding phenoseason show, that the differences in rainfall amount, duration, air temperature and VPD during the event among clusters are not associated only to the phenoseason. The complex interaction between phenoseasons and meteorological characteristics was already recognized as very complex (André et al., 2008; Mużyło et al., 2012; Iida et al., 2017). For example, Klamareus-Iwan and Witek (2018) observed that leaf wettability and water storage capacity are varying with seasons. However, to eliminate the influence of the phenoseason, we have compared the characteristics of the events observed only in the leafed period, which were grouped in clusters 2 and 3. The average air temperature for the events assigned to cluster 2 was higher (16.2°C) than for the events assigned to cluster 3 (14.4°C). In addition, the VPD was significantly higher ($p < 0.005$) for the events, assigned to cluster 2. Therefore, the difference in meteorological characteristics of the events was not related only to the season. Also the different response of stemflow, observed for clusters 2 and 3 was not the consequence of different canopy characteristics according to the phenoseasons. The results of hierarchical clustering (**Figure 4**) and analysis of the characteristics of the events per cluster (**Figure 5**) indicate that stemflow is more responsive to the rainfall input during colder events with the lower VPD conditions. Both, lower air temperature and lower VPD values indirectly decrease the evaporation, which may lead to more intense stemflow response.

The comparison of the meteorological conditions during the events, grouped in clusters, show no influence of wind characteristics (**Figure 5**). However, the influence of wind speed and direction on stemflow was already reported in numerous studies (Xiao et al., 2000; André et al., 2008; Staelens et al., 2008; Šraj et al., 2008; van Stan et al., 2014; Iida et al., 2017; Zabret et al., 2018; Zabret and Šraj, 2019). Additionally, the development of stemflow during the rainfall event was in detail analyzed by van Stan et al. (2011). The study showed the significant influence of wind-driven rainfall on stemflow development, taking into account 5-min time step data on wind direction during the event. Therefore, the observed influence of wind characteristics

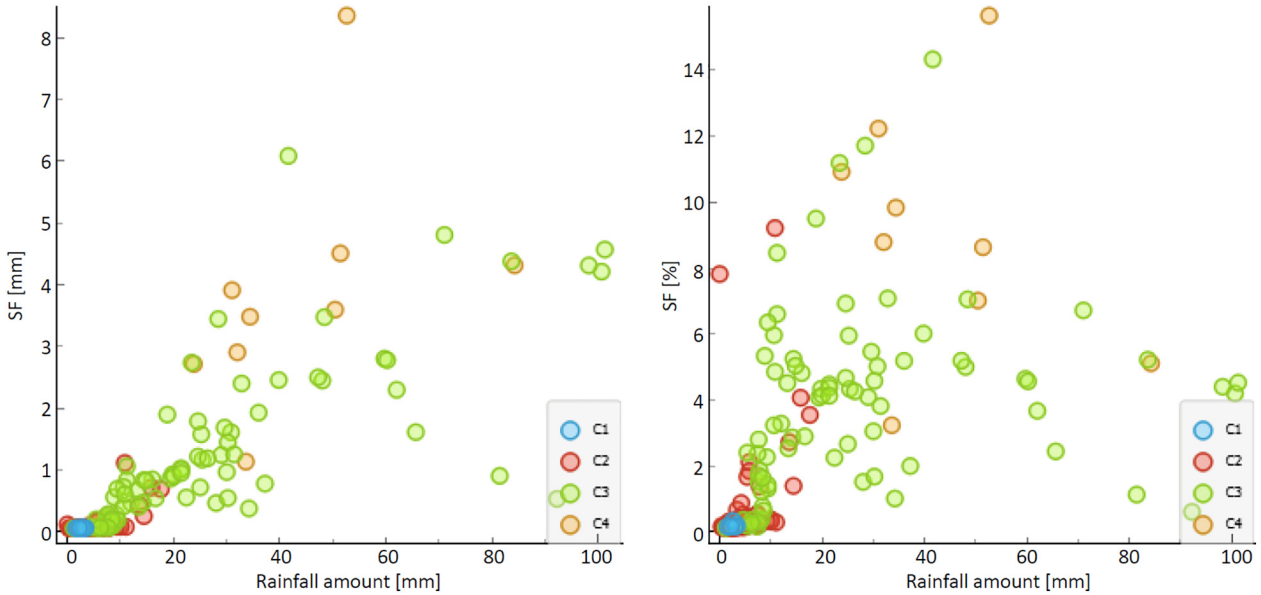

FIGURE 6 | Relationship between the rainfall amount and the corresponding stemflow according to clusters of stemflow response.

seems to be dependent on the method used for the analysis and the time step of the data taken into account (inter-event development of rainfall conditions). Thus, it appears that taking into account the average data on wind conditions during the event may lead to different results regarding the influence of wind conditions on stemflow response, as identified by clusters (**Figure 4**). Accordingly, we believe that the analysis of wind influence should be improved, taking into account shorter time step data, allowing to represent the changes in wind speed and direction during the event.

The Influence of the Stemflow Response on the Stemflow Volume

Values of the total stemflow and rainfall amount per event (**Figure 5**) show strong relationship with the observed response of the stemflow development during the event (**Figure 4**). This leads to a conclusion that stemflow response, defined through the process of hierarchical clustering, is significantly dependent on the total stemflow and rainfall amount per event. However, additional comparison of the results shows also a different interdependence. Events, delivering a similar amount of rainfall, as well as events with a similar proportion of stemflow according to the amount of rainfall in the open were assigned to different clusters (**Figure 6**). For example, events observed on 26 June 2016 and 3 October 2016 both delivered similar amounts of rainfall (15.2 mm and 15.6 mm, respectively), both occurred in the leafed phenoseason and after a similarly long dry period (10.4 and 9.8 h, respectively). However, the rainfall intensity and duration of both events were significantly different. The June event lasted for 1.1 h and had an average rainfall intensity of 13.2 mm/h, while the event in October lasted for 4.5 h, resulting in an average rainfall intensity of 3.5 mm/h. Additionally, air temperature and VPD were higher during the event in June (19.9°C and 0.31 kPa) than during the event in October (11.9°C and 0.13 kPa). According to different rainfall event characteristics and meteorological conditions, both events were grouped into different clusters, namely the June event in cluster 2 and the October event in cluster 3, indicating a different response of stemflow, and also resulting in a different proportion of the stemflow reaching the ground, i.e., 1.3% in June and 4.9% in October.

Such comparison of data confirms a large variability of stemflow among rainfall events, which was reported also by Cayuela et al. (2018). In the scope of the presented research, this variability/relationship seems to be also depended on the type of the stemflow response (**Figure 4**). Therefore, inter-event meteorological characteristics, in comparison to the phenophase, seem to dictate the stemflow response to rainfall occurrence and after all also the total amount of the stemflow reaching the ground. Somehow, this was suggested also by Swaffer et al. (2014), who compared the stemflow amount for two morphologically distinct tree species and observed a larger influence of inter-event variability than plot location or tree species characteristics. Similarly, the influence of meteorological variables in comparison to the canopy characteristics or plot location for stemflow occurrence was detected by Toba and Ohta (2005).

CONCLUSION

In this study a detailed analysis of the development of stemflow during 156 rainfall events for a single birch tree (*Betula pendula* Roth.) at the study plot in the city of Ljubljana, Slovenia, was conducted. For this purpose, a new approach was applied, namely the hierarchical clustering based on the graphical presentation of the rainfall and stemflow development during the event. In the next step, significant meteorological characteristics were

determined for each cluster of events in order to connect the stemflow development to the corresponding rainfall event characteristics and meteorological conditions during the event.

Four characteristic types of stemflow response were identified and connected to the corresponding event characteristics. In general, the results of the study demonstrate the response of stemflow is dependent to the rainfall amount per event, as larger events generate more responsive stemflow. However, if the rainfall events deliver less than 5 mm of rainfall, stemflow will show at least some response during longer and less intense events, while its response is expected to be negligible for shorter and intensive events. For the larger rainfall events in addition to rainfall amount also the rainfall duration has a significant influence on the stemflow response. However, more intense response is expected for the events occurring during lower air temperature and vapor pressure deficit. The fact that the response of stemflow during the events with similar rainfall amount can be substantially different due to the meteorological characteristics and other characteristics of the event, indicates that the type of the stemflow response influence also the total amount of stemflow reaching the ground.

By identifying the four groups of typical stemflow response to rainfall, we captured the complex relationships among the influencing factors, i.e., stemflow proportion and rainfall event characteristics (the amount, duration, and intensity of rainfall), as well as meteorological (air temperature, vapor pressure deficit, wind speed and wind direction), and vegetation (phenophases) conditions during the events. Furthermore, the identified types of typical stemflow response to rainfall correspond well to the examples from other locations and for other tree species that we were able to obtain from some other studies. However, further investigation is needed in terms of, e.g., a shorter time step of rainfall intensity and wind characteristics, additional variables (e.g., drop size distribution), new examples from different climates as well as for additional tree species in order to upgrade the proposed model of grouping.

DATA AVAILABILITY STATEMENT

The raw data supporting the conclusions of this article will be made available by the authors, without undue reservation.

AUTHOR CONTRIBUTIONS

KZ analyzed the data and drafted the manuscript. KZ and MŠ wrote the manuscript and revised it. Both authors contributed to the article and approved the submitted version.

REFERENCES

André, F., Jonard, M., and Ponette, Q. (2008). Influence of species and rain event characteristics on stemflow volume in a temperate mixed oak–beech stand. *Hydrol. Process.* 22, 4455–4466. doi: 10.1002/hyp.7048

ARSO (2020). *Meteorological Archive*. Available online at: http://www.meteo.si/met/sl/archive/ (accessed December 15, 2020).

Asadian, Y., and Weiler, M. (2009). A new approach in measuring rainfall interception by urban trees in coastal British Columbia. *Water Qual. Res. J. Can.* 44, 16–25.

Brasil, J. B., de Andrade, E. M., de Queiroz Palácio, H. A., dos Santos, J. C. N., and Medeiros, P. H. A. (2020). Temporal variability of throughfall as a function of the canopy development stage: from seasonal to intra-event scale. *Hydrolog. Sci. J.* 65, 1640–1651. doi: 10.1080/02626667.2020.1769105

Carlyle-Moses, D. E., Flores Laureano, J. S., and Price, A. G. (2004). Throughfall and throughfall spatial variability in Madrean oak forest communities of northeastern Mexico. *J. Hydrol.* 297, 124–135. doi: 10.1016/j.jhydrol.2004.04.007

Cayuela, C., Llorens, P., Sánchez-Costa, E., Levia, D. F., and Latron, J. (2018). Effect of biotic and abiotic factors on inter- and intra-event variability in stemflow rates in oak and pine stands in a Mediterranean mountain area. *J. Hydrol.* 560, 396–406. doi: 10.1016/j.jhydrol.2018.03.050

Crockford, R. H., and Richardson, D. P. (2000). Partitioning of rainfall into throughfall, stemflow and interception: effect of forest type, ground cover and climate. *Hydrol. Process.* 14, 2903–2920.

Demšar, J., Curk, T., Erjavec, A., Gorup, Č, Hočevar, T., Milutinovič, M., et al. (2013). Orange: data mining toolbox in Python. *J. Mach. Learn. Res.* 14, 2349–2353.

Germer, S., Werther, L., and Elsenbeer, H. (2010). Have we underestimated stemflow? Lessons from an open tropical rainforest. *J. Hydrol.* 395, 169–179. doi: 10.1016/j.jhydrol.2010.10.022

Guevara-Escobar, A., Gonzalez-Sosa, E., Veliz-Chavez, C., Ventura-Ramos, E., and Ramos- Salinas, M. (2007). Rainfall interception and distribution patterns of gross precipitation around an isolated *Ficus benjamina* tree in an urban area. *J. Hydrol.* 333, 532–541. doi: 10.1016/j.jhydrol.2006.09.017

Holder, C. D., and Gibbes, C. (2016). Influence of leaf and canopy characteristics on rainfall interception and urban hydrology. *Hydrolog. Sci. J.* 62, 182–190. doi: 10.1080/02626667.2016.1217414

Iida, S., Levia, D. F., Shimizu, A., Shimizu, T., Tamai, K., Nobuhiro, T., et al. (2017). Intrastorm scale rainfall interception dynamics in a mature coniferous forest stand. *J. Hydrol.* 548, 770–783. doi: 10.1016/j.jhydrol.2017.03.009

Inkiläinen, N. M., McHale, M. R., Blank, G. B., James, A. L., and Nikinmaa, E. (2013). The role of the residential urban forest in regulating throughfall: a case study in Raleigh, North Carolina, USA. *Landsc. Urban Plan.* 119, 91–103. doi: 10.1016/j.landurbplan.2013.07.002

Keim, R. F., Skaugset, A. E., and Weiler, M. (2006). Storage of water on vegetation under simulated rainfall of varying intensity. *Adv. Water Resour.* 29, 974–986. doi: 10.1016/j.advwatres.2005.07.017

Kermavnar, J., and Vilhar, U. (2017). Canopy precipitation interception in urban forests in relation to stand structure. *Urban Ecosyst.* 20, 1373–1387. doi: 10.1007/s11252-017-0689-7

Klamareus-Iwan, A., and Witek, W. (2018). Variability in the wettability and water storage capacity of common oak leaves (*Quercus robur* L.). *Water* 10:695. doi: 10.3390/w10060695

Levia, D. F., and Germer, S. (2015). A review of stemflow generation dynamics and stemflow-environment interactions in forests and shrublands. *Rev. Geophys.* 53, 673–714. doi: 10.1002/2015RG000479

Levia, D. F., and Herwitz, S. R. (2005). Interspecific variation of bark water storage capacity of three deciduous tree species in relation to stemflow yield and solute flux to forest soils. *Catena* 64, 117–137. doi: 10.1016/j.catena.2005.08.001

Levia, D. F., van Stan, J. T., Mage, S. M., and Kelley-Hauske, P. W. (2010). Temporal variability of stemflow volume in a beech-yellow poplar forest in relation to tree species and size. *J. Hydrol.* 380, 112–120. doi: 10.1016/j.jhydrol.2009.10.028

Li-COR (2015). *LAI-2200c Instruction Manual*. Lincoln, NE: Li-COR Biosciences.

Livesley, S. J., Baudinette, B., and Glover, D. (2014). Rainfall interception and stemflow by eucalypt street trees – the impacts of canopy density and bark type. *Urban For. Urban Green.* 13, 192–197. doi: 10.1016/j.ufug.2013.09.001

McPherson, G., Simpson, J. R., Peper, P. J., Maco, S. E., and Xiao, Q. (2005). Municipal forest benefits and costs in five US cities. *J. For.* 103, 411–416.

Mużyło, A., Llorens, P., and Domingo, F. (2012). Rainfall partitioning in a deciduous forest plot in leafed and leafless periods. *Ecohydrology* 5, 759–767. doi: 10.1002/eco.266

Nadbath, M. (2008). Meteorological station Ljubljana Bežigrad. *Naše Okolje* 15:1. (In Slovenian)

Park, A., and Cameron, J. L. (2008). The influence of canopy traits on throughfall and stemflow in five tropical trees growing in a Panamanian plantation. *For. Ecol. Manag.* 255, 1915–1925. doi: 10.1016/j.foreco.2007.12.025

Pérez-Harguindeguy, N., Diaz, S., Garnier, E., Lavorel, S., Poorter, H., Jaureguiberry, P., et al. (2013). New handbook for standardised measurement of plant functional traits worldwide. *Aust. J. Bot.* 61, 167–234. doi: 10.1071/BT12225

R Core Team (2020). *R: A Language and Environment for Statistical Computing*. Vienna: R Foundation for Statistical Computing.

Reid, L. M., and Lewis, J. (2009). Rates, timing, and mechanisms of rainfall interception loss in a coastal redwood forest. *J. Hydrol.* 375, 459–470. doi: 10.1016/j.jhydrol.2009.06.048

Sadeghi, S. M. M., Attarod, P., Van Stan, J. T., Pypker, T. G., and Dunkerley, D. (2015). Efficiency of the reformulated Gash's interception model in semiarid afforestations. *Agric. For. Meteorol.* 201, 76–85. doi: 10.1016/j.agrformet.2014.10.006

Sadeghi, S. M. M., Gordon, A., and van Stan, J. T. (2020). "A global synthesis of throughfall and stemflow hydrometeorology," in *Precipitation Partitioning by Vegetation: A Global Synthesis*, eds J. T. van Stan, E. Gutmann, and J. Friesen (Cham: Springer Nature), 49–70.

Schooling, J. T., and Carlyle-Moses, D. E. (2015). The influence of rainfall depth class and deciduous tree traits on stemflow production in an urban park. *Urban Ecosyst.* 18, 1261–1284. doi: 10.1007/s11252-015-0441-0

Siegert, C. M., and Levia, D. F. (2014). Seasonal and meteorological effects on differential stemflow funneling ratios for two deciduous tree species. *J. Hydrol.* 519, 446–454. doi: 10.1016/j.jhydrol.2014.07.038

Šraj, M., Brilly, M., and Mikoš, M. (2008). Rainfall interception by two deciduous Mediterranean forests of contrasting stature in Slovenia. *Agric. For. Meteorol.* 148, 121–134. doi: 10.1016/j.agrformet.2007.09.007

Staelens, J., de Schrijver, A., Verheyen, K., and Verhoest, N. E. C. (2008). Rainfall partitioning into throughfall, stemflow, and interception within a single beech (*Fagus sylvatica* L.) canopy: influence of foliation, rain event characteristics, and meteorology. *Hydrol. Process.* 22, 33–45. doi: 10.1002/hyp.6610

Su, L., Xu, W., Zhao, C., Xie, Z., and Ju, H. (2016). Inter- and intra-specific variation in stemflow for evergreen species and deciduous tree species in a subtropical forest. *J. Hydrol.* 537, 1–9. doi: 10.1016/j.jhydrol.2016.03.028

Swaffer, B. A., Holland, K. L., Doody, T. M., and Hutson, J. (2014). Rainfall partitioning, tree form and measurement scale: a comparison of two co-occurring, morphologically distinct tree species in a semi-arid environment. *Ecohydrology* 7, 1331–1344. doi: 10.1002/eco.1461

Toba, T., and Ohta, T. (2005). An observational study of the factors that influence interception loss in boreal and temperate forests. *J. Hydrol.* 313, 208–220. doi: 10.1016/j.jhydrol.2005.03.003

van Stan, J. T., Gay, T. E., and Lewis, E. S. (2016). Use of multiple correspondence analysis (MCA) to identify interactive meteorological conditions affecting relative throughfall. *J. Hydrol.* 533, 452–460. doi: 10.1016/j.jhydrol.2015.12.039

van Stan, J. T., and Gordon, D. A. (2018). Mini-Review: stemflow as a resource limitation to near-stem soils. *Front. Plant Sci.* 9:248. doi: 10.3389/fpls.2018.00248

van Stan, J. T., Siegert, C. M., Levia, D. F., and Scheick, C. E. (2011). Effects of wind-driven rainfall on interception and stemflow generation between two codominant tree species with differing crown characteristics. *Agric. For. Meteorol.* 151, 1277–1286. doi: 10.1016/j.agrformet.2011.05.008

van Stan, J. T., van Stan, J. H., and Levia, D. F. (2014). Meteorological influences on stemflow generation across diameter size classes of two morphologically distinct deciduous species. *Int. J. Biometeorol.* 58, 2059–2069. doi: 10.1007/s00484-014-0807-7

Wickham, H., Chang, W., Henry, L., Pedersen, T. L., Takahashi, K., Wilke, C., et al. (2020). *Package "ggplot2"*. Available online at: https://cran.r-project.org/web/packages/ggplot2/ggplot2.pdf (accessed February 25, 2021).

Xiao, Q., and McPherson, E. G. (2011). Rainfall interception of three trees in Oakland, California. *Urban Ecosyst.* 14, 755–769. doi: 10.1007/s11252-011-0192-5

Xiao, Q., McPherson, E. G., Ustin, S. L., Grismer, M. E., and Simpson, J. R. (2000). Winter rainfall interception by two mature open-grown trees in Davis, California. *Hydrol. Process.* 14, 763–784. doi: 10.1002/(SICI)1099-1085(200003)14:4<763::AID-HYP971<3.0.CO;2-7

Zabret, K. (2013). The influence of tree characteristics on rainfall interception. *Acta Hydrotech.* 26, 99–116. (In Slovenian)

Zabret, K., Rakovec, J., Mikoš, M., and Šraj, M. (2017). Influence of raindrop size distribution on throughfall dynamics under pine and birch trees at the rainfall event level. *Atmosphere* 8:240. doi: 10.3390/atmos8120240

Zabret, K., Rakovec, J., and Šraj, M. (2018). Influence of meteorological variables on rainfall partitioning for deciduous and coniferous tree species in urban area. *J. Hydrol.* 558, 29–41. doi: 10.1016/j.jhydrol.2018.01.025

Zabret, K., and Šraj, M. (2018). Spatial variability of throughfall under single birch and pine tree canopies. *Acta Hydrotech.* 31, 1–20.

Zabret, K., and Šraj, M. (2019). Rainfall interception by urban trees and their impact on potential surface runoff. *Clean Soil Air Water* 47:1800327. doi: 10.1002/clen.201800327

Zhang, H., Levia, D. F., He, B., Wu, H., Liao, A., Carlyle-Moses, D. E., et al. (2020). Interspecific variation in tree- and stand-scale stemflow funneling ratios in a subtropical deciduous forest in eastern China. *J. Hydrol.* 590:125455. doi: 10.1016/j.jhydrol.2020.125455

Conflict of Interest: The authors declare that the research was conducted in the absence of any commercial or financial relationships that could be construed as a potential conflict of interest.

frontiers in Forests and Global Change

ORIGINAL RESEARCH
published: 12 May 2021
doi: 10.3389/ffgc.2021.650665

How Is Bark Absorbability and Wettability Related to Stemflow Yield? Observations From Isolated Trees in the Brazilian Cerrado

Kelly Cristina Tonello[1], Sergio Dias Campos[2], Aparecido Junior de Menezes[3], Julieta Bramorski[4], Samir Leite Mathias[3] and Marcelle Teodoro Lima[1]*

[1] Research Group on Hydrology in Forest Ecosystem, Department of Environmental Science, Federal University of São Carlos, Sorocaba, Brazil, [2] Applied Mathematics Laboratory, Department of Physics, Chemistry and Mathematics, Federal University of São Carlos, Sorocaba, Brazil, [3] Research group of Polymers from Renewable Sources, Department of Physics, Chemistry and Mathematics, Federal University of São Carlos, Sorocaba, Brazil, [4] Research group on Hydrology in Forest Ecosystem, Department of Environment and Development, Federal University of Amapá, Macapá, Brazil

OPEN ACCESS

Edited by:
Anna Klamerus-Iwan, University of Agriculture in Krakow, Poland

Reviewed by:
Luiza Maria Teophilo Aparecido, Arizona State University, United States
Anna Ilek, Poznań University of Life Sciences, Poland

***Correspondence:**
Kelly Cristina Tonello
kellytonello@ufscar.br

Specialty section:
This article was submitted to Forest Hydrology, a section of the journal Frontiers in Forests and Global Change

Received: *07 January 2021*
Accepted: *07 April 2021*
Published: *12 May 2021*

Citation:
Tonello KC, Campos SD, Menezes AJ, Bramorski J, Mathias SL and Lima MT (2021) How Is Bark Absorbability and Wettability Related to Stemflow Yield? Observations From Isolated Trees in the Brazilian Cerrado. Front. For. Glob. Change 4:650665. doi: 10.3389/ffgc.2021.650665

Few investigations have examined the structural controls of bark on its water storage and influence on stemflow, despite the bark being considered a critical component that determines the time and magnitude of this process. This study seeks to answer the question: Do bark water absorbability and wettability estimates correlate with stemflow yield? We hypothesized that (1) the absorbability and wettability are correlated, that is, greater water absorbability implies greater wettability, and (2) high rates of bark water absorbability and wettability has a strong and negative correlation with stemflow generation. Stemflow yield (Sy) was monitored over 12 months for 31 trees, representing 9 species common to the Brazilian savanna ecosystem known as Cerrado. Bark absorbability, per unit dry weight, changes over time of the water absorbability (BWA - by submersion methodology), bark drying (BWD), bark absorbability rate (BWA_{rate}), bark drying rate (BWD_{rate}), and wettability (initial contact angle – CA_{in} and CA rate - CA_{rate}) were determined under laboratory conditions. As insoluble lignin may also act to alter bark water storage dynamics, for each species, the bark insoluble lignin content was characterized. Stemflow variability was significant across the study species. Funneling ratios (FR) indicates that all species' canopies diverted enough rainfall as stemflow to concentrate rainwaters at the surface around their stem bases ($FR > 1$). Differences in bark water absorbability were notable some of tree species. A decrease in the CA value as a function of time was not observed for all barks, which in association with stemflow yields, allowed a novel classification method of wettability, based on CA_{in} and it's rate of change: highly wettable ($CA_{in} \leq 75.3°$ and $CA_{rate} \geq 0.26°h^{-1}$) and non-wettable ($CA_{in} \geq 93.5°$ and $CA_{rate} \leq 0.13°h^{-1}$). So, only from the wettability classification could be observed that the non-wettable bark species presented higher Sy, FR, BWA, and BWA_{rate} than highly wettable bark species. The stemflow from species with highly wettable bark had a strong and positive correlation with BWA. On the other hand, non-wettable bark stemflow yield has a strongly and negative correlation with

FR, CA_{in}, and BWA_{rate}. Thus, bark wettability properties showed to deserves special attention. This novel classification of bark wettability had a substantial effect on stemflow yield comprehension and proved to be an important variable to link laboratory and field investigation for understanding the stemflow yield. These findings will improve our understanding of the stemflow dynamics, water balance and the ecohydrology processes of forest ecosystems.

Keywords: surface tension, water drop, water repellency, water storage capacity, insoluble lignin

INTRODUCTION

Many interactions between rainfall and forest canopy remain poorly understood. This is problematic because, for rainfall to reach a forest's soil, it must pass through tree canopies. Some rain droplets fall through canopy gaps, but most will interact with leaves, epiphytes, and/or bark surfaces. A result of these interactions is that a portion of the rainfall is evaporated back to the atmosphere, or intercepted by the canopy (Johnson and Lehmann, 2006; Ahmadi et al., 2013; Liu et al., 2014). The remaining rainwater reaches the forest soil surface as a drip (called throughfall) or as a flow of water down tree stems (stemflow). The stemflow water that reaches the soil are able to create complex spatial patterns, such as infiltration and groundwater recharge. Patterns of rainwater supply to soils via throughfall are highly heterogeneous, with spatial coefficients of variation often exceeding 50% in single events—and $>$ 100% in regions with complex canopies (Van Stan et al., 2020). Although stemflow may be $<$ 5% of the total rainfall across the canopy, its spatial variability is typically higher than observed for throughfall. This occurs because a fraction of rainfall across a single canopy can become highly magnified when locally drained (or "funneled") to a small area, 10^{-1} –10^{1} m^2 $tree^{-1}$ (Van Stan and Allen, 2020), next to a tree's stem base – sometimes resulting in stemflow volumes $>$ 100 times greater than open rainfall (Van Stan and Gordon, 2018). Another tree's stemflow volume may be so low that open rainfall is many times greater (Van Stan and Gordon, 2018).

Several mechanisms have been proposed to explain the high spatial variability of stemflow volumes within forests (Honda et al., 2015; Spencer and van Meerveld, 2016; Van Stan and Allen, 2020). First, one must consider the size of trees, where bigger canopies tend to capture greater rainfall (Zimmermann et al., 2015). Secondly, the structure of canopies can influence how effectively individual trees drain this capture rainfall, and currently it is hypothesized that there may be an optimum branch inclination angle that most efficiently drains rainwater to the stem (Levia, 2003; Sadeghi et al., 2020). Third, the orientation of canopies within the "tree neighborhood" is believed to impact stemflow generation – some dominant canopies overshadow others (Metzger et al., 2019) or gather wind-driven rainfall (Herwitz and Slye, 1995; Levia and Herwitz, 2005; Van Stan et al., 2011). Finally, bark structure, being the surface over which stemflow must flow, is considered a master variable. Specifically, smoother bark has been generally observed to generate greater stemflow due to lower water storage capacities and fewer flow obstructions (Levia et al., 2010; Van Stan and Levia, 2010; Van Stan et al., 2016).

Of course, all of these factors interact to control stemflow spatial variability (Metzger et al., 2019). However, in forests where tree density is low enough that canopies are rarely in close proximity (like the Cerrado of Brazil) (Honda et al., 2015), the tree neighborhood is unlikely to drive stemflow initiation and total volume per storm event. Rather, in this scenario, the individual canopy and stem bark structural variability is anticipated to drive spatial variability in stemflow across trees. This is because stemflow has persistent contact with the bark during draining while bark water storage capacity must be locally overcome for stemflow to initiate and drain. Thus, the amount of water flowing down the tree stem may depend more on bark properties (Crockford and Richardson, 2000; Levia and Herwitz, 2005) than other meteorological conditions (Voigt and Zwolinski, 1964). Crockford and Richardson (2000) found that bark wettability and water storage capacity are characteristics that greatly influence stemflow production. Moreover, barks may also have chemically heterogeneous compositions that could influence the water absorbability and wettability.

Tree barks contain significant amounts of lignin (sometimes with higher lignin content than their respective woods), a complex phenylpropanoid polymer that has a structural role in plant cell walls while also providing hydrophobicity and protection against infection (Neiva et al., 2020).

Similar as leaf wettability, bark wettability is the amount of water captured, and retained on bark surfaces. Bark has a greater water-holding capacity than foliar surfaces (Herwitz and Slye, 1995; Valová and Bieleszová, 2008) but stemflow generation can begin before the woody frame of a tree is completely wetted (Herwitz, 1987). As well-known, surface wettability is a physical parameter that can be experimentally measured. The liquid, in general, a simple droplet in controlled laboratory conditions, is brought in contact with a solid surface, forming a liquid-solid interface where a droplet shape is created. The shape of that droplet depends on the cohesive interactions present in the molecules of the liquid and the adhesive interactions between the solid and liquid phases of the material (Molnar et al., 2011). When the droplet is brought on the solid surface, a simple physical parameter, the so-called contact angle (CA), can be used to determine the wettability of such a surface. The CA is defined as the angle θ emerging at the contact between the three-phases, which can be measured by the tangent to the liquid-fluid interface and the solid surface. It is measured here counterclockwise, which means it is measured on the liquid side. The origins of this angle

probably go back to Galileo, passing through Young and others along the centuries [for a historical introduction and review see Good (1992) and Drelich et al. (2020)].

Hypothetically, the bark water storage capacity and wettability varies substantially between species, but relatively little is known about the dynamics of rainfall interception by the bark of stems and branches and the factors that regulate the process (Valová and Bieleszová, 2008; Ilek et al., 2017a). The differentiation of the bark surface is relatively hard to parametrize and there is little information on the methods of its measurement (Ilek and Jarosław, 2014). Some studies have examined bark water storage capacity (Levia and Frost, 2003; Levia and Wubbena, 2006; Valová and Bieleszová, 2008; Ilek and Jarosław, 2014; Ilek et al., 2015, 2017a,b) or leaf wettability properties (Aryal and Neuner, 2010; Klamerus-Iwan and Błońska, 2018; Papierowska et al., 2018; Klamerus-Iwan et al., 2020a,b,c). Indeed, leaf wettability observations and their relationship with rainfall interception processes are numerous enough to produce multiple critical reviews (e.g., Rosado and Holder, 2013; Holder, 2020), but no study known to the authors has yet evaluated the correlation of bark absorbability and bark wetting properties on stemflow yield. Thus, the focus of this research is to investigate how bark traits correlate to stemflow in an under-researched ecosystem. This investigation is the first to examine multiple factors regarding bark wettability (i.e., initial droplet contact angle and its rate of change with wetting; insoluble lignin content); and the first to discuss how this laboratory investigations of wettability correlated with the stemflow generation in the field.

The main purpose, therefore, of this investigation is to test whether and to what extent bark water absorbability and wettability influences stemflow in trees of Brazilian Cerrado savannah. Cerrado is the second largest biome in South America, as well as the main biome connecting four of the five Brazilian biomes and three important hydrographic basins in South America (Araguaia/Tocantins, São Francisco and Prata) that largely contribute to water recharge in Guarani Aquifer. Thus it has strategic value for several countries, mainly for the ones facing increasing water scarcity (de Leite and Ribeiro, 2018; Pereira et al., 2021). Stemflow variability was monitored over 12 months for 31 trees, representing 9 species common to the Cerrado. These data were used to answer the question: Do bark water absorbability and wettability estimates correlate with stemflow yields? We hypothesized that (1) the bark absorbability and wettability are correlated, that is, greater water absorbability imply greater wettability, and (2) that high rates of bark water absorbability and wettability has a strong and negative correlation with stemflow. Since the Cerrado is considered an arid ecosystem with high biodiversity (grasses, shrubs, and trees) there is a need for more information on how the hydrological processes of this environment are governed, as also as provide parameters for ecohydrological simulations in tropical forests.

MATERIALS AND METHODS

The experimental site was installed at the Private Natural Heritage Reserve (RPPN) Águas Perenes Forest (Perennial Water Forest), Brotas, São Paulo state, Brazil. The Águas Perenes Forest covers 812 ha and is characterized by secondary Cerrado and Cerradão vegetation (Pereira et al., 2021). The Köppen climate-type of the region is *Cwa* (Dubreuil et al., 2019), which corresponds to a subtropical climate (C), characterized by warm summers and dry, cool winters (w), such that the annual average temperature is 20°C (a), and the annual average rainfall is 1,337 mm. The predominant soil type is quartzarenicneosol (dos Santos et al., 2018).

Hydrometeorological Data

The study was carried out in sites under 11 years of passive restoration. Three sample units of 400 m^2 were installed and the stemflow volume [SF, L $tree^{-1}$ $storm^{-1}$], collectors were installed in all trees with DBH > 5cm, totalizing 31 trees distributed in 9 species (**Table 1**). The accumulated rainfall and stemflow were measured monthly from April 2018 to March 2019. Three The rainfall was measured in an open area without obstructions using three pluviometers made of polyethylene (storage capacity of 1.57 L) installed near the stand, with a maximum distance of 30 m. The pluviometers were installed at a height of 1.20 m. Stemflow collars were constructed by wrapping individual tree stems with a polyurethane gutter, fixed at 1.3 m from the ground (**Figure 1**). Water running down the stem was captured by these gutters, then drained by a 1.6 mm hose connected to 20L collection tanks. Evaporation from the stemflow collection tanks between storms was assumed to be negligible as the only opening in the tanks was < 2 mm (where the hose was connected). The collar material efficiently captured water. Event stemflow volumes were divided by each tree's projected canopy area [m^2 $tree^{-1}$] to estimate event stemflow yield [Sy, mm $tree^{-1}$ $storm^{-1}$]. Funneling ratio (FR) was computed *per specie* for mean annual storm and also, it was compared with a normalized stemflow yield (Gordon et al., 2020). While stemflow volume describes total flux to the forest floor, FR describes the efficiency with which individual trees are capable of capturing rainfall and generating stemflow (Siegert and Levia, 2014). Introduced by Herwitz (1986), FR ratio describes the efficiency of each tree to capture rainfall and to generate stemflow, and allows comparing stemflow amounts for plants with different DBH (Siegert and Levia, 2014; Levia and Germer, 2015; Corti et al., 2019). This parameter does not refer to the infiltration area at the soil surface but has the advantage of being related to easily measurable data. FR greater than 1 indicates the contribution of the outlying canopy to stemflow generation. This ratio is expressed by:

$$FR = \frac{Sy}{P * B} \quad (1)$$

where, *Sy*, stemflow yield, is the stemflow volume per tree, in L; P is the precipitation depth, in mm; B is the basal area of the trunk at breast height, in m^2.

Bark Water Absorbability (BWA) and Drying Rate (BWD)

By bark absorbability, we mean the ability of bark to absorb water in a given unit of time in full saturation conditions with the

TABLE 1 | Mean (standard errors) of diameter at breast high (DBH), height (H), outer bark thickness and bark texture of 9 Cerrado tree species, Brotas-Brazil.

Species	Family	*N*	DBH [m]	H [m]	Outer bark Thickness [cm]*	Bark Texture**
Anadenanthera peregrina	Fabaceae	6	32.1 (2.9)	9.2 (1.4)	2.2 (0.7)	Furrowed
Asconium subelegans	Annonaceae	1	9.6 (0.0)	3.9 (0.0)	0.8 (0.2)	Furrowed
Cedrela fissilis	Meliaceae	2	10.9 (1.1)	4.1 (0.4)	0.5 (0.0)	Furrowed/Smooth
Diospyros brasiliensis	Ebenaceae	4	10.4 (0.7)	6.2 (1.8)	0.5 (0.0)	Scaled
Eriotheca gracilipes	Malvaceae	3	9.3 (1.4)	4.4 (0.0)	1.0 (0.0)	Furrowed
Handroanthus ochraceus	Bignoniaceae	2	13.1 (0.3)	6.2 (0.4)	1.0 (0.2)	Furrowed
Machaerium acutifolium	Fabaceae	3	10.8 (1.0)	4.7 (0.0)	1.5 (0.0)	Fibrous
Qualea multiflora	Vochysiaceae	2	6.7 (1.0)	4.1 (0.4)	0.5 (0.0)	Scaled
Xylopia aromatica	Annonaceae	8	25.6 (0.7)	5.9 (0.4)	0.5 (0.0)	Scaled

*N, number of individuals. *Using a caliper (Graves et al., 2014; Astiani et al., 2017). **Klamerus-Iwan et al., 2020c.*

assumption that water is absorbed only by the outer bark layer. Analyses performed under laboratory conditions determined the bark water absorbability of species (N) over time. The outer bark samples were collected using a chisel, a saw, and a knife from the stems of similar size at the breast height (1.3 m) by cutting 3-5 rectangular pieces of bark (5 × 5 cm, approximately). Care was taken to ensure that the bark samples were collected from different locations around the stem at breast height. After that, the bark samples were dried at 35°C to constant mass and the weight of samples was the initial weight of the bark [dried mass – D_m, g]. Then, all side surfaces and the inner surface of the samples (surfaces not typically in contact with rainwater) were sealed with silicon prior to soaking, applied in such a way that, during the experiments, water was absorbed only by the outer layer of the bark (Ilek et al., 2017b). Next, the samples were reweighed to determine the dry weight of the insulating layer of individual samples.

Dried bark samples were submerged in deionized water and weighed every hour during the first 12 h, and then, weighed at intervals of 12 h until complete 96 h [saturated mass - S_m, g]. In each weighed, the samples were re-soaked every time. The experimental during time was determined due to no longer resulted in weight gain of individual bark samples. Bark water absorbability of these samples [BWA, %] was determined based on adaptation of a commonly applied submersion method used to obtain the litter water holding capacity (Blow, 1985). The difference in weight between a sample saturated with water and a dry one was related in each case to the weight of the sample in the dry state [equation (2)]. In this way, subsequent values of water absorbability (BWA) were obtained after successive times of immersion in water (BWA_1, BWA_2).

$$\mathrm{BWA}[\%] = \frac{(S_m - D_m)}{D_m} * 100 \tag{2}$$

where BWA is the dried bark water absorbability [%], S_m is the weight of a sample after a subsequent soaking stage [g], and D_m is the weight of a dry sample [g].

The bark water absorbability rate (% h^{-1}) was obtained by equation 3:

$$BWA_{rate}[\%\ h^{-1}\ ] = \frac{\left(BWA_f - BWA_i\right)}{t} \tag{3}$$

where BWA_i is the initial bark water absorbability [%], BWA_f is the final bark water absorbability [%], and t is the total time of absorbality [h].

Finished 96 h submersion time, the samples were exposed in the same environmental conditions (30°C mean temperature) and weighed as it dried out at intervals of 12, 24, 36, 48, 60, 72, 96, and 144 h. Similar as BWA, subsequent values of bark water drying [BWD,%] were obtained after successive times of drying until no longer resulted in weight loss of individual bark samples The BWD rate [BWD_{rate},%] was obtained on the same way as BWA_{rate} (equation 4):

$$BWD_{rate}[\%\ h^{-1}] = \frac{\left(BWD_f - BWD_i\right)}{t} \tag{4}$$

where BWD_i is the initial bark water drying [%], BWD_f is the final bark water drying [%], and t is the total time of drying [h].

Contact Angle and Bark Wettability

As aforesaid, the aim of this work is to present a novel methodology to study and measure the surface wettability of the bark in controlled laboratory conditions.

The contact surface can be idealized as homogeneous and smooth, which does not, in general, correspond to the samples measured in the laboratory. The non-idealized samples present a non-homogeneous composition and a non-smooth surface, i.e., it presents some roughness. **Figure 2** presents the rough solid surface (left panel) and the ideal surface (right panel). Roughly speaking, a smooth surface is characterized as hydrophilic or hydrophobic according to CA values. For a smooth surface, for $\theta < 90°$ is a feature of hydrophilic surfaces while for roughness surfaces, $\theta > 90°$. For a rough surface, the CA characterizing the hydrophilic/hydrophobic behavior is similar to the smooth case (For details and further explanations, please, see Drelich (2019) and references therein).

In the present work, we assume the evaporation of the droplets can be neglected, which can occur since the observation time scale is much shorter than the expected evaporation time (Butt et al., 2007). Of course, the greater the droplet (in microscopic scale), the greater the evaporation effects. Thus, the main goal here is to study the absorption time of the droplet by the bark surface.

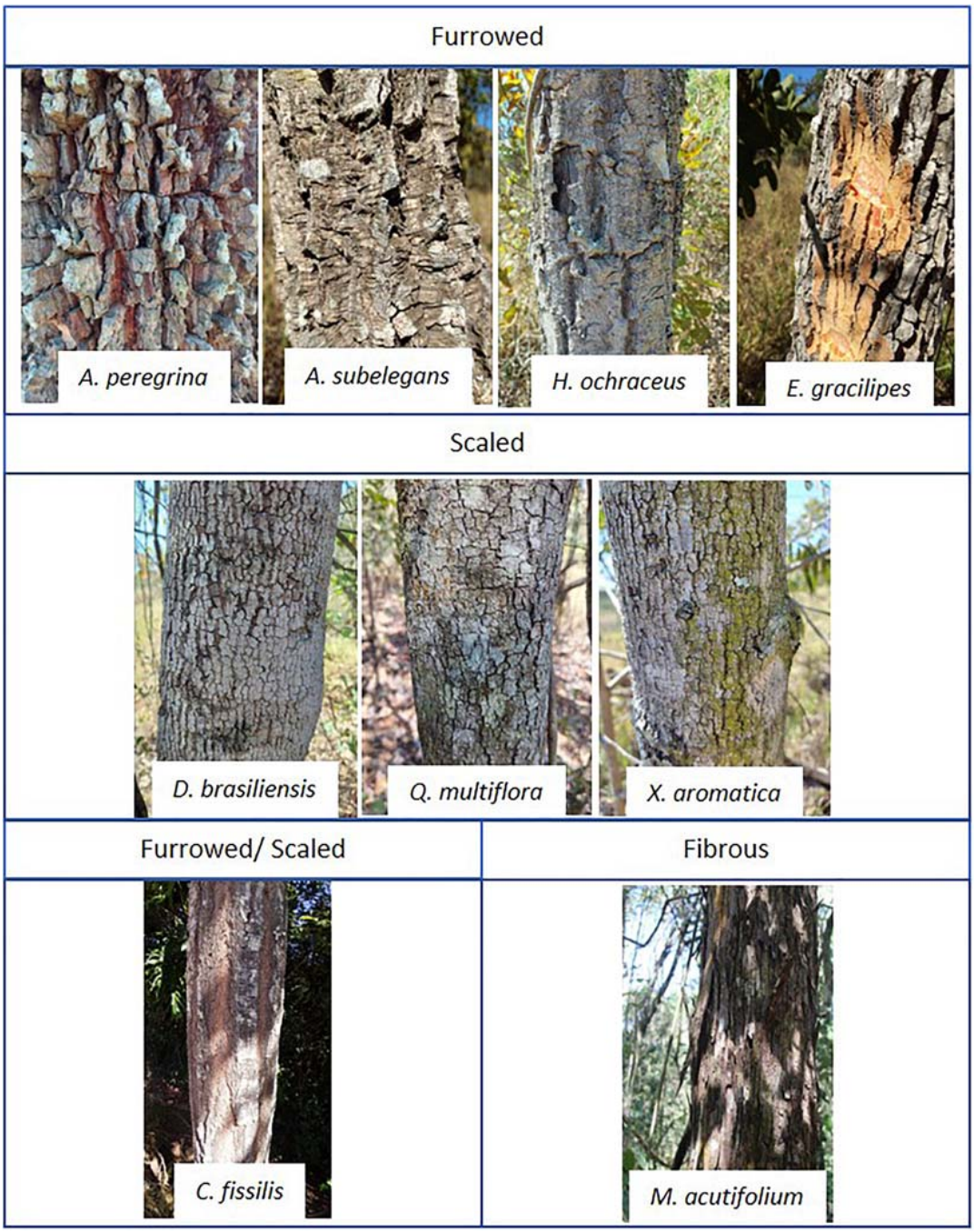

FIGURE 1 | Bark texture for 9 species studied in Brazilian Cerrado. Águas Perenes Forest, Brotas, Brazil.

Considering the above explanation, one way to characterize the wettability of a solid surface, or the interaction between a liquid and a solid, is through the contact angle between the two phases. One uses here the well-known sessile droplet method for its simplicity and relative accuracy to measure the CA, in which a droplet of liquid is deposited on a smooth, horizontal surface and the angle is measured between the solid surface and the tangent of the drop profile (Erbil, 2014; Sinderski, 2020).

Measurements of CA were conducted on bark samples in the laboratory at a constant temperature of 21°C. Considering the sessile droplet method, the Ramé-Hart goniometer (Ramé-Hart Instrument Co, Netcong, NJ, United States) was used to measure the CA on the bark surfaces. The instrument was connected to a computer equipped with image recording software, droplet shape analysis, and CA measurement tools. For each species, three bark samples were selected from different individuals. A distilled water

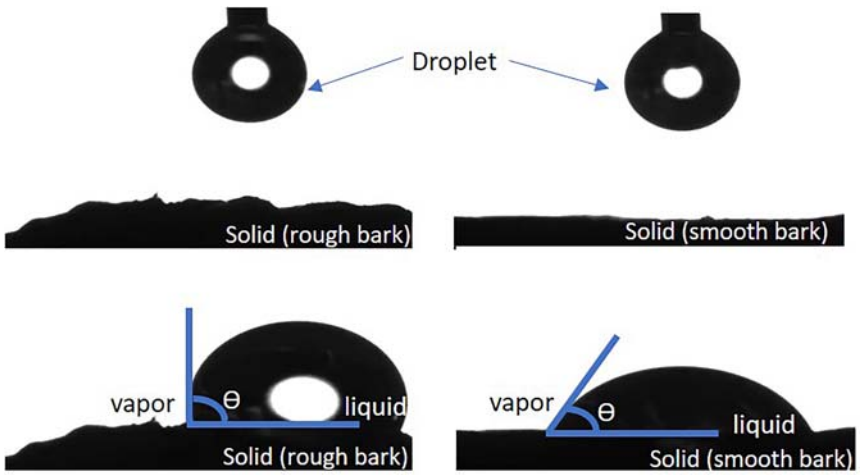

FIGURE 2 | Example for rough and smooth bark surface and the shape of water droplet (θ = contact angle, CA).

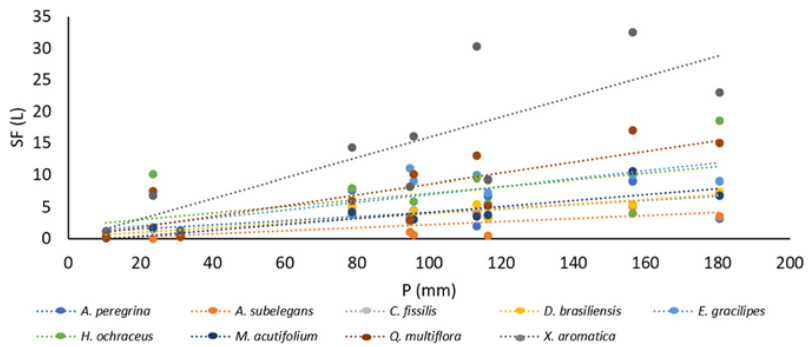

FIGURE 3 | Mean of stemflow [SF, L] and rainfall [P, mm] linear regression.

droplet (0.1 mL) was placed on external bark sides using a syringe with a 0.13 mm internal diameter needle.

The CA changed with time due to the absorption of the droplet by the solid surface. The shape of the droplet was recorded by the camera starting from second zero (placing the droplet on the bark) with 0.5-s intervals until the droplet was completely absorbed or until it reached the maximum interval of 480s adopted here. The following data were used for further analysis: the initial CA [CA_{in}, t = 0.5s], which represents the maximum of the CA (also known as the advancing CA), the final CA [maximum interval of 480s], representing the minimum of the CA (also known as receding CA), and for CA rate [CA_{rate} - difference between the initial and final CA divided per measurement time]. For each droplet, CAs from the right (CA_R) and left (CA_L) sides of the droplet were obtained, as well as the mean value of both results for every second of measurement. The mean of CA_{in} and CA_{rate} was used to characterize the species.

Bark Lignin Content

Different tree species may exhibit different behaviors based on bark constitution. Since lignin tends to be less hydrophilic than cellulose, we tried to determine the lignin content in the outer bark samples and to relate it to the contact angle. The bark lignin was determined according to the TAPPI standards for insoluble lignin (T222 om-02) (TAPPI, 2011). All characterizations were carried out in triplicates and the results correspond to the average values with their standard error.

Data Analyses

Descriptive statistics were compiled for all variables presented and regression analyses were performed to relate bark metrics to hydrologic variables. To characterized stemflow production across species, Analysis of variance (ANOVA) was applied to normal data through Tukey test at 5% probability level to analyze the means of the Sy (mm), BWA, CA_{in}, CA_{rate}, and lignin between the tree species. Data that did not meet ANOVA assumptions were subjected to non-parametric Kruskal-Wallis test. Cluster analyses was used to identify similar traits of species between contact angle and stemflow yield. The relation between bark metrics and their effects on stemflow was analyzed by Spearman correlation. All statistical analyses were performed using MinitabV16 (Minitab, Inc., State College, PA, United States).

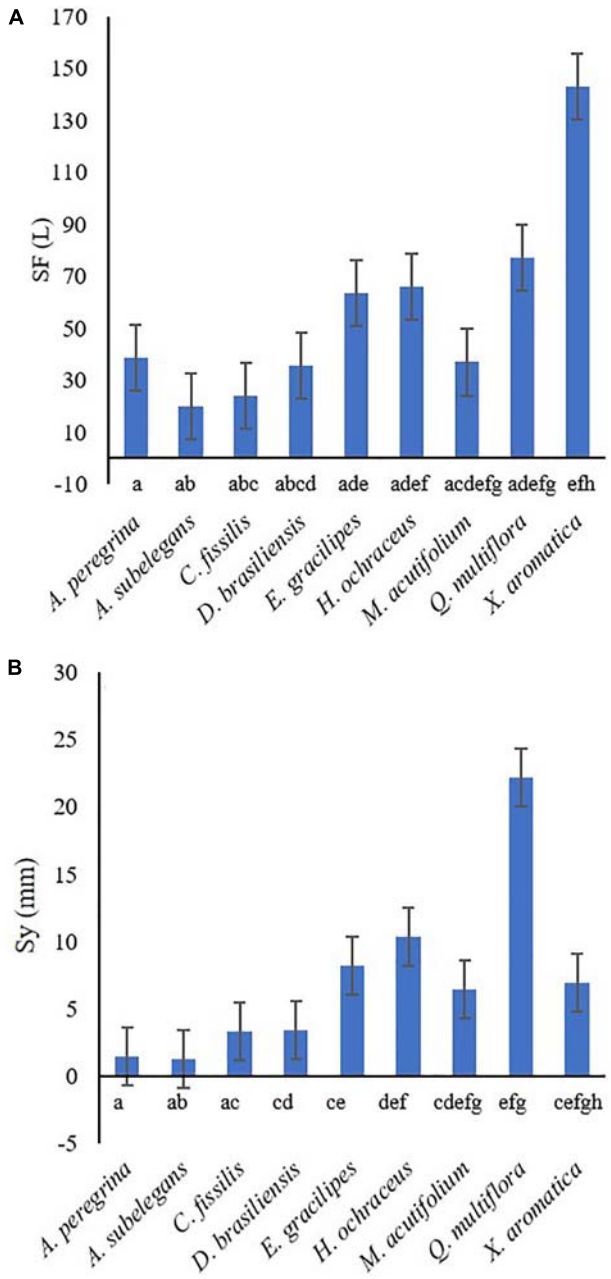

FIGURE 4 | Mean stemflow volume [SF, L] **(A)** and stemflow yield [Sy, mm] **(B)** in 9 tree species from April 2018 to March 2019. Águas Perenes Forest, Brotas, Brazil. Different letters indicate significant differences ($p < 0.05$) among species and vertical bars represent standard errors.

RESULTS

Stemflow Variability

Total rainfall during the study period was 900 mm and stemflow average was 56.1 ± 13.0 L tree^{-1}. Stemflow volume and monthly precipitation yield had a positive, significant linear association with rainfall for most species (**Figure 3** and **Supplementary Table 1**). Total stemflow during the study period was 63.6 mm. Of the total stemflow, two species contributed with the most yield: 35% was contributed by *Q. multiflora* (22.2 mm) and 16% (10.4 mm) by *H. ochraceus* (**Figure 4**). Funneling ratios indicates that all species captured most of the P and drained as stemflow (three plants' mean) to the surface around their stem bases (FR > 1) (**Figure 5**). Mean FR across all plants was 65.0 ± 24.1, however, *A. peregrina* was 99% lower than that. On the other hand, *Q. multiflora* and *E. gracilipes* were consistently high stemflow generators and were the only species that showed above average values.

Bark Absorbability and Drying

Differences in bark water absorbability (BWA) were noted among the tree species and varied from 70.3% (*C. fissilis*) to 337.1% (*M. acutifolium*) (**Table 2**). At subsequent time intervals, the bark water absorbability of all species increased, and large increments of water absorption were noted in bark samples irrespective of the species. Moreover, **Figure 6** shows that the species differ in their dynamics of absorbability (**Figure 6A**) as also in drying (**Figure 6B**). After each subsequent immersion time, the absorbability increment decreases. Interspecific differences are revealed in the amount of water absorbability and drying. It is also visible that water absorbability increases but tend to achieve the stability over time. For all species, BWD_{rate} were higher than BWA_{rate}. Despite *M. acutifolium* had the highest BWA, this specie also shown one of the highest BWD_{rate} (1.72% h^{-1}). While *Q multiflora* and *X. aromatica* had one of the lowest BWA_{rate}, they also had the highest BWD_{rate} (regression analysis for bark water absorbability (BWA) and water drying (BWD) among species are presented in **Supplementary Table 2**). In general, the relation between BWA and BWD are not related when analyzed with all species together ($r = 0.44$, $p = 0.23$). In contrast, the particular analysis by species points out that the BWAis has a indirect and strong relation with BWD (**Table 3**).

Bark Wettability and Lignin Content

Table 4 presents the initial CA values along with bark value changes over the period of the experiment duration (CA_{rate}). During measurements using the sessile droplet method, a decrease in the CA value as a function of time was not observed for all tested barks (**Figures 7** and **8**). Overall, the CA behavior could be divided in two groups based on time: (G1) the one in which the droplet was absorbed completely before 480s elapsing (*A. peregrina, C. fissilis, D. brasiliensis* and *X. aromatica*), characterized here as highly wettable ($CA_{in} \leq 75.3°$ and $CA_{rate} \geq 0.26°$ h^{-1}) and, (G2) the other one in which the droplet was not completely absorbed before 480s elapsed (*A. subelegans, E. gracilipes, H. ochraceus, M. acutifolium* and *Q. multiflora*), it means, non-wettable ($CA_{in} \geq 93.5°$ and $CA_{rate} \leq 0.13°$ h^{-1}). These groups were reinforced by cluster analysis of CA_{in} × SF (mm) presented in **Figure 9**. In general, the analysis of the bark lignin content has shown that the species with the lowest CA_{in} had the lowest insoluble lignin content. *A. peregrina* was an exception and showed the highest lignin content in the bark samples, but for this species, lignin did not necessarily imply the greatest CA_{in}.

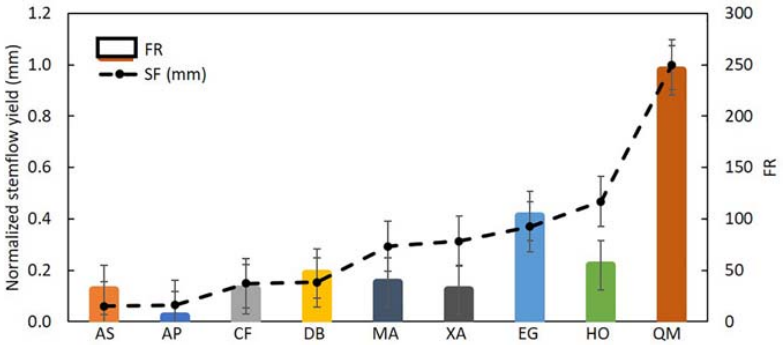

FIGURE 5 | Mean and standard deviation [SD] of normalized stemflow yield *per specie* and the associated funneling ratio. AS, *A. subelegans*; AP, *A. peregrina*; CF, *C. fissilis*; DB, *D. brasiliensis*; MA, *M. acutifolium*; XA, *X. aromatica*; EG, *E. gracilipes*; HO, *H. ochraceus*; QM, *Q. multiflora*.

TABLE 2 | Mean (standard error) of bark water absorbability [BWA] and rate [BWA_{rate}], and bark water drying [BWD] and rate [BWD_{rate}].

Specie	BWA* (%)	BWD** (%)	BWA_{rate} (% h^{-1})	BWD_{rate} (% h^{-1})
A.peregrina	93.4 (10.0) a	5.76	0.58	0.39
A.subelegans	211.0 (69.0) b	27.06	1.24	1.02
C. fissilis	70.3 (14.0) c	11.73	0.21	0.27
D. brasiliensis	128.1 (7.4) d	0.00	0.89	0.60
E. gracilipes	170.3 (48.1) e	0.00	0.65	0.89
H. ochraceus	179.9 (42.0) bef	3.18	0.49	0.92
M. acutifolium	337.1 (81.3) g	16.49	0.92	1.72
Q. multiflora	175.6 (60.1) def	1.28	0.34	1.81
X. aromatica	185.53 (31.0) b	0.00	0.33	1.04

*Different letters indicate significant differences ($p < 0.05$) among species. *after 96 h in submersion. **after 144 h drying in environmental conditions.*

Bark Traits by Contact Angle and Stemflow Correlations

To evaluate possible bark influences on stemflow variability, various directly measured metrics were compared. Few visible or strong statistical correlations or correspondences were found between bark structural variables and stemflow when the species were analyzed together (**Table 5**): a strong correlation was observed between CA_{in} × BWA and moderate for BWA_{rate} × SF (L) and Lignin × SF (mm).

However, the analysis from the wettability groups (section "Bark Wettability and Lignin Content") (highly wettable and non-wettable), showed that CA rate, lignin and SF (L) were approximately 700, 1, and 14% higher in highly wettable bark than in non-wettable bark. On the other hand, Sy, FR, BWA, and BWA_{rate} were, respectively, 158, 329, 80, and 46% higher in non-wettable bark (**Figure 10**). BWA showed a strong and positive correlation (direct relation) with stemflow (volume and depth) for highly wettable bark, whereas in non-wettable bark the correlation was weak/moderate and negative. BWA_{rate} and the classification by CA_{in} allowed a strong relation to estimate stemflow (volume and yield) in non-wettable bark, indicating a negative correlation. FR correlated strongly with CA and stemflow variables in non-wettable bark, indicating that with increase of CA_{in}, SF increases with FR. Finally, for highly wettable barks, lignin showed a strong and negative influence to FR, as well strong and negative correlation with CA_{rate} for non-wettable barks.

DISCUSSION

The knowledge of bark absorbability and wettability as well as the understanding of water retention processes on bark surfaces are particularly important and complex. Both bark water absorbability and bark water drying are dynamic processes, and they largely depend on the time during which samples are submersed in the water or exposed to the environment conditions. Considering the bark samples tested in the same way (i.e., in a controlled, systematic experiment), the features of bark water absorbability depended on the species. Apparently in this study, most of furrowed bark tends to absorb more water, although the drying behavior is independent of the bark texture. In terms of absorbability, the first 12 h of the experiment proved to be crucial for the analyzed bark samples, and a significant quantity of absorbed water was noted in the bark for all species during the experiment. After 60 h of the experiment, the bark samples showed an equilibrium tendency. In this case, only *M. acutifolium* was an exception, that despite presented a greater absorbability, it also presented, together with the *Q. multiflora*, a higher drying rate. Thus, some species can retain a big amount of water in their barks (> BWA) but they cannot store it for a longer time (< BWD_{rate}), e.g., *M. acutifolium* and *Q. multiflora*. Furthermore, some species can retain a small amount of water in their barks (< BWA) but they can store it for a longer time (< BWD_{rate}), e.g., *C.fissilis* and *A. peregrina* (**Table 2**). A similar pattern was observed in woody species bark in the Czech Republic (Valová and Bieleszová, 2008). This difference in the water absorption capacity of the bark between the species may be related to porosity and density. This variables were not measured in this study, but the literature shows that the bark with higher density and lower porosity, while having the same moisture, usually contains more water than the bark with lower

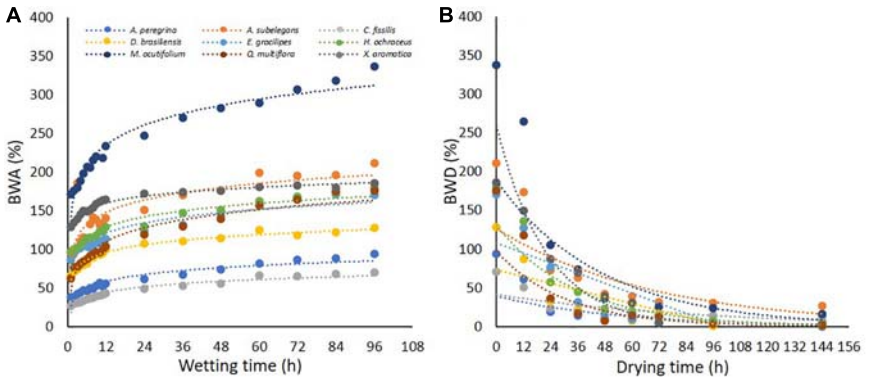

FIGURE 6 | Bark water absorbability [BWA,%] **(A)** and drying [BWD, %] **(B)** among tree Cerrado species.

TABLE 3 | Regression analyses for bark water drying (BWD) considering bark water absorbability (BWA).

Specie	Regression	R-adj	*r*	*p*
A. peregrina	$BWD = 645.32e^{-0.054*BWA}$	0.80	−0.75	0.03
A. subelegans	$BWD = 3152e^{-0.023*BWA}$	0.88	−0.84	0.01
C. fissilis	$BWD = 196.64e^{-0.039*BWA}$	0.80	−0.82	0.01
D. brasiliensis	BWD = −1.7992*BWA + 298.28	0.74	−0.86	0.01
E. gracilipes	BWD = −1.7992*BWA + 298.28	0.79	−0.89	0.00
H. ochraceus	$BWD = 198661e^{-0.059*BWA}$	0.92	−0.85	0.01
M. acutifolium	$BWD = 65600\ e^{-0.025*BWA}$	0.92	−0.82	0.01
Q. multiflora	$BWD = 196.64e^{-0.039*BWA}$	0.78	−0.79	0.02
X. aromatica	BWD = −7.2337*BWA + 1325.8	0.93	−0.96	0.00

TABLE 4 | Mean (standard error) of initial contact angle [CA_{in},°], CA rate [CA_{rate},° s^{-1}], and insoluble lignin [%] among species.

Species	CA_{in} (°)	CA_{rate} (° s^{-1})	Insoluble Lignin (%)
A.peregrina	72.2 (6.1)a	0.26 (0.10)^a	73.72 (0.69)^a
A.subelegans	120.8 (15.0)b	0.07 (0.03)^b	52.85 (0.58)^b
C. fissilis	63.4 (5.8)a	0.44 (0.11)^a	49.25 (1.77)^b
D. brasiliensis	51.3 (17.0)a	1.31 (0.43)^a	47.45 (0.61)^b
E. gracilipes	107.5 (5.5)b	0.09 (0.04)^b	53.76 (0.84)^b
H. ochraceus	105.0 (8.2)b	0.00 (0.00)^b	56.85 (0.43)^b
M. acutifolium	121.2 (12.0)b	0.12 (0.07)^b	59.67 (1.19)^b
Q. multiflora	93.5 (14.0)b	0.13 (0.04)^b	52.87 (1.03)^b
X. aromatica	75.3 (12.0)a	0.65 (0.08)^a	51.74 (0.14)^b
Mean (SE)	90.0 (8.5)	0.33 (0.14)	55.36 (2.06)

Different letters indicate significant differences ($p < 0.05$) among species.

density (Ilek et al., 2017a).Although the knowledge about bark absorbability is important to understand the bark and stemflow interaction, in this study these variables did not show a great correlation when we considered all species together (**Table 5**), and so, we could conclude that isolated BWA by submersion methodology could not be enough to relate to stemflow yield regardless of species. When the bark water storage was being studied, the main idea was that the initial condition necessary for water flow down the stem is the saturation of its bark with water (Kozlowski et al., 2010). In fact, in the bark submersion methodology, all bark surface is permanently exposed to water for a long period of time, forcing the bark to absorb water which does not happen in the field conditions. Nevertheless, in the field conditions, for the bark to absorb water as it drains down the stem, firstly, the amount of water must overcome the bark surface tension. But the field, the bark is not submerged in water. This fact could justify the strong correlations between BWA and SF for highly wettable barks, which showed a lower bark surface tension. In this way, the laboratory method seems to increase the bark saturation up to non-realistic values which cannot be found in natural conditions. Therefore, the wetting properties (rather than the lab-derived submersion estimates) could be crucial to improve the knowledge of stemflow and bark relations in the field conditions.

There is a good correlation between CA and penetration of coatings (solventborne alkyds and drying oils, for example) (Meijer, 2004), implying the wood should have a higher surface free energy than the coating (Nogalska et al., 2019). Thus, one can suppose the same occurs for the penetration of water in the bark. Different wetting processes need different approaches (Young, Wenzel or Cassie-Baxter equations) (Whyman et al., 2008). Thus, different barks may need different approaches and the evaluation of the processes that govern the stemflow generation from the CA in the controlled laboratory conditions seems to be more faithful to the field conditions. In general, small CA ($<< 90°$) implies a high wettability and high CA ($> > 90°$) corresponds to low wettability systems (Yuan and Lee, 2013; Prakash et al., 2017; Sinderski, 2020). It is important to consider that not only the initial CA value is relevant when assessing wettability, but also the time evolution of the drop (Papierowska et al., 2018). A non-wettable surface on which the droplet does not dissipate but retains its shape contributes to increasing stemflow yield more quickly, as could be observed by the inverse correlation between BWA_{rate} and SF/Sy in non-wettable barks. In turn, in highly wettable barks, the increase in stemflow is positively associated with bark water storage. It should be emphasized that this is the first study known to the authors to document the relation among bark wettability, absorbability and stemflow.

The investigation of stemflow process from bark wetting pointed to a different dynamic from that presented by other

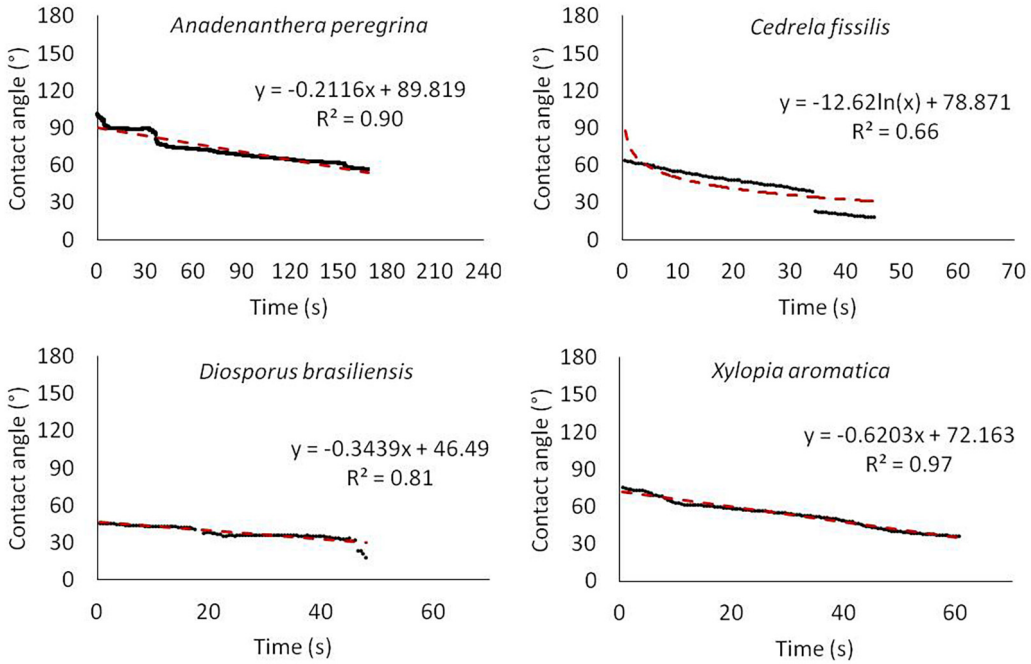

FIGURE 7 | Contact angle (CA) measurements for wettable bark vs. time for Cerrado species.

authors (Crockford and Richardson, 2000; Levia and Frost, 2003; Levia and Germer, 2015): the bark wettability groups were not formed by species with a single bark texture and it means that other bark properties must to be investigated. For highly wettable bark species there were two scaled bark species (*D. brasiliensis* and *X. aromatic*), one mixed (*C. fissilis*) and another with furrowed bark (*A. peregrina* – the thickest among those studied and with the highest lignin content), whereas in non-wettable bark group there were four furrowed and one scaled (*Q. multiflora*). One example of that is *M. acutifolium* that showed the highest BWA, and so, should have the lowest SF/Sy, but had the highest, as well as the second largest BWD_{rate} and highest CA_{in}. Thus, our results shown that stemflow yields are not a consequence of thick absorptive barks. Additionally, not only smooth and easily wetted bark has the potential for high stemflow yields. Although BWA was in the majority, higher for furrowed bark species, the evaluation by CA_{in} and CA_{rate} pointed out that there is greater water repellency through the bark of these same species (non-wettability), which reflected in weak correlations between BWA vs. SF. This pattern in non-wettable bark species was reinforced by the strong and positive correlations with FR, that is, the potential to generate stemflow. On the other hand, BWA for highly wettable bark species could be a good physical parameter to understand the SF yields, since they presented strong/positive correlations (**Table 5**).

The tree species did not differ in terms of bark lignin content - except *A. peregrina*. There exists the long-held belief that one of the functions of lignin in the wood cell wall is to provide waterproofing to aid in water transport (Notley and Norgren, 2010), so, this fact could justify a non-influence of lignin in the process of bark water absorbability, wetting, and stemflow. Evidence of lignin's importance relative to the wettability of wood comes from observations of the effects of weathering. Weathered wood tends to become depleted of lignin near to its surface, which is attributable to photodegradation of the aromatic structures (Hubbe et al., 2015). Indeed, the depletion of lignin in the surface layers of wood exposed to outdoor sunlight has been shown to result in increased wettability by water (Feist, 1993; Huang et al., 2012; Hubbe et al., 2015). Despite that, the association of stemflow and lignin showed that the best analyses were when we considered all species, independent of their wettability properties. In this situation, the lignin was associated with a lower stemflow yield. For highly wettable bark, the lignin had a moderate and inverse correlation with SF(L), and, thus, for these species lower lignin implies increases in stemflow generation. In contrast, for non-wettable bark species, the increment of lignin is associated with decreased of CA_{rate}, that on the other hand, is also implicated in the increment of bark water absorbability.

The dynamics of stemflow are a very important element of water balance in the environment. Knowledge gained from this study may augment our understanding in several aspects. Knowing the bark properties and stemflow dynamics for different tree species can help better understand and predict the role of forests in rainfall interception and water balance. Moreover, could be potentially used as a trait to determine plants that could be used for restoration projects, for example. Regarding the physiological ecology of forests, once bark provides a diverse substrate for a variety of these communities (Levia and Germer, 2015), the proposed method may have important implications for understanding the distribution and diversity of epiphytic

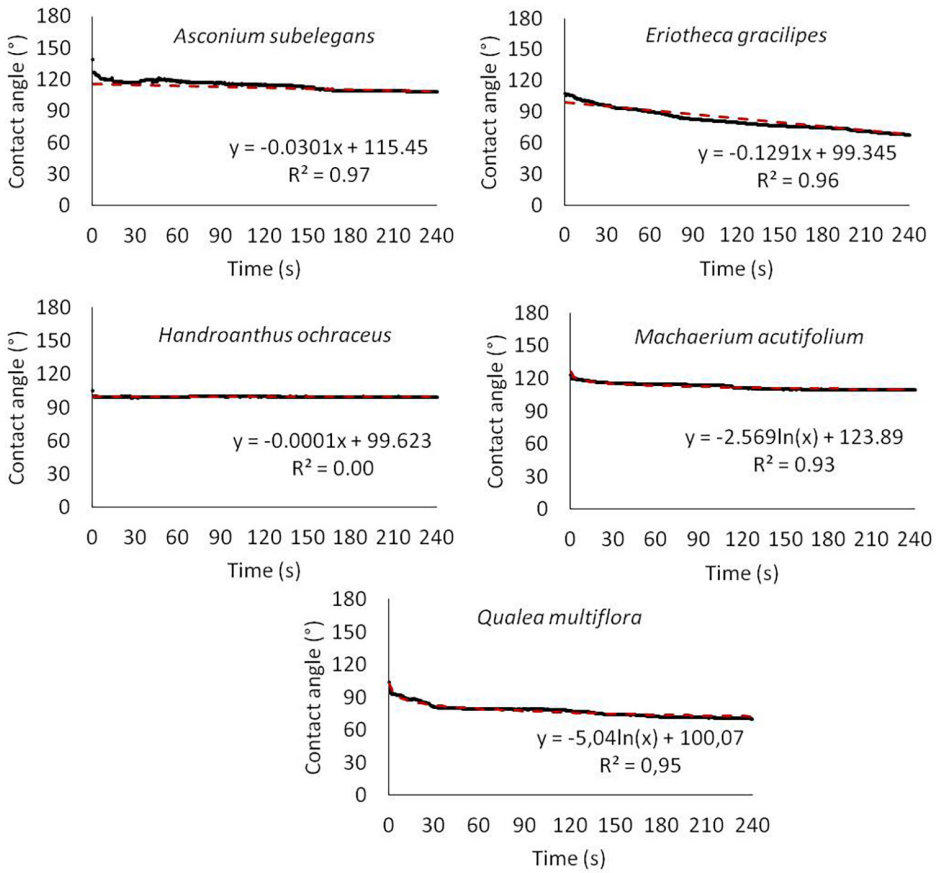

FIGURE 8 | Contact angle (CA) measurements for non-wettable bark vs. time for Cerrado species.

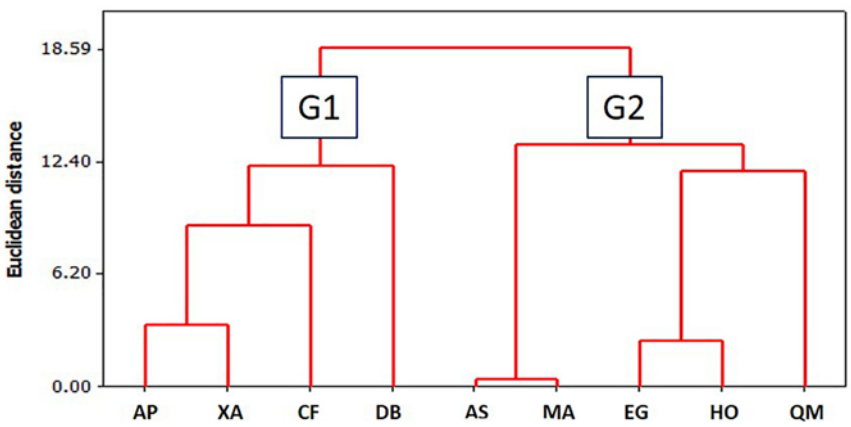

FIGURE 9 | Cluster analysis for CA_{in} x Sy (mm) groups. AP, *A. peregrina*; XA, *X. aromatica;* CF, *C. fissilis*; DB, *D. brasiliensis*; AS, *A. subelegans*; MA, *M. acutifolium*; EG, *E. gracilipes*; HO, *H. ochraceus*; QM, *Q. multiflora*; G1, highly wettable; G2, non-wettable.

lichens, bryophytes (Mitchell et al., 2005; Levia and Wubbena, 2006; Valová and Bieleszová, 2008; Van Stan and Pypker, 2015), fungal (Magyar et al., 2021) and metazoans (Ptatscheck et al., 2018), which, in turn, has a detectable and significant influence on stemflow chemistry (Pypker et al., 2011; Levia and Germer, 2015; Van Stan and Pypker, 2015) and, consequently, to the forest floor.

CONCLUSION

The present study shows how the tree bark traits is related to stemflow in 9 species commonly found in Cerrado. We investigated the association of bark absorbability, wettability, lignin content and stemflow yields. The results obtained here

TABLE 5 | Spearman correlations between bark properties and stemflow for all species together and per wettability groups (highly and non-wettability).

	Metrics	FR	BWA	BWA_{rate}	CA_{in}	CA_{rate}	Lignin
For all species together	CA_{in}	0.16	0.81	0.46	–	–	–
	CA_{rate}	−0.21	−0.42	−0.03	–	–	–
	Lignin	−0.26	0,02	0.04	0.15	−0.42	–
	Sy (mm)	0.24	0.10	−0.43	0.22	−0.33	−0.61
	SF (L)	0.24	0.11	−0.51	−0.09	0.09	0.12
Highly wettablity	CA_{in}	−0.72	0.29	−0.63	–	–	
	CA_{rate}	0.87	0.38	0.69	–	–	
	Lignin	−0.94	−0.26	0.07	0.54	−0.66	
	Sy (mm)	0.45	0.84	−0.35	0.30	0.24	−0.57
	SF (L)	0.05	0.91	−0.30	−0.63	0.00	−0.14
Non-wettability	CA_{in}	−0.87	0.69	0.93	–	–	–
	CA_{rate}	0.79	−0.52	−0.25	–	–	–
	Lignin	−0.50	0.78	0.07	0.42	−0.84	–
	Sy (mm)	0.93	−0.37	−0.89	−0.92	0.51	−0.22
	SF (L)	0.75	−0.56	−0.99	−0.94	0.32	−0.15

CA_{in}, initial contact angle; CA_{rate}, contact angle rate; SF (L), stemflow volume; Sy (mm), stemflow yield; FR, funneling ratio; BWA, bark water absorbability; BWA_{rate}, bark water absorbability rate.

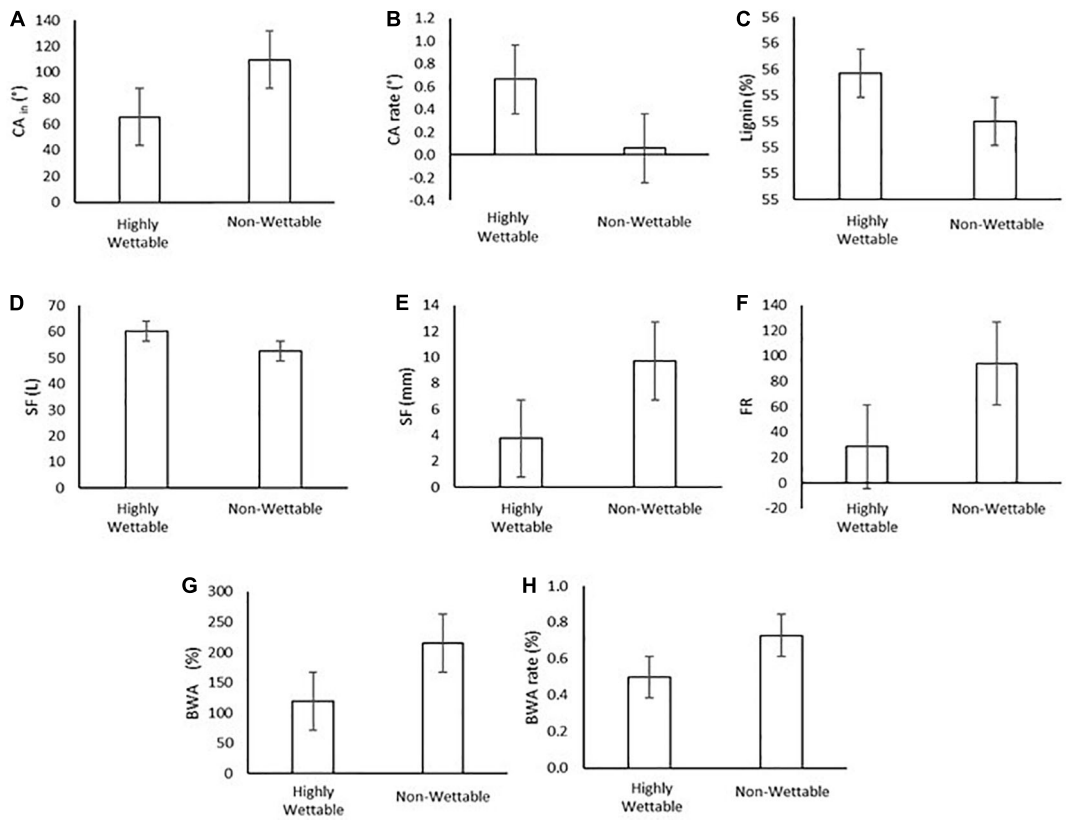

FIGURE 10 | Mean values of initial contact angle [CA_{in}] **(A)**, rate contact angle [CA_{rate}] **(B)**, lignin **(C)**, stemflow volume, SF (L) **(D)**, stemflow yield, Sy (mm) **(E)**, funneling ratio, FR **(F)**, bark water absorbability, BWA **(G)**, bark water absorbability rate, BWA_{rate} **(H)**.

confirm that bark absorbability and wetting depend on the tree species and reject the long-held paradigm that bark surface structure (smooth vs rough) is a major determinant of stemflow (at least in the Cerrado). We obtain important information on factors conditioning the stemflow yield, confirming how difficult is to consider the bark traits individually. The insoluble lignin did not differ among the most species but showed to have a moderate and negative association with stemflow. The combination of

wetting properties with stemflow, allowed to classify the species as highly wettable and non-wettable barks and then, the relations between bark traits and the stemflow dynamic became clearer. Highly wettable barks showed a strong and positive correlation between bark absorbability and stemflow, whereas for non-wettable barks the absorbability had a negative and moderate relation. Thus, the classification of wettability had a substantial effect on stemflow yield and proved to be an important variable to connect the laboratory and the field investigation, leading to a better understanding of the stemflow yield.

DATA AVAILABILITY STATEMENT

The original contributions presented in the study are included in the article/**Supplementary Material**, further inquiries can be directed to the corresponding author.

AUTHOR CONTRIBUTIONS

KT and AM contributed to conception and design of the experiment. KT, AM, and SM conducted the experiment and organized the database. KT, JB, and ML performed the statistical analyses and wrote the first draft of the manuscript. SC performed the physical analyses and part of the discussion. All authors contributed to manuscript revision, read, and approved the submitted version.

ACKNOWLEDGMENTS

The authors would like to thank the Brazilian National Council for Scientific and Technological Development (CNPq) and International Paper Co-Brazil.

SUPPLEMENTARY MATERIAL

The Supplementary Material for this article can be found online at: https://www.frontiersin.org/articles/10.3389/ffgc.2021.650665/full#supplementary-material

REFERENCES

Ahmadi, M. T., Attarod, P., and Bayramzadeh, V. (2013). The role of rainfall size in canopy interception loss: an observational study in a typical beech forest. *Middle-East J. Sci. Res.* 13, 876–882. doi: 10.5829/idosi.mejsr.2013.13.7.2721

Aryal, B., and Neuner, G. (2010). Leaf wettability decreases along an extreme altitudinal gradient. *Oecologia* 162, 1–9. doi: 10.1007/s00442-009-1437-3

Astiani, D., Mujiman, M., and Curran, L. M. (2017). Trees of tropical peatland forest influence on variability of water and carbon input through stemflow. *Biodiversitas* 18, 383–388. doi: 10.13057/biodiv/d180150

Blow, F. E. (1985). Quantity and hydrologic characteristics of litter under upland oak forests in eastern Tennessee. *J. For.* 53, 190–195.

Butt, H. J., Golovko, D. S., and Bonaccurso, E. (2007). On the derivation of young's equation for sessile drops: nonequilibrium effects due to evaporation. *J. Phys. Chem. B* 111, 5277–5283. doi: 10.1021/jp065348g

Corti, G., Agnelli, A., Cocco, S., Cardelli, V., Masse, J., and Courchesne, F. (2019). Soil affects throughfall and stemflow under Turkey oak (Quercus cerris L.). *Geoderma* 333, 43–56. doi: 10.1016/j.geoderma.2018.07.010

Crockford, R. H., and Richardson, D. P. (2000). Partitioning of rainfall into throughfall, stemslow∠d interception effect of forest type, ground cover and climate. *Hydrol. Process.* 14, 2903–2920.

de Leite, M. L. T. A., and Ribeiro, W. C. (2018). The Guarani Aquifer System (Gas) and the challenges for its management. *J. Water Resour. Prot.* 10, 1222–1241. doi: 10.4236/jwarp.2018.1012073

dos Santos, H. G., Jacomine, P. K. T., dos Anjos, L. H. C., de Oliveira, V. A., Lumbreras, J. F., Coelho, M. R., et al. (2018). *Sistema Brasileiro de Classificação de Solos*. Rio de Janeiro: Embrapa Solos.

Drelich, J. W. (2019). Contact angles: from past mistakes to new developments through liquid-solid adhesion measurements. *Adv. Colloid Interface Sci.* 267, 1–14. doi: 10.1016/j.cis.2019.02.002

Drelich, J. W., Boinovich, L., Chibowski, E., Della Volpe, C., Hołysz, L., Marmur, A., et al. (2020). Contact angles: history of over 200 years of open questions. *Surf. Innov.* 8, 3–27. doi: 10.1680/jsuin.19.00007

Dubreuil, V., Fante, K. P., Planchon, O., and Sant'Anna Neto, J. L. (2019). Climate change evidence in Brazil from Köppen's climate annual types frequency. *Int. J. Climatol.* 39, 1446–1456. doi: 10.1002/joc.5893

Erbil, H. Y. (2014). The debate on the dependence of apparent contact angles on drop contact area or three-phase contact line: a review. *Surf. Sci. Rep.* 69, 325–365. doi: 10.1016/j.surfrep.2014.09.001

Feist, W. C. (1993). "Weathering and surface protection of wood," in *Proceeding of the Seventy-Ninth Annual Meeting of the American Wood-Preservers' Association*, (Stevensville, MD: American Wood- Preservers' Association), 195–205. doi: 10.1016/B978-081551500-5.50016-1

Good, R. J. (1992). Contact angle, wetting and adhesion. *J . Adhes. Sci. Technol.* 6, 1269–1302.

Gordon, D. A. R., Coenders-Gerrits, M., Sellers, B. A., Sadeghi, S. M. M., and Van Stan, J. T. (2020). Rainfall interception and redistribution by a common North American understory and pasture forb, Eupatorium capillifolium (Lam. dogfennel). *Hydrol. Earth Syst. Sci.* 24, 4587–4599. doi: 10.5194/hess-24-4587-2020

Graves, S. J., Rifai, S. W., and Putz, F. E. (2014). Outer bark thickness decreases more with height on stems of fire-resistant than fire-sensitive Floridian oaks (*Quercus spp*. Fagaceae). *Am. J. Bot.* 101, 2183–2188. doi: 10.3732/ajb.1400412

Herwitz, S. R. (1986). Infiltration-excess caused by Stemflow in a cyclone-prone tropical rainforest. *Earth Surf. Process. Landforms* 11, 401–412. doi: 10.1002/esp.3290110406

Herwitz, S. R. (1987). Raindrop impact and water flow on the vegetative surfaces of trees and the effects on stemfow and throughfall generation. *Earth Surf. Process. Landforms* 12, 425–432. doi: 10.1002/esp.3290120408

Herwitz, S. R., and Slye, R. E. (1995). Three-dimensional modeling of canopy tree interception of wind-driven rainfall. *J. Hydrol.* 168, 205–226. doi: 10.1016/0022-1694(94)02643-P

Holder, C. D. (2020). "Advances and future research directions in the study of leaf water repellency," in *Forest-Water Interactions*, ed. D. F. Levia (Cham: Springer), 261–278. doi: 10.1007/978-3-030-26086-6

Honda, E. A., Mendonça, A. H., and Durigan, G. (2015). Factors affecting the stemflow of trees in the Brazilian Cerrado. *Ecohydrology* 8, 1351–1362. doi: 10.1002/eco.1587

Huang, X., Kocaefe, D., Kocaefe, Y., Boluk, Y., and Pichette, A. (2012). Changes in wettability of heat-treated wood due to artificial weathering. *Wood Sci. Technol.* 46, 1215–1237. doi: 10.1007/s00226-012-0479-6

Hubbe, M. A., Gardner, D. J., and Shen, W. (2015). Contact angles and wettability of cellulosic surfaces: a review of proposed mechanisms and test strategies. *BioResources* 10, 8657–8749.

Ilek, A., and Jarosław, K. (2014). Hydrological properties of bark of selected forest tree species. Part I: the coefficient of development of the interception surface of bark. *Trees - Struct. Funct.* 28, 831–839. doi: 10.1007/s00468-014-0995-0

Ilek, A., Kucza, J., and Morkisz, K. (2017a). Hygroscopicity of the bark of selected forest tree species. *IForest - Biogeosci. Forestry* 10, 220–226. doi: 10.3832/ifor1979-009

Ilek, A., Kucza, J., and Morkisz, K. (2017b). Hydrological properties of bark of selected forest tree species. Part 2: interspecific variability of bark water storage capacity. *Folia For. Pol. Ser. A* 59, 110–122. doi: 10.1515/ffp-2017-0011

Ilek, A., Kucza, J., and Szostek, M. (2015). The effect of stand species composition on water storage capacity of the organic layers of forest soils. *Eur. J. For. Res.* 134, 187–197. doi: 10.1007/s10342-014-0842-2

Johnson, M. S., and Lehmann, J. (2006). Double-funneling of trees: stemflow and root-induced preferential flow. *Écoscience* 13, 324–333. doi: 10.2980/i1195-6860-13-3-324.1

Klamerus-Iwan, A., and Błońska, E. (2018). Canopy storage capacity and wettability of leaves and needles: the effect of water temperature changes. *J. Hydrol.* 559, 534–540. doi: 10.1016/j.jhydrol.2018.02.032

Klamerus-Iwan, A., Łagan, S., Zarek, M., Słowik-Opoka, E., and Wojtan, B. (2020a). Variability of leaf wetting and water storage capacity of branches of 12 deciduous tree species. *Forests* 11:1158. doi: 10.3390/f11111158

Klamerus-Iwan, A., Lasota, J., and Blonska, E. (2020b). Interspecific variability of water storage capacity and absorbability of deadwood. *Forests* 11:575. doi: 10.3390/f11050575

Klamerus-Iwan, A., Link, T. E., Klein, R. F., and Van Stan, J. T. (2020c). "Storage and routing of precipitation through canopies," in *Precipitation Partitioning by Vegetation: A Global Synthesis*, eds T. John, Van Stan, and J. F. Ethan Gutmann (Berlin: Springer Nature Switzerland), 17–34.

Kozlowski, R., Józwiak, M. A., and Borowska, E. (2010). "Porównanie wybranych metod do obliczania wysokosci opadu splywajacego po pniach [Comparison of selected methods for calculation of stemflow volume]," *Monitoring Srodowiska Przyrodniczego*, (Kielce: Kieleckie Towarzystwo Naukowe, 11: 25–33.

Levia, D. F. (2003). Winter stemflow leaching of nutrient-ions from deciduous canopy trees in relation to meteorological conditions. *Agric. For. Meteorol.* 117, 39–51. doi: 10.1016/S0168-1923(03)00040-6

Levia, D. F., and Frost, E. E. (2003). A review and evaluation of stemflow literature in the hydrologic and biogeochemical cycles of forested and agricultural ecosystems. *J. Hydrol.* 274, 1–29. doi: 10.1016/S0022-1694(02)00399-2

Levia, D. F., and Germer, S. (2015). A review of stemflow generation dynamics and stemflow-environment interactions in forests and shrublands. *Rev. Geophys.* 53, 673–714.

Levia, D. F., and Herwitz, S. R. (2005). Interspecific variation of bark water storage capacity of three deciduous tree species in relation to stemflow yield and solute flux to forest soils. *Catena* 64, 117–137. doi: 10.1016/j.catena.2005.08.001

Levia, D. F., Van Stan, J. T., Mage, S. M., and Kelley-Hauske, P. W. (2010). Temporal variability of stemflow volume in a beech-yellow poplar forest in relation to tree species and size. *J. Hydrol.* 380, 112–120. doi: 10.1016/j.jhydrol.2009.10.028

Levia, D. F., and Wubbena, N. P. (2006). Vertical variation of bark water storage capacity of *Pinus strobus* L. (Eastern White Pine) in Southern Illinois. *Northeast. Nat.* 13, 131–137.

Liu, G., Du, S., Peng, S., and Wang, G. (2014). Rainfall interception in two contrasting forest types in the mount gongga area of eastern tibet. *China. Hydrol. Curr. Res.* 4, 1–6. doi: 10.4172/2157-7587.1000161

Magyar, D., Van Stan, J. T., and Sridhar, K. R. (2021). Hypothesis and theory: fungal spores in stemflow and potential bark sources. *Frontiers in Forests and Global Change 4* 4: 1–18. doi: 10.3389/ffgc.2021.623758

Meijer, M. (2004). "A review of interfacial aspects in wood coatings: wetting, surface energy, substrate penetration and adhesion," in *Proceedings of the COST E18*, (Paris), 1–16.

Metzger, J. C., Schumacher, J., Lange, M., and Hildebrandt, A. (2019). Neighbourhood and stand structure affect stemflow generation in a heterogeneous deciduous temperate forest. *Hydrol. Earth Syst. Sci.* 23, 4433–4452. doi: 10.5194/hess-23-4433-2019

Mitchell, R. J., Truscot, A. M., Leith, I. D., Cape, J. N., Van Dijk, N., Tang, Y. S., et al. (2005). A study of the epiphytic communities of Atlantic oak woods along an atmospheric nitrogen deposition gradient. *J. Ecol.* 93, 482–492. doi: 10.1111/j.1365-2745.2005.00967.x

Molnar, I. L., O'Carroll, D. M., and Gerhard, J. I. (2011). Impact of surfactant-induced wettability alterations on DNAPL invasion in quartz and iron oxide-coated sand systems. *J. Contam. Hydrol.* 119, 1–12. doi: 10.1016/j.jconhyd.2010.08.004

Neiva, D. M., Rencoret, J., Marques, G., Gutiérrez, A., Gominho, J., Pereira, H., et al. (2020). Lignin from tree barks: chemical structure and valorization. *ChemSusChem* 13, 4537–4547. doi: 10.1002/cssc.202000431

Nogalska, A., Trojanowska, A., Tylkowski, B., and Garcia-Valls, R. (2019). Surface characterization by optical contact angle measuring system. *Phys. Sci. Rev.* 5, 1–13. doi: 10.1515/psr-2019-0083

Notley, S. M., and Norgren, M. (2010). Surface energy and wettability of spin-coated thin films of lignin isolated from wood. *Langmuir* 26, 5484–5490. doi: 10.1021/la1003337

Papierowska, E., Szporak-Wasilewska, S., Szewińska, J., Szatyłowicz, J., Debaene, G., and Utratna, M. (2018). Contact angle measurements and water drop behavior on leaf surface for several deciduous shrub and tree species from a temperate zone. *Trees - Struct. Funct.* 32, 1253–1266. doi: 10.1007/s00468-018-1707-y

Pereira, L. C., Balbinot, L., Matus, G. N., Dias, H. C. T., and Tonello, K. C. (2021). Aspects of forest restoration and hydrology: linking passive restoration and soil – water recovery in Brazilian Cerrado. *J. For. Res.* doi: 10.1007/s11676-021-01301-3

Prakash, C. G. J., Clement Raj, C., and Prasanth, R. (2017). Fabrication of zero contact angle ultra-super hydrophilic surfaces. *J. Colloid Interface Sci.* 496, 300–310. doi: 10.1016/j.jcis.2017.01.007

Ptatscheck, C., Milne, P. C., and Traunspurger, W. (2018). Is stemflow a vector for the transport of small metazoans from tree surfaces down to soil? *BMC Ecol.* 18:43. doi: 10.1186/s12898-018-0198-4

Pypker, T. G., Levia, D. F., Staelens, J., and Van Stan, J. T. (2011). "Canopy structure in relation to hydrological and biogeochemical fluxes," in *Forest Hydrology and Biogeochemistry, Synthesis of Past Research and Future Directions*, eds D. F. Levia, D. Carlyle-Moses, and T. Tanaka (Dordrecht: Springer), doi: 10.1007/978-94-007-1363-5

Rosado, B. H. P., and Holder, C. D. (2013). The significance of leaf water repellency in ecohydrological research: a review. *Ecohydrology* 6, 150–161. doi: 10.1002/eco.1340

Sadeghi, S. M. M., Gordon, D. A., and Van Stan, J. T. (2020). "A global synthesis of throughfall and stemflow hydrometeorology," in *Precipitation Partitioning by Vegetation: A Global Synthesis*, eds T. John, J. F. Van Stan, E. Gutmann, and J. Friesen (Berlin: Springer Nature Switzerland), 49–70. doi: 10.1007/978-3-030-29702-2

Siegert, C. M., and Levia, D. F. (2014). Seasonal and meteorological effects on differential stemflow funneling ratios for two deciduous tree species. *J. Hydrol.* 519, 446–454. doi: 10.1016/j.jhydrol.2014.07.038

Sinderski, L. G. Z. (2020). Ângulo de contato e rugosidade de madeiras, uma breve revisão. *Rev. Ciência da Madeira* 11, 1–11. doi: 10.12953/2177-6830/rcm.v11n1p1-11

Spencer, S. A., and van Meerveld, H. J. (2016). Double funnelling in a mature coastal British Columbia forest: spatial patterns of stemflow after infiltration. *Hydrol. Process.* 30, 4185–4201. doi: 10.1002/hyp.10936

TAPPI (2011). *Lignin in Wood and Pulp*. Atlanta: TAPPI.

Valová, M., and Bieleszová, S. (2008). Interspecific variations of bark's water storage capacity of chosen types of trees and the dependance on occurance of epiphytic mosses. *Geosci. Eng. LIV* 4, 45–51.

Van Stan, J. T., and Allen, S. T. (2020). What we know about stemflow's infiltration area. *Front. For. Glob. Chang.* 3:61. doi: 10.3389/ffgc.2020.00061

Van Stan, J. T., and Gordon, D. A. (2018). Mini-Review: stemflow as a resource limitation to near-stem soils. *Front. Plant Sci.* 9:248. doi: 10.3389/fpls.2018.00248

Van Stan, J. T., and Levia, D. F. (2010). Inter- and intraspecific variation of stemflow production from *Fagus grandifolia* ehrh. (American beech) and *Liriodendron tulipifera* L. (yellow poplar) in relation to bark microrelief in the eastern United States. *Ecohydrology* 3, 11–19. doi: 10.1002/eco

Van Stan, J. T., Lewis, E. S., Hildebrandt, A., Rebmann, C., and Friesen, J. (2016). Impact of interacting bark structure and rainfall conditions on stemflow

variability in a temperate beech-oak forest, central Germany. *Hydrol. Sci. J.* 61, 2071–2083. doi: 10.1080/02626667.2015.1083104

Van Stan, J. T., and Pypker, T. G. (2015). A review and evaluation of forest canopy epiphyte roles in the partitioning and chemical alteration of precipitation. *Sci. Total Environ.* 536, 813–824. doi: 10.1016/j.scitotenv.2015.07.134

Van Stan, J. T., Siegert, C. M., Levia, D. F., and Scheick, C. E. (2011). Effects of wind-driven rainfall on stemflow generation between codominant tree species with differing crown characteristics. *Agric. For. Meteorol.* 151, 1277–1286. doi: 10.1016/j.agrformet.2011.05.008

Van Stan, J. T., Hildebrandt, A., Friesen, J., Metzger, J. C., and Yankine, S. A. (2020). "Spatial variability and temporal stability of local net precipitation patterns," in *Precipitation Partitioning by Vegetation*, eds T. John, J. F. Van Stan, E. Gutmann, and J. Friesen (Cham: Springer), 89–104.

Voigt, G. K., and Zwolinski, M. J. (1964). Absorption of stem ow by bark of young red and white pines sign in oxford academic account sign in via society site sign in via your institution short-term access. *For. Sci.* 10, 277–282. doi: 10.1093/forestscience/10.3.277

Whyman, G., Bormashenko, E., and Stein, T. (2008). The rigorous derivation of young, cassie-baxter and wenzel equations and the analysis of the contact angle hysteresis phenomenon. *Chem. Phys. Lett.* 450, 355–359. doi: 10.1016/j.cplett.2007.11.033

Yuan, Y., and Lee, T. R. (2013). "Contact angle and wetting properties," in *Surface Science Techniques*, eds G. Bracco and B. Holst (Berlin: Springer-Verlag), 1–32. doi: 10.1007/978-3-642-34243-1

Zimmermann, A., Uber, M., Zimmermann, B., and Levia, D. F. (2015). Predictability of stemflow in a species-rich tropical forest. *Hydrol. Process.* 29, 4947–4956. doi: 10.1002/hyp.10554

Conflict of Interest: The authors declare that the research was conducted in the absence of any commercial or financial relationships that could be construed as a potential conflict of interest.

frontiers in Forests and Global Change

ORIGINAL RESEARCH
published: 07 July 2021
doi: 10.3389/ffgc.2021.691321

Localized Augmentation of Net Precipitation to Shrubs: A Case Study of Stemflow Funneling to Hummocks in a Salinity-Intruded Swamp

Scott T. Allen[1]* *and William H. Conner*[2]

[1] Department of Natural Resources and Environmental Science, University of Nevada, Reno, NV, United States, [2] Baruch Institute of Coastal Ecology and Forest Science, Clemson University, Georgetown, SC, United States

OPEN ACCESS

Edited by:
Anna Klamerus-Iwan, University of Agriculture in Krakow, Poland

Reviewed by:
Krzysztof Owsiak, University of Agriculture in Krakow, Poland
Kelly Cristina Tonello, Federal University of São Carlos, Brazil

***Correspondence:**
Scott T. Allen
scottallen@unr.edu

Specialty section:
This article was submitted to Forest Hydrology, a section of the journal Frontiers in Forests and Global Change

Received: *06 April 2021*
Accepted: *15 June 2021*
Published: *07 July 2021*

Citation:
Allen ST and Conner WH (2021) Localized Augmentation of Net Precipitation to Shrubs: A Case Study of Stemflow Funneling to Hummocks in a Salinity-Intruded Swamp. Front. For. Glob. Change 4:691321. doi: 10.3389/ffgc.2021.691321

The interception of precipitation by plant canopies can alter the amount and spatial distribution of water inputs to ecosystems. We asked whether canopy interception could locally augment water inputs to shrubs by their crowns funneling (freshwater) precipitation as stemflow to their bases, in a wetland where relict overstory trees are dying and persisting shrubs only grow on small hummocks that sit above mesohaline floodwaters. Precipitation, throughfall, and stemflow were measured across 69 events over a 15-months period in a salinity-degraded freshwater swamp in coastal South Carolina, United States. Evaporation of intercepted water from the overstory and shrub canopies reduced net precipitation (stemflow plus throughfall) across the site to 91% of gross (open) precipitation amounts. However, interception by the shrub layer resulted in increased routing of precipitation down the shrub stems to hummocks – this stemflow yielded depths that were over 14 times larger than that of gross precipitation across an area equal to the shrub stem cross-sectional areas. Through dimensional analysis, we inferred that stemflow resulted in local augmentation of net precipitation, with effective precipitation inputs to hummocks equaling 100–135% of gross precipitation. Given that these shrubs (wax myrtle, *Morella cerifera*) are sensitive to mesohaline salinities, our novel findings prompt the hypothesis that stemflow funneling is an ecophysiologically important mechanism that increases freshwater availability and facilitates shrub persistence in this otherwise stressful environment.

Keywords: ecohydrology, critical zone, precipitation partitioning, microtopography, coastal wetland, canopy interception

INTRODUCTION

In flooded wetlands, microtopographic high areas (e.g., hummocks) can serve as local refugia. Microtopographic highs can foster seed germination and seedling survival in environments where they would otherwise be excluded by flooding (Conner et al., 1986; Souther and Shaffer, 2000); this is especially true when floodwaters are saline (Rheinhardt and Faser, 2001) because salinity is often a critical physiological stressor to both juvenile and mature trees (Allen et al., 2019). Thus, hummocks, which are often composed of partially decomposed organic material, such as stumps or logs, and are common in diverse wetland types (Andrus et al., 1983; Jones et al., 1996; Shimamura and Momose, 2005; Stine et al., 2011), can affect community structure by providing a preferential zone for establishment (Huenneke and Sharitz, 1986; Duberstein and Conner, 2009). Hummocks allow roots to avoid and sit above saline waters (Light et al., 2007). Hsueh et al. (2016) showed that salinity sensitive trees occupying hummocks in a mesohaline wetland used water from the hummocks which was less saline than the surrounding floodwaters; others have also observed coastal woody plants avoiding uptake of saline water despite its availability and proximity to roots (Ish-Shalom et al., 1992). In this study, we examine the input of freshwater to hummocks, which can facilitate plants' avoidance of saline conditions.

Precipitation is often the primary freshwater input to ecosystems, although the amount and spatial distributions of that input can be substantially modified by canopy interception before it reaches plant roots. Interception can substantially reduce precipitation inputs, with interception losses in closed-canopy forests often exceeding 10–20% of gross precipitation (Carlyle-Moses and Gash, 2011). Thus, throughfall and stemflow, which together constitute the net precipitation input to soils, can be considerably less than gross precipitation. However, precipitation inputs to specific locations can be substantially augmented by interception processes because tree crowns can redistribute water and result in temporally stable spots of especially high precipitation inputs (Keim et al., 2005). Perhaps the greatest localized input is that of stemflow, which is routed down stems to the stem-soil interface and, hypothetically, to roots (Martinez-Meza and Whitford, 1996; Liang et al., 2009). Thus, a consequence of canopies routing throughfall and stemflow may be local augmentations to the amount of water that infiltrates near stems (Li et al., 2009).

In this study, we investigate how canopy interception affects precipitation inputs to a permanently flooded wetland where salinity intrusion has yielded an ecosystem composed of sparse relict trees with submerged roots (Williams et al., 2014) and midstory shrubs rooted on hummocks. The dominant shrub, wax myrtle (*Morella cerifera*) can have wide crowns and smooth bark, which are characteristics associated with high stemflow rates (Levia and Germer, 2015). In our study site, their crowns extended far beyond the extent of the above-water hummock areas (here defined as microtopographic highs supporting woody vegetation). Thus, we hypothesized that stemflow inputs to hummocks could augment the net precipitation, and thus the influx of freshwater, to exceed that of gross precipitation. If this were true, this could be ecologically important given that wax-myrtle shrubs are stressed by salinities as low as five practical salinity units (PSU) (Tolliver et al., 1997), which is within the range of values observed in floodwaters of the study site (Duberstein et al., 2018).

MATERIALS AND METHODS

Site Description

The study site was Strawberry Swamp in coastal South Carolina (33°19′49″N, 79°14′54″W), a permanently flooded wetland with ∼30 ha watershed (Williams et al., 2014) that drains into the Winyah Bay estuary (1.2 km to the west); the site is also proximal to the Atlantic Ocean (8 km to the east). The region's climate can be classified as humid subtropical with a mean July temperature of 27.6°C, a mean January temperature of 8.2°C, and an annual total precipitation of 133 cm, which is highest from July–September (mean of 17 cm month^{-1}; from the National Climate Data Center). Salinity enters the site from periodic storm surges or by backflooding from the estuary during severe events. This salinity is associated with widespread tree mortality and replacement by shrub cover (Williams et al., 2014), as well as reduced biomass (Liu et al., 2017) and transpiration (Duberstein et al., 2020).

The throughfall and stemflow measurement locations spanned freshwater and mesohaline conditions (**Table 1**). This salinity gradient occurs over a roughly 50–100 m distance so freshwater and saltier zones are not discrete or spatiotemporally constant. The sampling design was oriented around a 500-m-long, 0.3-m-wide boardwalk. The boardwalk is composed of two transects in a "v" shape (**Figure 1**) from freshwater to mesohaline to freshwater zones. While the boardwalk location is not random, its placement was for spanning the salinity gradient and not with attention to small-scale biases regarding its position under the canopy.

Canopy and tree or shrub characteristics were quantified. Uncorrected leaf area index (LAI) was quantified by light attenuation using paired canopy analyzers (LAI-2000, LI-COR, Lincoln, NE) with 76° view angles (Cutini et al., 1998), which yields reasonable relativistic values in baldcypress swamps (Allen et al., 2015). Measurements were taken on an approximately 6-m interval over the length of the boardwalk (88 measurements) in July 2015 (**Figure 1**). LAI values ranged from one, in the mesohaline zone, to over five, in the freshwater zone (**Figure 1**). Stand basal areas were quantified across this gradient in previous studies (Liu et al., 2017; Duberstein et al., 2020) that discretized the site into zones classified as freshwater, intermediate, and mesohaline; those studies measured trees and shrubs with diameters at breast height (dbh, at 1.3 m) over 10 cm in two 20 × 25 m plots in each zone. In this study, we use site-averaged basal areas (BA), using the average of all six plots from these previous studies. We also refer to "Freshwater" and "Mesohaline" zones, which is an *ad hoc* classification used for communication purposes.

TABLE 1 | Forest characteristics—salinity, basal area (BA), dominant species (>15% of BA), density, and size—for the overstory trees by zone, and shrub characteristics across the whole site (Liu et al., 2017; Duberstein et al., 2020).

Zone	Salinity (psu)	Plots[a]	BA (m^2 ha^{-1})	Species[b]	Trees ha^{-1}	Diameter[c] (cm)
Fresh (Overstory)	0.7 ± 0.4	2	59	TD,NB,NA	800	30.6
Intermediate (Overstory)	2.6 ± 0.9	2	65	TD,NA	610	36.8
Saline (Overstory)	3.0 ± 1.0	2	58	TD	590	35.5
All (Overstory)		6	61	TD,NA	670	34.0
All (Shrub)		27/9	13[d]	MC	9481	3.3

[a]*For overstory measurements, 20 × 25 m plots were used; for the shrub midstory, 27 5.0 × 1.0 m plots were used to quantify tree ha-1 and nine hummocks of various size were used to characterize BA and diameter.* [b]*Taxodium distichum, Nyssa aquatica, Nyssa biflora, and Morella cerifera.* [c]*Quadratic-mean diameter.* [d]*In the nine hummocks, basal area densities were 119 ± 23 m^2 ha^{-1} of hummock area (mean ± 1SE) then scaled up to stand by hummock area per site (11.1 ± 3.5%) based on 27 plots of 5 m^2.*

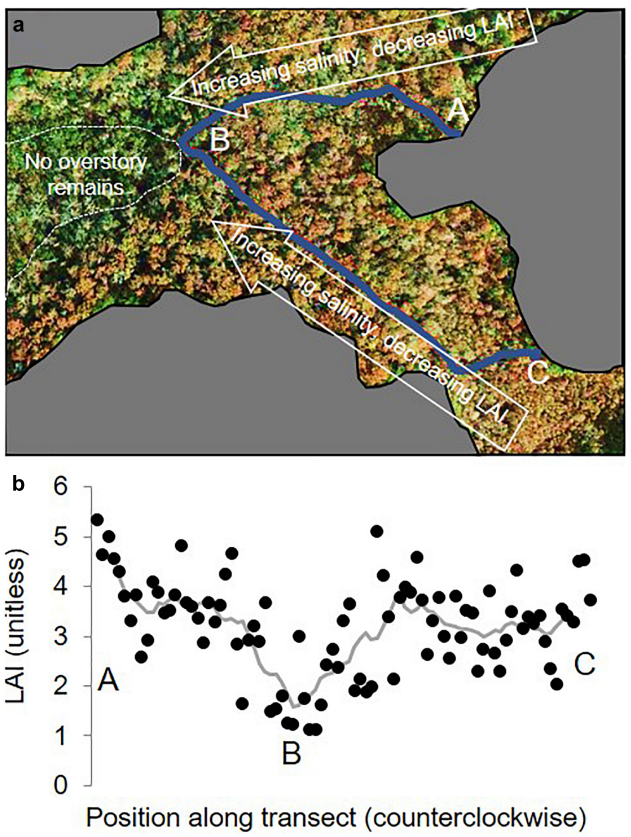

FIGURE 1 | (a) Aerial image of site (with upland areas excluded), showing the boardwalk along which sampling was conducted (in blue) and showing the shift in structure with salinity. The marked "A", "B", and "C" correspond with the LAI measurements in **(b)**, which are measured at 6-m intervals along the site boardwalk. Imagery was downloaded from Google Earth (Google Inc., Mountain View, CA, United States). The gray line in panel **(b)** is a running mean using a nine-measurement moving window.

Despite similarities in basal areas among zones (**Table 1**), the freshwater and mesohaline zones differed substantially in ecosystem structure: baldcypress (*Taxodium distichum* var. *distichum*) and water tupelo (*Nyssa aquatica*) occurred in both zones, but swamp tupelo (*Nyssa biflora*) and sweetgum (*Liquidambar styraciflua*) only occurred in the freshwater zone. In the mesohaline zone, there were fewer, larger trees and they were predominantly baldcypress (**Table 1**). The midstory was composed of wax myrtle shrubs (*Morella cerifera*) in both zones, although the freshwater zone midstory also had younger cohorts of baldcypress.

This wetland is always flooded, although wetter conditions reduce the above-water ground area. Based on our experience wading through the floodwaters, we estimate water depths to largely range between 0.5 and 1.5 m. However, they are not easily quantified because they vary tremendously in space. Furthermore, the soils are unconsolidated and contain substantial amounts of coarse woody debris, further challenging a quantitative description of water depth. Both the freshwater and mesohaline zones have hummocks, and both have deep (>1.0 m) water. In general, water levels vary with major events, seasons, and prolonged droughts, but are minimally responsive to small events in summer. For example, in the week before our hummock survey, 3.8 and 1.6 cm precipitation events resulted in 3.5 and 2.3-cm water level rises that receded back to prior conditions in less than a week. However, a historic 60-cm precipitation event in 2015 caused water levels to rise to 1.1 m over the median depth.

All observed shrub stems were rooted in hummocks (e.g., **Figure 2**), not in soils under the floodwater as was generally the case for large, mature trees; this pattern has been reported elsewhere (Rheinhardt and Faser, 2001).

Net and Gross Precipitation Measurements

To measure gross precipitation, a precipitation collector was placed in an open field 500 m away from the study site. This precipitation collector, as well as each of the throughfall collectors, was composed of a 2.0-liter plastic jug with a 11.7 cm diameter funnel; water passed through a >5-cm length of tubing to impede evaporation from the collectors. Collectors were placed on a pole that was roughly one meter above the soil or floodwater surface. They were designed so that the collectors could haphazardly pivot around the poles, so that they would not be in an identical position each time they were sampled and put back on the pole; non-stationary sampling strategies such as this reduce uncertainties because they mitigate the likelihood of drip points being consistently represented or missed as a function of collector location (Holwerda et al., 2006).

FIGURE 2 | Wax myrtle stems on hummocks of different heights and sizes at the Strawberry Swamp field site; in the top left panel, a ∼0.3 m ruler is shown.

To measure throughfall, 29 collectors were placed along the boardwalk. They were placed to span both fresh and mesohaline zones, up to the edge of the entirely treeless zone (**Figure 1a**). In addition to the previously described LAI measurements along the boardwalk, LAI was also characterized above each collector, using the LAI-2000 instrument. In the field, each collector was categorized as being associated with the freshwater or mesohaline zones as a function of its position along the gradient and the change in canopy (i.e., with minimal evidence of tree recruitment in recent decades in the mesohaline zone). These classifications were admittedly subjective; however, they were established prior to any precipitation sampling and they reflected our best visual assessment of a step-shift in forest structure.

Stemflow was measured on six wax-myrtle shrub stems. The stems varied from 5.0 to 7.5 cm dbh. Stemflow was collected using an approximately 5-cm thick ring of wax inside of a plastic cylinder sealed around them (Safeeq and Fares, 2014); a length of tubing conveyed water to a 2.0- or 4.0-liter container (depending on tree size). We did not measure overstory-tree stemflow because they all have rough bark, which is generally associated with low *SF* (Rothacher, 1963; Van Stan and Gordon, 2018); its potential effects were not ignored in calculations, however (as described in section "Analyses").

Overall, precipitation from 69 events was collected from 14 April 2015 to 8 July 2016. The stemflow collectors were installed on 3 July 2015. Occasionally, back-to-back rain events occurred, preventing collection in between events; thus, some so-called events included multiple storms. The measurements were continuous, with the exception of one excluded record precipitation event of 60 cm in 5 days in Oct 2015. Over the study, 2% of throughfall samples were lost due to collectors coming off the poles or mis-transferring water into the measuring graduated cylinder. In all cases where cumulative throughfall or stemflow depths are compared to cumulative gross precipitation, only matched respective events are used (i.e., if a collector failed for one event, gross precipitation is also omitted for that event when, e.g., quantifying ratios of throughfall to gross precipitation).

Hummock and Shrub Measurements

Intensive measurements of shrubs and hummocks were made to scale stemflow measurements and quantify those fluxes across the site, across hummocks, and across shrubs.

To determine fractional hummock area for the swamp, we assumed the boardwalk to represent an unbiased transect through the swamp and took systematic measurements of hummocks along that track. A 5.0-by-1.0-m plot was established precisely every 18-m of length along the boardwalk (27 plots in total), extending perpendicularly on the outside of the boardwalk loop. In each plot, area of water versus area of above-water-level ground (hummocks) was quantified; water levels at the time of the survey were 5 cm below the median water level over the study duration, and water levels were within 5 cm

of this height for 55% of the growing season, so they were assumed to reasonably represent typical conditions. Hummocks were defined as any ground above the water level that had accumulated soil or litter and had vegetation growing on it. Hummock areas were approximated by assuming each hummock was rectangular in shape, with area calculated from average lengths and average widths measured using a measuring tape. The number of woody stems on hummocks within plots was counted. Across the 5.0 m^2 plots, the number of hummocks per plot ranged from zero (in five of the 27 plots) to four, the individual hummock sizes (within the plot bounds) ranged from 0.01 to 2.5 m^2, and the shrub stem density averaged 9 ± 5 stems per m^2 of hummock and was as high as 17 per plot and 67 per m^2 of hummock area. Hummocks averaged 11 ± 3.5% (Mean ± 1SE) of the area in plots (and thus floodwater and submerged tree stems were 89% of plot area); this was assumed to be representative of the site.

More intensive diameter inventories were measured on nine additional hummocks, selected because they contained or were near the wax-myrtle shrubs on which stemflow was measured. These nine hummocks are reasonably representative of the site, as indicated by the similarity in stem density (10 ± 4 stems per m^2 of hummock; Mean ± 1SE) to that observed across the effectively-random hummock plots described above. Hummock area, hummock height, and total crown area of all shrubs on each hummock were measured (**Supplementary Table 1**). In these nine hummocks, the total crown area of shrubs was twenty times greater than the area of hummocks they occupied (**Supplementary Table 1**); shrub crowns also overlapped with shrubs on other hummocks. Diameters of every woody plant over 1.0 cm in dbh were measured, which were almost exclusively wax myrtle; no diameters exceeded 8 cm. Basal areas were calculated for each stem, and summed for the nine hummocks and divided by hummock areas, showing that stem areas were 1.2 ± 0.2% of hummock areas (mean ± 1 SE); this number was multiplied by the fractional area of hummocks across the site (previous paragraph) to yield the mean fractional shrub basal area ($F_{BA-shrub}$), which was 0.13 ± 0.05% of the site area (or 13 ± 5 m^2 ha^{-1} of site area), with the SE estimated by Gaussian error propagation.

Analyses

Interception loss was calculated across the site using the following equation:

$$Interception\ loss\ =\ P_g - Net\ Precipitation\ =$$
$$P_g - [(1 - F_{BA-all})\ \times\ TF\ +\ SF_{overstory}\ +\ SF_{shrub}], \quad (1)$$

where P_g is the gross precipitation measured in the clearing, TF is the throughfall across the site, SF_{shrub} is the upscaled site-level wax-myrtle stemflow, and $SF_{overstory}$ is the assumed overstory stemflow, and F_{BA-all} is the fractional basal area of all trees and shrubs; F_{BA-all} was calculated as the sum of $F_{BA-shrub}$ and overstory tree basal areas divided by respective plot areas ($F_{BA-overstory}$). The "1- F_{BA-all}" term is included because throughfall cannot fall where stems are located. To report all fluxes as depths, measured P_g and TF volumes were divided by the area of the collector funnels. For SF_{shrub}, depths were first calculated by dividing cumulative collector volumes for each stem by its basal area. These depths were averaged across the six wax-myrtle shrubs and multiplied by $F_{BA-shrub}$ to yield SF_{shrub}, integrated across the stand. To fill gaps of events where stemflow was not measured, SF_{shrub} was estimated by multiplying event P_g by the mean shrub funneling ratio (FR_{shrub}: cumulative SF_{shrub} divided by cumulative P_g, over the same events). Values for $SF_{overstory}$ are assumed by multiplying P_g by $F_{BA-overstory}$ and an assumed overstory funneling ratio (1.0); a higher value (3.0) and a lower value (0.0) were also used to understand the sensitivity of our findings to the overstory trees potentially having unexpectedly small or large funneling ratios (see, e.g., Van Stan and Gordon, 2018).

Interception losses were calculated as site-integrated, cumulative values, but we also stratified results among small events (<1 cm), medium events (≥1 and <3 cm), and large events (≥3 cm), as well as by growing and dormant season (April-October and November-March, respectively; readers should note that wax myrtle is evergreen). For error calculations in cumulative values, by-event standard errors (reflecting variability among collectors) were added in quadrature to propagate errors through analyses. Errors in overstory-basal-area and gross-precipitation values are treated as negligible compared to other sources of errors in eq. 1.

Stemflow volumes exceeded the collector capacities in many larger events, with potentially overtopped collectors representing 19% of the entire dataset. This is a substantial amount, and thus all reported observed stemflow values are likely underestimates. In collectors that overtopped, we assumed their values to be the observed maximum collectable volume (i.e., 1600 or 3600 ml for 2000 or 4000 ml containers). We assume all reported observed SF_{shrub} values to underestimate actual values, but the magnitude of that bias is unknown, and thus, we preface stemflow values as being "at least" what we report them to be.

Analyses were performed in MATLAB (Mathworks, Natick, MA, United States). All uncertainties are expressed as ± one standard error (SE) unless described otherwise.

RESULTS AND DISCUSSION

Precipitation Partitioning

Over the 15-months measurement period, net precipitation was 91.4 ± 0.7% of P_g (**Table 2**), implying that interception losses were 8.6 ± 0.7% of P_g, or less, given that stemflow was underestimated (as described in section "Analyses"). Interception losses were greatest for small storms (<1.0 cm) during the growing season (**Table 2**). Throughfall, the dominant component of net precipitation, ranged from 63% to 112% of P_g in storms larger than >1.0 cm and from 39% to 142% of P_g in storms <1.0 cm. Throughfall exceeded precipitation in only eight events, with an amount-weighted mean among those events of only 1.06% of P_g. Interception loss fractions were lower in the dormant

TABLE 2 | Cumulative depth of gross precipitation (P_g), throughfall (*TF*), shrub stemflow (SF_{shrub}), and shrub *SF* funneling ratio (FR_{shrub}), and interception loss (IL) over the 15-months-measuring period, stratified by event size (small < 1 cm, 1 cm ≤ medium < 3 cm, and large ≥ 3 cm) and season (dormant versus growing seasons).

Period	Size	Number of events	P_g (cm)	*TF* (cm)	SF_{shrub} (cm)	IL (cm)	IL (%)	FR_{shrub} (unitless)
Dormant	Small	2	1.0	1.1 ± 0.0	0.06 ± 0.01	−0.1 ± 0.0	−12.4 ± 4.5	42.1 ± 9.7
	Med	8	17.1	16.2 ± 0.4	0.56 ± 0.06	0.4 ± 0.4	2.4 ± 2.6	24.9 ± 2.0
	Large	9	43.1	40.8 ± 1.0	0.92 ± 0.06	1.4 ± 1.0	3.2 ± 2.3	16.2 ± 0.9
Growing Season	Small	20	10.3	8.2 ± 0.1	0.13 ± 0.01	1.9 ± 0.1	18.7 ± 1.3	9.9 ± 0.8
	Med	15	25.6	22.0 ± 0.3	0.48 ± 0.04	3.2 ± 0.3	12.4 ± 1.1	14.0 ± 0.9
	Large	15	87.7	77.1 ± 0.7	1.29 ± 0.05	9.2 ± 0.7	10.5 ± 0.8	11.2 ± 0.5
All	**All**	**69**	**184.9**	**166 ± 1**	**3.44 ± 0.11**	**15.9 ± 1.3**	**8.6 ± 0.7**	**14.1 ± 0.4**

season, as indicated by the several SEs of separation between dormant- and growing-season mean values (**Table 2**).

Across the salinity gradient, throughfall amounts increased in sparser-canopy zones (**Figure 3**). The $TF{:}P_g$ ratios decreased with increasing LAI, although one outlier (i.e., a drip point in the mesohaline zone) weakened the least-squares-fit regression relationship ($R^2 = 0.04$); however, by using a robust-fit regression to down-weight the influence of outliers, we found that $TF{:}P_g$ decreased by 0.033 (mm mm^{-1}) per unit of LAI (adjusted $R^2 = 0.25$, $p < 0.01$). The collectors in the mesohaline zone yielded cumulative $TF{:}P_g$ ratios of 0.92 ± 0.05 ($n = 15$; mean ± 1SE), compared to those in the freshwater zone of 0.87 ± 0.03 ($n = 14$), and thus they did not differ significantly ($p = 0.4$). Accordingly, we assume that *TF* is similar across the site in all site-level analyses, despite the relationships shown in **Figures 1**, **3**.

To account for the uncertainties associated with assuming that overstory tree stemflow equaled P_g depths across the overstory tree BAs (i.e., an assumed funneling ratio of one), we evaluated the sensitivity of interception loss estimates to assuming overstory funneling ratios of zero and three; resulting interception losses were 9.2 and 7.4% of P_g, respectively, and thus errors in our interception loss calculations (reported above as ±0.7% of P_g) may be more on the scale of ± 2% of P_g.

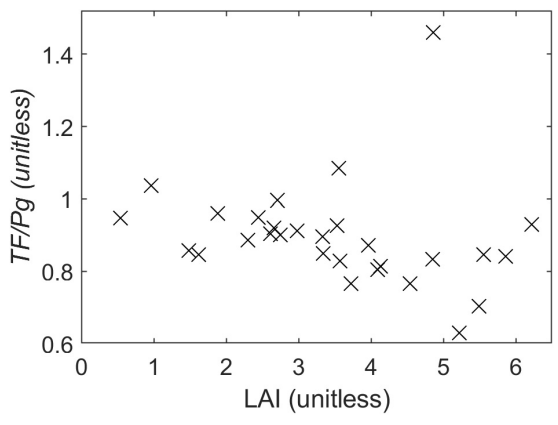

FIGURE 3 | The ratio of cumulative throughfall (*TF*) to cumulative gross precipitation (P_g) by *TF* collector, regressed against LAI measured above each collector. Areas under denser canopy generally receive less throughfall.

Stemflow to Hummocks

Given that most precipitation must fall on the floodwater surface, as opposed to the hummock soils, the routing of stemflow to hummocks could be important for increasing freshwater availability to shrubs on those hummocks.

The mean cumulative funneling ratio (FR_{shrub}) of the six instrumented wax-myrtle stems was 14.1 ± 0.4, implying that the depth of stemflow resulting from one mm of precipitation would be 14.1 mm across an area equal to the stem's basal area. Although stemflow was only a small component (i.e., 2%) of net precipitation (**Table 2**), this input comes down shrub stems which only represent 0.13 ± 0.05% of the site area. Given that shrub crowns are much more expansive than stems, with a crown-area to stem-basal-area ratio of 2228 ± 198 m^2 m^{-2} for shrubs on the nine intensively measured hummocks, only 0.6% of the precipitation potentially falling on those shrub crowns would need to be intercepted and routed to stemflow to yield funneling ratios of 14.1. Small amounts of precipitation collected across larger areas can be funneled to stems to locally augment inputs.

If we were to assume that all of shrub stemflow were to infiltrate into hummocks, stemflow can represent a substantial augmentation of freshwater, given that hummocks were small and the shrub stemflow was high. Hummocks were 11.1 ± 3.5% of the site area, and thus net precipitation can be calculated specifically for the hummocks by assuming that they receive all of the shrub stemflow (SF_{shrub}) and the same depths of *TF* as the rest of the site. To do so, we re-calculate SF_{shrub} for only the hummock area (i.e., $SF_{hummocks}$ is equal to SF_{shrub} divided by 11.1 ± 3.5%) and then calculate hummock net precipitation as TF + $SF_{hummocks.}$ Using the mean fractional hummock area, we estimate that the cumulative $SF_{hummocks}$ would be 31.1 ± 1.0 cm, and that hummock net precipitation would be 197 ± 2 cm, representing 106% of P_g (**Figure 4**). To account for error in the fractional hummock area (a major source of uncertainty), we recalculate these values for the confidence intervals of fractional hummock area using the mean ± 2SE (i.e., with hummocks representing 4.1% and 18.1% of site area); this yields an interval of net precipitation to hummock of 185–250 cm, representing 100–135% of P_g. We remind readers that these estimates are coarse, but they are also underestimated because stemflow was under-captured by the collectors. Thus, net precipitation inputs to hummocks likely ranged from equaling to substantially exceeding P_g, despite site-integrated net precipitation being approximately 9% lower than P_g.

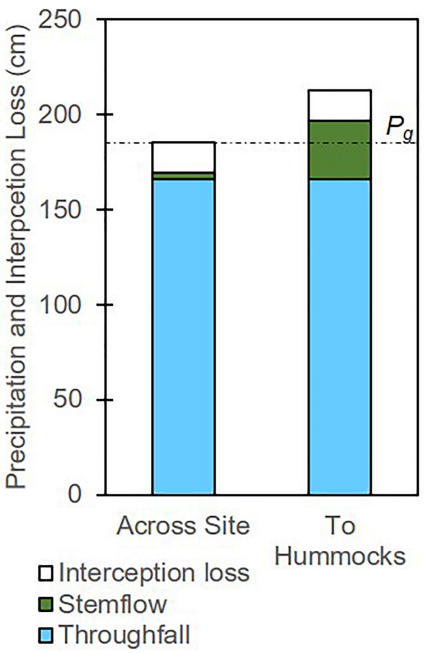

FIGURE 4 | Partitioning of precipitation among interception loss, stemflow, and throughfall across the site and across hummock area, assuming all shrub stemflow infiltrates into hummocks. The dotted line indicates the depth of gross precipitation across the study period, equal to the sum of across-site stemflow, interception loss, and throughfall, but exceeded by the sum of those values to hummocks (because of stemflow funneling in shrubs on hummocks).

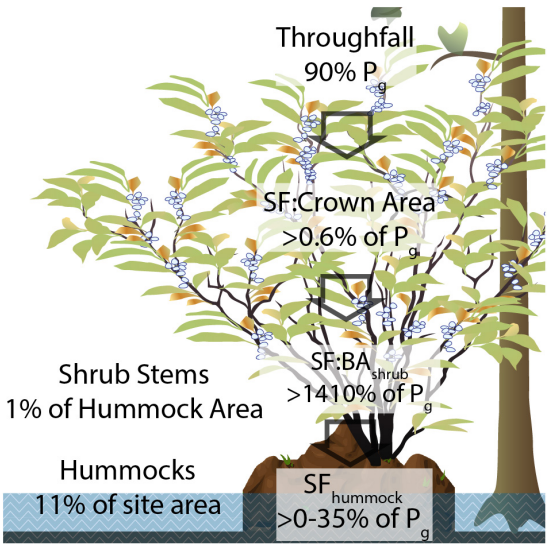

FIGURE 5 | Diagram of stemflow input scaling in the shrub layer, where input is *TF* from the overstory (90% of gross precipitation, P_g). Across shrub crown areas, 0.6% of P_g is routed to stemflow, which equates to over 14.1 times the depth of P_g across shrub stem basal areas. Across hummocks, stemflow averaged 17% of P_g depths, amounting to hummock net precipitation inputs that were 106% of P_g. The plant illustrations are adapted from artwork by Jane Hawkey (Integration and Application Network, University of Maryland Center for Environmental Science; ian.umces.edu/imagelibrary/).

Implications and Synthesis

The effect of interception – accounting for losses and redistribution – involved net losses at the site level but local augmentation of precipitation to hummocks (**Figure 4**). These losses are not especially surprising, although the interception loss estimates (mean of 9%, assuming $FR_{overstory}$ of one) were below average values of mixed forests (Carlyle-Moses and Gash, 2011), likely because the site included sparse canopy areas with low LAI (**Figure 1**). The denser canopy in the freshwater zone yielded *TF*:P_g ratios (**Figure 3**) that are comparable to global mean interception losses from forests (13–19% in broadleaf forests and 22% in conifers; Miralles et al., 2010). Both the effects of season (*TF* during leafed period > leafless) and event size (*TF* fraction during small events was less than during large events) were also consistent with others' observations (e.g., Mużyło et al., 2012). Given that the observed patterns in interception loss are typical, we focus this discussion on the previously undescribed phenomenon of stemflow funneling to hummocks.

The augmentation of net precipitation to hummocks was likely attributable to (1) high funneling ratios, (2) stems restricted to rooting on small hummocks, and (3) broad crowns extending well beyond the spatial extents of the hummock (**Figure 5** and **Supplementary Table 1**).

The observed cumulative funneling ratio of wax-myrtle shrubs (14 ± 0.4) was high, although funneling ratios over 20 are not uncommon for smooth-barked or large-crowned species (Levia and Germer, 2015). Moreover, the reported funneling ratios may be severely underestimated by us using too-small collectors (i.e., with maximum volumes of 3600 and 1600 ml for four and two of the collectors, respectively). More evidence that these values are underestimated is shown in **Table 2**: smaller events (less likely to overflow the collectors) had larger funneling ratios, which is a pattern that contrasts with other studies (Mużyło et al., 2012; Siegert and Levia, 2014). Collector overtopping even occurred in events as small as 1.6 cm, indicating that the under-catch of stemflow in larger events could have been substantial. Thus, actual net precipitation to hummocks may far exceed the 100–135% of P_g that we can infer from our data.

The association of wax-myrtle shrubs with hummocks may represent a system that benefits from stemflow-augmented net precipitation. Although wax myrtle is commonly associated with mesohaline environments, it is stressed by salinities as low as five PSU and it is often absent from zones of higher salinities (Young et al., 1994; Tolliver et al., 1997). In the mesohaline zones, 9% of measurements across the study exceeded 5 PSUs (see salinity measurements for stations "St4", "St5", and "T" in this dataset: Duberstein et al., 2018). Thus, the above-floodwater volume of these hummocks, which could store freshwater, may hypothetically provide a freshwater refuge to salinity-intolerant shrubs that enables of separation of roots from the surrounding mesohaline floodwaters. The measured hummock elevations (**Supplementary Table 1**) were similar in magnitude to the

rooting depths of wax myrtle and other coastal shrubs reported elsewhere (Young et al., 1994). Others have used stable-isotope tracing to demonstrate that coastal vegetation can use hummock and shallow-soil water to avoid using saline floodwaters or groundwater (Sternberg et al., 1991; Hsueh et al., 2016). Given the limited heights and spatial extents of hummocks, and thus their limited potential volume of freshwater storage, we hypothesize that canopy-interception-induced precipitation augmentation to hummocks could be a mechanism by which plant-water status and site favorability is improved.

Potential ecohydrological implications of stemflow routing have been discussed and demonstrated elsewhere. The routing of stemflow has been shown to augment moisture locally around stems (Návar and Bryan, 1990; Liang et al., 2009), notably in water-limited shrublands (Martinez-Meza and Whitford, 1996). Researchers have described a "double funneling" effect where not only does stemflow funnel from a broad canopy funnel to a stem, it also preferentially infiltrates around the stem as a high-flux-density input (Martinez-Meza and Whitford, 1996; Levia et al., 2011; Spencer and Van Meerveld, 2016). There is a paucity of evidence showing how stemflow infiltrates or influences plant-water relations (see discussions in Allen et al., 2020; Carlyle-Moses et al., 2020; Van Stan and Allen, 2020); however, the potential physiological benefits of augmented net precipitation to hummocks with limited water storage capacities seem likely, given that precipitation is the freshwater source to the shrubs located in the mesohaline zone. Otherwise, unfortunately, our study was not designed to directly measure the roles of stemflow in hummock water balances, the pore-water salinities in hummocks, or wax-myrtle water uptake sources; perhaps a manipulative experiment in which stemflow is diverted from shrubs and hummocks in a subset of stems could elucidate the ecophysiological importance of stemflow to wax myrtle on hummocks.

Ultimately, this first study showing the potential magnitude of net precipitation to hummocks prompts new questions about the importance of this phenomenon. For example, given that dormant season events (i.e., when less overstory canopy is intercepting precipitation) showed much higher wax-myrtle funneling ratios, we wonder whether progressive mortality of overstory trees will increase shrub funneling ratios (year-round) and thereby further increase hummock net precipitation. For another example, these findings prompt us to ask how much water can be stored above floodwaters in these hummock soils, and how much of the net precipitation inputs are retained and held against gravity. More mechanistic research is warranted to understand the importance of hummock water balances in maintaining this precipitation-controlled and potentially water-limited ecotone.

CONCLUSION

Canopy interception losses were 9% of gross precipitation in a disturbed forested wetland in coastal South Carolina, measured across 69 storm events over a 15-months period. Despite these losses, net precipitation to hummocks equaled or exceeded gross precipitation (by an additional 0–35% of gross precipitation). These augmentations were a result of high stemflow rates in the shrub layer, which is assumed to have infiltrated into the hummocks on which the shrubs were rooted. Given that these shrubs are generally stressed by salinity, we present a novel hypothesis that the additional freshwater inputs provided by this localized net precipitation augmentation can facilitate the shrubs' avoidance of using the mesohaline waters that surrounded the hummocks.

DATA AVAILABILITY STATEMENT

The raw data supporting the conclusion of this article will be made available by the authors, without undue reservation.

AUTHOR CONTRIBUTIONS

SA conceived and established the study, conducted the analysis, and wrote this manuscript. WC developed the study site and facilitated on-site activities, led the field sampling, and contributed to the editing of the manuscript. All authors contributed to the article and approved the submitted version.

FUNDING

Funding was provided by the Wetland Foundation Research Travel Grant, the CUAHSI Pathfinder Fellowship, and by the National Institute of Food and Agriculture, United States Department of Agriculture, under award number SCZ-1700590. Technical Contribution No. 6967 of the Clemson University Experiment Station.

ACKNOWLEDGMENTS

Special thanks to the Baruch Foundation for use of their land during the study. We thank and remember Stephen "Hutch" Hutchinson for his assistance. Ryan Marsh and other Clemson University staff members also provided assistance. We also thank reviewers for their thoughtful comments and suggestions, which improved the manuscript.

SUPPLEMENTARY MATERIAL

The Supplementary Material for this article can be found online at: https://www.frontiersin.org/articles/10.3389/ffgc.2021.691321/full#supplementary-material

REFERENCES

Allen, S. T., Aubrey, D. P., Bader, M. Y., Coenders-Gerrits, M., Friesen, J., Gutmann, E. D., et al. (2020). "Key questions on the evaporation and transport of intercepted precipitation," in *Precipitation Partitioning by Vegetation: A Global Synthesis*, eds I. Van Stan, T. John, E. Gutmann, and J. Friesen (New York, NY: Springer International Publishing), 269–280. doi: 10.1007/978-3-030-29702-2_16

Allen, S. T., Keim, R. F., and Dean, T. J. (2019). Contrasting effects of flooding on tree growth and stand density determine aboveground production, in baldcypress forests. *For. Ecol. Manage.* 432, 345–355. doi: 10.1016/j.foreco.2018.09.041

Allen, S. T., Whitsell, M. L., and Keim, R. F. (2015). Leaf area allometrics and morphometrics in baldcypress. *Can. J. For. Res.* 45, 963–969. doi: 10.1139/cjfr-2015-0039

Andrus, R. E., Wagner, D. J., and Titus, J. E. (1983). Vertical zonation of Sphagnum mosses along hummock-hollow gradients. *Can. J. Bot.* 61, 3128–3139. doi: 10.1139/b83-352

Carlyle-Moses, D. E., and Gash, J. H. (2011). *Rainfall interception loss by forest canopies, in: Forest Hydrology and Biogeochemistry*. Netherlands: Springer, 407–423.

Carlyle-Moses, D. E., Iida, S., Germer, S., Llorens, P., Michalzik, B., Nanko, K., et al. (2020). Commentary: What we know about stemflow's infiltration area. *Front. For. Glob. Change* 3:577247. doi: 10.3389/ffgc.2020.577247

Conner, W. H., Toliver, J. R., and Sklar, F. H. (1986). Natural regeneration of baldcypress (Taxodium distichum (L.) Rich.) in a Louisiana swamp. *For. Ecol. Manage* 14, 305–317. doi: 10.1016/0378-1127(86)90176-3

Cutini, A., Matteucci, G., and Mugnozza, G. S. (1998). Estimation of leaf area index with the Li-Cor LAI 2000 in deciduous forests. *For. Ecol. Manage* 105, 55–65. doi: 10.1016/S0378-1127(97)00269-7

Duberstein, J. A., and Conner, W. H. (2009). Use of hummocks and hollows by trees in tidal freshwater forested wetlands along the Savannah River. *For. Ecol. Manage* 258, 1613–1618. doi: 10.1016/j.foreco.2009.07.018

Duberstein, J. A., Krauss, K. W., Allen, S. T., and Baldwin, M. J. (2018). *Sap flow data from a long-hydroperiod forested wetland undergoing salinity intrusion in South Carolina, USA*: U.S. Geological Survey data release. doi: 10.5066/P9IR2XUO

Duberstein, J. A., Krauss, K. W., Baldwin, M. J., Allen, S. T., Conner, W. H., Salter, J. S., et al. (2020). Small gradients in salinity have large effects on stand water use in freshwater wetland forests. *For. Ecol. Manage* 473:118308. doi: 10.1016/j.foreco.2020.118308

Holwerda, F., Scatena, F. N., and Bruijnzeel, L. A. (2006). Throughfall in a Puerto Rican lower montane rain forest: A comparison of sampling strategies. *J. Hydro.* 327, 592–602. doi: 10.1016/j.jhydrol.2005.12.014

Hsueh, Y.-H., Chambers, J. L., Krauss, K. W., Allen, S. T., and Keim, R. F. (2016). Hydrologic exchanges and baldcypress water use on deltaic hummocks, Louisiana, USA. *Ecohydrol* 2016:1738. doi: 10.1002/eco.1738

Huenneke, L. F., and Sharitz, R. R. (1986). Microsite abundance and distribution of woody seedlings in a South Carolina cypress-tupelo swamp. *Am. Midl. Nat.* 115, 328–335. doi: 10.2307/2425869

Ish-Shalom, N., Sternberg, L., da, S. L., Ross, M., O'Brien, J., and Flynn, L. (1992). Water utilization of tropical hardwood hammocks of the Lower Florida Keys. *Oecologia* 92, 108–112. doi: 10.1007/BF00317270

Jones, R. H., Lockaby, B. G., and Somers, G. L. (1996). Effects of Microtopography and Disturbance on Fine-Root Dynamics in Wetland Forests of Low-Order Stream Floodplains. *Am. Midl. Nat.* 136, 57–71. doi: 10.2307/2426631

Keim, R. F., Skaugset, A. E., and Weiler, M. (2005). Temporal persistence of spatial patterns in throughfall. *J. Hydrol.* 314, 263–274. doi: 10.1016/j.jhydrol.2005.03.021

Levia, D. F., and Germer, S. (2015). A review of stemflow generation dynamics and stemflow-environment interactions in forests and shrublands. *Rev. Geophys.* 53:2015RG000479. doi: 10.1002/2015RG000479

Levia, D. F., Keim, R. F., Carlyle-Moses, D. E., and Frost, E. E. (2011). "Throughfall and stemflow in wooded ecosystems," in *Forest Hydrology and Biogeochemistry, Ecological Studies*, eds D. F. Levia, D. Carlyle-Moses, and T. Tanaka (Netherlands: Springer), 425–443. doi: 10.1007/978-94-007-1363-5_21

Li, X.-Y., Yang, Z.-P., Li, Y.-T., and Lin, H. (2009). Connecting ecohydrology and hydropedology in desert shrubs: stemflow as a source of preferential flow in soils. *Hydrol. Earth Syst. Sci. Discuss.* 6, 1551–1580.

Liang, W.-L., Kosugi, K., and Mizuyama, T. (2009). A three-dimensional model of the effect of stemflow on soil water dynamics around a tree on a hillslope. *J. Hydrol.* 366, 62–75. doi: 10.1016/j.jhydrol.2008.12.009

Light, H. M., Darst, M. R., and Mattson, R. A. (2007). *Ecological characteristics of tidal freshwater forests along the lower Suwannee River, Florida, in: Ecology of Tidal Freshwater Forested Wetlands of the Southeastern United States*. Netherlands: Springer, 291–320. doi: 10.1007/978-1-4020-5095-4_11

Liu, X., Conner, W. H., Song, B., and Jayakaran, A. D. (2017). Forest composition and growth in a freshwater forested wetland community across a salinity gradient in South Carolina. USA. *For. Ecol. Manage.* 389, 211–219. doi: 10.1016/j.foreco.2016.12.022

Martinez-Meza, E., and Whitford, W. G. (1996). Stemflow, throughfall and channelization of stemflow by roots in three Chihuahuan desert shrubs. *J. Arid. Environ.* 32, 271–287. doi: 10.1006/jare.1996.0023

Miralles, D. G., Gash, J. H., Holmes, T. R. H., de Jeu, R. A. M., and Dolman, A. J. (2010). Global canopy interception from satellite observations. *J. Geophys. Res.* 115:D16122. doi: 10.1029/2009JD013530

Mużyło, A., Llorens, P., and Domingo, F. (2012). Rainfall partitioning in a deciduous forest plot in leafed and leafless periods. *Ecohydrology* 5, 759–767. doi: 10.1002/eco.266

Návar, J., and Bryan, R. (1990). Interception loss and rainfall redistribution by three semi-arid growing shrubs in northeastern Mexico. *J. Hydrol.* 115, 51–63. doi: 10.1016/0022-1694(90)90197-6

Rheinhardt, R. D., and Faser, K. (2001). Relationship between hydrology and zonation of freshwater swale wetlands on lower Hatteras Island, North Carolina, USA. *Wetlands* 21, 265–273. doi: 10.1672/0277-5212(2001)021[0265:rbhazo]2.0.co;2

Rothacher, J. (1963). Net precipitation under a Douglas-fir forest. *For. Sci.* 9, 423–429.

Safeeq, M., and Fares, A. (2014). Interception losses in three non-native Hawaiian forest stands. *Hydrol. Process.* 28, 237–254. doi: 10.1002/hyp.9557

Shimamura, T., and Momose, K. (2005). Organic matter dynamics control plant species coexistence in a tropical peat swamp forest. *Proc. R. Soc. Lon. B: Biol. Sci.* 272, 1503–1510. doi: 10.1098/rspb.2005.3095

Siegert, C. M., and Levia, D. F. (2014). Seasonal and meteorological effects on differential stemflow funneling ratios for two deciduous tree species. *J. Hydrol.* 519, 446–454. doi: 10.1016/j.jhydrol.2014.07.038

Souther, R. F., and Shaffer, G. P. (2000). The effects of submergence and light on two age classes of baldcypress (Taxodium distichum (L.) Richard) seedlings. *Wetlands* 20, 697–706. doi: 10.1672/0277-5212(2000)020[0697:teosal]2.0.co;2

Spencer, S. A., and Van Meerveld, H. J. (2016). Double funnelling in a mature coastal British Columbia forest: spatial patterns of stemflow after infiltration. *Hydrol. Process.* 30, 4185–4201. doi: 10.1002/hyp.10936

Sternberg, L., da, S. L., Ish-Shalom-Gordon, N., Ross, M., and O'Brien, J. (1991). Water relations of coastal plant communities near the ocean/freshwater boundary. *Oecologia* 88, 305–310. doi: 10.1007/bf00317571

Stine, M. B., Resler, L. M., and Campbell, J. B. (2011). Ecotone characteristics of a southern Appalachian Mountain wetland. *CATENA* 86, 57–65. doi: 10.1016/j.catena.2011.02.006

Tolliver, K. S., Martin, D. W., and Young, D. R. (1997). Freshwater and saltwater flooding response for woody species common to barrier island swales. *Wetlands* 17, 10–18. doi: 10.1007/BF03160714

Van Stan, J. T. I., and Allen, S. T. (2020). What We Know About Stemflow's Infiltration Area. *Front. For. Glob. Change* 3:61. doi: 10.3389/ffgc.2020.00061

Van Stan, J. T., and Gordon, D. A. (2018). Mini-Review: Stemflow as a resource limitation to near-stem soils. *Front. Plant Sci* 9:248. doi: 10.3389/fpls.2018.00248

Williams, B. J., Song, B., Williams, T. M., and Chow, A. (2014). "GIS analysis of impact of sea level change on a freshwater tidal forested wetland," in *Proceedings of the 9th Southern Forestry and Natural Resource Management GIS Conference. Presented at the Proceedings of the 9th Southern Forestry and Natural Resource Management GIS Conference*, eds K. Merry, P. Bettinger, T. Brown, C. Cieszewski, I.-K. Hung, and Q. Meng (Athens, GA).

Young, D. R., Erickson, D. L., and Semones, S. W. (1994). Salinity and the small-scale distribution of three barrier island shrubs. *Can. J. Bot.* 72, 1365–1372. doi: 10.1139/b94-167

Conflict of Interest: The authors declare that the research was conducted in the absence of any commercial or financial relationships that could be construed as a potential conflict of interest.

The handling editor declared a past co-authorship with one of the author SA.

frontiers in Forests and Global Change

ORIGINAL RESEARCH
published: 12 July 2021
doi: 10.3389/ffgc.2021.704190

Stand-Level Variation Drives Canopy Water Storage by Non-vascular Epiphytes Across a Temperate-Boreal Ecotone

*Kate Hembre[1], Abigail Meyer[1], Tana Route[1], Abby Glauser[1,2] and Daniel E. Stanton[1]**

[1] Department of Ecology, Evolution and Behavior, University of Minnesota, St. Paul, MN, United States, [2] College of Arts and Sciences, University of Colorado, Boulder, Boulder, CO, United States

Epiphytes, including bryophytes and lichens, can significantly change the water interception and storage capacities of forest canopies. However, despite some understanding of this role, empirical evaluations of canopy and bole community water storage capacity by epiphytes are still quite limited. Epiphyte communities are shaped by both microclimate and host plant identity, and so the canopy and bole community storage capacity might also be expected to vary across similar spatial scales. We estimated canopy and bole community cover and biomass of bryophytes and lichens from ground-based surveys across a temperate-boreal ecotone in continental North America (Minnesota). Multiple forest types were studied at each site, to separate stand level and latitudinal effects. Biomass was converted into potential canopy and bole community storage on the basis of water-holding capacity measurements of dominant taxa. Bole biomass and potential water storage was a much larger contributor than outer canopy. Biomass and water storage capacity varied greatly, ranging from 9 to >900kg ha^{-1} and 0.003 to 0.38 mm, respectively. These values are lower than most reported results for temperate forests, which have emphasized coastal and old-growth forests. Variation was greatest within sites and appeared to reflect the strong effects of host tree identity on epiphyte communities, with conifer-dominated plots hosting more lichen-dominated epiphyte communities with lower potential water storage capacity. These results point to the challenges of estimating and incorporating epiphyte contributions to canopy hydrology from stand metrics. Further work is also needed to improve estimates of canopy epiphytes, including crustose lichens.

Keywords: interception, stemflow, water-holding capacity (WHC), bryophytes, lichen, canopy hydrology

OPEN ACCESS

Edited by:
Anna Klamerus-Iwan, University of Agriculture in Krakow, Poland

Reviewed by:
Paolo Giordani, University of Genoa, Italy
John T. Van Stan, Georgia Southern University, United States

****Correspondence:***
Daniel E. Stanton
stan@umn.edu;
stan0477@umn.edu

Specialty section:
This article was submitted to Forest Hydrology, a section of the journal Frontiers in Forests and Global Change

Received: *01 May 2021*
Accepted: *11 June 2021*
Published: *12 July 2021*

Citation:
Hembre K, Meyer A, Route T, Glauser A and Stanton DE (2021) Stand-Level Variation Drives Canopy Water Storage by Non-vascular Epiphytes Across a Temperate-Boreal Ecotone. Front. For. Glob. Change 4:704190. doi: 10.3389/ffgc.2021.704190

INTRODUCTION

The storage and evaporation of atmospheric waters by forest canopies cannot only directly impact precipitation inputs to the surface but also indirectly influence transpiration by lowering canopy VPD (Van Stan et al., 2020). Forest canopies are extensive and structurally complex spaces, made up not only of the surfaces of the tree itself (branches and leaves), but also sometimes highly diverse epiphytic communities (Zotz, 2016). Epiphytes have been found to significantly increase canopy water storage in a range of ecosystems (Van Stan and Pypker, 2015; Porada et al., 2018; Mendieta-Leiva et al., 2020).

However, despite their potential importance, studies of the hydrological role of epiphytes have been geographically patchy, focusing on ecosystems with very large amounts of vascular or non-vascular epiphytes such as old growth wet temperate (Pypker et al., 2006, 2017), tropical montane forests (Chang et al., 2002; Villegas et al., 2008; Ah-Peng et al., 2017) or other exceptionally epiphyte-rich ecosystems (Stanton et al., 2014). For example, while Porada et al. (2018) cite a number of studies of epiphyte biomass and water storage from boreal and temperate ecosystems, the majority of these were conducted in old-growth forests in humid coastal or mountainous areas: ideal conditions for the development of dense non-vascular epiphyte cover (Gehrig-Downie et al., 2011). While valuable for asserting the importance of non-vascular epiphytes, such studies may be difficult to extend to drier or younger forests at the same latitudes, on which the epiphyte communities are notably less developed. In such ecosystems, the dominant epiphytes may be small bryophytes (e.g., *Frullania*, *Orthotrichum*, and *Pylaisia*), microfoliose lichens (e.g., *Physcia, Physconia,* and associated genera), and crustose lichens. These taxa have drawn less attention from hydrologists due to their small size and therefore individually limited water-holding capacity, such that their impact is poorly quantified but a recent study of crustose lichens in dry forests found comparable biomasses to larger-bodied lichens (Miranda-González and McCune, 2020).

Here we focus on the potential water storage of non-vascular epiphytes across a range of continental temperate to boreal forests in central North America. Vascular epiphytes are essentially absent from such forests, and epiphyte communities are dominated by non-vascular epiphytes: lichens, mosses, and liverworts. Non-vascular epiphytes are notable for their dynamic water content (poikilohydry), which is often associated with considerable water storage capacity. The water-holding capacity of lichens and bryophytes can be quite substantial given their relatively small mass and/or size. For example, lichens can store up to 3,360% of their dry weight in water and some bryophytes even more (Cornelissen et al., 2007; Elumeeva et al., 2011; Gauslaa and Coxson, 2011; Klamerus-Iwan et al., 2020).

In evaluating the epiphyte communities and their potential hydrologic effects we consider several scales of organization. Firstly, location within canopy: the communities on the bole and bases of large branches are often quite different from those in the upper and outer regions of the canopy (Zotz, 2016). In continental temperate forests the former are more often dominated by bryophytes, crustose and foliose lichens while the latter can harbor more fruticose lichens. The likely hydrologic impacts also differ: while both may influence canopy interception and storage, bole epiphyte communities primarily intercept stemflow whereas the outer canopy community may have more impact on through-fall (Mendieta-Leiva et al., 2020). Furthermore, north- and south-facing sides of the bole differ in their microclimate and sometimes epiphyte communities (Ellis, 2012). These are important hydrological and ecological factors to consider as canopy interception remains largely under-studied (Van Stan et al., 2020; Zheng and Jia, 2020; Linhoss and Siegert, 2020).

Secondly, epiphyte communities can vary with host tree due to light-penetration, crown architecture, and bark texture and chemistry (Smith, 1982; Ellis, 2012; Zotz, 2016). Tree species may also shape stand-level microclimate, which can vary greatly between forest types. Lastly, macroclimate can also greatly shape epiphyte communities following changing temperature and precipitation across latitudinal and longitudinal (Smith et al., 2020) or altitudinal scales (Rodriguez-Quiel et al., 2019).

To systematically evaluate the potential hydrologic impacts of epiphytes in northern temperate forests we evaluated epiphytic communities of dominant forest types across a latitudinal gradient marking the transition from savanna and temperate forest to boreal forest in Minnesota, United States. The sites span the ecotone of three of the major biomes of continental North America (Prairie, Eastern temperate deciduous forest, Laurentian boreal forest) and each include a mosaic of upland and lowland forests with differing dominant trees. Because this range abuts the edge of extensive forests (forest-prairie ecotone), it covers an ecologically important if climatically narrow range of temperature and precipitation. We hypothesized that epiphyte biomass and water storage potential would increase with latitude, reflecting decreasing evaporative stresses that might favor the development of epiphyte communities.

MATERIALS AND METHODS

Sites

Epiphyte communities were sampled on or near University of Minnesota field stations (**Figure 1A**), namely Cedar Creek Ecosystem Science Reserve (East Bethel, MN, United States), Cloquet Forestry Center (Cloquet, MN, United States), Itasca State Park (Park Rapids, MN, United States), and Hubachek Wilderness Research Center (Ely, MN, United States). Dominant forest communities as described by the Minnesota Department of Natural Resources (MDNR)'s Native Plant Community classification (Aaseng et al., 2011) were sampled at each site (**Figure 1B**), and site specific data are presented in **Table 1**. These 4 sites were chosen because they span the western limit of the Eastern Deciduous Forest biome and the ecotones with Laurentian Shield Boreal and Prairie biomes in North America, encompassing some of the largest North-American biomes in a small geographic space.

Plots were chosen by overlaying MDNR GIS maps[1] of the selected dominant forest communities onto our sites, then marking a coordinate that was (a) well away from the community edges and (b) easily accessible to the field team. The field team then used the MDNR Native Plant Community classification system to confirm the forest community type upon arrival at the coordinate. If the forest community was correct and far enough away from community edges and disturbances, a plot was set up. If the coordinates were too close to an edge, not the best representation, or showed disturbance, the field team chose a

[1]MNDNR (Minnesota Department of Natural Resources) – Division of Ecological and Water Resources - Biological Survey. MDNR Native Plant Communities. Accessed May 2020. Retrieved from: https://gisdata.mn.gov/dataset/biota-dnr-native-plant-comm

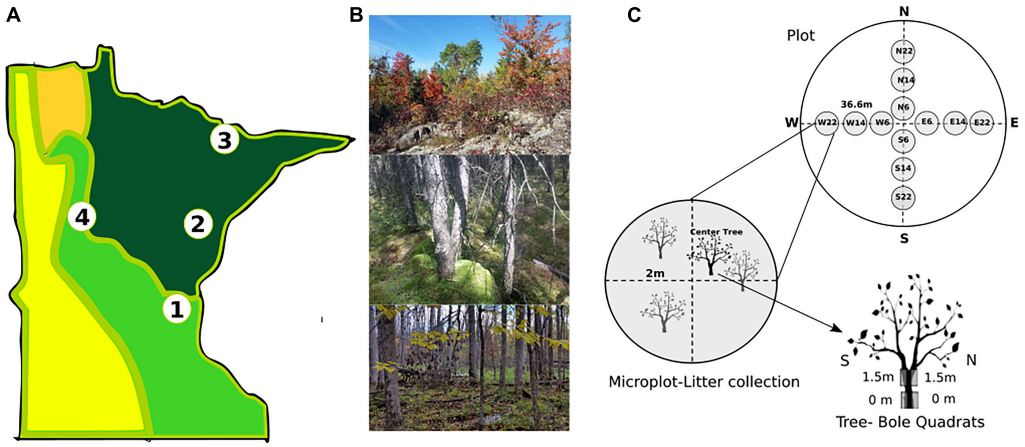

FIGURE 1 | Sampling design at state **(A)**, site **(B)**, and plot **(C)** scales. A-Sites (1-Cedar Creek Ecosystem Reserve, 2-Cloquet Forestry Center, 3-Hubachek Wilderness Research Center, and 4-Itasca State Park) are located across the eastern temperate (light green) to boreal (dark green) forest transition. **(B)** Within each site plots were selected to represent in forest types (top-Aspen-Birch, middle-Tamarack-Black Spruce bog, and bottom- Black Ash swamp). **(C)** Each plot includes 2 m-radius microplots for litter collection and 20 cm × 50 cm quadrats at 4 locations on 12 microplot center trees for bole epiphyte sampling. Photo credit: A. Glauser and D. Stanton.

different coordinate. Plot centers were in a few occasions moved 5–20 m to avoid edge effects or overlap with adjacent forest types.

Temperature and precipitation data for each site was obtained from the nearest weather station in the Climate Data Online repository[2] with a 10 years record of daily means (January 01, 2010–December 31, 2020): Cambridge MN (for Cedar Creek), Cloquet, Itasca University of Minnesota and Ely 25 E (for HWRC). From these we calculated the median rainfall event size for each site.

Biomass estimation: Plots were established as circular plots of 36.6 m (120 ft) radius with care to avoid patch edges. Forest type was assigned following the Minnesota Native Plant Community Classification (Aaseng et al., 2011) and basal area measured using a wedge prism (Jim-Gem Rectangular prism, Forestry Suppliers). Within each plot, transects were traced in the 4 cardinal directions, and microplots (2 m radius circles) established at 6, 14, and 22 m from plot center (**Figure 1C**). Upper canopy communities were estimated by harvesting all recently fallen litter (epiphytes or twigs/branches with epiphytes attached) as an indirect measure (modified from McCune, 1993). The living tree nearest to the microplot center was used for bole community surveys. Trees for bole community estimates (12/plot) were identified to species and diameter at breast height (DBH) recorded. Quadrats (20 cm × 50 cm) were affixed to the bole on the north and south sides of the trunk at ground level and 1.5 m height (4 total per tree). Within each quadrat the relative cover of each epiphyte functional group was recorded. Taxa were assigned to the following functional groups based on growth form: Crustose Lichen (e.g., *Lecanora*), Cyanolichen (e.g., *Peltigera*), Small Foliose Lichen (e.g., *Physcia* and *Physconia*), Large Foliose Lichen (e.g., *Parmelia* and *Platismatia*), Tufted Fruticose Lichen (e.g., *Ramalina* and *Usnea*), Pendulous Fruticose Lichen (e.g., *Bryoria*), Jelly Lichen (e.g., *Leptogium*), Small Prostrate Bryophyte (e.g., *Frullania*), Large Prostrate Bryophyte (e.g., *Anomodon*), Feathermoss Bryophyte (e.g., *Pleurozium*), Small Bryophyte Cushion (e.g., *Orthotrichum*), Large Bryophyte Cushion (e.g., *Dicranum*) and Pendent Bryophyte Mat (e.g., *Neckera* and *Porella*). Results of species surveys and ground sampling will be presented in a forthcoming publication (Route et al., in prep).

Water-Holding Capacity Measurements

Water-holding capacity (WHC) and Specific Mass (SM) were measured for representative lichen and bryophyte taxa following established methods (Esseen et al., 2017; Ure and Stanton, 2019). Briefly, individual lichen thalli and bryophyte clumps were detached from their substrate and cleaned of debris in the lab before hydration. To hydrate, samples were placed over mesh and sprayed three times with distilled water at 2 min intervals for at least 15 min (20 min for large samples), flipping the sample between sprays to ensure even hydration. Following hydration the lichen thalli were placed between two mesh pieces and gently shaken three times on each side. After which filter paper is used to absorb the external water still remaining, thus leaving the internal water. Between each of these processes the wet mass was recorded. Once fully hydrated wet mass was recorded with a Mettler BB2400 digital scale (Mettler Toledo, Columbus, OH, United States) following gentle blotting (internal WHC). After these measurements the thalli were placed between two glass plates and a ruler was added for scale. A photograph of the hydrated sample projected area was taken using a light-table (to emphasize contrast) and a vertically mounted Canon EOS 80D DSLR camera (Canon U.S.A., Inc., Melville, NY, United States). The areas were measured from photographs using ImageJ 2.0 (Rueden et al., 2017). Samples were air dried for at least 48 h to obtain a dry mass.

[2]Climate Data Online, National Centers for Environmental Information https://www.ncdc.noaa.gov/cdo-web/

TABLE 1 | Locations and characteristics of the plots included in the study.

Site	Plot number	Latitude	Longitude	Native plant community	Native plant community subtype	Physiography	Elevation (m)	Basal area (m2/hectare)	Percent conifer	Mean annual temperature C	Mean annual precipitation mm	Median 24 h precipitation mm
Cedar Creek Ecosystem Science Reserve	1	45.407943	−93.200673	Central dry-mesic oak-aspen forest	Red oak – sugar maple – basswood forest	Upland	281.00	48.68	0.00	6.30	743	6.3
	2	45.421263	−93.186181	Northern poor conifer swamp	Poor tamarack – black spruce swamp – tamarack subtype	Lowland	281.03	7.81	100.00	6.22	741	6.3
	3	45.422013	−93.193017	Northern poor conifer swamp	Poor Tamarack – black spruce swamp	Lowland	280.11	28.47	95.16	6.22	742	6.3
	4	45.407130	−93.199308	Northern wet cedar forest	Lowland white cedar forest	Lowland	277.06	45.46	87.90	6.27	744	6.3
	5	45.388098	−93.197993	Southern dry savanna	Dry barrens oak savanna – oak subtype	Upland	281.03	21.58	0.00	6.30	743	6.3
	6	45.386515	−93.194518	Southern dry savanna	Dry barrens oak savanna – oak subtype	Upland	282.85	30.31	0.00	6.30	743	6.3
	7	45.386010	−93.198141	Southern dry savanna	Dry barrens oak savanna – oak subtype	Upland	280.11	29.85	0.00	6.30	743	6.3
	8	45.387208	−93.193052	Southern dry savanna	Dry barrens oak savanna – oak subtype	Upland	281.94	20.20	0.00	6.30	743	6.3
	9	45.395476	−93.181468	Southern dry savanna	Dry barrens oak savanna – oak subtype	Upland	282.85	33.06	0.00	6.28	744	6.3
Cloquet Forestry Center	1	46.692676	−92.533366	Aspen plantation	Aspen plantation	Upland	388.00	30.31	0.06	3.94	790	2.5
	2	46.696150	−92.515188	Aspen plantation	Aspen plantation	Upland	385.00	41.33	0.02	3.97	792	2.5
	3	46.694825	−92.533031	Northern dry-mesic mixed woodland	Red pine – white pine woodland	Upland	391.97	40.87	96.63	3.95	788	2.5
	4	46.696630	−92.526570	Northern dry-mesic mixed woodland	Red pine – white pine woodland	Upland	390.00	45.92	80.00	3.95	788	2.5
	5	46.694495	−92.528925	Northern dry-mesic mixed woodland	Red pine – white pine woodland	Upland	391.06	59.70	100.00	3.95	788	2.5
	6	46.679040	−92.522600	Northern poor conifer swamp	Poor black spruce swamp	Lowland	373.99	40.87	100.00	4.03	789	2.5
Itasca State Park	1	47.185760	−95.173620	Central dry-mesic oak-aspen forest	Red oak – sugar maple – basswood forest	Upland	500.00	45.00	0.00	3.65	670	1.8
	2	47.209343	−95.171426	Central dry-mesic oak-aspen forest	Red oak – sugar maple – basswood forest	Upland	483.00	32.14	0.00	3.56	673	1.8
	3	47.202830	−95.163410	Central dry-mesic pine-hardwood forest	Red pine – white pine forest	Upland	466.00	33.98	38.00	3.59	671	1.8
	4	47.195249	−95.214209	Northern mesic hardwood forest	Aspen – birch – basswood forest	Upland	465.00	44.08	0.00	3.67	669	1.8
	5	47.199527	−95.218984	Northern rich tamarack swamp	Extremely rich tamarack swamp	Lowland	447.00	15.61	100.00	3.71	668	1.8

(Continued)

TABLE 1 | Continued

Site	Plot number	Latitude	Longitude	Native plant community	Native plant community subtype	Physiography	Elevation (m)	Basal area (m2/hectare)	Percent conifer	Mean annual temperature C	Mean annual precipitation mm	Median 24 h precipitation mm
Hubachek Wilderness Research Center	1	47.954007	−91.754419	Northern mesic mixed forest	Aspen-birch forest – balsam fir subtype	Upland	427.94	35.80	41.00	2.77	711	2.8
	2	47.958538	−91.754682	Northern mesic mixed forest	Aspen-birch forest	Upland	428.85	14.20	22.58	2.79	713	2.8
	3	47.954682	−91.746495	Northern very wet ash swamp	Black ash – yellow birch – red maple – alder swamp	Lowland	403.86	27.09	10.17	2.82	707	2.8

Native plant community classification is based on Aaseng et al., 2011. Sites are listed from South to North.

Calculations and Analyses

All calculations and analyses were carried out R 4.0.5 (R Core Team, 2021). Specific Mass was calculated as: SM = oven dry mass (DM)/blotted wet area (Awet). Water-holding capacity as calculated as (WHC) = (wet mass (WM) − DM)/Awet.

Data from multiple species was used to calculate a mean SM and WHC for each functional group, which are presented in **Table 2**. Although these properties may also vary within a functional group depending on site and species characteristics, this will be explored in a forthcoming study.

The functional group mean values of Specific Mass and WHC were then multiplied by cover to calculate the quadrat-scale SM and WHC attributable to each functional group:

$$Mass_{quadrat} = \sum SM_{Funct.Group} \times Cover_{Funct.Group}$$

These were then summed to calculate four quadrat-level Biomass and WHC values for each bole (North and South aspects at 0 and 1.5 m, respectively).

To convert quadrat-level values to tree-level we approximated each tree bole as a 10 m cylinder of constant diameter. Mean Biomass and WHC from the North and South ground level quadrats was used to calculate Biomass and WHC of the base of the tree 0–0.5 m; mean SM and WHC from the North and South 1.5 m quadrats was used to calculate Biomass and WHC of the rest (0.5–10 m):

$$Mass_{Bole} = \frac{Mass_{0,N} + Mass_{0,S}}{2} \times 0.5 \times 2\pi r + \frac{Mass_{1.5,N} + Mass_{1.5,S}}{2} \times 9.5 \times 2\pi r$$

Stand-scale estimates were made by dividing the total basal area of trees by the mean bole cross-sectional area to approximate the number of trees:

$$Biomass_{ha} = \overline{Mass_{Bole}} \times N_{trees/ha}$$

TABLE 2 | Mean attributes of each non-vascular epiphyte functional group.

Organism	Functional group	Number of replicates	Specific mass (SM) g cm^{-2}	Internal water holding capacity (WHCblot) g H_2O cm^{-2}
Lichen	Crustose	8	0.0551	0.0447
	Cyanolichen	10	0.0202	0.0475
	Jelly lichen	1	0.0111	0.0299
	Large foliose	45	0.0240	0.0501
	Pendulous fruticose	4	0.0093	0.0093
	Small foliose	13	0.0215	0.0432
	Tufted fruticose	28	0.0172	0.0300
Bryophyte	Feathermoss	15	0.0992	0.7670
	Large cushion	3	0.0400	0.2662
	Large prostrate	10	0.0447	0.3987
	Pendent mat	16	0.0278	0.1445
	Small cushion	3	0.0400	0.2662
	Small prostrate	3	0.0362	0.3681

All data analysis was conducted in R 4.0.5 (R Core Team, 2021). Linear regressions were used to evaluate the relationships between epiphyte community properties (biomass and potential water storage capacity) and broad geographic (Latitude), macroclimatic (Mean Annual Precipitation) and forest structure (% conifers, physiographic position).

RESULTS

A total of 23 plots were studied across 4 sites, encompassing 7 major forest types and 11 different native plant communities according to the MN DNR Classification. Biomass and potential water storage capacity varied across 2 orders of magnitude, ranging from ∼9 to >900 kg ha^{-1} and 0.003–0.38 mm, respectively (**Table 3**). The nearly full spectrum of variation was present within sites and even sometimes within native plant communities, indicating stand-level variation in epiphyte biomass and potential water storage. Nearly all of the estimated biomass was due to bole epiphytes, with canopy epiphyte biomass 100–300 times smaller.

Bole biomass showed no significant change with latitude (t = 1.934, $F_{1,21}$ = 3.739, p = 0.0668, adj-R^2 = 0.11, **Figure 2A**) or precipitation (t = −0.497, $F_{1,21}$ = 0.2472, p = 0.624, adj-R^2 = −0.035, **Figure 2B**). There was no correlation between bole and canopy biomass (t = 0.878, $F_{1,21}$ = 0.7713, p = 0.0.39, adj-R^2 = −0.01, **Figure 2C**) or water storage capacity. Canopy biomass and thus water holding capacity was much lower than on the boles, but showed stronger responses to latitude and climate. Canopy biomass increased with latitude (t = 2.303, $F_{1,21}$ = 5.305, p = 0.0319, adj-R^2 = 0.16), and a slight but significant decrease with precipitation (t = −2.152, $F_{1,21}$ = 4.631, p = 0.0432, adj-R^2 = 0.14).

These translate into equivalent patterns with bole community water storage capacity: no change with latitude (t = 0.046, $F_{1,21}$ = 0.002, p = 0.9637, adj-R^2 = −0.05, **Figure 2D**) or precipitation (t = −1.910, $F_{1,21}$ = 3.648, p = 0.0699, adj-R^2 = 0.11, **Figure 2E**). Water storage capacity on the bole community was significantly related to forest composition, with lower capacity in conifer-dominated forests (t = −2.814, $F_{1,21}$ = 7.92, p = 0.0104, adj-R^2 = 0.24, **Figure 2F**). As with biomass, patterns were more marked in canopy water storage capacity: increase with latitude (t = 2.208, $F_{1,2}1$ = 4.855, p = 0.0388, adj-R^2 = 0.15) and decrease with precipitation (t = 2.131, $F_{1,21}$ = 4.539, p = 0.0451, adj-R^2 = 0.14).

Water-holding capacity was much greater in the bryophytes than the lichens (**Figure 3A**). As a result, total water storage was strongly inversely correlated with the proportion of lichens in the epiphyte community (t = −3.787, $F_{1,21}$ = 14.34, p = 0.001, adj-R^2 = 0.38, **Figure 3B**). The proportion of lichens varied considerably within sites, ranging from 10 to >95%, but with no significant relationship with latitude. Due to the greater water capacity of bryophytes in our study sites, this translated into a usually <50% contribution of lichens to bole community water capacity but no significant latitudinal pattern (t = 0.949, $F_{1,21}$ = 0.9004, p = 0.3535, adj-R^2 = −0.004,

TABLE 3 | Biomass and potential water-holding capacity (as both L/ha and mm depth equivalent) of bole, canopy and total epiphyte communities at each study site.

Site	Plot number	Native plant community (Abbr.)	Bole biomass kg/ha	Bole H2O L/ha	Bole WHC mm	Canopy biomass kg/ha	Canopy H2O L/ha	Total biomass g	Total WHC mm
Cedar Creek Ecosystem Science Reserve	1	Dry-Mesic Oak-Aspen Forest	339.01	1341.91	0.13	0.84	2.95	339.85	0.13
	2	Conifer swamp	9.31	34.51	0.00	0.39	1.34	9.70	0.00
	3	Conifer swamp	84.97	175.00	0.02	0.36	1.26	85.33	0.02
	4	Wet cedar forest	247.60	1948.34	0.19	0.08	0.28	247.68	0.19
	5	Dry savanna	123.40	959.64	0.10	1.18	4.13	124.58	0.10
	6	Dry savanna	378.82	3524.88	0.35	1.26	4.47	380.09	0.35
	7	Dry savanna	159.23	1051.58	0.11	0.29	1.03	159.53	0.11
	8	Dry savanna	362.47	2776.80	0.28	0.76	2.64	363.22	0.28
	9	Dry savanna	491.44	3768.65	0.38	0.37	1.28	491.80	0.38
Cloquet Forestry Center	1	Aspen plantation	112.02	422.00	0.04	0.00	0.00	112.02	0.04
	2	Aspen plantation	473.53	888.52	0.09	0.00	0.00	473.53	0.09
	3	Dry-mesic mixed woodland	253.72	359.59	0.04	1.98	6.32	255.70	0.04
	4	Dry-mesic mixed woodland	241.47	323.07	0.03	3.13	10.22	244.60	0.03
	5	Dry-mesic mixed woodland	928.46	1120.92	0.11	3.88	13.73	932.34	0.11
	6	Conifer swamp	660.21	906.90	0.09	1.96	6.11	662.17	0.09
Itasca State Park	1	Dry-mesic oak-aspen forest	534.49	2020.07	0.20	3.34	11.53	537.83	0.20
	2	Dry-mesic oak-aspen forest	456.42	1485.80	0.15	1.10	2.77	457.52	0.15
	3	Dry-mesic pine-hardwood forest	413.29	2787.46	0.28	4.49	15.45	417.77	0.28
	4	Mesic hardwood forest	795.78	2496.04	0.25	1.96	6.69	797.74	0.25
	5	Tamarack swamp	227.12	524.18	0.05	9.64	32.52	236.77	0.06
Hubachek Wilderness Research Center	1	Mesic mixed forest	482.71	2406.40	0.24	1.58	5.15	484.30	0.24
	2	Mesic mixed forest	361.28	843.47	0.08	1.36	4.69	362.64	0.08
	3	Very wet ash swamp	335.04	2835.47	0.28	2.52	8.03	337.56	0.28

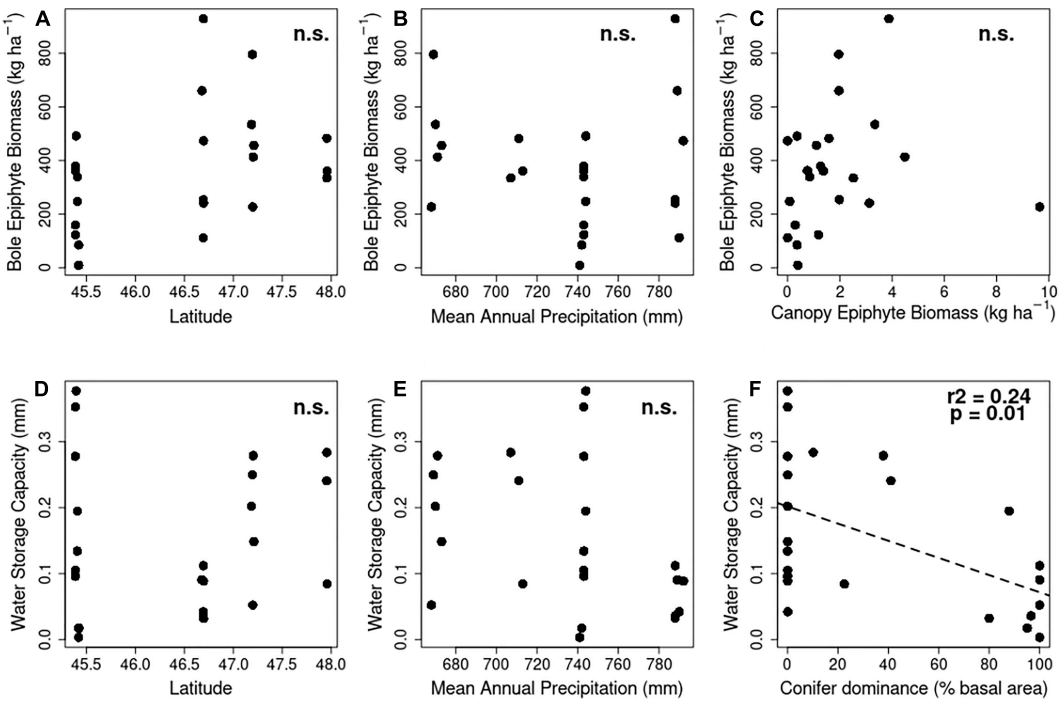

FIGURE 2 | Relationships of bole epiphyte community biomass **(A–C)** and potential water storage capacity **(D–F)** to plot and site characteristics, including site latitude **(A,C)**, mean annual precipitation **(B,E)** and stand composition **(F)**. Results of linear regressions are reported in each sub-panel. n.s., not significant at $p < 0.05$.

Figure 3C). Proportion of lichens was significantly greater in conifer-dominated stands ($t = 4.557$, $F_{1,21} = 20.76$, $p = 0.0002$, adj-$R^2 = 0.47$, **Figure 3D**).

Potential water storage by bole and canopy epiphytes amounted to 5–15% of the median 24 h rainfall at the study sites (**Figure 4**), with a significantly greater potential impact at the driest site (Itasca State Park; $F_3 = 8.568$, $p < 0.0008$). This pattern was driven more by differences in rain event size (**Table 3**) than epiphyte biomass.

DISCUSSION

Estimated biomass and water storage potential of epiphytes on boles was significant, but varied greatly between and even within forest types. Contrary to expectation, bole biomass did not show a clear latitudinal or climatic pattern across the ranges considered, which cover the transition between continental temperate and boreal forests in North America. Although estimated potential water storage by epiphytes was lower than reported for more epiphyte rich coastal and montane temperate environments, it reached hydrologically important levels in some stands.

We hypothesized a latitudinal increase in epiphyte biomass and storage capacity, based on decreasing potential evapotranspiration typically favoring greater epiphyte cover. Contrary to expectations, bole epiphyte biomass showed no response to latitude, and a negative correlation with annual precipitation. In contrast, canopy biomass, which represented only a minor fraction of the estimated biomass, increased with latitude and decreased with precipitation. A likely explanation for this result is the extensive cover of crustose lichens and small bryophytes at our lower latitude sites. These groups are less showy than the larger bodied macrolichens, and have often been overlooked in studies of ecosystem roles of epiphytes due to their small size. However, some studies of crustose lichen communities have found that they can represent comparable biomass to macrolichens (Miranda-González and McCune, 2020). Although the total estimated biomass of crustose lichens at our sites was far less than reported for tropical dry forests by Miranda-González and McCune (2020), it is nonetheless indicative of an under-valued component of canopy communities.

In the absence of macroclimatic predictors of epiphyte biomass and potential water storage, forest type appeared to be a strong driver of epiphyte community properties. Non-vascular epiphytes communities are known to be strongly influenced by host tree species, reflecting effects of bark texture, chemistry, and light availability (Ellis, 2012; Mitchell et al., 2021). Canopy structure also influences the partitioning of rainfall between throughfall and stemflow (Levia and Frost, 2003; Levia et al., 2019; Van Stan et al., 2020), which can further influence bole epiphyte communities. This effect of tree species can be seen in the strong correlations between potential water storage capacity and hardwood dominance: conifer-dominated plots had more lichen-dominated epiphyte communities and lower potential water storage. However, this broad pattern is insufficient to

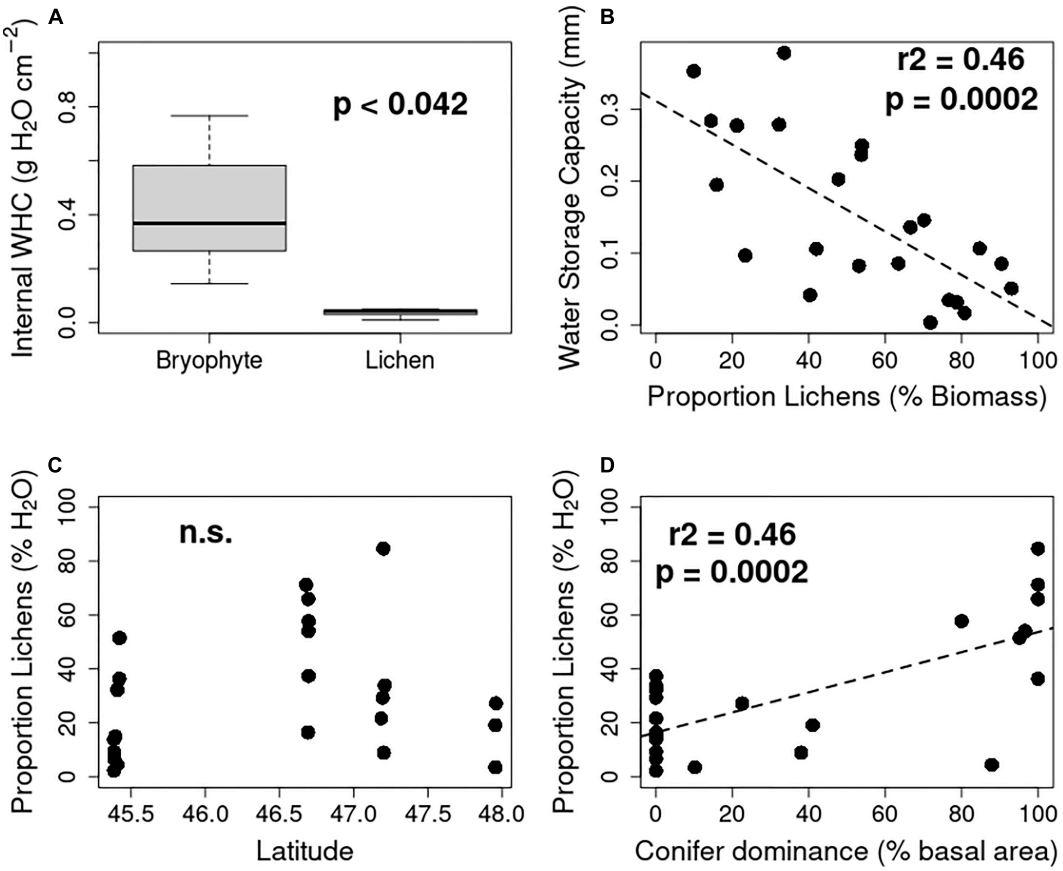

FIGURE 3 | Contrasting impacts of bryophytes and lichens on potential canopy water storage. Bryophytes tended to have greater internal water holding capacity across all functional groups **(A)**, leading to a negative relationship between lichen dominance and potential water storage **(B)**. Lichen dominance of epiphyte communities was not explained by latitude **(C)** but increased significantly in conifer dominated stands **(D)**. n.s., not significant at $p < 0.05$.

account for the full variation in potential water storage, especially in hardwood-dominated plots, which may be attributable in part to variation in specific host tree species. This impact of host tree identity suggests that future attempts to incorporate epiphytes into temperate-boreal ecohydrology need to account for the interactions between epiphytes, trees and climate. Preferably, species-specific allometries of canopy structure might also be applied to obtain more precise estimates of epiphyte biomass than the coarse and conservative scaling estimates presented here.

Potential storage capacity is not necessarily the same as realized capacity in natural rain events. Because of the focus on the bole, the epiphyte communities documented here primarily influence stemflow, and may have limited impacts on throughfall. Some additional factors also influence the realized storage capacity. Water storage in many bryophytes and lichens can be external as well as internal, with external water holding capacity sometimes equally or exceeding internal (e.g., Elumeeva et al., 2011; Esseen et al., 2017). Because external water-holding capacity estimates were not available for all functional groups, and external water-holding capacity is less closely correlated to mass and area (Eriksson et al., 2018), we chose to only focus on internal water storage. This likely under-estimated potential water storage capacity.

Other factors may decrease realized storage capacity when compared to estimated potential. As with leaves and bark (Eller et al., 2013; Holder, 2013; Klamerus-Iwan and Błońska, 2018), the surface hydrophobicity of lichens and bryophytes can vary not just across species, but also with hydration status, with dry thalli often more hydrophobic than those "primed" by high humidity or wetting (Lakatos et al., 2006). Epiphytes may also still be retaining water from previous precipitation or fog (Hargis et al., 2019). As such, the humidity conditions preceding a rain event may impact the amount of water retained by epiphytes. Secondly, stemflow does not proceed equally down the bole, and so some regions of the bole may contribute more than others to canopy interception. Experimental validation of epiphyte interception is needed for future work. Experimental measurements of epiphyte impacts on stem flow have been conducted in other forests (Van Stan and Pypker, 2015; Chen et al., 2019; Van Stan et al., 2020), and these methods might be adapted to temperate non-vascular epiphytes.

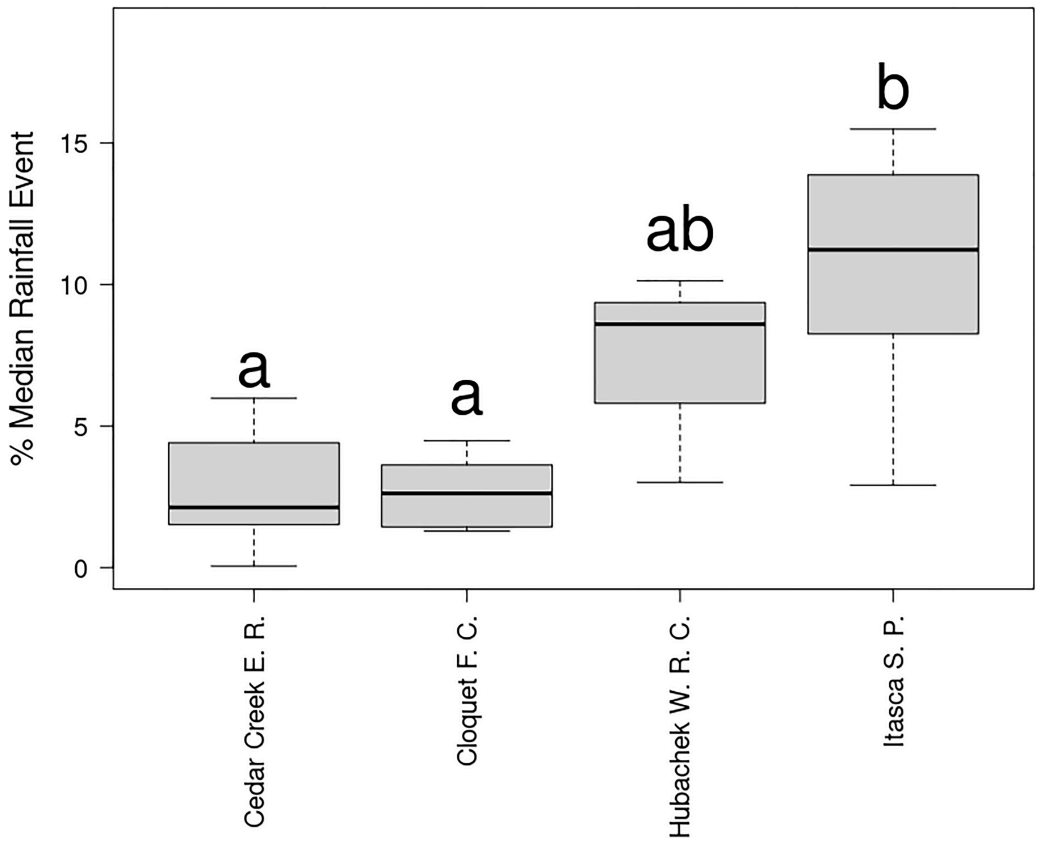

FIGURE 4 | Potential canopy water storage by epiphytes as a proportion of median rainfall event size (median 24 h precipitation 2010–2020) at study sites. Letters indicate significantly different groups ($p < 0.05$) according to Tukey HSD post-hoc tests.

The estimations of epiphyte biomass applied here were ground-based, which is far more efficient than climbing or crane-based approaches but rely on assumptions of relative vertical homogeneity of epiphyte properties. Epiphyte communities can vary with vertical position in the canopy (Ellis, 2012), such that ground-based observations only capture a portion of the cover and diversity. Many non-vascular epiphytes are slow-growing, and epiphytes communities vary with branch age as well as position (Woods, 2017).However, we sought to minimize these impacts through conservative estimates of bole surface area, ignoring large branches and any portions of the main stem >10 m. Our ground-based estimate of canopy epiphyte biomass is also intended to be a conservative estimate, emphasizing the larger-bodied epiphytes on terminal branches that are most likely to be collected in litter-fall (McCune, 1993; Dettki and Esseen, 2003).

Forest age is also likely to be an important factor. In contrast to many prior studies in older forests (e.g., Liu et al., 2000; Köhler et al., 2007; Pypker et al., 2017), only one site in the present study was >100 years (Cloquet Forestry Center *Pinus resinosa* forest). This age bias reflects both natural disturbance from fire and windthrow and a history of logging in Minnesota, such that few centennial stands of forest persist (Friedman and Reich, 2005; Vogeler et al., 2020). The potential hydrological importance of epiphytes and other components of old-growth forests is a strong argument for their conservation, but may not represent regional patterns in areas where forest cover is more dynamic, such as Eastern and Central North America. Our estimated potential water storage capacities lie toward the lower end of the range estimated by Porada et al. (2018) in their global model of canopy interception in temperate forests.

While the results reported here suggest greater microclimatic than macroclimatic effects on epiphyte water storage potential, extension to regional patterns is limited by the low number of sites and uneven replication of forest types. Macroclimate patterns in Minnesota reflect the intersection of a South to North decreasing gradient in temperature and a South-East to North-West gradient of decreasing precipitation. These combine to create a longitudinal gradient in Potential Evapotranspiration, with PET increasing from East to West. Although our selection of sites captured the latitudinal range in Temperature, all but one of the sites (Itasca State Park) were at the same longitude. Furthermore the clustering of plots within macrosites (due to logistical constraints of accessibility) limits the interpretation of macroclimate as a linear variable. Further studies are currently ongoing to broaden the geographic, macroclimatic and vegetational range of data.

CONCLUSION

Although easily overlooked, non-vascular epiphytes have the potential to impact forest hydrology even in continental environments where their apparent biomass can seem small. The potential impact on forest hydrology found in our sites across the temperate-boreal ecotone was lower than that reported in more humid, coastal temperate and sub-boreal forests where most prior studies have been conducted. This potential canopy storage by epiphytes was site and forest-type specific, with considerable variation even in nearly adjacent plots. While approximate, we hope that the relatively rapid and easy techniques presented here might serve a wider survey of the potential roles of epiphytes in forest hydrology, one that does not just consider the large-bodied non-vascular and vascular components, but also the small but extensive cover of small non-vascular epiphytes as well.

DATA AVAILABILITY STATEMENT

The original contributions presented in the study are included in the article/**Supplementary Material**, further inquiries can be directed to the corresponding author/s.

AUTHOR CONTRIBUTIONS

DS and AG designed the study. AG and TR oversaw site selection, sample collection, and processing. AG, TR, AM, and KH collected data and processed samples. KH and DS analyzed the data. KH, AM, and DS wrote the manuscript, with contributions from TR. All authors contributed to the article and approved the submitted version.

FUNDING

Funding for this project was provided by the Minnesota Environmental and Natural Resources Trust Fund Project M.L. 2018, Chp. 214, Art. 4, Sec. 02, Subd. 03e (Assessing Natural Resource Benefits Provided by Lichens and Mosses) awarded to DS.

ACKNOWLEDGMENTS

Work at each of the sites was made possible by the invaluable assistance of station staff, including K. Gill, B. Prange, S. Oberg, L. Domine, L. Knoll, M. Lauzon, T. Mielke, K. Worm, and others. Field and labwork collecting and processing samples for biomass estimation included the assistance of J. Ure, K. Stone, M. Valentin, D. Last, H. Bjorklund, L. Liulevicius, M. Syed, and S. Treuchel. O. Gockman, J. Thayer, T. McDonald, T. Clark, and members of the Stanton lab provided valuable feedback on project design and manuscript drafts.

SUPPLEMENTARY MATERIAL

The Supplementary Material for this article can be found online at: https://www.frontiersin.org/articles/10.3389/ffgc.2021.704190/full#supplementary-material

REFERENCES

Aaseng, N. E., Almendinger, J. C., Dana, R. P., Hanson, D. S., Lee, M. D., Rowe, E. R., et al. (2011). *Minnesota's Native Plant Community Classification: A Statewide Classification of Terrestrial and Wetland Vegetation Based on Numerical Analysis of Plot Data*. Biological Report No. 108. Minnesota County Biological Survey, Ecological Land Classification Program, and Natural Heritage and Nongame Research Program. St. Paul: Minnesota Department of Natural Resources.

Ah-Peng, C., Cardoso, A. W., Flores, O., West, A., Wilding, N., Strasberg, D., et al. (2017). The role of epiphytic bryophytes in interception, storage, and the regulated release of atmospheric moisture in a tropical montane cloud forest. *J. Hydrol.* 548, 665–673. doi: 10.1016/j.jhydrol.2017.03.043

Chang, S.-C., Lai, I.-L., and Wu, J.-T. (2002). Estimation of fog deposition on epiphytic bryophytes in a subtropical montane forest ecosystem in northeastern Taiwan. *Atmospheric Res.* 64, 159–167. doi: 10.1016/s0169-8095(02)00088-1

Chen, L.-C., Wang, L.-J., Martin, C. E., and Lin, T.-C. (2019). Mediation of stemflow water and nutrient availabilities by epiphytes growing above other epiphytes in a subtropical forest. *Ecohydrology* 12:e2140.

R Core Team (2021). *R: A Language and Environment for Statistical Computing*. Vienna: R Foundation for Statistical Computing.

Cornelissen, J. H. C., Lang, S. I., Soudzilovskaia, N. A., and During, H. J. (2007). Comparative cryptogam ecology: a review of bryophyte and lichen traits that drive biogeochemistry. *Ann. Bot.* 99, 987–1001. doi: 10.1093/aob/mcm030

Dettki, H., and Esseen, P.-A. (2003). Modelling long-term effects of forest management on epiphytic lichens in northern Sweden. *Forest Ecol. Manag.* 175, 223–238. doi: 10.1016/s0378-1127(02)00131-7

Eller, C. B., Lima, A. L., and Oliveira, R. S. (2013). Foliar uptake of fog water and transport belowground alleviates drought effects in the cloud forest tree species, Drimys brasiliensis (Winteraceae). *New Phytol.* 199, 151–162. doi: 10.1111/nph.12248

Ellis, C. J. (2012). Lichen epiphyte diversity: A species, community and trait-based review. *Perspect. Plant Ecol. Evol. Syst.* 14, 131–152. doi: 10.1016/j.ppees.2011.10.001

Elumeeva, T. G., Soudzilovskaia, N. A., During, H. J., and Cornelissen, J. H. C. (2011). The importance of colony structure versus shoot morphology for the water balance of 22 subarctic bryophyte species: Factors affecting bryophyte water balance. *J. Veget. Sci.* 22, 152–164. doi: 10.1111/j.1654-1103.2010.01237.x

Eriksson, A., Gauslaa, Y., Palmqvist, K., Ekström, M., and Esseen, P.-A. (2018). Morphology drives water storage traits in the globally widespread lichen genus Usnea. *Fungal Ecol.* 35, 51–61. doi: 10.1016/j.funeco.2018.06.007

Esseen, P.-A., Rönnqvist, M., Gauslaa, Y., and Coxson, D. S. (2017). Externally held water – a key factor for hair lichens in boreal forest canopies. *Fungal Ecol.* 30, 29–38. doi: 10.1016/j.funeco.2017.08.003

Friedman, S. K., and Reich, P. B. (2005). Regional legacies of logging: departure from presettlement forest conditions in Northern Minnesota. *Ecol. Appl.* 15, 726–744. doi: 10.1890/04-0748

Gauslaa, Y., and Coxson, D. (2011). Interspecific and intraspecific variations in water storage in epiphytic old forest foliose lichens. *Botany* 89, 787–798. doi: 10.1139/b11-070

Gehrig-Downie, C., Obregón, A., Bendix, J., and Gradstein, S. R. (2011). Epiphyte biomass and canopy microclimate in the tropical lowland cloud forest of French Guiana: Epiphyte abundance in lowland cloud forest. *Biotropica* 43, 591–596. doi: 10.1111/j.1744-7429.2010.00745.x

Hargis, H., Gotsch, S. G., Porada, P., Moore, G. W., Ferguson, B., and Van Stan, J. T. (2019). Arboreal epiphytes in the soil-atmosphere interface: how often are the biggest "buckets" in the canopy empty? *Geosciences* 9:342. doi: 10.3390/geosciences9080342

Holder, C. D. (2013). Effects of leaf hydrophobicity and water droplet retention on canopy storage capacity. *Ecohydrology* 6, 483–490. doi: 10.1002/eco.1278

Klamerus-Iwan, A., and Błońska, E. (2018). Canopy storage capacity and wettability of leaves and needles: the effect of water temperature changes. *J. Hydrol.* 559, 534–540. doi: 10.1016/j.jhydrol.2018.02.032

Klamerus-Iwan, A., Kozłowski, R., Przybylska, J., Solarz, W., and Sikora, W. (2020). Variability of water storage capacity in three lichen species. *Biologia* 75, 899–906. doi: 10.2478/s11756-020-00437-7

Köhler, L., Tobón, C., Frumau, K. F. A., and Bruijnzeel, L. A. (2007). Biomass and water storage dynamics of epiphytes in old-growth and secondary montane cloud forest stands in Costa Rica. *Plant Ecol.* 193, 171–184. doi: 10.1007/s11258-006-9256-7

Lakatos, M., Rascher, U., and Büdel, B. (2006). Functional characteristics of corticolous lichens in the understory of a tropical lowland rain forest. *New Phytol.* 172, 679–695. doi: 10.1111/j.1469-8137.2006.01871.x

Levia, D. F., and Frost, E. E. (2003). A review and evaluation of stemflow literature in the hydrologic and biogeochemical cycles of forested and agricultural ecosystems. *J. Hydrol.* 274, 1–29. doi: 10.1016/s0022-1694(02)00399-2

Levia, D. F., Nanko, K., Amasaki, H., Giambelluca, T. W., Hotta, N., Iida, S., et al. (2019). Throughfall partitioning by trees. *Hydrol. Process.* 33, 1698–1708. doi: 10.1002/hyp.13432

Linhoss, A. C., and Siegert, C. M. (2020). Calibration reveals limitations in modeling rainfall interception at the storm scale. *J. Hydrol.* 584:124624. doi: 10.1016/j.jhydrol.2020.124624

Liu, C., Ilvesniemi, H., and Westman, C. J. (2000). Biomass of arboreal lichens and its vertical distribution in a boreal coniferous forest in central Finland. *Lichenologist* 32, 495–504. doi: 10.1006/lich.2000.0288

McCune, B. (1993). Gradients in epiphyte biomass in three Pseudotsuga-Tsuga forests of different ages in western Oregon and Washington. *Bryologist* 96, 405–411. doi: 10.2307/3243870

Mendieta-Leiva, G., Porada, P., and Bader, M. Y. (2020). "Interactions of epiphytes with precipitation partitioning," in *Precipitation Partitioning by Vegetation: A Global Synthesis*, eds I. Van Stan John, T. E. Gutmann, and J. Friesen (Cham: Springer International Publishing), 133–146. doi: 10.1007/978-3-030-29702-2_9

Miranda-González, R., and McCune, B. (2020). The weight of the crust: biomass of crustose lichens in tropical dry forest represents more than half of foliar biomass. *Biotropica* 52, 1298–1308. doi: 10.1111/btp.12837

Mitchell, R. J., Hewison, R. L., Beaton, J., and Douglass, J. R. (2021). Identifying substitute host tree species for epiphytes: the relative importance of tree size and species, bark and site characteristics. *Appl. Veget. Sci.* 24:e12569.

Porada, P., Stan, J. T. V., and Kleidon, A. (2018). Significant contribution of non-vascular vegetation to global rainfall interception. *Nat. Geosci.* 11, 563–567. doi: 10.1038/s41561-018-0176-7

Pypker, T. G., Unsworth, M. H., and Bond, B. J. (2006). The role of epiphytes in rainfall interception by forests in the Pacific Northwest. II. Field measurements at the branch and canopy scale. *Can. J. Forest Res.* 36, 819–832. doi: 10.1139/x05-286

Pypker, T. G., Unsworth, M. H., Van Stan, J. T., and Bond, B. J. (2017). The absorption and evaporation of water vapor by epiphytes in an old-growth Douglas-fir forest during the seasonal summer dry season: implications for the canopy energy budget: Impact of epiphytes on the canopy hydrology of Douglas-fir forests. *Ecohydrology* 10:e1801. doi: 10.1002/eco.1801

Rodriguez-Quiel, E. E., Mendieta-Leiva, G., and Bader, M. Y. (2019). Elevational patterns of bryophyte and lichen biomass differ among substrates in the tropical montane forest of Barú Volcano, Panama. *J. Bryol.* 41, 95–106. doi: 10.1080/03736687.2019.1584433

Rueden, C. T., Schindelin, J., Hiner, M. C., DeZonia, B. E., Walter, A. E., Arena, E. T., et al. (2017). ImageJ2: IMAGEJ for the next generation of scientific image data. *BMC Bioinform.* 18:529. doi: 10.1186/s12859-017-1934-z

Smith, A. J. (1982). *Bryophyte Ecology*. Dordrecht: Springer Netherlands.

Smith, R. J., Jovan, S., Stanton, D., and Will-Wolf, S. (2020). Epiphytic macrolichen communities indicate climate and air quality in the U.S. Midwest. *Bryo* 123, 517–533.

Stanton, D. E., Huallpa Chávez, J., Villegas, L., Villasante, F., Armesto, J., Hedin, L. O., et al. (2014). Epiphytes improve host plant water use by microenvironment modification. *Funct. Ecol.* 28, 1274–1283. doi: 10.1111/1365-2435.12249

Ure, J. D., and Stanton, D. E. (2019). Co-dominant anatomically disparate lichens converge in hydrological functional traits. *Bryo* 122, 463–470. doi: 10.1639/0007-2745-122.3.463

Van Stan, J. T., Gutmann, E., and Friesen, J. (2020). *Precipitation Partitioning by Vegetation: A Global Synthesis*. Salmon Tower Building, NY: Springer International Publishing.

Van Stan, J. T., and Pypker, T. G. (2015). A review and evaluation of forest canopy epiphyte roles in the partitioning and chemical alteration of precipitation. *Sci. Total Environ.* 536, 813–824. doi: 10.1016/j.scitotenv.2015.07.134

Villegas, J. C., Tobón, C., and Breshears, D. D. (2008). Fog interception by non−vascular epiphytes in tropical montane cloud forests: dependencies on gauge type and meteorological conditions. *Hydrol. Process.* 22, 2484–2492. doi: 10.1002/hyp.6844

Vogeler, J. C., Slesak, R. A., Fekety, P. A., and Falkowski, M. J. (2020). Characterizing over four decades of forest disturbance in Minnesota. USA. *Forests* 11:362. doi: 10.3390/f11030362

Woods, C. L. (2017). Primary ecological succession in vascular epiphytes: the species accumulation model. *Biotropica* 49, 452–460. doi: 10.1111/btp.12443

Zheng, C., and Jia, L. (2020). Global canopy rainfall interception loss derived from satellite earth observations. *Ecohydrology* 13:e2186.

Zotz, G. (2016). *Plants on Plants – The Biology of Vascular Epiphytes*. Salmon Tower Building, NY: Springer International Publishing.

Conflict of Interest: The authors declare that the research was conducted in the absence of any commercial or financial relationships that could be construed as a potential conflict of interest.

frontiers in Forests and Global Change

ORIGINAL RESEARCH
published: 19 July 2021
doi: 10.3389/ffgc.2021.657850

Bark Effects on Stemflow Chemistry in a Japanese Temperate Forest II. The Role of Bark Anatomical Features

Ayano Oka[1], Junko Takahashi[2], Yoshikazu Endoh[3] and Tatsuyuki Seino[2,4]*

[1] Graduate School of Life and Environmental Sciences, University of Tsukuba, Tsukuba, Japan, [2] Faculty of Life and Environmental Sciences, University of Tsukuba, Tsukuba, Japan, [3] Ikawa Forest Station, Mountain Science Center, University of Tsukuba, Shizuoka, Japan, [4] Yatsugatake Forest Station, Mountain Science Center, University of Tsukuba, Minamimaki, Japan

OPEN ACCESS

Edited by:
Anna Klamerus-Iwan, University of Agriculture in Krakow, Poland

Reviewed by:
John T. Van Stan, Georgia Southern University, United States
Salli F. Dymond, University of Minnesota Duluth, United States
Wojciech Piaszczyk, University of Agriculture in Krakow, Poland

***Correspondence:**
Ayano Oka
sbtn.notchi@gmail.com

Specialty section:
This article was submitted to Forest Hydrology, a section of the journal Frontiers in Forests and Global Change

Received: *24 January 2021*
Accepted: *21 June 2021*
Published: *19 July 2021*

Citation:
Oka A, Takahashi J, Endoh Y and Seino T (2021) Bark Effects on Stemflow Chemistry in a Japanese Temperate Forest II. The Role of Bark Anatomical Features. Front. For. Glob. Change 4:657850. doi: 10.3389/ffgc.2021.657850

A fraction of rainfall drains to the soil surface down tree stems (as "stemflow"), and the resulting stemflow waters can be highly enriched with dissolved nutrients due to prolonged bark contact. To date, stemflow chemistry has been examined mostly in regards to the external morphology of the bark, while its relationship with bark anatomy has received little attention. Arguably, this represents a major knowledge gap, because bark anatomical traits are linked to the storage and transport of soluble (and insoluble) organic materials, and control the proximity of these materials to passing stemflow waters. To initiate this line of investigation, here, we examine bark-water leaching rates for common leachable macronutrient ions (Mg^{2+}, Ca^{2+}, and K^{+}) across six different tree species with varying bark anatomical traits (four deciduous broadleaved and two evergreen coniferous species). These different bark types were subjected to laboratory experiments, including observations of bark anatomy and soaking experiments. Laboratory-derived estimates of leaching rates for Mg^{2+}, Ca^{2+}, and K^{+} were then analyzed alongside bark anatomical traits. Leaching rates of Mg^{2+} and Ca^{2+} appear to be controlled by the thickness of the rhytidome and periderm; while K^{+} leaching rates appeared to be driven by the presence of cellular structures associated with resource storage (parenchyma) and transfer (sieve cells). Other species-specific results are also identified and discussed. These results suggest that the anatomical features of bark and the concentration of leachable macronutrient ions in stemflow are related, and that these relationships may be important to understand nutrient cycle through the bark. We also conclude that future work on the mechanisms underlying stemflow solute enrichment should consider bark anatomy.

Keywords: bark anatomy, bark morphology, forest hydrology, rainfall, stemflow

INTRODUCTION

> "L'écorce est une fiere travailleuse"
> [1]"The bark is a proud worker" (Fabre, 1867).

The bark, or the outermost part of the tree stem, is the boundary between the stem and its surrounding environment. This bark boundary protects the internal stem tissues from invasion dryness, fire, and severe external temperatures (Rosell et al., 2014; Pausas, 2015). Bark also plays important roles in forests as an intermediary between the outside environment and the inside of the tree, e.g.: hosting lichens and other corticolous epiphytic life, acting as an exchange site for aerosols and substances within precipitation, and being a pathway for rainfall that drains to the surface as stemflow (Van Stan et al., 2021). Stemflow may also be highly enriched in solutes, resulting in significant, locally concentrated nutrient inputs (Dovey et al., 2011; Germer et al., 2012). Past studies suggested that the amount of stemflow and its solute concentration are strongly coupled to the traits of the bark over which stemflow must drain (Levia and Germer, 2015).

Stemflow chemistry can be influenced by bark contact in several ways. Externally, stemflow can wash off aerosols that were deposited on the bark surface between storms (Levia et al., 2011). The amount of materials captured on the bark varies with the external bark structure–where rough bark on stems, for instance, has been observed to capture nearly 10 times more particles (by mass) than the same area of smoother branch bark surfaces (Xu et al., 2019). There are several studies that have examined the interactions between stemflow chemistry and bark surface structure (Levia and Germer, 2015), and this was the topic for the first part of our research (Oka et al., 2021). Within the bark, however, there are concentrated intracellular solutions that the draining stemflow waters may be able to leach (Klemm et al., 1989). Past work suggests that bark contact may preferentially increase leaching of NH_4^+, K^+, NO_3^-, SO_4^{2-}, and H^+, with the degree of leaching being dependent on bark structure (André et al., 2008). As the bark is capable of taking up external waters, it can also take up solutes (André et al., 2008). The ability for draining stemflow to leach solutes from the bark may depend on bark anatomy, but this has not been investigated to our knowledge. Thus, this manuscript details research that continues from Oka et al. (2021), examining relationships between bark external anatomical traits and stemflow chemistry. Oka et al. (2019, 2021) suggested that Cl^- and Na^+, which are thought to be derived from dry deposition on the tree surface, are easily washed away in the stemflow of smooth bark, while species with coarsely split bark are more likely to leach cations and organic matter, especially Mg^{2+}, Ca^{2+}, and K^+. The external morphology of bark makes a significant contribution to the solute composition and concentration of stemflow, while the thickness and internal morphology of bark are also expected to affect the mechanisms of this bark-water solute exchange. Thus, the anatomical point of view is important for exploring the mechanism of stemflow chemistry (Levia and Herwitz, 2005; Van Stan et al., 2021).

The purpose of this study is to examine how solute leaching [focusing on Mg^{2+}, Ca^{2+}, and K^+ per the results of Oka et al. (2021)] relates to bark anatomical differences among six study tree species in Japan to evaluate bark functions in the exchange of macronutrient cations with stemflow. To accomplish this aim, laboratory experiments were designed to observe the amount, timing, and rates of different solutes leached from the surface of various types of bark. Anatomical observations of the bark were also made to gain insight into the possible connections between bark physiological structures and interspecies solute leaching differences.

MATERIALS AND METHODS

Target Species

The target species were selected according to their bark morphology by moderate, roughness, coarse, and with or without longitudinal tear as following a previous study by Oka et al. (2021). The smooth and mottled bark surface types was represented by *Clethra barbinervis* Sieb. et Zucc.; whereas, the smooth, lateral bark surface types was represented by *Padus grayana* (Maxim.) C. K. Schneid. A moderate bark roughness type was represented by *Magnolia obovata* Thunb. Coarse and deep longitudinal tears distinguished *Castanea crenata* Sieb. et Zucc., as a very rough bark structure. These species were deciduous broad-leaved trees. Evergreen conifers were also selected, where moderate bark roughness was represented by *Abies firma* Sieb. et Zucc., and coarse bark morphology was represented by *Tsuga sieboldii* Carr (**Figure 1**).

Sample Collection and Anatomical Observations

Sample collections were carried out in Tashiro, Shizuoka, central Japan (35.307672N, 138.199925E). The site elevation is 966 m a.s.l., the annual rainfall is 3110.1 mm, and the annual mean temperature is 11.4°C (statistical period according to AMeDAS: 1981–2010, Ministry of Land, Infrastructure, Transport, and Tourism Meteorological Agency HP, https://www.data.jma.go.jp/obd/stats/etrn/index.php, last viewed on December 6, 2019). Forest vegetation of the site is mixed forest of deciduous broad-leaved trees and evergreen conifers (Seino and Endoh, 2019). The site is approx. 48 km far from the nearest coast, and the site is surrounded by natural forests, and there are almost no factories or residential area in the area. Therefore, the mineral supply from the ocean (especially Cl^-) and the influence of pollutants (some nitrogen oxides) from human activities are expected to low (**Figure 2**).

Bark samples for anatomical analysis approximately 4 cm^2 were collected at the site in September 2019. This sampling time was selected to minimize the effects of mineral leaching from the bark due to heavy rainfall caused by the Japanese rainy season and typhoons. The samples were obtained from sound individuals with minimal observable surface damage, not covered with lichen or epiphytes, and collected at a height of approx. 1 m above the ground using a chisel. The thickness of each bark sample was measured at three points using a manual caliper. Anatomical analysis was carried out in the laboratory of the Yatsugatake Forest Station, Mountain Science Center,

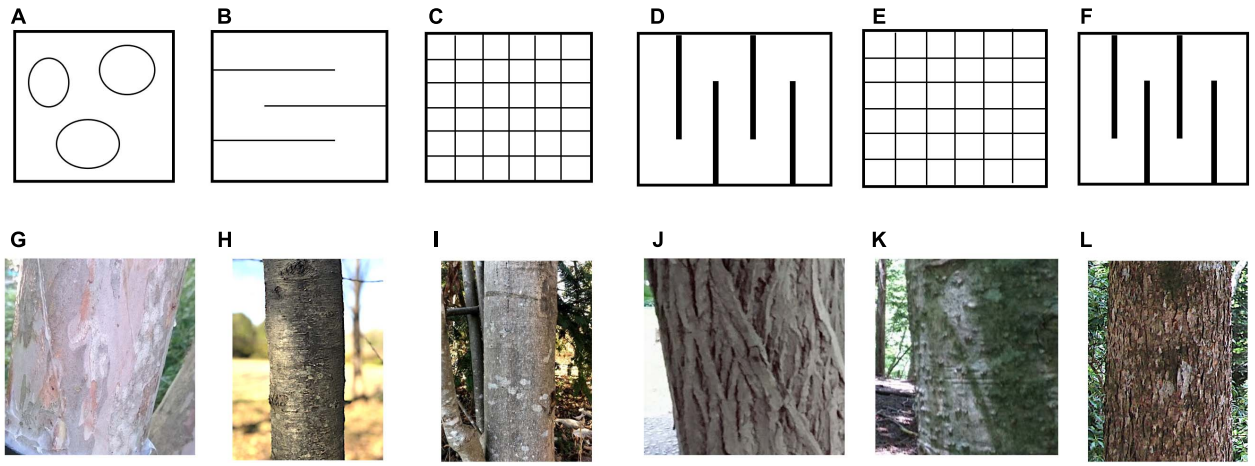

FIGURE 1 | Schematic diagram of bark surface and photographs of the bark of target tree species. The upper row is a schematic drawing of the bark surface, **(A)** smooth and mottled surface type, **(B)** smooth lateral skin type, **(C)** moderate roughness type, **(D)** coarse and deep longitudinal tear type, **(E)** moderate type of conifer, and **(F)** coarse type of conifer. The middle row shows bark photographs of the trees in which soaking experiments of the bark were conducted, **(G)** *Clethra barbinervis,* **(H)** *Padus grayana,* **(I)** *Magnolia obovata,* **(J)** *Castanea crenata,* **(K)** *Abies firma,* and **(L)** *Tsuga sieboldii.*

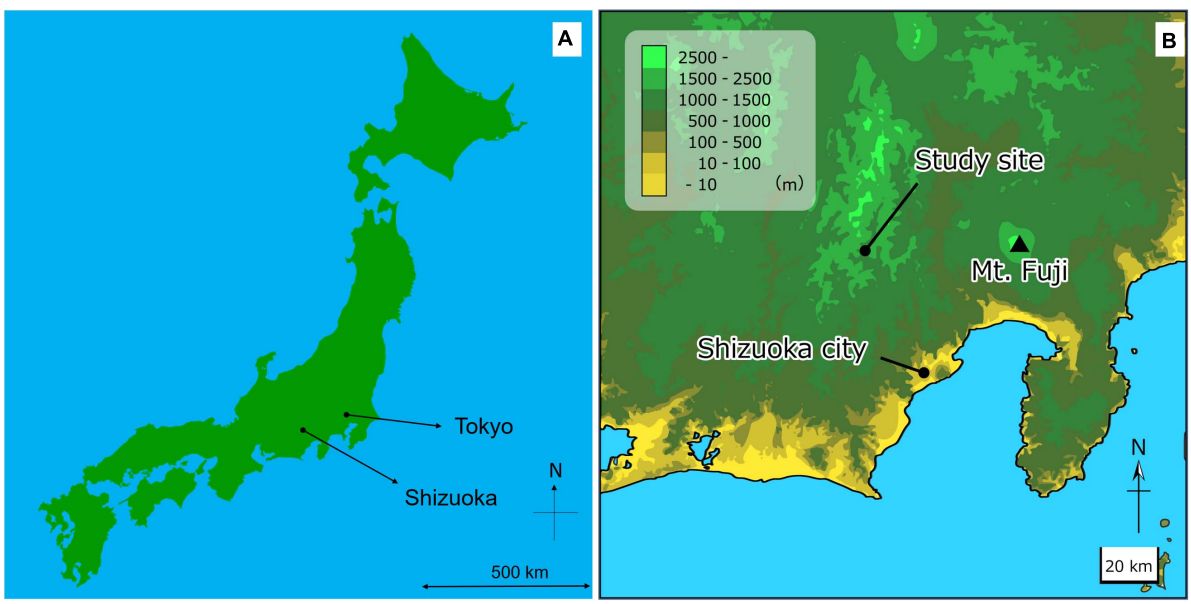

FIGURE 2 | Map of the sample collection area. **(A)** Map of Japan, and **(B)** Map of around the sample collection site.

University of Tsukuba, Japan. The bark samples were fixed and softened in 99.5% ethanol, and lateral sections were prepared using a sliding microtome (TU-213, Yamato Kohki Industrial, Saitama, Japan). Cross sections (30 μm thick) were obtained from the bark samples. Cross sections were dehydrated in an ethanol series and sequentially stained with safranin and methyl blue. Permanent preparations were made for observations of the morphology and arrangement of the cells with an optical microscope (BX53, Olympus, Tokyo, Japan), and anatomical photographs were taken with a digital camera (EOS Kiss X7i, Canon, Tokyo, Japan).

The general structures of bark were defined as follows (Shimaji et al., 1976; Trockenbrodt, 1990; Angyalossy et al., 2016). The bark encompasses all of the tissues outside the cambium of a tree. It is broadly divided from the outside into the epidermis, periderm, cortex, and secondary phloem. The epidermis, the outermost cell with a thick cell wall, is responsible for preventing water loss from inside the tree and protecting the tree body from external stimuli. The periderm, which serves as secondary lateral meristem to the disrupted epidermal layer, consists of phellem, phellogen, and phelloderm. The cortex is the foundation of the periderm. The secondary phloem includes radiation tissue–which

is responsible for the transport of materials and for their storage– as well as bast fiber and sclereids–which provide mechanical strength. According to the above definitions, the anatomical findings of the bark structures of each species are described.

Bark-Soaking Experiment

Bark samples for soaking experiments were collected at the site in September 2019, with three bark samples of approximately 9 cm^2 from each, for a total of 18 samples at the laboratory of University of Tsukuba, Japan. The reason for the sample size was that there was a limit to the number of individuals suitable for bark collection and due to the time constraint in the process of immersion experiments. The inner surfaces and sections of the bark samples were coated with paraffin wax and soaked for the first time in 200 ml of distilled water after 12 h. The samples were placed in a petri dish so that the outer bark was immersed in water. The water samples were collected continuously throughout the soaking experiment by removing 4 ml samples from the petri dish every 24 h. The soaking time was set to maximum at 96 h due to the expectation that the extracted minerals would reach at a saturation concentration by that time. The concentrations of target inorganic ions (Mg^{2+}, Ca^{2+}, and K^{+}) were measured in a total of 90 water samples using ion chromatography (Prominence series, Shimadzu, Kyoto). Calibration curves were tested using five mixed standard solution for the peak area of each ion and organic carbon, and quantification was performed after confirming their correlation coefficients. The reproducibility of the peak area, was regularly confirmed that the CV is 2% or less.

Data Analysis

To evaluate patterns leaching cations from the bark, we applied a Principal Components Analysis using the online ClustVis application[1] by Metsalu and Vilo (2015). A PCA analysis was performed to explore possible interrelations of K^{+}, Mg^{2+}, and Ca^{2+} leaching rates with bark anatomical traits.

RESULTS

Anatomical Findings of Species

According to the above-mentioned definitions by Shimaji et al. (1976); Trockenbrodt (1990), and Angyalossy et al. (2016), the anatomical findings of the bark structures of each bark type by species are described and summarized in **Table 3**. Anatomical pictures are included in the **Supplementary Figures**. The bark surface morphology was already described in a previous research by Oka et al. (2021).

The smooth and mottled bark of *Clethra barbinervis* has a thin cortex from the epidermis and well-developed radiating tissue that is distinct (**Table 3**). We observed a raised epidermis over the extension of the radiation tissue. The epidermis of *Padus grayana* has a thin cork phelloderm on the periderm that forms a linear rhytidome. Gaps are also common at the border between the cortex and the secondary phloem for *P. grayana*. This species radiation tissue is developed in three to five rows of cells, and there are gaps along this radiation tissue as well. Parenchyma were also observed in a distinct, cross-sectional direction for *P. grayana*. For the moderately-rough barked *Magnolia obovata*, the epidermis is mostly absent, with uneven, slightly developed phellem. The *M. obovata* cortex has a rare supra-grain sclereid, is spongy with many gaps, and characterized by the expansion and development of the radiation tissue toward the cortex in the middle of the secondary phloem. Circumferential parenchyma and bast fibers are also well developed and distinct in the *M. obovata* samples. The coarse, deep, longitudinal tears of *Castanea crenata* bark is related to a wave-patterned periderm that forms its rhytidome. A thin radiation tissue consisting of one or two rows of cells was found in the secondary phloem of *C. crenata*. This species also has thick bast fibers alternating with parenchyma at equal intervals. Bark of the conifer, *Abies firma*, shows several layers of thin, smooth periderm overlap with a thickly developed mosaic-like layer of skin mixed with live cells and sclereids. There were also many gaps in *A. firma* samples, which was common in the broadleaved moderate bark (i.e., *M. obovata*). The secondary phloem of *A. firma* is thinner than that of the other broad-leaved trees, and the radiation tissue is thin and indistinct. The coarse bark conifer, *Tsuga sieboldii*, has an outer rhytidome and porous bark layer that appears similar to *A. firma*. The old periderm of *T. sieboldii* has scattered ball-shaped sclerae, while the inner new phelloderm is wavy and well-developed. The parenchyma of the secondary phloem of this species indistinctly intrudes into the cortex and are characterized by the presence of many clustered sclereids.

Bark-Soaking Experiment

For minerals leaching from a tree body, such as K^{+}, Ca^{2+}, and Mg^{2+}, their concentrations differed among species and with soaking time (**Figure 3** and **Table 1**). All studied cations increased until settling near the maximum (i.e., 96-h) concentration (**Figure 3** and **Table 2**). Mg^{2+} concentrations tended to be low in *Padus grayana* (7.64–39.61 μmol L^{-1}), *T. sieboldii* (5.12–25.42 μmol L^{-1}), *A. firma* (13.25–30.61 μmol L^{-1}), and *C. barbinervis* (8.39–29.05 μmol L^{-1}), but concentrations of Mg^{2+} were generally higher in *M. obovata* (24.56–88.57 μmol L^{-1}) and *C. crenata* (24.62–34.03 μmol L^{-1}) (ANOVA, $F_{[5,58]} = 5.19$, $p < 0.001$ by species). For all trees,

TABLE 1 | Leaching rates (μmol L^{-1} h^{-1}) of K^{+}, Mg^{2+}, and Ca^{2+} by species, estimated as the slope of a linear regression relating concentration and time of saturation during the soaking experiment.

Species	K^{+}		Mg^{2+}		Ca^{2+}	
	Mean	Range	Mean	Range	Mean	Range
Clethra barbinervis	0.40	0.15–0.53	0.18	0.10–0.28	0.32	0.09–0.74
Padus grayana	0.53	0.29–0.77	0.17	0.08–0.25	0.28	NA
Magnolia obovata	2.11	0.24–3.51	0.27	0.23–0.28	0.75	0.71–0.79
Castanea crenata	0.19	0.15–0.24	0.50	0.20–0.90	1.01	0.35–1.48
Abies firma	1.85	0.26–2.84	0.19	0.07–0.35	0.26	0.09–0.70
Tsuga sieboldii	0.70	0.19–1.64	0.15	0.05–0.23	0.23	0.20–0.26

[1]https://biit.cs.ut.ee/clustvis/

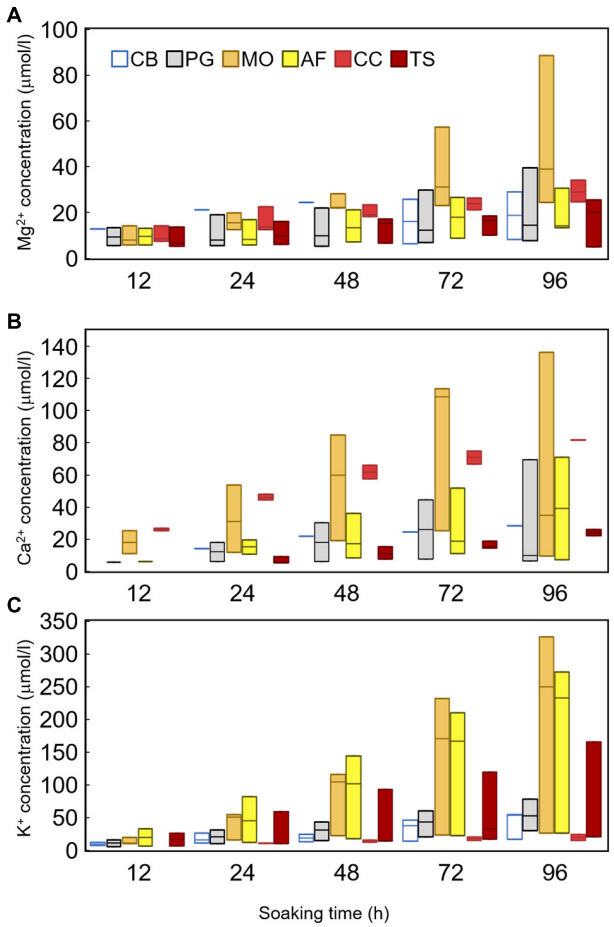

FIGURE 3 | Box-plot of concentrations of inorganic ion, **(A)** Mg^{2+}, **(B)** Ca^{2+}, and **(C)** K^{+} extracted from the bark by soaking experiment. Colors mean each species as *Clethra barbinervis* (white), *Padus grayana* (gray), *Magnolia obovata* (orange), *Abies firma* (yellow), *Castanea crenata* (light red), and *Tsuga sieboldii* (deep red). Bars in figure are SD.

Mg^{2+} concentrations increased over time of the soaking experiment, especially for *M. obovata* (**Figure 4**). Concentrations of Ca^{2+} in *A. firma* (7.04–71.07 μmol L^{-1}) and *C. crenata* (81.77 μmol L^{-1}) were higher than those for other species (**Figure 4**). In *M. obovata*, Ca^{2+} concentrations were lower and often undetectable in some samples. Up to 48 h, *C. crenata* had the highest concentrations of Ca^{2+} (57.34–74.73 μmol L^{-1}), after which its concentration exceeded those of *M. obovata* during the same soaking times [ANOVA, $F_{(5,42)} = 4.66$, $p < 0.01$ by soaking time]. The highest concentrations of K^{+} were, in order, *M. obovata* (26.22–325.74 μmol L^{-1}), *A. firma* (26.19–232.85 μmol L^{-1}), *T. sieboldii* (20.38–165.23 μmol L^{-1}), *P. grayana* (29.76–77.99 μmol L^{-1}), *C. barbinervis* (16.79–54.20 μmol L^{-1}), and *C. crenata* (15.08–24.47 μmol L^{-1}). For all tree species, K^{+} concentrations increased over time, while in the same order [ANOVA, $F_{(4,53)} = 6.16$, $p < 0.001$ by soaking time] (**Figure 4**). As for the leaching rate and their linearity along a time course, there were no remarkable relations. The bark types such as *C. crenata* and *T. sieboldii* tended to leach more easily than others (**Tables 2**, **3**).

Two principal components were identified that represented ∼60% of the variability within these data: 37% in component 1 (PC1) and 23% in component 2 (PC2). The three bark samples from each species (indicated by symbol color) clustered together across the PC space; however, these species-specific clusters are generally distinct from each other (**Figure 5**). The loadings (lower right) suggest that the leaching rates of Mg^{2+} and Ca^{2+} across the studied tree species may be possibly driven by similar anatomical features of the bark. Specifically, Mg^{2+} and Ca^{2+} leaching rates load alongside the rhytidome thickness (Rhy), periderm thickness (Per), and the presence of bast fibers (Bst) (**Figure 5**). K^{+} leaching rates, on the other hand, seem to be influenced by the presence of cavities (Cav), parenchyma (Par), sieve cells (Siv), and cortical thickness (Ctx) (**Figure 3**). The spread among species and their clusters in the PCA plot is larger along the direction of loading by K^{+} and its affiliated bark anatomical features (i.e., from quadrants 2 to 4), compared to the influence of Mg^{2+} and Ca^{2+} leaching rates/bark features (**Figure 5**). The exception to this is *A. firma*, for which one of the samples plotted relatively far from the other two samples in both major loading directions.

DISCUSSION

Comparison of Anatomical Structures by Bark Type

From the results of this study, the anatomical characteristics of the inner bark are not simply determined by the thickness of the outer bark, which is often how comparisons have been drawn between solute concentrations and their sources in the rain waters that have drained through tree canopies (Levia and Frost, 2003; Levia and Germer, 2015; Lu et al., 2017; Oka et al., 2021). These anatomical descriptions and the assessment of their interactions with the select macronutrient cations in this study may provide a roadmap for future work on the biogeochemical interactions between bark and stemflow or branchflows. Many of the anatomical structures identified in this study are analogous to other species' bark. The structure of the *P. grayana* periderm, for example, which contains a thin, smooth, lateral phellem has also been observed in *Betula platyphylla* Sukaczev var. *japonica* (Miq.) H. Hara (Shibui and Sano, 2018) which bark surface is

TABLE 2 | Coefficients of the relationship between time and percentage of maximum concentration over the soaking experiment.

Species	K^{+}	Mg^{2+}	Ca^{2+}
Clethra barbinervis	0.93*	0.93**	0.93***
Padus grayana	0.97***	0.97***	0.79**
Magnolia obovata	0.89*	1.01***	0.89**
Castanea crenata	0.72*	0.84*	0.92***
Abies firma	0.90**	0.95***	0.88**
Tsuga sieboldii	0.95**	0.54*	0.90***

*Asterisks denote p value (*p < 0.05; **p < 0.01; ***p < 0.001).*

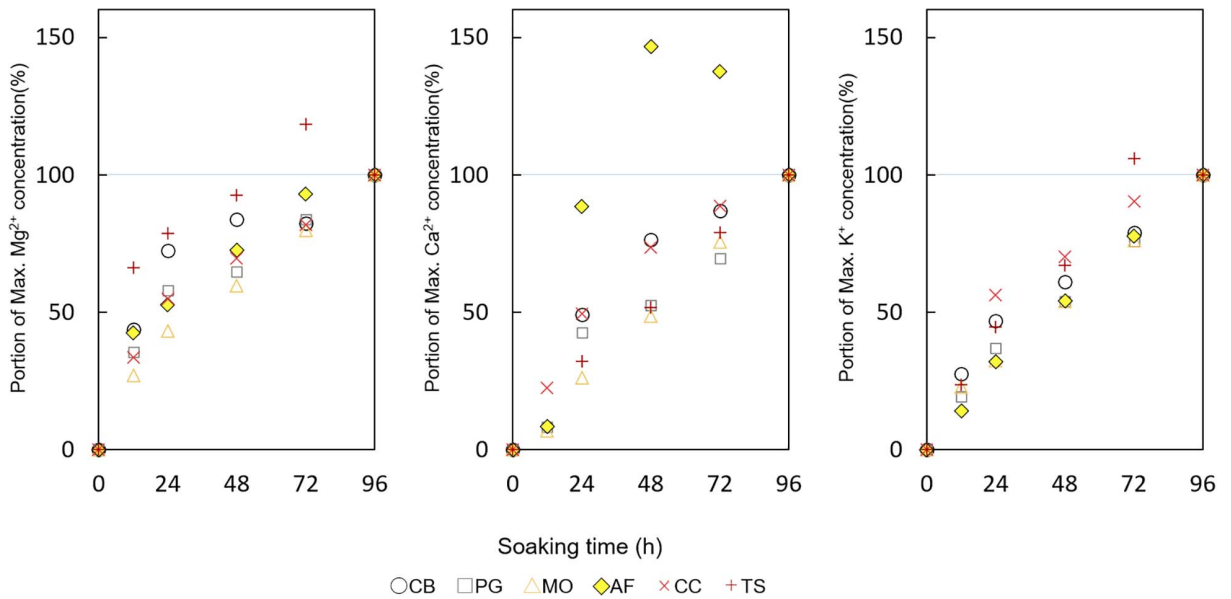

FIGURE 4 | The portions of maximum Mg^{2+}, Ca^{2+}, and K^{+} concentration (%) by soaking time (hr). Colors mean each species as CB *Clethra barbinervis* (white circle), PG as *Padus grayana* (gray square), MO as *Magnolia obovata* (orange triangle), AF as *Abies firma* (yellow diamond), CC as *Castanea crenata* (light red x), and TS as *Tsuga sieboldii* (deep red cross).

similar to that of *P. grayana*. Some bark anatomical traits were similar across coniferous and broadleaved study species. For the moderately rough bark types, such as *M. obovata* and *A. firma*, both had gaps and sclereids at the border between the periderm and the secondary phloem. The bark of these moderate types was also similar to that of *P. grayana* except for the characteristics of the periderm. The coarse, deep, longitudinal structure of the thick rhytidome and the structure of the secondary phloem were similar in both *C. crenata* and *T. sieboldii*. Some features were only observed in one of the species. For example, the characteristically well-developed radiation tissue was observed only in *M. obovata*. Across the studied species, however, the internal anatomy of smooth, moderate, and coarse bark types did differ greatly.

These different bark anatomies suggested that the possible solute exchange between the bark and the drained rainwater is related to tree growth. For example, Shibata and Sakuma (1996) and Staelens et al. (2007) have shown that seasonal changes in the dynamics of the chemistry of deciduous broadleaf tree stemflow were related to tree growth, especially leaf phenology such as leaf flush, expansion, and defoliation. Carmo et al. (2016) analyzed minerals in the bark of *Copaifera langsdorffii* Desf. (Fabaceae) by correlating chemical analysis with anatomical characteristics. Carmo et al. (2016) also analyzed the relationship between bark anatomies such as its thickness and the mineral source within each tissue. The results of this study provide a prospect to explore the mechanisms of solute enrichment by bark-water interactions from the following soaking experiments.

Bark-Soaking Experiment

A trend of increasing concentration over soaking time was observed for all species' bark samples for Mg^{2+}, Ca^{2+}, and K^{+}, which are solubilizing substances. For Mg^{2+} and Ca^{2+}, the concentrations of *C. crenata* were high up to 24 h later–and at similar concentrations to those of stemflow samples from the field (Oka et al., 2021); however, after 48 h, the concentrations were higher in *M. obovata*. This suggests that the bark of *M. obovata* is particularly prone to the accumulation of substances, and that there may be a time lag in the leaching of these cations to water contacting the bark. We note that the residence time of rainwater on bark may be exaggerated in our soaking experiments; however, to our knowledge, no residence time estimates for stemflow in tree canopies currently exist. Thus, there are no observations or estimates of the appropriate time duration that one could have used to guide the soaking experiment. We assume that the length of our soaking experiment represents a maximum residence time, yet storms may last several days and snow residence time on bark (before melt) may last 96 h or longer (Klamerus-Iwan et al., 2020). It may be that the amount of cation accumulation that is leachable during these soaking experiments was related to the internal structure of the bark, such as the cortex, rather than the surface structure.

Much attention has been focused on the water storage capacity of bark (Levia and Herwitz, 2005; Van Stan et al., 2016) and its function as a source of minerals (Wetzel and Greenwood, 1989; Wetzel et al., 1989; Wolterbeek et al., 1996). In the case of those bark-derived leaching cations examined in this study (Ca^{2+}, Mg^{2+}, and K^{+}), Ca^{2+} tended to be more abundant in tree bodies (Jones et al., 2019), while Mg^{2+} and K^{+} tend to be more concentrated in leaves, which is closely related to their physiological in individual trees (Shibata and Sakuma, 1996; Jones et al., 2019). It has been suggested that the leaching of these cations from tree body is related to the water-storage function of the bark because, hypothetically,

TABLE 3 | Summarized of anatomical characteristics of each species.

			Anatomical characteristics										
	Bark morphology		**Species**		**Perderm**			**Cortex**		**Secondary phloem**			
			Thickness (mm)	**Epodermis**		**(apr. mm)**	**Rhytidomes**		**(apr. mm)**	**Sclereid**	**Radiation tissue**	**Sieve cell**	**Parenchyma**	**Bast fiber**
Broad-leaved trees	Smooth and mottled surface	*Clethra barbinervis*	0.54 ± 0.05^{a}	Very thin	Very thin	0.02	×	Very thin	0.065	×	Well-developed	Scatter	×	×
	Smooth with lateral skin	*Padus grayana*	3.69 ± 0.20^{ac}	×	Horizontal straight	0.44	Thin pericarp layered	Cavity	0.39	×	Well-developed	Well-developed	Circumferential	×
	Moderate roughness	*Magnolia obovate*	6.08 ± 0.36^{cd}	×	Slightly developed	0.26	Mono layered	Many cavities	1.17	○	Expanding outward	Obscure	Well-developed	Well-developed
	Coarse and deep longitudinal tear	*Castanea crenata*	6.57 ± 1.48^{cd}	×	Developed	1.96	Wavy development, layered	Thin	0.26	×	Narrow	Well-developed	Well-developed	○
Conifers	Moderate roughness	*Abies firma*	6.53 ± 0.40^{cd}	×	Thin	0.39	Thin pericarp overlaps	Mosaic with cabity	5.33	○	×	×	Obscure	×
	Coarse and deep longitudinal tear	*Tsuga sieboldii*	6.29 ± 0.59^{bcd}	×	Thick outside thick inside	0.39	Wavy development	Mosaic with cabity	0.84	○ Ball shaped develop	×	×	Obscure	×

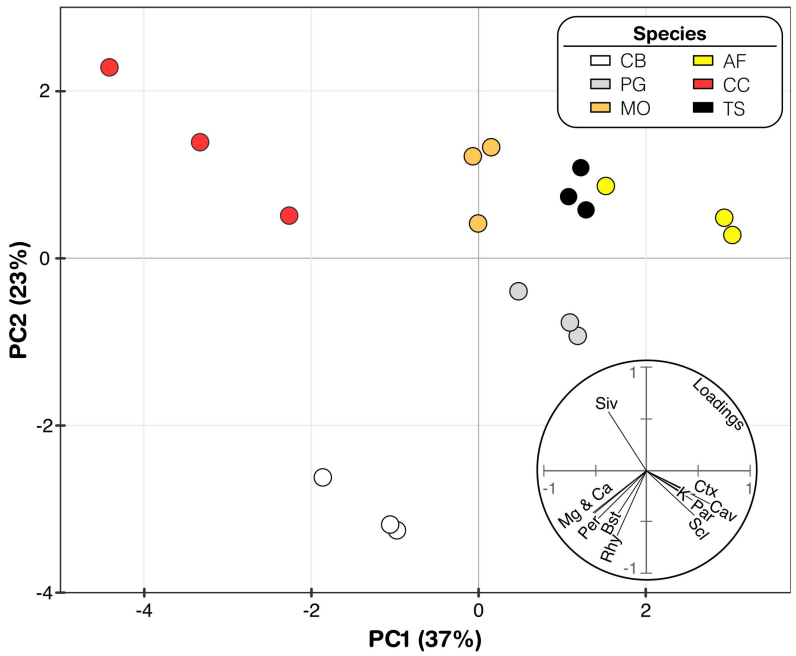

FIGURE 5 | Principal component analysis with Mg^{2+}, Ca^{2+}, and K^{+} concentrations related to anatomical components. The arrows represent variable plotted by the first two PCA axes. Species abbreviations are *Clethra barbinervis* (CB) *Padus grayana* (PG), *Magnolia obovata* (MO), *Castanea crenata* (CC), *Abies firma* (AF), and *Tsuga sieboldii* (TS), respectively.

greater water storage equates to longer bark-water contact times (Levia and Herwitz, 2005; Abbasian et al., 2015). To date, however, the physiological mechanisms of the bark-water interactions that underlie the enrichment of stemflow with the macronutrient ions remain relatively undescribed–especially compared to leaching mechanisms in leaves (Aubrey, 2020). This may be a result of common methods for estimating leaching rates in throughfall and stemflow requiring no knowledge of bark anatomy and physiology, e.g.: (i) multiple regression modeling (Lovett and Lindberg, 1984); (ii) parsing washoff and leaching from intrastorm trends in water chemistry (Kazda and Glatzel, 1986; Kazda, 1990); or (iii) using tracer solutes (Staelens et al., 2008; Turpault et al., 2021). Our results suggest that bark anatomy plays an important role in the leaching of macronutrient cations into waters draining through woody plant canopies.

From the principal components analysis, leaching of Mg^{2+} and Ca^{2+} appears to be driven by similar bark anatomical traits such as a thickness of rhytidome and periderm, as well as bast fibers. The thickness of the rhytidome and periderm may influence these leaching rates by influencing the distance between living cells (beyond the rhytidome) and the stored or draining rainwaters (as similarly hypothesized by André et al., 2008). Given that bast fibers primarily provide stabilizing or mechanical support functions, it's relationship with the leaching of Mg^{2+} and Ca^{2+} is uncertain. K^{+} appears to be driven by the presence of cavities, parenchyma, sieve cells, sclereids and cortex thickness. The statistical inference of a relationship between K^{+} leaching rates and some of these anatomical features seems reasonable, particularly given that parenchyma are generally specialized storage tissue (which may hold a variety of materials, like starches, oils, resins, etc.: Zabel and Morrell, 2020), and that sieve cells may conduct sugars and can be associated with parenchyma (Simpson, 2019). Bark anatomical results by Carmo et al. (2016), observed cavities, sclereids, cortex thickness of *C. langsdorfifii* bark, and detected chemical composition in the fractionation of extractives. K^{+} plays an important role in photosynthesis, ion transport, and osmotic adjustment in plants. Therefore, it would be important to know that K^{+} compartments present and related to their ecophysiological activity, and the thickness of the sclerotium as its storage function. In addition, since sclereids are formed by changes in old sieve cells, if the relationship between the process of formation and the concentration of K^{+} is detected it can be expected to indicate the process of bark development and the physiological activity at the crown through the chemistry of the stemflow.

Although our study focused on K^{+}, Mg^{2+}, and Ca^{2+}, there are other solutes meritorious of investigation with regard to their bark-water interactions. Wetzel et al. (1989) reported on the nitrogen storage function of bark from the perspective of bark anatomy. Past research on the composition of organic chemical components in *Pinus densiflora* Siebold and Zucc., bark aimed at the effective use of bark as a residue of timber production (Hata and Sogo, 1956). Others have examined tannin extraction from the bark of species useful for wood (Ohara, 2009). For one of the target tree species in this research, past work has examined essential oil components in the bark of

M. obovata (Fujita et al., 1973). Research on the bark of *Fraxinus lanuginosa* Koidz. f. *serrata* (Nakai) Murata has also been done for the isolation of naturally occurring antioxidants (Hayafuji, 2018) which may be useful in assessing the quality of medicinal components. Thus, this work builds on a long, but sparse, history of research on bark anatomy and its relationship with water and solutes by shedding new insights into the possible role of bark anatomical traits in the dynamics of inorganic components leached from the bark to stemflow.

CONCLUSION

Current theory on the influence of bark on stemflow chemistry solely considers the influence of external bark surface morphology, neglecting the role of bark anatomy. The results of this study suggest that bark anatomical traits are related to stemflow chemistry for commonly leached macronutrient ions (K^+, Mg^{2+}, and Ca^{2+}) across a wide range of bark types studied here (six species from coniferous and broadleaved trees). These results further suggest that the stemflow-bark interactions can play an important role in the transfer and intrasystem cycling of macronutrients between the inside of the tree and the external environment. Across bark samples of varying anatomy, Mg^{2+} and Ca^{2+} leaching rates were driven by the thickness of the rhytidome and periderm–hypothetically reducing leaching rates as the distance between living cells (beyond the rhytidome) and stemflow is increased. K^+ leaching rates appeared to be driven by the presence of anatomical features associated with resource storage (parenchyma) and transfer (sieve cells). For some bark types, such as *Abies firma* and *Magnolia obovata*, that had a spongy anatomy, with gaps were found at the boundary between the epidermis and the secondary phloem that appear to delay bark-stemflow solute exchange. The concentrations of tree body derived leachates were higher in the stemflow of study trees like *Castanea crenata* and *Tsuga sieboldii*, suggesting that the rhytidome thickness and the presence or absence of sieve cells and associated parenchyma are related. Even in the coarse bark type, there was a difference in the internal structure between conifers and hardwoods, which may have resulted in a difference in the tendency of the stemflow chemistry. We recommend that future work seeking to mechanistically explain variability in stemflow solute concentration, composition, and especially leaching from bark surfaces, examine bark anatomical traits.

DATA AVAILABILITY STATEMENT

The original contributions presented in the study are included in the article/**Supplementary Material**, further inquiries can be directed to the corresponding author.

AUTHOR CONTRIBUTIONS

All authors conceived and designed the research plan. AO, YE, and TS collected the samples. AO and JT carried out chemical analyses. AO and TS operated anatomical analyses. All authors contributed to the manuscript writing.

FUNDING

This study was partly supported by a Grant-in-Aid from the Mountain Research Center, University of Tsukuba.

ACKNOWLEDGMENTS

We are grateful to reviewers, Anna Klamerus-Iwan, John Van Stan, Yoshihiko Tsumura, Takashi Kamijo, and laboratory member of Ikurinken for their fruitful advice; Shozo Kato of Kato Limited Partnership Company and staff member of the Ikawa Forest Station, Mountain Research Center, University of Tsukuba for kind support during fieldwork. Miho Sato for providing the photograph of *Juglans mandshurica* var. *sachalinensis* in **Figure 1**.

SUPPLEMENTARY MATERIAL

The Supplementary Material for this article can be found online at: https://www.frontiersin.org/articles/10.3389/ffgc.2021.657850/full#supplementary-material

Supplementary Figure 1 | Cross-section pictures of *Clethra barbinervis*. Abbreviations for anatomical terms are described in the anatomical observations section of the text; epidermis (ep), periderm (pd), phelloderm (pld), cortex (cor), secondary phloem (sp), sieve cell (s), and radiating tissue (r). The photograph was taken at 40×.

Supplementary Figure 2 | Cross-section pictures of *Padus grayana.* Abbreviations for anatomical terms are described in the anatomical observations section of the text; periderm (pd), phellem (pl), phellogen (plg), phelloderm (pld), ritidome (rd), cortex (cor), sclereid (sc), origin sclereid (osc), secondary phloem (sp), parenchyma (p), sieve cell (s), and radiating tissue (r). The photograph was taken at 40×. The picture was combined multiple photos.

Supplementary Figure 3 | Cross-section pictures of *Magnolia obovata.* Abbreviations for anatomical terms are described in the anatomical observations section of the text; periderm (pd), phellem (pl), phellogen (plg), phelloderm (pld), ritidome (rd), cortex (cor), sclereid (sc), origin sclereid (osc), secondary phloem (sp), parenchyma (p), sieve cell (s), radiating tissue (r), and bast fiber (f). The photographs were taken at 40×. Picture was combined multiple photos.

Supplementary Figure 4 | Cross-section pictures of *Castanea crenata.* Abbreviations for anatomical terms are described in the anatomical observations section of the text; periderm (pd), ritidome (rd), cortex (cor), sclereid (sc), origin sclereid (osc), secondary phloem (sp), parenchyma (p), sieve cell (s), radiating tissue (r), and bast fiber (f). The photograph was taken at 40×. The picture was combined multiple photos.

Supplementary Figure 5 | Cross-section pictures of *Abies firma.* Abbreviations for anatomical terms are described in the anatomical observations section of the text; periderm (pd), ritidome (rd), cortex (cor), sclereid (sc), origin sclereid (osc), secondary phloem (sp), parenchyma (p), and radiating tissue (r). The photograph was taken at 40×. Picture was combined multiple photos.

Supplementary Figure 6 | Cross-section pictures of *Tsuga sieboldii.* Abbreviations for anatomical terms are described in the anatomical observations section of the text; periderm (pd), ritidome (rd), cortex (cor), sclereid (sc), and radiating tissue (r). The photograph was taken at 40×. Picture was combined multiple photos.

REFERENCES

Abbasian, P., Attarod, P., Sadeghi, S. M. M., Van Stan, J. T., and Hojjati, S. M. (2015). Throughfall nutrients in a degraded indigenous Fagus orientalis forest and a Picea abies plantation in the of North of Iran. *Forest Syst.* 24:1. doi: 10.5424/fs/2015243-06764

André, F., Jonard, M., and Ponette, Q. (2008). Effects of biological and meteorological factors on stemflow chemistry within a temperate mixed oak–beech stand. *Sci. Total Environ.* 393, 72–83. doi: 10.1016/j.scitotenv.2007.12.002

Angyalossy, V., Pace, M. R., Evert, R. F., Marcati, C. R., Oskolski, A. A., Terrazas, T., et al. (2016). IAWA list of microscopic bark features. *IAWA J.* 37, 517–615. doi: 10.1163/22941932-20160151

Aubrey, D. P. (2020). *Relevance of precipitation partitioning to the tree water and nutrient balance. In Precipitation partitioning by vegetation*. Cham: Springer, 147–162.

Carmo, J. F., Miranda, I., Quilhó, T., Sousa, V. B., Cardoso, S., Carvalho, A. M., et al. (2016). Copaifera langsdorffii bark as a source of chemicals: structural and chemical characterization. *J. Wood Chem. Technol.* 36, 305–317. doi: 10.1080/02773813.2016.1140208

Dovey, S. B., du Toit, B., and de Clercq, W. (2011). Nutrient fluxes in rainfall, throughfall and stemflow in Eucalyptus stands on the Zululand coastal plain, South Africa. *Southern Forests J. Forest Sci.* 73, 193–206. doi: 10.2989/20702620.2011.639506

Fabre, J. H. (1867). *Histoire de la Bûche - Récits sur la Vie des Plantes*. Whitefish, MT: Kessinger Publishing.

Fujita, M., Itokawa, H., and Sashida, Y. (1973). Studies on the components of Magnolia obovata Thunb. II. On the components of the methanol extract of the bark. *Yakugaku Zasshi* 93, 422–428. doi: 10.1248/yakushi1947.93.4_415

Germer, S., Zimmermann, A., Neill, C., Krusche, A. V., and Elsenbeer, H. (2012). Disproportionate single-species contribution to canopy-soil nutrient flux in an Amazonian rainforest. *Forest Ecol. Manage.* 267, 40–49. doi: 10.1016/j.foreco.2011.11.041

Hata, K., and Sogo, M. (1956). Chemical studies on the bark I. Chemical composition and some chemical properties of the bark of Japanese red pine (Pines densiflora S. et Z.). *J. Jap. Forestry Soc.* 38, 473–478. doi: 10.11519/jjfs1953.38.12_473

Hayafuji, A. (2018). Search of antioxidative constituents of the bark of Fraxinus lanuginosa. *JSSE Res. Rep.* 32, 11–14. doi: 10.14935/jsser.32.8_11

Jones, J. M., Heineman, K. D., and Dalling, J. W. (2019). Soil and species effects on bark nutrient storage in a premontane tropical forest. *Plant Soil* 438, 347–360. doi: 10.1007/s11104-019-04026-9

Kazda, M. (1990). "Sequential stemflow sampling for estimation of dry deposition and crown leaching in beech stands," in *Nutrient cycling in terrestrial ecosystems: field methods, application and interpretation*, eds A. F. Harrison, P. Ineson, and O. W. Heal (London: Elsevier Applied Science), 46–55.

Kazda, M., and Glatzel, G. (1986). *Dry deposition, retention and wash-off processes of heavy metals in beech crowns: Analysis of sequentially sampled stemflow. In Atmospheric Pollutants in Forest Areas*. Dordrecht: Springer, 215–222.

Klamerus-Iwan, A., Lasota, J., and Błońska, E. (2020). Interspecific variability of water storage capacity and absorbability of deadwood. *Forests* 11:575. doi: 10.3390/f11050575

Klemm, O., Kuhn, U., Beck, E., Katz, C., Oren, R., Schulze, E. D., et al. (1989). *Leaching and uptake of ions through above-ground Norway spruce tree parts. In Forest decline and air pollution*. Berlin, Heidelberg: Springer, 210–237.

Levia Jr, D. F., and Frost, E. E. (2003). A review and evaluation of stemflow literature in the hydrologic and biogeochemical cycles of forested and agricultural ecosystems. *J. Hydrol.* 274, 1–29. doi: 10.1016/S0022-1694(02)00399-2

Levia, D. F., and Germer, S. (2015). A review of stemflow generation dynamics and stemflow-environment interactions in forests and shrublands. *Rev. Geophys.* 53, 673–714. doi: 10.1002/2015RG000479

Levia, D. F., and Herwitz, S. R. (2005). Interspecific variation of bark water storage capacity of three deciduous tree species in relation to stemflow yield and solute flux to forest soils. *Catena* 64, 117–137. doi: 10.1016/j.catena.2005.08.001

Levia, D. F., Van Stan, J. T., Siegert, C. M., Inamdar, S. P., Mitchell, M. J., Mage, S. M., et al. (2011). Atmospheric deposition and corresponding variability of stemflow chemistry across temporal scales in a mid-Atlantic broadleaved deciduous forest. *Atmospheric Environ.* 45, 3046–3054. doi: 10.1016/j.atmosenv.2011.03.022

Lovett, G. M., and Lindberg, S. E. (1984). Dry deposition and canopy exchange in a mixed oak forest as determined by analysis of throughfall. *J. Appl. Ecol.* 21, 1013–1027. doi: 10.2307/2405064

Lu, J., Zhang, S., Fang, J., Yan, H., and Li, J. (2017). Nutrient fluxes in rainfall, throughfall, and stemflow in *Pinus densata* natural forest of Tibetan Plateau. *Clean - Soil, Air, Water*. 45, 1–9. doi: 10.1002/clen.201600008

Metsalu, T., and Vilo, J. (2015). ClustVis: a web tool for visualizing clustering of multivariate data using Principal Component Analysis and heatmap. *Nucleic Acids Res.* 43, W566–W570.

Ohara, S. (2009). Chemical characteristics of bark tannis and their chemical and enzymatic conversions. *J. Jap. Wood Res. Soc.* 55, 59–68. doi: 10.2488/jwrs.55.59

Oka, A., Takahashi, J., Endoh, Y., and Seino, T. (2019). Effect of bark characteristics on stemflow and its chemical components. *Chubu Forestry Res.* 67, 29–34. doi: 10.18999/chufr.67.29

Oka, A., Takahashi, J., Endoh, Y., and Seino, T. (2021). Bark effects on stemflow chemistry in a Japanese temperate forest I. The role of bark surface morphology. *Front. Forests Global Change* 4:654375. doi: 10.3389/ffgc.2021.654375

Pausas, J. G. (2015). Bark thickness and fire regime. *Funct. Ecol.* 29, 315–327. doi: 10.1111/1365-2435.12372

Rosell, J. A., Gleason, S., Méndez-Alonzo, R., Chang, Y., and Westoby, M. (2014). Bark functional ecology: Evidence for tradeoffs, functional coordination, and environment producing bark diversity. *New Phytol.* 201, 486–497. doi: 10.1111/nph.12541

Seino, T., and Endoh, Y. (2019). Ecological positions of conifers on the stand structure of the temperate forest in central Japan. *Chubu Forestry Res.* 67, 25–28. doi: 10.18999/chufr.67.25

Shibata, H., and Sakuma, T. (1996). Canopy modification of precipitation chemistry in deciduous and coniferous forests affected by acidic deposition. *Soil Sci. Plant Nutr.* 42, 1–10. doi: 10.1080/00380768.1996.10414683

Shibui, H., and Sano, Y. (2018). Structure and formation of phellem of Betula maximowicziana. *IAWA J.* 39, 18–36. doi: 10.1163/22941932-20170186

Shimaji, K., Sudo, S., and Harada, H. (1976). *Organization of Wood*. Tokyo: Morikita Publishing.

Simpson, M. G. (2019). *Evolution and Diversity of Vascular Plants. In Plant Systematics*, Third Edn. Cambridge, MA: Academic Press, 75–130.

Staelens, J., De Schrijver, A., and Verheyen, K. (2007). Seasonal variation in throughfall and stemflow chemistry beneath a European beech (Fagus sylvatica) tree in relation to canopy phenology. *Can. J. Forest Res.* 37, 1359–1372. doi: 10.1139/X07-003

Staelens, J., Houle, D., De Schrijver, A., Neirynck, J., and Verheyen, K. (2008). Calculating dry deposition and canopy exchange with the canopy budget model: review of assumptions and application to two deciduous forests. *Water Air Soil Pollut.* 191, 149–169. doi: 10.1007/s11270-008-9614-2

Trockenbrodt, M. (1990). Survey and discussion of the terminology used in bark anatomy. *IAWA Bull.* 11, 141–166. doi: 10.1163/22941932-90000511

Turpault, M. P., Kirchen, G., Calvaruso, C., Redon, P. O., and Dincher, M. (2021). Exchanges of major elements in a deciduous forest canopy. *Biogeochemistry* 152, 51–71. doi: 10.1007/s10533-020-00732-0

Van Stan, J. T., Dymond, S. F., and Klamerus-Iwan, A. (2021). Bark-water interactions across ecosystem states and fluxes. *Front. Forests Global Change* 4:660662. doi: 10.3389/ffgc.2021.660662

Van Stan, J. T., Lewis, E. S., Hildebrandt, A., Rebmann, C., and Friesen, J. (2016). Impact of interacting bark structure and rainfall conditions on stemflow variability in a temperate beech-oak forest, central Germany. *Hydrol. Sci. J.* 61, 2071–2083. doi: 10.1080/02626667.2015.1083104

Wetzel, S., Demmers, C., and Greenwood, J. S. (1989). Seasonally fluctuating bark proteins are a potential form of nitrogen storage in three temperate hardwoods. *Planta* 178, 275–281. doi: 10.1007/BF00391854

Wetzel, S., and Greenwood, J. S. (1989). Proteins as a potential nitrogen storage compound in bark and leaves of several softwoods. *Trees* 3, 149–153. doi: 10.1007/BF00226650

Wolterbeek, H. T., Verburg, P. K., Wamelink, G. W. W., and Van Dobben, H. (1996). Relations between sulphate, ammonia, nitrate, acidity and trace element

concentrations in tree bark in the Netherlands. *Environ. Monit. Assess.* 40, 185–201. doi: 10.1007/BF00414391

Xu, X., Yu, X., Mo, L., Xu, Y., Bao, L., and Lun, X. (2019). Atmospheric particulate matter accumulation on trees: A comparison of boles, branches and leaves. *J. Cleaner Produc.* 226, 349–356. doi: 10.1016/j.jclepro.2019.04.072

Zabel, R. A., and Morrell, J. J. (2020). "The decay setting: Some structural, chemical, and moisture features of wood features of wood in relation to decay development," in *Wood Microbiology*, Second Edn, eds R. A. Zabel and J. J. Morrell (Cambridge, MA: Academic Press), 149–183. doi: 10.1016/b978-0-12-819465-2.00006-1

Conflict of Interest: The authors declare that the research was conducted in the absence of any commercial or financial relationships that could be construed as a potential conflict of interest.

frontiers in Forests and Global Change

MINI REVIEW
published: 27 July 2021
doi: 10.3389/ffgc.2021.675299

Beneath the Bark: Assessing Woody Stem Water and Carbon Fluxes and Its Prevalence Across Climates and the Woody Plant Phylogeny

Z. Carter Berry[1†], Eleinis Ávila-Lovera[2†], Mark E. De Guzman[3†], Kimberly O'Keefe[4†] and Nathan C. Emery[5†]*

[1] Department of Biology, Wake Forest University, Winston-Salem, NC, United States, [2] Smithsonian Tropical Research Institute, Panama City, Panama, [3] Department of Environmental Science and Policy, University of California, Davis, Davis, CA, United States, [4] Department of Ecosystem Science and Management, University of Wyoming, Laramie, WY, United States, [5] Department of Plant Biology, Michigan State University, East Lansing, MI, United States

OPEN ACCESS

Edited by:
John T. Van Stan, Georgia Southern University, United States

Reviewed by:
Brett Wolfe, Louisiana State University Agricultural Center, United States
Salli F. Dymond, University of Minnesota Duluth, United States

***Correspondence:**
Z. Carter Berry
zcberry@gmail.com

† These authors have contributed equally to this work

Specialty section:
This article was submitted to Forest Hydrology, a section of the journal Frontiers in Forests and Global Change

Received: *02 March 2021*
Accepted: *25 June 2021*
Published: *27 July 2021*

Citation:
Berry ZC, Ávila-Lovera E, De Guzman ME, O'Keefe K and Emery NC (2021) Beneath the Bark: Assessing Woody Stem Water and Carbon Fluxes and Its Prevalence Across Climates and the Woody Plant Phylogeny. Front. For. Glob. Change 4:675299. doi: 10.3389/ffgc.2021.675299

While woody stems are known to influence carbon and water dynamics, direct exchange with the atmosphere is seldom quantified, limiting our understanding of how these processes influence the exchange of mass and energy. The presence of woody stem chlorophyll in a diversity of climates and across a range of species suggests an evolutionary advantage to sustaining carbon assimilation and water relations through permeable stem tissue. However, no formal evaluation of this hypothesis has been performed. In this mini-review, we explore the interactions between woody stems and the atmosphere by examining woody stem photosynthesis and bark-atmosphere water exchange. Specifically, we address the following questions: (1) How do water and carbon move between the atmosphere and woody stems? (2) In what climate space is woody stem photosynthesis and bark water uptake advantageous? (3) How ubiquitous across plant families is woody stem photosynthesis and bark-atmosphere water exchange? In the literature, only seven species have been identified as exhibiting bark water uptake while over 300 species are thought to conduct woody stem photosynthesis. The carbon dioxide and water gained from these processes can offset respiration costs and improve plant water balance. These species span diverse biomes suggesting a broad prevalence of bark-atmosphere permeability. Finally, our results demonstrate that there may be an evolutionary component as demonstrated by a high Pagel's lambda for the presence of stem photosynthesis. We end with recommendations for future research that explores how bark water and carbon interactions may impact plant function and mass flow in a changing climate.

Keywords: woody stem interaction with the atmosphere, woody stem photosynthesis, phylogenetic signal, water flux, carbon flux, bark water uptake

INTRODUCTION

The global cycling of water and carbon is driven by small-scale forces that move these molecules through different pools in the environment. Plants play a major role in this cycling by absorbing and releasing both water and carbon through multiple plant organs. Most research has focused on leaves and roots as the integral locations where water and carbon fluxes occur while suberized tissue,

such as stem bark, is stereotyped as an impermeable, enigmatic shield. Bark is known to protect plants from pathogens and fire (Morris and Jansen, 2016; Loram-Lourenco et al., 2020), provide mechanical support (Niklas, 1999), and transport and store various compounds (Lintunen et al., 2016; Ilek et al., 2021). The role of permeable bark in governing plant carbon and water budgets through direct exchange of these molecules with the atmosphere is largely considered trivial. Stems release carbon dioxide (respiration) and water as other plant surfaces do. The movement of these molecules can occur in the opposite direction too, but these phenomena are less studied. Justifiably, measured rates of stem photosynthesis and water uptake are generally small compared to total plant and ecosystem fluxes. Nevertheless, recent work has shown that bark carbon dioxide and water uptake can mitigate environmental stress by providing an additional subsidy of carbon and water (e.g., Teskey et al., 2008; Ávila et al., 2014; Earles et al., 2016). For example, stem net photosynthesis can range from 0.5 in *Syringa vulgaris* (Pilarski, 2002) to 43.9 μmol $m^{-2}s^{-1}$ in *Bebbia juncea* (Ávila-Lovera et al., 2019) and, across several species, compensate for all of the carbon that would otherwise be lost to the atmosphere through respiration. To date, at least 341 species have been empirically shown to exhibit bark water uptake or woody stem photosynthesis (7 for water, 334 for carbon; **Supplementary Table 1**). While this count is surely a subset of the total prevalence and significance of these processes, we leverage these studies to provide predictions and hypotheses about the broad role of bark in carbon and water exchange with the atmosphere.

Woody stem carbon dioxide uptake is largely considered to be an evolutionary relic because the earliest land plants primarily photosynthesized through their stems (Stewart and Rothwell, 1993; Nilsen, 1995). Woody stem assimilation of carbon dioxide can be classified into two types: *stem net photosynthesis* (Ávila et al., 2014), in which stems can directly absorb carbon dioxide from the atmosphere, and *stem recycling photosynthesis*, in which stems utilize carbon dioxide from internal respiration of root and stem tissue and often lack stomata on the stem (Nilsen, 1995; Ávila et al., 2014). Stem recycling photosynthesis can account for 7–126% of carbon dioxide refixation (Teskey et al., 2008; Ávila et al., 2014). The actual site of chlorophyll and woody stem photosynthesis can vary widely from the inner bark (living cortex) all the way to the pith (Cannon, 1908). Considerable work has explored carbon reassimilation dynamics within stems but only recently has research identified permeable bark as a novel source for water and carbon in woody species. Investigations of stem net photosynthesis has been largely limited by methods, because leaf chambers for gas exchange systems are not able to accommodate large stems or detect low fluxes.

The few studies that have explored this pathway find that carbon uptake is commonly facilitated by lenticels, stomata, cracks, or wounds (Grosse, 1997; Groh et al., 2002; Teskey and McGuire, 2005). The process of water uptake is less well understood, but likely occurs via symplastic pathways through hydrophilic regions of the phellem cell wall (Schönherr and Ziegler, 1980; Earles et al., 2016). The direct absorption of carbon and water from the atmosphere relies on similar bark structure and porosity meaning that species capable of carbon dioxide uptake likely can take up water as well. Liu et al. (2019), for instance, found that stem photosynthesis promoted bark water uptake and embolism repair in *Salix matsudana*. The interconnected exchange of carbon and water through permeable bark also suggests that, while bark water uptake is considerably understudied, hypotheses regarding this process may be developed from broad scale assessments of the more commonly studied stem photosynthesis.

In this mini-review, we survey the literature to demonstrate the prevalence and significance of bark in affecting woody stem carbon and water dynamics. We define woody stems as stems with secondary growth, i.e., having wood with a combination of living and non-living cells exterior to the cambium. Collectively, all the tissues beyond the cambium are known as bark. Our composite of all species where water or carbon dioxide uptake has occurred allows us to assess broad-scale environmental factors affecting bark permeability to these molecules. We then use two publicly available, large data sets from China (Prentice et al., 2011; Wang et al., 2018; accessed in TRY, Kattge et al., 2020) with information about the prevalence of stem photosynthesis to consider the biophysical environments and clades where we might expect significant bark carbon dioxide and water uptake to occur. These data allow us to hypothesize climates and contexts where researchers should explore the role of woody stem water and carbon uptake. With these new ideas, we hope to inspire colleagues to investigate stem gas and water exchange in their study systems and enhance our knowledge base of these understudied processes.

How Do Water and Carbon Move Between Woody Stems and the Atmosphere?

As with water movement throughout the soil-plant-atmosphere continuum, water is able to move radially through woody tissue based on water potential gradients. This movement can be bidirectional – water can be lost to evaporation or absorbed through bark water uptake. The few studies focused on bark water uptake investigated how water absorbed by bark affects xylem hydraulic function and whole plant water status (e.g., Earles et al., 2016). The amount of water mobilized and the directionality will depend on broad anatomical features such as the differences in space partitioning among vessel, fiber, and xylem parenchyma cell types, emergent hydraulic functional traits (e.g., wood density and capacitance; Pratt and Jacobsen, 2017), and environmental drivers such as soil water availability and vapor pressure deficit (VPD) (Laur and Hacke, 2014; Fontes et al., 2020). Stems with stomata have conductance values that range from 0.03 mmol $m^{-2}s^{-1}$ in *Ruscus microglossum* (cuticular conductance) (Pivovaroff et al., 2014) to 472.64 mmol $m^{-2}s^{-1}$ in *B. juncea* (maximum stomatal conductance) (Ávila-Lovera et al., 2019), which can result in substantial water loss. Stems without stomata have conductance values ranging from 0.86 to 12.98 mmol $m^{-2}s^{-1}$ (Wolfe, 2020). More recent research focused on the absorption of water by woody stems demonstrated that bark water uptake likely requires high relative humidity or wet surfaces but can improve plant water status and xylem hydraulic

conductivity (Earles et al., 2016; Carmichael et al., 2020). While still sparse in number, the current literature suggests that bark water uptake likely benefits plant hydraulic functioning.

Woody stems that have the ability to photosynthesize have a protective tissue that is permeable to light and movement of carbon dioxide and water. Some species with secondary growth (i.e., secondary xylem or wood) delay periderm formation (Gibson, 1983) and maintain their epidermis with stomata during the lifetime of the stem (Lindorf et al., 2006). These stems appear green and exchange carbon dioxide and water regularly with the surrounding atmosphere. Similar to leaves, stem net photosynthesis responds to light availability, atmospheric carbon dioxide concentration, VPD, and air temperature (Nilsen, 1995). CO_2 concentrations inside stems are an order of magnitude higher than atmospheric CO_2 concentration: 0.1–26.3% in stems (Teskey et al., 2008) vs. ∼0.04% in air, hence most CO_2 movement occurs from the stem to the atmosphere. However, when stem CO_2 concentrations decreased to values lower than that of the atmosphere, carbon dioxide from the atmosphere can diffuse through the stem protective layers and be assimilated within the bark (Berveiller et al., 2007). Even in stems with an epidermis but closed stomata, water, and carbon dioxide can continue moving through the cuticle given sufficient concentration gradients (Ávila-Lovera et al., 2017).

The coordination of woody stem photosynthesis and bark water uptake is likely linked but rarely studied in tandem. One recent study on the coordination of woody stem photosynthesis and hydraulic traits showed that there is a positive relationship between stem photosynthetic rate and cuticular conductance to water (Ávila-Lovera et al., 2017). This suggests that structures enabling permeability in periderms and cuticles have the ability to influence carbon dioxide uptake, water loss, and potentially water uptake. Another study found that photosynthetic cells in the stems can increase the amount of water stored in the tissue through modification of the starch supply, influencing the osmotic potential of water through the bark (Liu et al., 2019). Bark conductance to water and carbon dioxide, and the environmental drivers that lead to bidirectional exchange will be key parameters for integrating carbon and water budgets. What remains unknown is the magnitude of these carbon and water fluxes, how prevalent they are, how they vary in time and space, and how they influence the whole-plant carbon and water economy.

In What Climate Space Are Bark Water Uptake and Woody Stem Photosynthesis Advantageous?

Stem net photosynthesis may benefit plant functioning by maintaining some carbon gain during periods of low or no leaf gas exchange (Nilsen and Sharifi, 1997) and by increasing water-use efficiency (Osmond et al., 1987). Stem water uptake may also benefit plants by promoting embolism repair (Earles et al., 2016; Liu et al., 2019). Consequently, permeable bark should be more common in climate conditions where these physiological effects are particularly advantageous. Photosynthetic woody stems should be beneficial in warm, dry environments where an additional source of carbon and, consequently, enhanced whole-plant water-use efficiency may be adaptive (e.g., high-latitude deserts; Ávila et al., 2014). Bark water uptake may also be adaptive in these ecosystems if bark wetting from small precipitation or fog/dew events facilitates localized hydraulic recovery despite a generally dry environment (Earles et al., 2016). For example, Earles et al. (2016) demonstrates that branch wetting from fog events improves plant water status in coastal redwood trees that experience summer drought. However, to our knowledge, this hypothesis has not been formally tested. Here, we explored if this is supported by mapping the occurrence of woody stem photosynthesis and bark water uptake in climatic niche space using Whittaker biome classifications (Whittaker, 1962). We created two figures that plotted: (1) occurrences of woody stem photosynthesis, bark conductance, and bark water uptake from our literature review, and (2) occurrences of reported stem photosynthesis from two datasets that surveyed the flora of China (Prentice et al., 2011; Wang et al., 2018).

Woody stem photosynthesis was widespread across Whittaker biomes for both our literature review (**Figure 1**), and the Prentice et al. (2011) and Wang et al. (2018) datasets (**Figure 2**). As expected, woody stem photosynthesis reported within our literature review was prevalent across warm, dry biomes such as temperate grasslands/deserts and subtropical deserts. However, this phenomenon was also observed across tropical seasonal forest/savanna, woodland/shrubland, boreal forest, temperate seasonal forest, and temperate rainforest biomes, and spanned a climate range of 6.7–248.1 cm of mean annual precipitation (MAP) and −2.2–28.8°C of mean annual temperature (MAT). Stem photosynthesis reported by Prentice et al. (2011) and Wang et al. (2018) showed a similar distribution across climate space but did not occur in temperate rain forest or subtropical desert (MAP 1.5–186.8 cm and MAT −5.3 to 22.9°C). Bark water uptake, which was investigated in far fewer studies from our literature review (seven species; **Supplementary Table 1**), occurred in temperate grassland/desert, woodland/shrubland, temperate seasonal forest, and tropical seasonal forest/savanna (MAP 48.7–131.8 mm and MAT 4.3–20.2°C). While there is bias in the spatial sampling of these biomes, these results demonstrate that stem photosynthesis and bark water uptake occur across a wide range of temperature and rainfall environments and are thus likely more prevalent than previously considered.

While woody stem photosynthesis likely occurs in most biomes, broad-scale climate factors such as MAP and MAT might not be good predictors of where this phenomenon occurs. Rather, variability in small-scale environmental factors (e.g., topography, soil texture, water availability in the rhizosphere, and light availability) may be more important environmental drivers for bark carbon dioxide uptake. Although a large number of observations occurred in subtropical desert and woodland/shrublands, these data do not necessarily indicate that woody stem photosynthesis is more likely to occur in this climate space simply because much of the existing woody stem photosynthesis research has occurred in these ecosystems (e.g., Ehleringer et al., 1987; Comstock et al., 1988; Tinoco-Ojanguren, 2008; Pivovaroff et al., 2016; Ávila-Lovera et al., 2019). Likewise, few studies have investigated bark water uptake

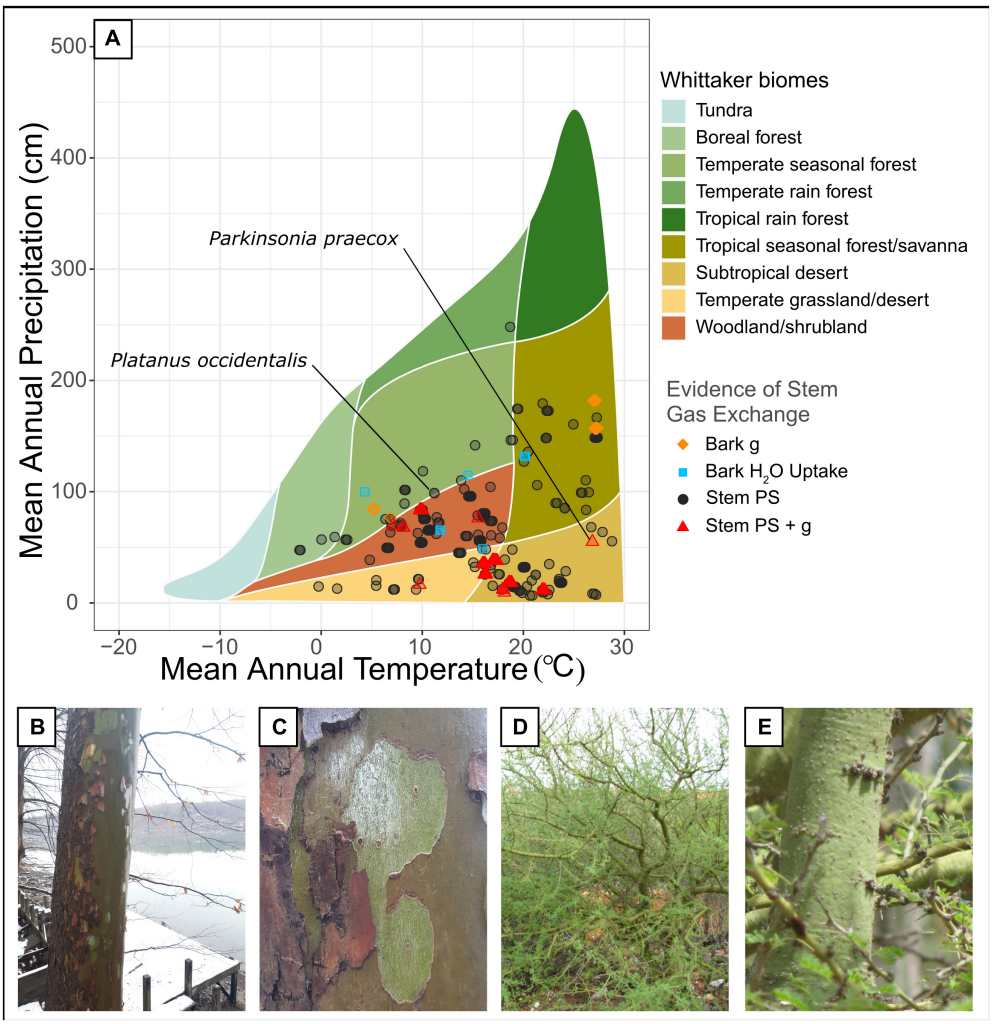

FIGURE 1 | (A) Whittaker plot showing the biomes where stem carbon dioxide and water exchange have been quantified (data come from **Supplementary Table 1**). Shown are observations where only bark photosynthesis was observed (including both net CO_2 uptake and CO_2 reassimilation, "Stem PS"), bark photosynthesis and bark conductance were both observed ("Stem PS + g"), only bark conductance was observed ("Bark g"), and bark water uptake was observed ("Bark H_2O Uptake"). Observations were plotted as semi-transparent points in order to improve clarity of clustered points. **(B,C)** Sycamore tree (*Platanus occidentalis*) with green, deciduous bark, photographed at Cheat Lake, West Virginia (photos by N. Emery). **(D,E)** Foothill Palo Verde (*Parkinsonia praecox*) with bright green bark, photographed in a xerophytic woodland in Venezuela (photos by W. Tezara).

(e.g., Mayr et al., 2014; Earles et al., 2016; Yu et al., 2018; Liu et al., 2019), inherently limiting its known distribution across climate space. Given that stem carbon and water uptake should be linked through permeable periderms and cuticles (Ávila-Lovera et al., 2017), stem water uptake likely occurs in similar climate space as woody stem photosynthesis. This notion is further supported by our observation that stem conductance was reported within a similar climate space as stem photosynthesis (**Figure 1**). This analysis opens up new opportunities for researchers to explore the interwoven processes of woody stem photosynthesis and bark water uptake across different biomes and ecological gradients to better understand their global frequency and distribution, and to determine the role these processes may play in mediating plant responses to a changing climate.

How Ubiquitous Across Plant Families Is Woody Stem Photosynthesis and Bark-Atmosphere Water Exchange?

Permeable stems are likely the ancestral state of all terrestrial vascular plants, as some of the earliest land plants conducted photosynthesis exclusively from stems (Stewart and Rothwell, 1993; Nilsen, 1995). However, as plants evolved woody tissue and secondary phloem (inner bark), this permeability might have been replaced with thicker, more robust bark, which inherently decreases light transmission (Rosell et al., 2015). Within species, younger, more light-exposed stems tend to have higher chlorophyll content (Pfanz et al., 2002), suggesting that bark permeability is age-related and light interception may be a primary factor limiting the retention of this trait

(Pfanz and Aschan, 2001, Aschan and Pfanz, 2003). For example, Rosell et al. (2015) found all 85 species studied had photosynthesis in small stems but only 43 of those species retained this trait in main trunks. In our data set, the presence of stem photosynthesis exists across a diversity of plant families (**Figure 2**). Whether this is a reversal to an ancestral trait or convergent evolution requires further investigation.

We conducted a phylogenetic analysis using Pagel's λ to determine if stem photosynthesis had a phylogenetic signal across a broad range of woody species. We only analyzed woody plant species based on life form designation within the data sets (see **Supplementary Methods 1**). Our phylogenetic analysis of 685 woody plant species (Prentice et al., 2011; Wang et al., 2018) indicates that stem photosynthesis is clustered across the tree with some families containing many species exhibiting stem photosynthesis and others with few (**Figure 2**). This is demonstrated by the high Pagel's λ ($\lambda = 0.87$, $p < 0.0001$) which indicates a significant phylogenetic signal in stem photosynthesis (Pagel, 1999). A significant phylogenetic signal indicates that the similarity between species is related to their phylogenetic relatedness (Losos, 2008). Both mapping the stem photosynthesis trait and estimating Pagel's λ suggest that relatives resemble each other more than they resemble species sampled at random from the tree (Blomberg and Garland, 2002). The uneven distribution of stem photosynthesis across the vascular plant phylogeny suggests that multiple evolutionary events may have led to permeable bark tissue that facilitates carbon dioxide and water exchange (Nilsen, 1995; Gibson, 1996; Ávila-Lovera and Ezcurra, 2016). Thus, retaining bark permeability in mature stems may indeed provide a functional advantage for woody plants. However, a few limitations should be noted. First, it is possible that the analysis cannot separate stem photosynthesis from stem and plant size. In other words, plants that are smaller would have smaller stems and thus be more likely to be registered as having photosynthetic stems. Secondly, we cannot know from the data set whether the species exhibit stem recycling photosynthesis or if they take up carbon dioxide from the atmosphere although both types improve carbon balance of plants. Ultimately, this large data set provides great power for analysis but also comes with limitations of extensive inference. This leaves many fascinating questions around stem photosynthesis and the potential prevalence of bark water uptake. Future work that investigates bark water uptake across a broad range of species and climate space would also be able to utilize these data to reveal novel insights regarding the prevalence of bark water uptake across the woody plant phylogeny and its functional significance.

Similar to the biome analysis, we find stem photosynthesis represented across a broad swath of species, ranging from gymnosperms (Ephedraceae and Gnetaceae, 269–104 Mya) to Asteraceae (91–36 Mya). Out of a total of 719 species reported in the data set, stem photosynthesis was present in 125 species and absent in 594 species. Trees, shrubs, and vines were all represented including temperate 30 m tall trees (*Machilus yunnanensis*, Lauraceae), desert shrubs (*Atraphaxis bracteata*, Polygonaceae), and tropical climbing vines (*Psychotria serpens*, Rubiaceae). The widespread prevalence of stem photosynthesis across our woody plant phylogeny suggests that this trait is likely advantageous and possibly evolves under different abiotic and biotic pressures. Given the similar constraints of carbon dioxide and water exchange with the atmosphere, we infer that stem permeability is adaptive as well.

UNANSWERED QUESTIONS AND CONCLUSIONS

Across biomes, climates, and clades, stems absorb water and photosynthesize. Bark water and carbon dioxide exchange can repair embolisms (Earles et al., 2016), reduce localized water stress, recover up to 100% of respired carbon, and can even result in a net carbon gain (Teskey et al., 2008). But as with most scientific endeavors, new discovery opens up many new unanswered questions. First and foremost, methods that increase the precision and throughput capacity of quantifying carbon and water uptake would dramatically increase research capacity. This should include exploring new tracers, engineering new sensors to detect uptake, and permanent modification to current gas exchange chambers. Additional mechanistic and functional questions fall into two broad categories: (1) the structural and microclimatic conditions that drive woody stem water–carbon exchange and consequences for physiological functioning, and (2) the implications for these processes on ecosystem water–carbon budgets, natural selection, and climate change.

To determine the drivers of woody stem water and carbon exchange, studies need to simultaneously explore woody stem structural variation combined with microclimatic drivers that will affect these fluxes. Similar to leaves, specific bark area is positively related to stem photosynthetic rate (Cernusak and Marshall, 2000; Berveiller et al., 2007; Ávila-Lovera et al., 2017), meaning that long and thin stems have higher rates than thick, short stems. Age is another factor that affects the ability of stems to conduct photosynthesis, with increasingly older stems having lower photosynthetic capacity (Nilsen et al., 1989; Aschan et al., 2001). But to what extent do specific bark area and age affect bark water uptake and do these relationships hold across broad bark anatomies of the plant kingdom? From there, understanding the implications of bark permeability and other traits to whole plant function will also be important to unravel. For example, does a dew event in the midst of a summer drought improve plant hydraulic function and photosynthetic rates through direct bark uptake? Are the water and carbon balances of woody stems tightly linked to leaf carbon and water dynamics? Additionally, is bark permeability to water and carbon comparable and consistent across all contexts? What microclimatic conditions promote bark water and carbon uptake? Do these processes tend to occur in similar environmental conditions or at separate moments, allowing for plants to maximize carbon and water balance at different times? Many of these questions are beginning to be explored, with fascinating results, but a more holistic understanding is still needed.

Finally, even fewer studies have explored bark water and carbon uptake with a focus on larger scale implications.

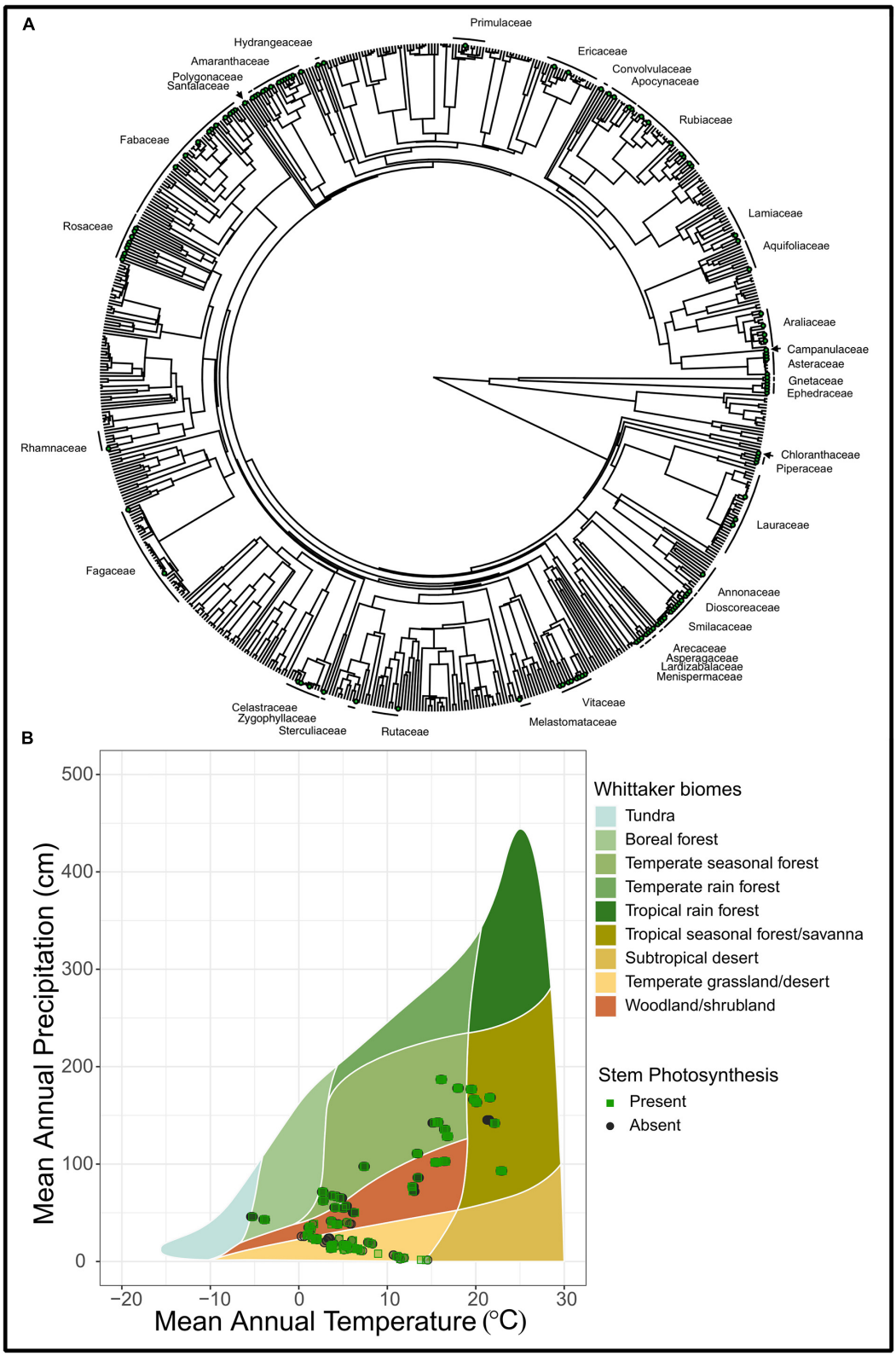

FIGURE 2 | (A) A phylogenetic tree of 685 species from Prentice et al. (2011) and Wang et al. (2018) that demonstrate stem photosynthesis. Green points represent species with stem photosynthesis and families that have at least a single species are labeled on the outside of the tree. **(B)** A Whittaker plot illustrating the climatic space of stem photosynthesis. Shown are observations where stem photosynthesis was recorded as present ("Present") and those where stem photosynthesis was recorded as absent ("Absent"). Out of a total of 719 species in this plot, stem photosynthesis was present in 125 species and absent in 594 species. Observations were plotted as semi-transparent points in order to improve clarity of clustered points.

While bark water and carbon fluxes are small compared to ecosystem budgets, there are likely periods where they play a disproportionate role. Can we identify when woody stem exchange is important and use that information to refine ecosystem models? How much water can be absorbed by bark in different species? Here we find a phylogenetic pattern to woody stem photosynthesis, but it is still unclear if this leads to a competitive advantage for some plant species. Do the clear benefits to carbon or water balance lead to some greater likelihood for survival and reproduction? If so, has this trait been lost and regained in certain clades and what are the conditions driving the reemergence? All of these questions should also be considered within the context of climate change. As ecosystems experience more variable rainfall patterns, temperatures, and frequencies of extreme events (e.g., drought, fire, and flood), how will that affect the role of bark exchange in species persistence? Will this alternative strategy for maintaining physiological function drive ecosystem resilience following extreme events? These questions all push at the boundaries of our understanding and will continue to reveal new linkages between plant and ecosystem processes.

AUTHOR CONTRIBUTIONS

All authors listed have contributed equally and made a substantial, direct and intellectual contribution to the work, and approved if for publication.

ACKNOWLEDGMENTS

We would like to genuinely thank all contributions to the two data sets that were used to conduct our analyses. This paper would not be possible without the data sets in Prentice et al. (2011) and Wang et al. (2018). We also would like to acknowledge that some of these data were accessed through the TRY database requests 12687 and 12688. We are thankful for the time, support, and conversations had with each other as fellow early-career scientists. We would also like to acknowledge our grant support: USDA-NIFA Award 2020-67014-30916 (ZC Berry), USDA-NIFAAward 2020-67014-30915 (E Avila-Lovera), Smithsonian Tropical Research Institute Earl S. Tupper Postdoctoral Fellowship (E Avila-Lovera), and DOE TES Award DESC0019037 (K O'K).

SUPPLEMENTARY MATERIAL

The Supplementary Material for this article can be found online at: https://www.frontiersin.org/articles/10.3389/ffgc.2021.675299/full#supplementary-material

Supplementary Table 1 | List of species that exhibit evidence of bark CO_2 uptake (Bark PS), bark conductance (Bark g), bark CO_2 uptake, and bark conductance (Bark PS + g), and bark water uptake. Also shown are corresponding citations and GPS coordinates of observation, when available.

Supplementary Methods 1 | Description of the methods used to conduct the literature review, estimate phylogenetic signal and trait mapping, and to classify stems as "photosynthetic" in the China Plant Trait Database.

REFERENCES

Aschan, G., and Pfanz, H. (2003). Non-foliar photosynthesis–a strategy of additional carbon acquisition. *Flora-Morphol. Distrib. Funct. Ecol. Plants* 198, 81–97. doi: 10.1078/0367-2530-00080

Aschan, G., Wittmann, C., and Pfanz, H. (2001). Age-dependent bark photosynthesis of aspen twigs. *Trees* 15, 431–437. doi: 10.1007/s004680100120

Ávila, E., Herrera, A., and Tezara, W. (2014). Contribution of stem CO_2 fixation to whole-plant carbon balance in nonsucculent species. *Photosynthetica* 52, 3–15. doi: 10.1007/s11099-014-0004-2

Ávila-Lovera, E., and Ezcurra, E. (2016). "Stem-succulent trees from the Old and New World tropics," in *Tropical tree physiology*, eds G. Goldstein and L. S. Santiago (Switzerland: Springer), 45–65. doi: 10.1007/978-3-319-27422-5_3

Ávila-Lovera, E., Haro, R., Ezcurra, E., and Santiago, L. S. (2019). Costs and benefits of photosynthetic stems in desert species from southern California. *Funct. Plant Biol.* 46, 175–186. doi: 10.1071/fp18203

Ávila-Lovera, E., Zerpa, A. J., and Santiago, L. S. (2017). Stem photosynthesis and hydraulics are coordinated in desert plant species. *New Phytol.* 216, 1119–1129. doi: 10.1111/nph.14737

Berveiller, D., Kierzkowski, D., and Damesin, C. (2007). Interspecific variability of stem photosynthesis among tree species. *Tree Physiol.* 27, 53–61. doi: 10.1093/treephys/27.1.53

Blomberg, S. P., and Garland, T. (2002). Tempo and mode in evolution: phylogenetic inertia, adaptation and comparative methods. *J. Evol. Biol.*15, 899–910. doi: 10.1046/j.1420-9101.2002.00472.x

Cannon, W. A. (1908). *The topography of the chlorophyll apparatus in desert plants*. Washington, DC: Carniege Institution of Washington.

Carmichael, M. J., White, J. C., Cory, S. T., Berry, Z. C., and Smith, W. K. (2020). Foliar water uptake of fog confers ecophysiological benefits to four common tree species of southeastern freshwater forested wetlands. *Ecohydrology* 13:e2240.

Cernusak, L., and Marshall, J. (2000). Photosynthetic refixation in branches of western white pine. *Funct. Ecol.* 14, 300–311. doi: 10.1046/j.1365-2435.2000.00436.x

Comstock, J. P., Cooper, T. A., and Ehleringer, J. R. (1988). Seasonal patterns of canopy development and carbon gain in nineteen warm desert shrub species. *Oecologia* 75, 327–335. doi: 10.1007/bf00376933

Earles, J. M., Sperling, O., Silva, L. C., McElrone, A. J., Brodersen, C. R., North, M. P., et al. (2016). Bark water uptake promotes localized hydraulic recovery in coastal redwood crown. *Plant Cell Environ.* 39, 320–328. doi: 10.1111/pce.12612

Ehleringer, J. R., Comstock, J. P., and Cooper, T. A. (1987). Leaf-twig carbon isotope ratio differences in photosynthetic-twig desert shrubs. *Oecologia* 71, 318–320. doi: 10.1007/bf00377301

Fontes, C. G., Fine, P. V. A., Wittmann, F., Bittencourt, P. R. L., Piedade, M. T. F., Higuchi, N., et al. (2020)). Convergent evolution of tree hydraulic traits in Amazonian habitats: implications for community assemblage and vulnerability to drought. *New Phytol.* 228, 106–120. doi: 10.1111/nph.16675

Gibson, A. C. (1983). Anatomy of photosynthetic old stems of nonsucculent dicotyledons from North American deserts. *Bot. Gaz.* 144, 347–362. doi: 10.1086/337383

Gibson, A. C. (1996). *Structure-function relations of warm desert plants*. Berlin: Springer.

Groh, B., Hübner, C., and Lendzian, K. J. (2002). Water and oxygen permeance of phellems isolated from trees: the role of waxes and lenticels. *Planta* 215, 794–801. doi: 10.1007/s00425-002-0811-8

Grosse, W. (1997). "Gas transport of trees," in *Trees: contributions to modern tree physiology*, eds H. Rennenberg, W. Escrich, and H. Ziegler (Leiden: Backhuys), 57–74.

Ilek, A., Siegert, C. M., and Wade, A. (2021). Hygroscopic contriutions to bark water storage and controls exerted by internal bark stucture over water vapor absorption. *Trees* 35, 831–843. doi: 10.1007/s00468-021-02084-0

Kattge, J., Boenisch, G., and Diaz, S. (2020). TRY plant trait database - enhanced coverage and open access. *Glob. Change Biol.* 26, 119–188.

Laur, J., and Hacke, U. G. (2014). Exploring P icea glauca aquaporins in the context of needle water uptake and xylem refilling. *New Phytol.* 203, 388–400. doi: 10.1111/nph.12806

Lindorf, H., Parisca, L. D., and Rodríguez, P. (2006). *Botánica. Clasificación, estructura, reproducción., 2nd. edition*. Caracas: Ediciones de la Biblioteca de la Universidad Central de Venezuela.

Lintunen, A., Paljakka, T., Jyske, T., Peltoniemi, M., Sterck, F., Von Arx, G., et al. (2016). Osmolality and non-structural carbohydrate composition in the secondary phloem of trees across a latitudinal gradient in Europe. *Front. Plant Sci.* 7:726. doi: 10.3389/fpls.2016.00726

Liu, J., Gu, L., Yu, Y., Huang, P., Wu, Z., Zhang, Q., et al. (2019). Corticular photosynthesis drives bark water uptake to refill embolized vessels in dehydrated branches of Salix matsudana. *Plant Cell Environ.* 42, 2584–2596. doi: 10.1111/pce.13578

Loram-Lourenco, L., Farnese, F. D. S., Sousa, L. F. D., Alves, R. D. F. B., Andrade, M. C. P. D., Almeida, S. E. D. S., et al. (2020). A structure shaped by fire, but also water: ecological consequences of the variability in bark properties across 31 species from the brazilian cerrado. *Front. Plant Sci.* 10:1718. doi: 10.3389/fpls.2019.01718

Losos, J. B. (2008). Phylogenetic niche conservatism, phylogenetic signal and the relationship between phylogenetic relatedness and ecological similarity among species. *Ecol. Lett.* 11, 995–1003. doi: 10.1111/j.1461-0248.2008.01229.x

Mayr, S., Schmid, P., Laur, J., Rosner, S., Charra-Vaskou, K., Dämon, B., et al. (2014). Uptake of water via branches helps timberline conifers refill embolized xylem in late winter. *Plant Physiol.* 164, 1731–1740. doi: 10.1104/pp.114.236646

Morris, H., and Jansen, S. (2016). Secondary xylem parenchyma–from classical terminology to functional traits. *Iawa J.* 37, 1–15. doi: 10.1163/22941932-20160117

Niklas, K. J. (1999). The mechanical role of bark. *Am. J. Bot.* 86, 465–469. doi: 10.2307/2656806

Nilsen, E. T. (1995). "Stem photosynthesis: extent, patterns, and role in plant carbon economy," in *Plant stems: physiology and functional morphology*, ed. B. L. Gartner (San Diego: Academic Press), 223–240. doi: 10.1016/b978-012276460-8/50012-6

Nilsen, E. T., and Sharifi, M. R. (1997). Carbon isotopic composition of legumes with photosynthetic stems from Mediterranean and desert habitats. *Am. J. Bot.* 84, 1707–1713. doi: 10.2307/2446469

Nilsen, E. T., Meinzer, F. C., and Rundel, P. W. (1989). Stem photosynthesis in *Psorothamnus spinosus* (smoke tree) in the Sonoran Desert of California. *Oecologia* 79, 193–197. doi: 10.1007/bf00388478

Osmond, C. B., Smith, S. D., Gui-Ying, B., and Sharkey, T. D. (1987). Stem photosynthesis in a desert ephemeral. Eriogonum inflatum. *Oecologia* 72, 542–549. doi: 10.1007/bf00378980

Pagel, M. (1999). Inferring the historical patterns of biological evolution. *Nature* 401, 877–884. doi: 10.1038/44766

Pfanz, H., and Aschan, G. (2001). *The existence of bark and stem photosynthesis in woody plants and its significance for the overall carbon gain. An eco-physiological and ecological approach in Progress in botany*. Berlin: Springer, 477–510.

Pfanz, H., Aschan, G., Langenfeld-Heyser, R., Wittmann, C., and Loose, M. (2002). Ecology and ecophysiology of tree stems: corticular and wood photosynthesis. *Naturwissenschaften* 89, 147–162. doi: 10.1007/s00114-002-0309-z

Pilarski, J. (2002). Diurnal and seasonal changes in the intensity of photosynthesis in stems of lilac (Syringa vulgaris L.). *Acta Physiol. Plant.* 24, 29–36. doi: 10.1007/s11738-002-0018-4

Pivovaroff, A. L., Pasquini, S. C., De Guzman, M. E., Alstad, K. P., Stemke, J. S., and Santiago, L. S. (2016). Multiple strategies for drought survival among woody plant species. *Funct.Ecol.* 30, 517–526. doi: 10.1111/1365-2435.12518

Pivovaroff, A. L., Sharifi, R., Scoffoni, C., Sack, L., and Rundel, P. (2014). Making the best of the worst of times: traits underlying combined shade and drought tolerance of *Ruscus aculeatus* and *Ruscus microglossum* (Asparagaceae). *Funct. Plant Biol.* 41, 11–24. doi: 10.1071/fp13047

Pratt, R. B., and Jacobsen, A. L. (2017). Conflicting demands on angiosperm xylem: Tradeoffs among storage, transport and biomechanics. *Plant Cell Environ.* 40, 897–913. doi: 10.1111/pce.12862

Prentice, I. C., Meng, T., Wang, H., Harrison, S. P., Ni, J., and Wang, G. (2011). Evidence of a universal scaling relationship for leaf CO2 drawdown along an aridity gradient. *New Phytol.* 190, 169–180. doi: 10.1111/j.1469-8137.2010.03579.x

Rosell, J. A., Castorena, M., Laws, C. A., and Westoby, M. (2015). Bark ecology of twigs vs. main stems: functional traits across eighty-five species of angiosperms. *Oecologia* 178, 1033–1043. doi: 10.1007/s00442-015-3307-5

Schönherr, J., and Ziegler, H. (1980). Water permeability of *Betula* periderm. *Planta* 147, 345–354. doi: 10.1007/bf00379844

Stewart, W. N., and Rothwell, G. W. (1993). *Paleobotany and the evolution of plants*. Cambridge, MA: Cambridge University Press.

Teskey, R. O., and McGuire, M. A. (2005). CO 2 transported in xylem sap affects CO 2 efflux from *Liquidambar styraciflua* and Platanus occidentalis stems, and contributes to observed wound respiration phenomena. *Trees* 19, 357–362. doi: 10.1007/s00468-004-0386-z

Teskey, R. O., Saveyn, A., Steppe, K., and Mcguire, M. A. (2008). Origin, fate and significance of CO2 in tree stems. *New Phytol.* 177, 17–32. doi: 10.1111/j.1469-8137.2007.02286.x

Tinoco-Ojanguren, C. (2008). Diurnal and seasonal patterns of gas exchange and carbon gain contribution of leaves and stems of Justicia californica in the Sonoran Desert. *J. Arid. Environ.* 72, 127–140. doi: 10.1016/j.jaridenv.2007.06.004

Wang, H., Harrison, S. P., Prentice, I. C., Yang, Y., Bai, F., Togashi, H. F., et al. (2018). The China plant trait database: Toward a comprehensive regional compilation of functional traits for land plants. *Ecology* 99:500. doi: 10.1002/ecy.2091

Whittaker, R. H. (1962). Classification of natural communities. *Bot. Rev.* 28, 1–239. doi: 10.1007/bf02860872

Wolfe, B. T. (2020). Bark water vapour conductance is associated with drought performance in tropical trees. *Biol. Lett.* 16:20200263. doi: 10.1098/rsbl.2020.0263

Yu, H., Shang, H., Cao, J., and Chen, Z. (2018). How important is woody tissue photosynthesis in EuCahetus dunnii Maiden and Osmanthus fragrans (Thunb.) Lour. under O 3 stress? *Environ. Sci. Pollut. Res.* 25, 2112–2120. doi: 10.1007/s11356-017-0584-z

Conflict of Interest: The authors declare that the research was conducted in the absence of any commercial or financial relationships that could be construed as a potential conflict of interest.

Publisher's Note: All claims expressed in this article are solely those of the authors and do not necessarily represent those of their affiliated organizations, or those of the publisher, the editors and the reviewers. Any product that may be evaluated in this article, or claim that may be made by its manufacturer, is not guaranteed or endorsed by the publisher.

frontiers in Forests and Global Change

MINI REVIEW
published: 05 August 2021
doi: 10.3389/ffgc.2021.716557

Accumulator, Transporter, Substrate, and Reactor: Multidimensional Perspectives and Approaches to the Study of Bark

*Alexandra G. Ponette-González**

Department of Geography and the Environment, University of North Texas, Denton, TX, United States

Woody ecosystems have a relatively thin but aerially extensive and dynamic layer of bark that, like leaves, regulates material exchange at the interface of air, water, and biota. Through interception, retention, and leaching of materials and interactions with epiphytic communities, bark alters the chemistry and composition of water draining over its surface during precipitation. This mini-review explores different perspectives and approaches to the study of bark and what they reveal about the myriad ways bark surfaces influence the quality of sub-canopy precipitation. Observational studies conducted over the past five decades in the fields of environmental science, ecohydrology, epiphyte ecology, and microbiology demonstrate that bark is an accumulator, transporter, substrate, and reactor. Bark passively accumulates materials from the atmosphere, water, and canopies, and also serves as an active transport surface, exchanging materials laterally and longitudinally. In addition, bark substrates influence epiphyte diversity, composition, and distribution, which, in turn, affect material cycling. Bark surfaces are dynamic over time, changing in response to disturbances (e.g., insect outbreaks, aging, and tree death)—how such changes influence the chemical and elemental composition of throughfall and stemflow merits further study. Moving forward, integration of diverse perspectives and approaches is needed to elucidate the influence of bark surfaces on solute and particulate transport and cycling within woody ecosystems.

Keywords: biomonitoring, epiphytes, forests, microorganisms, stemflow, throughfall, woody ecosystems

OPEN ACCESS

Edited by:
Anna Klamerus-Iwan, University of Agriculture in Krakow, Poland

Reviewed by:
Beate Michalzik, Friedrich Schiller University Jena, Germany
Dawid Kupka, University of Agriculture in Krakow, Poland
Bernard Okoński, Poznań University of Life Sciences, Poland

***Correspondence:**
Alexandra G. Ponette-González
alexandra.ponette@unt.edu

Specialty section:
This article was submitted to Forest Hydrology, a section of the journal Frontiers in Forests and Global Change

Received: *28 May 2021*
Accepted: *16 July 2021*
Published: *05 August 2021*

Citation:
Ponette-González AG (2021) Accumulator, Transporter, Substrate, and Reactor: Multidimensional Perspectives and Approaches to the Study of Bark. Front. For. Glob. Change 4:716557. doi: 10.3389/ffgc.2021.716557

INTRODUCTION

The outer bark of tree branches and stems (i.e., phellem or rhytidome) constitutes a critical interface between the atmosphere, water, and vegetation that has important implications for the cycling of materials in woody plant-dominated ecosystems. Bark is a passive receptor surface to which materials deposit during precipitation (wet deposition) and *via* dry deposition. Some fraction of these materials can sorb to or be absorbed by bark surfaces, resulting in retention. Materials also leach from bark surfaces, moving through the bark into external solution that drains to the surface during storms. Growing on and within bark surfaces, epiphytic plants (e.g., mosses, ferns, and bromeliads) intercept, retain, and leach substances (Mendieta-Leiva et al., 2020), while bark-dwelling microorganisms and fauna produce, transform, and decompose materials (Aguirre-von-Wobeser, 2020). Exchanges between epiphytic communities and their substrates

create additional pathways for material cycling within and below canopies. Thus, bark surfaces directly and indirectly influence the physical, chemical, and biological characteristics of water flowing through woody canopies (Ponette-González et al., 2020).

Water that drips from leaves, twigs, and branches (throughfall) and that flows down tree stems (stemflow) washes canopy surfaces, integrating deposition, retention, and leaching processes and the outcomes of bark-epiphyte interactions (Decina et al., 2020). As such, understanding the complete network of surfaces—including the non-leafy components—that links the top of the canopy to the soil is critical for a more complete and comprehensive view of how woody plants alter biogeochemical inputs to soils and the potential consequences for ecosystem functions, such as carbon and nutrient cycling (Van Stan et al., 2021a).

Bark exhibits a diverse array of physical and chemical properties that affect the chemistry and composition of waters draining over its surface (Oka et al., 2021). Importantly, bark can comprise a significant proportion of the total plant or ecosystem surface area available for passive interception and active exchange (i.e., uptake and leaching) of materials. Early estimates from temperate deciduous forest indicate that branch and stem bark surface areas combined range from 1.5 to 2.8 m^2 per m^2, while leaf surface area ranges from 3 to 6 m^2 per m^2 (Whittaker and Woodwell, 1967). Recent estimates from temperate evergreen coniferous forest dominated by redwood (*Sequoia sempervirens*) show exceptionally high and nearly equivalent bark and leaf surface areas (Sillett et al., 2019). In other words, as much as 30–50% of the total plant or ecosystem surface area exposed to the atmosphere (and precipitation) is bark. While the relative importance of the bark interface varies spatially due to species- and community-specific differences in outer surface areas, the bark interface varies temporally as well. The ratio of bark to leaf surfaces increases with tree age (Whittaker and Woodwell, 1967), during periods of leaf abscission, and after disturbances (e.g., hurricanes and insect outbreaks) that result in partial or complete canopy defoliation. Bark surfaces are also more temporally persistent than leaves (Van Stan et al., 2021a), meaning that they accumulate and exchange materials continuously over multiple seasons, years, and often over the entirety of a plant's life.

Bark surfaces are rough, porous, hygroscopic (absorb and retain water), and sorptive (**Supplementary Figure 1**), characteristics that influence deposition, leaching, and retention and interactions with epiphytes. The sorptive properties of bark and its effectiveness at removing metal ions from aqueous solution has resulted in growing interest in using bark in water and wastewater treatment (Şen et al., 2015). The hygroscopicity of bark is of relevance as it represents a potentially significant component of total bark water storage. In temperate forests, water adsorbed from the atmosphere during dry periods can constitute 10–30% of maximum bark water storage capacity, with values exceeding 60% at humid forest sites (Ilek et al., 2016, 2021). These findings suggest that bark surfaces with lower hygroscopicity will retain more water during storms, increasing water residence time and opportunities for canopy exchange on bark. Surface roughness is another bark property affecting both bark water storage and dry deposition. As is the case with leaves and whole canopies (Rindy et al., 2019), increased roughness enhances particulate capture (Oka et al., 2021). Deposited particulates can wash off bark surfaces or accumulate within porous bark "traps" (Magyar et al., 2021; **Supplementary Figure 1**). Additionally, some tree species, such as paper birch (*Betula papyrifera*) and copperwood (*Bursera simaruba*), undergo periodic exfoliation. Bark shedding releases materials retained on and in bark tissues and leads to renewal of the bark surface. Finally, bark surfaces are diverse in chemical and elemental composition. Species differ in resource allocation to chemical defenses against insects, pests, and pathogens (e.g., Franceschi et al., 2005) and may translocate elements such as manganese to the bark to avoid toxic concentrations in leaves and other tissues (Hauck and Paul, 2005). Taken together, the structural heterogeneity and complex composition of bark give rise to unique associations with flora and fauna that in turn participate in material cycling and alteration of water quality.

The role and potential significance of the outer bark in atmosphere-water-vegetation interactions is often examined qualitatively or overlooked in field and modeling studies (Butler et al., 2020; Pace and Grote, 2020). In many fields, leaves still rule. As a result, the processes of deposition, retention, leaching, and washoff are relatively well described for leaves, but not so for bark. This precludes our ability to fully understand how woody plants influence the quality of water transported within (branch bark) and below (stem bark) tree canopies. In this mini-review, I briefly explore diverse perspectives and approaches to the study of bark and what they reveal about the myriad ways bark surfaces influence the chemistry and composition of sub-canopy precipitation.

PERSPECTIVES ON BARK ARE DIVERSE BUT COMPLEMENTARY

Bark interactions with the atmosphere, water, and vegetation have been the subject of research in the fields of environmental science, ecohydrology, epiphyte ecology, and microbiology for over five decades (e.g., Staxäng, 1969; Johnsen and Søchting, 1976; Farmer et al., 1991). A review of selected peer-reviewed literature indicates that within these fields bark is conceptualized as: (1) accumulator and biomonitor of atmospheric pollution; (2) transport surface; (3) substrate for epiphytic communities; and (4) reactor.

A Web of Science search for articles published between 1945 and present conducted with the terms "bark" and "biomonitoring" (n = 148), "bark" and "stemflow" (n = 122), and "bark" and "epiphytes" (n = 212) suggests that bark is most often considered in the context of plant ecology. Less than 10% of the articles identified in the "bark" and "epiphytes" group focused on microorganisms and animals. While the number of publications in all research areas has grown steadily since 1976 (**Supplementary Figure 2**), there are important differences in where, at what scale, and how bark is studied (**Figure 1**).

Bark biomonitoring often takes place within urban and industrial areas, where atmospheric pollution is a health and environmental concern. Bark is considered advantageous

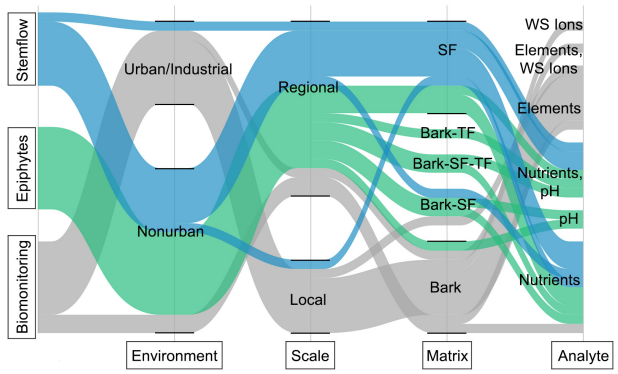

FIGURE 1 | Parallel plot illustrating approaches to the study of bark in three research areas: bark and biomonitoring (n = 10 studies), bark and stemflow (n = 8 studies), and bark and epiphytes (n = 9 studies). The y-axis depicts the three research areas. The width of the parallel lines represents the frequency of studies falling in each category along the x-axis. The x-axis categories include the environment in which the study was conducted (urban/industrial or nonurban), the spatial scale at which the study was conducted (local or regional), the environmental matrix sampled [bark, stemflow (SF), and throughfall (TF)], and the dissolved or particulate analytes. Analytes include water-soluble ions (ws ions), trace and major elements (elements), dissolved and soluble nutrients (nutrients), and pH.

in biomonitoring research given its widespread distribution, accessibility, and capacity to intercept and retain pollutants. Indeed, bark is widely used to map and measure past and present impacts of airborne pollution downwind of point sources (e.g., incinerator and smelter; Cocozza et al., 2016) and near city and heavily trafficked roads (e.g., Catinon et al., 2012). The objective often is to monitor pollution changes over long-time frames or on local scales (e.g., Guéguen et al., 2012)—that is, within kilometers of major emissions sources. Most studies that utilize tree bark as a passive biomonitor determine trace element concentrations in bark tissue, with heavy metals such as lead, copper, cadmium, mercury, and uranium of particular interest due to their toxicity to human populations (e.g., Fujiwara et al., 2011; Chiarantini et al., 2016). For example, Flett et al. (2021) determined uranium concentrations in tree bark on tribal lands in the western United States and found that these were highest along an abandoned mine access road and near a mill where uranium was processed; concentrations decreased with increasing distance from pollution hotspots. The effectiveness of bark relative to other biomonitors such as leaves, lichens, and mosses has also been examined. Comparisons of multiple biomonitors consistently show that pollutant concentrations decrease in the order lichen/moss > bark > leaf surface > leaf wax (e.g., Cucu-Man and Steinnes, 2013).

Insights on how bark alters stemflow material inputs to soils generally derive from measurements conducted in non-urban forests. In this context, stemflow water is generally collected and analyzed for dissolved inorganic nutrients, organic carbon, organic nitrogen, and pH. While bark characteristics influence solute chemistry and fluxes, beyond the role of bark in altering stemflow water volumes, it is unclear how (Levia and Germer, 2015). In ecohydrological research, rarely are concentrations in bark leachate compared to those in stemflow (but see Tucker et al., 2020).

Ecologists and microbiologists frequently investigate bark-epiphyte interactions in non-urban forested environments. For example, in the northeastern United States, United Kingdom, and Sweden, pollution gradient studies underscore the effects of increasing pollutant deposition and acidification on bark substrates and epiphytic lichens and bryophytes along their length (e.g., Schmull et al., 2002; Mitchell et al., 2005; Fritz et al., 2009). In contrast to studies focused on epiphytic vegetation, we are only beginning to understand the role of bark and resident epiphytes as habitat for microorganisms and faunal communities (e.g., Aguirre-von-Wobeser, 2020). To understand the various factors influencing epiphytic microbial, plant, and animal communities, it is not uncommon for researchers to collect samples from diverse environmental matrices, including bark, precipitation (rainfall, throughfall, and stemflow), epiphytic tissue, and in some cases soils, for analysis of nutrients and pollutants (e.g., Farmer et al., 1991). Despite differences in scale, approach, and method, knowledge gained from all research areas elucidates how bark can influence biogeochemical cycling in woody ecosystems now and in the future.

BARK AS ACCUMULATOR, TRANSPORTER, SUBSTRATE, AND REACTOR

Bark as Accumulator

Bark accumulates particulates from the atmosphere and plant canopies (Van Stan et al., 2021b), including organic matter (e.g., pollen and microbes), crustal matter (i.e., dust), and pollutants (e.g., heavy metals). It has been estimated that ∼80% of a tree's bark surface deposit is organic matter, with the remaining 20% comprising similar amounts of crustal and anthropogenic particulates (Catinon et al., 2009).

Field and laboratory experiments, in some instances coupled with microscopy, demonstrate that particulate accumulation on bark surfaces is a highly complex process varying as a function of meteorological (e.g., rain), bark, and particle factors. In a series of sorption experiments, Su et al. (2013) found that spruce bark has a strong affinity for metals, such as iron, lead, copper, and cadmium, which explains why outer bark surfaces are typically enriched in these metals near pollution sources such as industrial plants and highways (Suzuki, 2006; Catinon et al., 2009). Less is known about the deposition of plant limiting nutrients, such as nitrogen, on tree bark, although bark may reflect broad-scale spatial gradients in N deposition (Boltersdorf et al., 2014). Accumulation of water-soluble ions can also be significant, representing ∼20% of the total particulate mass on bark surfaces (Xu et al., 2019). Proximity and location relative to pollution sources (e.g., downwind or facing) influence the composition of accumulated particles as well as their size. Near industrial pollution sources and roads, bark particulates are frequently <10 μm in diameter (Suzuki, 2006; Tye et al., 2006). In contrast, bark surfaces distant from these sources have been

found to accumulate higher proportions of large (10–100 μm in diameter) particulates (Xu et al., 2019). Accumulation is also dependent on location within the bark (e.g., Chiarantini et al., 2016). Suberized cells within the outer bark tissue have been shown to preferentially accumulate elements derived from crustal and anthropogenic pollution sources (Catinon et al., 2011), whereas non-suberized cells are subject to the wear and tear of precipitation. Combining measurements of elemental composition in bark tissue, stemflow, and xylem sap, Catinon et al. (2012) showed that outer bark surface deposits are subject to intense washoff during storms. Taken together, these studies show that bark surface deposits are mixtures of materials whose composition reflects diverse sources and processes.

Bark as Transporter

Water travels over complex bark topography as it moves from the atmosphere to the ground below. Bark physical properties affect the volume and routing of water in ways that matter for material inputs to soil during precipitation (Levia and Herwitz, 2005). Given its effects on stemflow volume and water residence time, bark water storage capacity is of particular relevance.

Bark water storage capacity is significantly greater than that of foliage and can account for as much as 80% of total tree water storage (Herwitz, 1985), albeit the amount of water retained by bark varies considerably within and among species. Rough-barked species typically have higher water storage capacities than smooth-barked species (Levia and Herwitz, 2005) and therefore lower stemflow volumes (Ponette-González et al., 2010). High-resolution (0.1 mm vertical resolution) characterization of tree trunks reveals the influence of bark microrelief on intra- and inter-specific variability in water storage capacity. One study found that a pedunculate oak (*Quercus robur*) tree with highly ridged and steeply sloped bark could retain >2.5-fold more water than a smooth-barked European beech (*Fagus sylvatica*) tree of similar size (Van Stan et al., 2016). Bark water storage was recently shown to vary over meters distance along single tree stems (Sioma et al., 2018). In that study, four of five species sampled had higher bark water interception potential at 1.5 m compared to 15 m height due to a larger volume of water-accumulating space. Because bark water storage capacity is positively related to water residence time, higher storage results in increased chemical concentrations as well increased time available for exchange processes across and along the bark surface. Indeed, Oka et al. (2021) found that stemflow concentrations of calcium and potassium (ions easily leached from canopy surfaces; Ponette-González et al., 2016), increased along a gradient from smooth- to rough-barked species presumably as a result of longer water residence times. The research by Sioma et al. (2018) suggests that the lower sections of tree stems, where the downward transport of materials and higher water storage combine, could represent biogeochemical hotspots within tree canopies, providing a more nuanced explanation for high solute fluxes to near-stem soils during rainfall.

Measurements of stemflow (and throughfall) under tree canopies during leaf-on and leaf-off periods or along gradients of tree decay/death also demonstrate how bark surfaces modify water chemistry and composition (e.g., Siegert et al., 2018). In a Belgian oak forest, nitrate and ammonium concentrations were lower in stemflow compared to rainfall during the leaf-off season suggesting net uptake by bark surfaces (André et al., 2008). In an old-growth forest with varying levels of decay, stemflow collected under snags with little decay had higher calcium, potassium, and zinc concentrations compared to stemflow under live trees and snags with advanced decay. The pulse of elements with decay onset was attributed to release from decaying wood; release from deeper layers of bark and wood exposed with decay; or transport from outer wood to bark with stem evaporation (Bade et al., 2015).

Compared to bark effects on the downward flux of materials in stemflow, less is known about how the bark transport surface alters ionic and elemental exchanges horizontally across the bark membrane. Direct water (and nutrient) uptake through the bark may be more prevalent and significant than once thought (Berry et al., in press). Moving in the other direction, stem transpiration can result in calcium and potassium leaching from the xylem and subsequent re-deposition on the bark surface (Catinon et al., 2012). Despite knowledge limitations, bark appears to be a reactive substrate that exerts important controls over the materials transported by draining stormwater.

Bark as Substrate

Tree bark is a substrate whose physical and chemical properties affect epiphytic plant communities directly and indirectly through effects on branchflow and stemflow quality. Numerous studies highlight the importance of bark pH in epiphyte community composition, especially in polluted areas, where nitrogen and sulfur deposition can lead to bark acidification (e.g., Mitchell et al., 2005; Cleavitt et al., 2011). In these landscapes, both ammonium and nitrate have been associated with decreasing bryophyte and lichen cover (Schmull et al., 2002; Mitchell et al., 2005). Bark also represents a source of micronutrients, such as manganese, which is readily leached from bark into stemflow, but that can be toxic to epiphytes when supplied in excess (Hauck and Paul, 2005). Intraspecific changes in bark properties and associated nutrient gradients that occur with tree age represent an additional, though less well studied, control on epiphyte communities. For example, cation leaching from damaged areas on older trees may increase stemflow pH, thereby providing microhabitats for epiphytes of conservation value (Fritz et al., 2009). McGee et al. (2019) demonstrated that bark substrates become enriched in nutrients as tree bark thickness increases with tree size and age, and that enrichment correlates positively with the cover of several mesophytic and calciphilic epiphytes. In turn, epiphytes alter the chemistry and composition of draining waters. The magnitude and extent of chemical alteration is beyond the scope of this mini-review but the subject of an extensive review by Van Stan and Pypker (2015).

Bark as Reactor

Compared to research on interactions between bark and epiphytic vegetation, we are only beginning to understand the role of bark and resident epiphytes as habitat for microorganisms and faunal communities (e.g., Aguirre-von-Wobeser, 2020). Bark

contains high levels of microbial diversity (Lambais et al., 2014), a diversity that is often intermediate between, and distinctive in composition from, adjacent leaves and soils (Leff et al., 2015). Bark microbial communities also have been shown to vary by season (Beck et al., 2014) and spatially along bark surfaces (Leff et al., 2015). For instance, Leff et al. (2015) found higher microbial diversity near the interior and on the underside of branches. Such variations in diversity and composition are attributable to micro-environmental differences in UV radiation exposure, water, nutrient and carbon availability, as well as the presence of antimicrobial compounds (e.g., Magyar et al., 2021).

What functions do bark-dwelling microbes and fauna perform? Increasing evidence highlights the important roles bark bacterial communities play in the cycling of carbon and nitrogen (Jeffrey et al., 2021). Abundant photosynthetic genes identified in microbes sampled from bark tissues indicate the potential for bacterial primary production on bark surfaces that could help sustain heterotrophic bacteria (Aguirre-von-Wobeser, 2020). In turn, heterotrophic bacterial and fungal communities associated with decaying wood and bark (Martins et al., 2013) decompose complex carbon compounds. The potential for methane consumption by bark-dwelling methane-oxidizing bacteria was recently demonstrated by Jeffrey et al. (2021), illustrating yet another pathway by which bark bacterial communities influence carbon cycling. Some bacteria and lichens also add nitrogen to canopies through nitrogen fixation (Aguirre-von-Wobeser, 2020). Although less well studied, faunal communities within bark epiphytes (e.g., foliose lichens) and on bark surfaces make up part of a complex and rich bark food web that remains poorly understood (Anderson, 2014; Asplund et al., 2018). In sum, although nascent, this research points to the potential for significant transfers of microorganismal and faunal biomass *via* throughfall and stemflow to the ground below (Guidone et al., 2021; Magyar et al., 2021) along with important fluxes of dissolved and suspended materials.

FUTURE DIRECTIONS

Bark is a passive accumulator, an active transport surface, a substrate, and a reactor. Although bark has been shown to accumulate considerable amounts of particulates, the contribution of bark to total nutrient and pollutant loading has not been quantified. Further, we know little about exchanges of both water, nutrients, and pollutants across tree branch and stem surfaces. In the future, changes in atmospheric composition, precipitation, and disturbance regimes will alter what is deposited to bark surfaces, as well as woody plant species composition and species' expression of bark. The latter may occur *via* changes in the age structure of stands or intraspecific variation in bark structure and chemistry. In sum, the interaction of bark and stormy conditions may represent a critical influence on the accumulation, exchange and transport of elements between atmosphere, water, and vegetation.

AUTHOR CONTRIBUTIONS

AGP-G conceived the mini-review, reviewed the literature, created the figures, and wrote the manuscript.

FUNDING

Partial funding for manuscript publication fees was provided through a *Frontiers* fee support grant.

ACKNOWLEDGMENTS

I would like to acknowledge John Van Stan II for constructive comments on two versions of this manuscript and my three hound dogs for inspiring me with every bark.

SUPPLEMENTARY MATERIAL

The Supplementary Material for this article can be found online at: https://www.frontiersin.org/articles/10.3389/ffgc.2021.716557/full#supplementary-material

REFERENCES

Aguirre-von-Wobeser, E. (2020). Functional metagenomics of bark microbial communities from avocado trees (*Persea americana* Mill.) reveals potential for bacterial primary productivity. *bioRxiv [Preprint]* doi: 10.1101/2020.09.05.284570

Anderson, O. R. (2014). Microbial communities associated with tree bark foliose lichens: a perspective on their microecology. *J. Eukaryot. Microbiol.* 61, 364–370. doi: 10.1111/jeu.12116

André, F., Jonard, M., and Ponette, Q. (2008). Effects of biological and meteorological factors on stemflow chemistry within a temperate mixed oak–beech stand. *Sci. Total Environ.* 393, 72–83. doi: 10.1016/j.scitotenv.2007.12.002

Asplund, J., Strandin, O. V., and Gauslaa, Y. (2018). Gastropod grazing of epiphytic lichen-dominated communities depends on tree species. *Basic Appl. Ecol.* 32, 96–102. doi: 10.1016/j.baae.2018.07.007

Bade, C., Jacob, M., Leuschner, C., and Hauck, M. (2015). Chemical properties of decaying wood in an old-growth spruce forest and effects on soil chemistry. *Biogeochemistry* 122, 1–13. doi: 10.1007/s10533-014-0015-x

Beck, A., Peršoh, D., and Rambold, G. (2014). First evidence for seasonal fluctuations in lichen-and bark-colonising fungal communities. *Folia Microbiol.* 59, 155–157. doi: 10.1007/s12223-013-0278-y

Berry, Z. C., Ávila-Lovera, E., De Guzman, M. E., O'Keefe, K., and Emery, N. C. (in press). Beneath the bark: assessing woody stem water and carbon fluxes and its prevalence across climates and the woody plant phylogeny. *Front. For. Glob. Chang.*

Boltersdorf, S. H., Pesch, R., and Werner, W. (2014). Comparative use of lichens, mosses and tree bark to evaluate nitrogen deposition in Germany. *Environ. Pollut.* 189, 43–53. doi: 10.1016/j.envpol.2014.02.017

Butler, E. E., Chen, M., Ricciuto, D., Flores-Moreno, H., Wythers, K. R., Kattge, J., et al. (2020). Seeing the canopy for the branches: Improved within canopy scaling of leaf nitrogen. *J. Adv. Model. Earth Syst.* 12:e2020MS002237.

Catinon, M., Ayrault, S., Boudouma, O., Asta, J., Tissut, M., and Ravanel, P. (2012). Atmospheric element deposit on tree barks: the opposite effects of rain and transpiration. *Ecol. Indic.* 14, 170–177. doi: 10.1016/j.ecolind.2011.07.013

Catinon, M., Ayrault, S., Clocchiatti, R., Boudouma, O., Asta, J., Tissut, M., et al. (2009). The anthropogenic atmospheric elements fraction: a new interpretation of elemental deposits on tree barks. *Atmos. Environ.* 43, 1124–1130. doi: 10.1016/j.atmosenv.2008.11.004

Catinon, M., Ayrault, S., Spadini, L., Boudouma, O., Asta, J., Tissut, M., et al. (2011). Tree bark suber-included particles: a long-term accumulation site for elements of atmospheric origin. *Atmos. Environ.* 45, 1102–1109. doi: 10.1016/j.atmosenv.2010.11.038

Chiarantini, L., Rimondi, V., Benvenuti, M., Beutel, M. W., Costagliola, P., Gonnelli, C., et al. (2016). Black pine (*Pinus nigra*) barks as biomonitors of airborne mercury pollution. *Sci. Total Environ.* 569, 105–113. doi: 10.1016/j.scitotenv.2016.06.029

Cleavitt, N. L., Ewing, H. A., Weathers, K. C., and Lindsey, A. M. (2011). Acidic atmospheric deposition interacts with tree type and impacts the cryptogamic epiphytes in Acadia National Park Maine, USA. *Bryologist* 114, 570–582. doi: 10.1639/0007-2745-114.3.570

Cocozza, C., Ravera, S., Cherubini, P., Lombardi, F., Marchetti, M., and Tognetti, R. (2016). Integrated biomonitoring of airborne pollutants over space and time using tree rings, bark, leaves and epiphytic lichens. *Urban For. Urban Green.* 17, 177–191. doi: 10.1016/j.ufug.2016.04.008

Cucu-Man, S.-M., and Steinnes, E. (2013). Analysis of selected biomonitors to evaluate the suitability for their complementary use in monitoring trace element atmospheric deposition. *Environ. Monit. Assess.* 185, 7775–7791. doi: 10.1007/s10661-013-3135-1

Decina, S. M., Ponette-González, A. G., and Rindy, J. E. (2020). "Urban tree canopy effects on water quality via inputs to the urban ground surface," in *Forest-Water Interactions*, eds D. Levia, D. Carlyle-Moses, S. Iida, B. Michalzik, K. Nanko, and A. Tischer (Chem: Springer), 433–457. doi: 10.1007/978-3-030-26086-6_18

Farmer, A. M., Bates, J. W., and Bell, J. N. B. (1991). Seasonal variations in acidic pollutant inputs and their effects on the chemistry of stemflow, bark and epiphyte tissues in three oak* woodlands in NW Britain. *New Phytol.* 118, 441–451. doi: 10.1111/j.1469-8137.1991.tb00026.x

Flett, L., McLeod, C. L., McCarty, J. L., Shaulis, B. J., Fain, J. J., and Krekeler, M. P. S. (2021). Monitoring uranium mine pollution on native american lands: insights from tree bark particulate matter on the spokane reservation, Washington, USA. *Environ. Res.* 194:110619. doi: 10.1016/j.envres.2020.110619

Franceschi, V. R., Krokene, P., Christiansen, E., and Krekling, T. (2005). Anatomical and chemical defenses of conifer bark against bark beetles and other pests. *New Phytol.* 167, 353–376. doi: 10.1111/j.1469-8137.2005.01436.x

Fritz, Ö, Brunet, J., and Caldiz, M. (2009). Interacting effects of tree characteristics on the occurrence of rare epiphytes in a Swedish beech forest area. *Bryologist* 112, 488–505. doi: 10.1639/0007-2745-112.3.488

Fujiwara, F. G., Gómez, D. R., Dawidowski, L., Perelman, P., and Faggi, A. (2011). Metals associated with airborne particulate matter in road dust and tree bark collected in a megacity (Buenos Aires, Argentina). *Ecol. Indic.* 11, 240–247. doi: 10.1016/j.ecolind.2010.04.007

Guéguen, F., Stille, P., Geagea, M. L., and Boutin, R. (2012). Atmospheric pollution in an urban environment by tree bark biomonitoring–Part I: Trace element analysis. *Chemosphere* 86, 1013–1019. doi: 10.1016/j.chemosphere.2011.11.040

Guidone, M., Gordon, D. A., and Van Stan, J. T. (2021). Living particulate fluxes in throughfall and stemflow during a pollen event. *Biogeochemistry* 153, 323–330. doi: 10.1007/s10533-021-00787-7

Hauck, M., and Paul, A. (2005). Manganese as a site factor for epiphytic lichens. *Lichenol.* 37, 409–423. doi: 10.1017/s0024282905014933

Herwitz, S. R. (1985). Interception storage capacities of tropical rainforest canopy trees. *J. Hydrol.* 77, 237–252. doi: 10.1016/0022-1694(85)90209-4

Ilek, A., Kucza, J., and Morkisz, K. (2016). Hygroscopicity of the bark of selected forest tree species. *iForest-Biogeosciences For.* 10:220. doi: 10.3832/ifor1979-009

Ilek, A., Siegert, C. M., and Wade, A. (2021). Hygroscopic contributions to bark water storage and controls exerted by internal bark structure over water vapor absorption. *Trees* 35, 831–843. doi: 10.1007/s00468-021-02084-0

Jeffrey, L. C., Maher, D. T., Chiri, E., Leung, P. M., Nauer, P. A., Arndt, S. K., et al. (2021). Bark-dwelling methanotrophic bacteria decrease methane emissions from trees. *Nat. Commun.* 12:2127.

Johnsen, I., and Søchting, U. (1976). Distribution of cryptogamic epiphytes in a Danish city in relation to air pollution and bark properties. *Bryologist* 79, 86–92. doi: 10.2307/3241873

Lambais, M. R., Lucheta, A. R., and Crowley, D. E. (2014). Bacterial community assemblages associated with the phyllosphere, dermosphere, and rhizosphere of tree species of the Atlantic forest are host taxon dependent. *Microb. Ecol.* 68, 567–574. doi: 10.1007/s00248-014-0433-2

Leff, J. W., Del Tredici, P., Friedman, W. E., and Fierer, N. (2015). Spatial structuring of bacterial communities within individual G inkgo biloba trees. *Environ. Microbiol.* 17, 2352–2361. doi: 10.1111/1462-2920.12695

Levia, D. F., and Germer, S. (2015). A review of stemflow generation dynamics and stemflow-environment interactions in forests and shrublands. *Rev. Geophys.* 53, 673–714. doi: 10.1002/2015rg000479

Levia, D. F., and Herwitz, S. R. (2005). Interspecific variation of bark water storage capacity of three deciduous tree species in relation to stemflow yield and solute flux to forest soils. *Catena* 64, 117–137. doi: 10.1016/j.catena.2005.08.001

Magyar, D., Van Stan, J. T., and Sridhar, K. R. (2021). Hypothesis and theory: fungal spores in stemflow and potential bark sources. *Front. For. Glob. Chang.* 4, 1–18.

Martins, G., Lauga, B., Miot-Sertier, C., Mercier, A., Lonvaud, A., Soulas, M.-L., et al. (2013). Characterization of epiphytic bacterial communities from grapes, leaves, bark and soil of grapevine plants grown, and their relations. *PLoS One* 8:e73013. doi: 10.1371/journal.pone.0073013

McGee, G. G., Cardon, M. E., and Kiernan, D. H. (2019). Variation in *Acer saccharum* Marshall (sugar maple) bark and stemflow characteristics: implications for epiphytic bryophyte communities. *Northeast. Nat.* 26, 214–235. doi: 10.1656/045.026.0118

Mendieta-Leiva, G., Porada, P., and Bader, M. Y. (2020). "Interactions of epiphytes with precipitation partitioning," in *Precipitation Partitioning by Vegetation*, eds J. T. Van Stan, E. Gutmann, and J. Friesen (Cham: Springer), 133–146. doi: 10.1007/978-3-030-29702-2_9

Mitchell, R. J., Truscot, A. M., Leith, I. D., Cape, J. N., Van Dijk, N., Tang, Y. S., et al. (2005). A study of the epiphytic communities of Atlantic oak woods along an atmospheric nitrogen deposition gradient. *J. Ecol.* 93, 482–492. doi: 10.1111/j.1365-2745.2005.00967.x

Oka, A., Takahashi, J., Endoh, Y., and Seino, T. (2021). Bark effects on stemflow chemistry in a Japanese temperate forest I. The role of bark surface morphology. *Front. For. Glob. Chang.* 4:654375. doi: 10.3389/ffgc.2021.654375

Pace, R., and Grote, R. (2020). Deposition and resuspension mechanisms into and from tree canopies: a study modeling particle removal of conifers and broadleaves in different cities. *Front. For. Glob. Chang.* 3:26. doi: 10.3389/ffgc.2020.00026

Ponette-González, A. G., Ewing, H. A., and Weathers, K. C. (2016). "Interactions between precipitation and vegetation canopies," in *A Biogeoscience Approach to Ecosystems*, eds E. A. Johnson and Y. Martin (New York, NY: Cambridge University Press), 215–253. doi: 10.1017/cbo9781107110632.009

Ponette-González, A. G., Van Stan, J. T. II, and Magyar, D. (2020). "Things seen and unseen in throughfall and stemflow," in *Precipitation Partitioning by Vegetation*, eds J. T. Van Stan, II, E. Gutmann, and J. Friesen (Cham: Springer), 71–88. doi: 10.1007/978-3-030-29702-2_5

Ponette-González, A. G., Weathers, K. C., and Curran, L. M. (2010). Water inputs across a tropical montane landscape in Veracruz, Mexico: synergistic effects of land cover, rain and fog seasonality, and interannual precipitation variability. *Glob. Chang. Biol.* 16, 946–963. doi: 10.1111/j.1365-2486.2009.01985.x

Rindy, J. E., Ponette-González, A. G., Barrett, T. E., Sheesley, R. J., and Weathers, K. C. (2019). Urban trees are sinks for soot: elemental carbon accumulation by two widespread oak species. *Environ. Sci. Technol.* 53, 10092–10101. doi: 10.1021/acs.est.9b02844

Schmull, M., Hauck, M., Vann, D. R., Johnson, A. H., and Runge, M. (2002). Site factors determining epiphytic lichen distribution in a dieback-affected spruce-fir forest on Whiteface Mountain, New York: stemflow chemistry. *Can. J. Bot.* 80, 1131–1140. doi: 10.1139/b02-106

Şen, A., Pereira, H., Olivella, M. A., and Villaescusa, I. (2015). Heavy metals removal in aqueous environments using bark as a biosorbent. *Int. J. Environ. Sci. Technol.* 12, 391–404. doi: 10.1007/s13762-014-0525-z

Siegert, C. M., Renninger, H. J., Sasith Karunarathna, A. A., Riggins, J. J., Clay, N. A., Tang, J. D., et al. (2018). "Biogeochemical hotspots around bark-beetle killed trees," in *Proceedings of the 19th Biennial Southern Silvicultural Research Conference*, Washington, DC.

Sillett, S. C., Van Pelt, R., Carroll, A. L., Campbell-Spickler, J., Coonen, E. J., and Iberle, B. (2019). Allometric equations for *Sequoia sempervirens* in forests of different ages. *For. Ecol. Manage.* 433, 349–363. doi: 10.1016/j.foreco.2018.11.016

Sioma, A., Socha, J., and Klamerus-Iwan, A. (2018). A new method for characterizing bark microrelief using 3D vision systems. *Forests* 9:30. doi: 10.3390/f9010030

Staxäng, B. (1969). Acidification of bark of some deciduous trees. *Oikos* 20, 224–230. doi: 10.2307/3543190

Su, P., Granholm, K., Pranovich, A., Harju, L., Holmbom, B., and Ivaska, A. (2013). Sorption of metal ions from aqueous solution to spruce bark. *Wood Sci. Technol.* 47, 1083–1097. doi: 10.1007/s00226-013-0562-7

Suzuki, K. (2006). Characterisation of airborne particulates and associated trace metals deposited on tree bark by ICP-OES, ICP-MS, SEM-EDX and laser ablation ICP-MS. *Atmos. Environ.* 40, 2626–2634. doi: 10.1016/j.atmosenv.2005.12.022

Tucker, A., Levia, D. F., Katul, G. G., Nanko, K., and Rossi, L. F. (2020). A network model for stemflow solute transport. *Appl. Math. Model.* 88, 266–282. doi: 10.1016/j.apm.2020.06.047

Tye, A. M., Hodgkinson, E. S., and Rawlins, B. G. (2006). Microscopic and chemical studies of metal particulates in tree bark and attic dust: evidence for historical atmospheric smelter emissions, Humberside, UK. *J. Environ. Monit.* 8, 904–912. doi: 10.1039/b605729b

Van Stan, J. T. II, and Pypker, T. G. (2015). A review and evaluation of forest canopy epiphyte roles in the partitioning and chemical alteration of precipitation. *Sci. Total Environ.* 536, 813–824. doi: 10.1016/j.scitotenv.2015.07.134

Van Stan, J. T., Dymond, S. F., and Klamerus-Iwan, A. (2021a). Bark-water interactions across ecosystem states and fluxes. *Front. For. Glob. Chang.* 4:28.

Van Stan, J. T., Lewis, E. S., Hildebrandt, A., Rebmann, C., and Friesen, J. (2016). Impact of interacting bark structure and rainfall conditions on stemflow variability in a temperate beech-oak forest, central Germany. *Hydrol. Sci. J.* 61, 2071–2083. doi: 10.1080/02626667.2015.1083104

Van Stan, J. T., Ponette-González, A. G., Swanson, T., and Weathers, K. C. (2021b). Throughfall and stemflow are major hydrologic highways for particulate traffic through tree canopies. *Front. Ecol. Environ* (in press). doi: 10.1002/fee.2360

Whittaker, R. H., and Woodwell, G. M. (1967). Surface area relations of woody plants and forest communities. *Am. J. Bot.* 54, 931–939. doi: 10.1002/j.1537-2197.1967.tb10717.x

Xu, X., Yu, X., Mo, L., Xu, Y., Bao, L., and Lun, X. (2019). Atmospheric particulate matter accumulation on trees: a comparison of boles, branches and leaves. *J. Clean. Prod.* 226, 349–356. doi: 10.1016/j.jclepro.2019.04.072

Conflict of Interest: The author declares that the research was conducted in the absence of any commercial or financial relationships that could be construed as a potential conflict of interest.

Publisher's Note: All claims expressed in this article are solely those of the authors and do not necessarily represent those of their affiliated organizations, or those of the publisher, the editors and the reviewers. Any product that may be evaluated in this article, or claim that may be made by its manufacturer, is not guaranteed or endorsed by the publisher.

frontiers in Forests and Global Change

ORIGINAL RESEARCH
published: 21 October 2021
doi: 10.3389/ffgc.2021.687907

Vertical Variability in Bark Hydrology for Two Coniferous Tree Species

Anna Ilek[1,2], John T. Van Stan[3], Karolina Morkisz[2] and Jarosław Kucza[2]*

[1] Department of Botany and Forest Habitats, Faculty of Forestry and Wood Technology, Poznań University of Life Sciences, Poznań, Poland, [2] Department of Forest Utilization, Engineering and Forest Technology, Faculty of Forestry, University of Agriculture in Krakow, Krakow, Poland, [3] Department of Biological, Geological, and Environmental Sciences, Cleveland State University, Cleveland, OH, United States

As the outermost layer of stems and branches, bark is exposed to the influence of atmospheric conditions, i.e., to changes in the air's relative humidity and wetting during storms. The bark is involved in water interception by tree canopies and stemflow generation, but bark–water relations are often overlooked in ecohydrological research and insufficiently understood. Relative to other canopy ecohydrological processes, little is known about vertical variation in bark properties and their effect on bark hydrology. Thus, the objective of this study was to analyze changes in physical properties (thickness, outer to total bark thickness ratio, density, and porosity) and hydrology (bark absorbability, bark water storage capacity, and hygroscopicity) vertically along stems of Norway spruce [*Picea abies* (L.) Karst.] and silver fir (*Abies alba* Mill.) trees. Our null hypotheses were that bark hydrology is constant both with tree height and across measured physical bark properties. We found that bark thickness and the ratio of outer-to-total bark thickness decreased with tree height for both species, and this was accompanied by an increase in the bark water storage capacity. In contrast, the bark's density, porosity, and hygroscopicity remained relatively constant along stems. These results inform ecohydrological theory on water storage capacity, stemflow initiation, and the connection between the canopy water balance and organisms that colonize bark surfaces.

Keywords: forest hydrology, bark water storage capacity, bark hygroscopicity, *Picea abies* (L.) H. Karst., *Abies alba* (Mill.)

OPEN ACCESS

Edited by:
Heidi Asbornsen, University of New Hampshire, United States

Reviewed by:
Paolo Giordani, University of Genoa, Italy
Brett Wolfe, Louisiana State University Agricultural Center, United States

****Correspondence:***
Anna Ilek
anna.ilek@up.poznan.pl

Specialty section:
This article was submitted to Forest Hydrology, a section of the journal Frontiers in Forests and Global Change

Received: *30 March 2021*
Accepted: *24 September 2021*
Published: *21 October 2021*

Citation:
Ilek A, Van Stan JT, Morkisz K and Kucza J (2021) Vertical Variability in Bark Hydrology for Two Coniferous Tree Species. Front. For. Glob. Change 4:687907. doi: 10.3389/ffgc.2021.687907

INTRODUCTION

When rain falls over forests, a hydrologically and ecologically relevant portion of that water (up to several mm event^{-1}, depending on storm and canopy conditions) is retained on the canopy's leaves, epiphytes, and bark (Klamerus-Iwan et al., 2020). This canopy water storage fuels a major part of the Earth's terrestrial evaporation flux by returning rainwater back to the atmosphere as canopy interception (Porada et al., 2018). Canopy interception and the resulting changes in top-of-atmosphere albedo (i.e., related cloud formation) has been estimated to impact air temperatures by −0.6 °C globally and −1.9°C regionally (Davies-Barnard et al., 2014) and can provide city-to-watershed scale stormwater ecoservices valued at millions (of USD) year^{-1}

(Nowak et al., 2020). Precipitation stored on wet leaves, epiphytes, and bark may be taken up by plants – and recent interest in these ecohydrological processes is growing (Berry et al., 2019; Aubrey, 2020; Carmichael et al., 2020; Miller et al., 2021). Water storage dynamics in canopy habitats have been linked to various ecological processes of societal importance. For example, the timing and extent of leaf wetness can influence plant pathogen infection and transport (DeBary, 1853; Rowlandson et al., 2015). Rainwater storage dynamics in pitcher-like leaves (phytotelmata) or in treeholes (dendrotelmata) can inform mosquito management (Maguire, 1971; Anosike et al., 2007). The dynamics of inner (living portion of) bark water storage have been linked to a suite of plant functions (Rosell et al., 2015; Wolfe and Kursar, 2015; Loram-Lourenco et al., 2020). However, research on the outer (non-living) bark's capacity and filling-and-emptying dynamics is comparatively under-represented.

Based on the available observations to date, bark merits improved representation in the canopy water balance. Bark is present all year round in woody ecosystems, unlike leaves, and its specific water storage capacity can be larger than leaves from the same species (Klamerus-Iwan et al., 2020). There are two important caveats regarding these bark water storage capacity estimates. First, most past estimates come from methods that rely on samples taken near the stem base (e.g., Liu, 1998; Llorens and Gallart, 2000; Van Stan et al., 2016); however, the vertical variability of bark structure in single trees can be visually striking. When examined, this vertical bark structural variability has been found to result in substantial variability in bark water storage capacity, where the capacity of the lower bark was roughly double that of the upper-canopy bark (Levia and Wubbena, 2006). Characterizing the vertical variability in bark water storage capacity may shed light on the dynamics of multiple rainwater drainage pathways through tree canopies (i.e., branchflow, throughfall drip points, and stemflow). The upper canopy's bark water storage will influence the generation of branchflows and throughfall drip points (Herwitz, 1987; Van Stan et al., 2021). Along the lower portion of the stem, bark water storage can influence the generation of stemflow (Zhang et al., 2021). To advance understanding of this topic, this study examines vertical variability in bark water storage capacity (and other hydrological parameters) for two common tree species {Norway spruce [*Picea abies* (L.) Karst.] and silver fir trees (*Abies alba* Mill.)} alongside bark physical traits. The second caveat is that most of the past bark water storage capacity estimates assume there is no partial filling of this storage by water vapor during dry (or non-rainy) periods (Ilek et al., 2017b, 2021).

To understand the timing of water receipt below canopies *via* throughfall drip points and stemflow, it is not only important to know (i) how much water the bark can store and (ii) how this storage varies vertically – we must also understand (iii) how much of the water storage capacity is available for interception prior to the storm. One (rarely researched) way in which bark water storage (at any height in the canopy) may remain at an intermediate saturation state between storms is via bark's passive exchange with water vapor (i.e., hygroscopicity). Previous work has found that a meaningful fraction of bark water storage capacity may be occupied by hygroscopic water (Ilek et al., 2017b, 2021). For several tree species in a continental, temperate forest site, hygroscopic water within bark could account for 10–30% of bark water storage capacity (Ilek et al., 2017b). At a more humid (subtropical) forest site, Ilek et al. (2021) found that hygroscopic water could account for an even greater fraction of bark water storage capacity, even exceeding 60% at times. However, our understanding of bark hygroscopicity shares an uncertainty (that is unresearched, to the knowledge of the authors) with our understanding bark water storage capacity: its vertical variability. To advance understanding on this topic, our vertical assessment of bark water storage capacity is complemented by a vertical assessment of the hygroscopic fraction of this storage capacity for two study tree species.

The vertical sampling of bark and estimation of its variability in water storage capacity and hygroscopic fraction, alongside its physical characteristics, enabled the testing of various hypotheses. The null hypotheses tested in this study include: (1) bark water storage capacity is constant with height; (2) hygroscopic water represents a similar fraction of this storage capacity with height; (3) bark water absorbability and absorption rates are constant with height; and (4) these bark hydrologic properties are constant across measured physical bark properties (i.e., porosity, bulk density, and thickness). Rejecting these null hypotheses would suggest physical mechanisms exist that vertically drive bark water storage and its hygroscopic fraction for these study species, meriting further research on this topic and, where confirmed, its integration into canopy water balances.

MATERIALS AND METHODS

Study Area and Bark Sample Collection

Bark samples were collected from felled Norway spruce [*Picea abies* (L.) Karst.] and silver fir trees (*Abies alba* Mill.) located in the Beskid Żywiecki Mountains (49.9211°N, 19.3606°E) within the State Forests (Jeleśnia Forest District) in southern Poland, at heights ranging from about 800 to 840 masl (**Figure 1**). The study area belongs to the Carpathian climate zone situated in a temperate climate area. The average annual temperature is 5°C, and the average annual precipitation is 1095 mm. The average temperature and precipitation within the growing season are 14°C and 450 mm, respectively. Dominant canopy trees at the site include Norway spruce, silver fir, European beech (*Fagus sylvatica* L.), and in some places, sycamore maple (*Acer pseudoplatanus* L.), and European larch (*Larix decidua* Mill.)[1].

We chose three lichen-free and bark beetle-free trees per species with stem diameters at breast height between 34 and 39 cm. After cutting down the trees, we measured their length and collected rectangular total bark samples every 1–2 m from the bottom to the trees' top using a knife, chisel, and hammer. The location of a given bark sample on a tree stem was expressed as a proportion of tree height, i.e., as a ratio of the distance measured from the bark sampling place to the tree's bottom by the stem

[1] www.bdl.lasy.gov.pl/portal/mapy-en

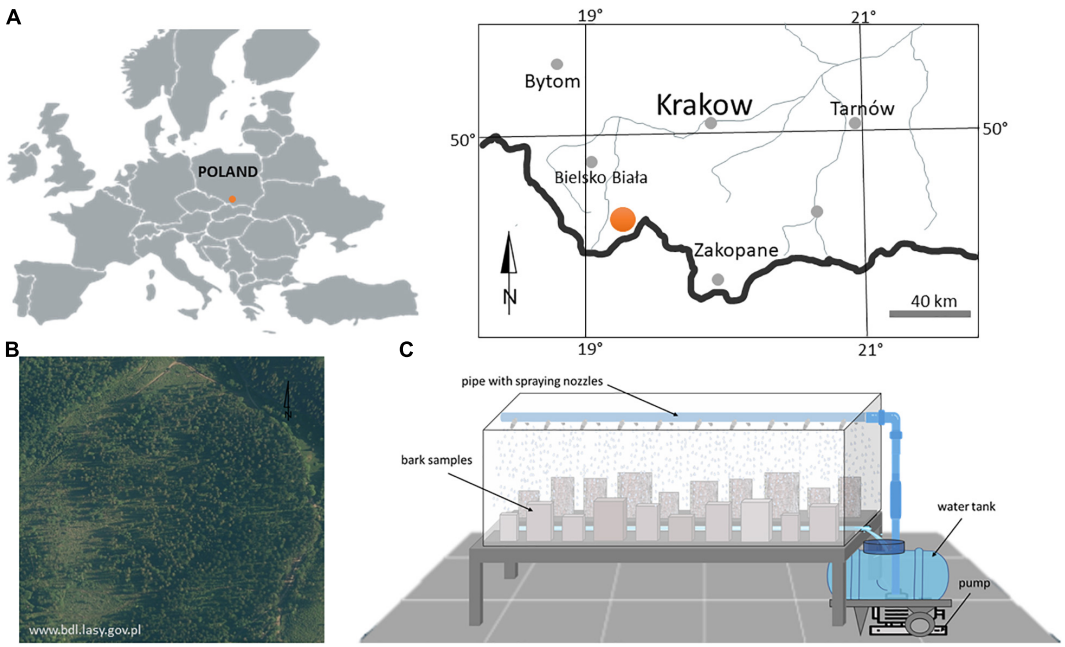

FIGURE 1 | Location of the study area **(A)** with a view of the stand where bark samples were collected **(B)** and rainfall simulator construction **(C)**.

length. In total, we collected 56 samples of fir bark and 63 samples of spruce bark with an approximate area of 20–100 cm^2, and each sample was classified by their height on the stem: bottom (0–33% of tree height), middle (34–66% of tree height), or top (67–100% of tree height). Additionally, we collected several dozen smaller samples with an area of about 5 cm^2 from each of the three sections of all trees.

Laboratory Tests

We determined bark absorbability, water absorption rate, bark water storage capacity, bark hygroscopicity, the ratio of bark hygroscopicity and water storage capacity, bark thickness, outer to total bark thickness ratio, bulk density, and total porosity of bark during laboratory tests. All bark samples were first oven-dried at 35°C to constant mass, and then we measured total, outer, and inner bark thickness using a digital caliper. Next, all internal and side surfaces of rectangular bark samples with an area of 20–100 cm^2 were sealed with colorless silicon (Soudal) and dried at 35°C again. These samples were used to determine bark absorbability, water absorption rate, and bark water storage capacity under rainfall simulation conditions. The same procedure was applied to the one part of smaller bark samples (∼5 cm^2) that were used to determine bark hygroscopicity. We applied silicon to seal the areas of bark samples that would not be exposed *in situ* (i.e., the inner tangential and radial sides of the bark samples) and to ensure water absorption only through the bark's outer layer during particular experiments.

A portion of bark samples was not sealed with silicone to allow water absorption estimates per the commonly used submersion methods of past research. In this case, measurement of bark absorbability began by determining the average time of water absorption by non-silicone bark samples with an area of ∼ 5 cm^2 collected from the bottom, middle, and top parts of individual trees (we used on average 50 bark samples per individual part of each tree species). After drying the bark at 35°C, the samples were immersed in water and covered from above with a damp cotton material. The time of water absorption was measured from the moment the bark samples were immersed in water until bark fell to the bottom of the beaker, i.e., until the given bark sample reached a density >1 g cm^{-3} (Kucza and Urbaś, 2005; Ilek et al., 2019). The samples that had sunk to the bottom of the beaker were removed at least once a day, and then we determined their mass, their volume by the displacement of water in a graduated cylinder and their dry mass after drying at 105°C. Based on dry mass, m (g), and volume of bark, v (cm^3), we calculated its bulk density, ρ_d (g cm^{-3}), according to the equation:

$$\rho_d = m/v \tag{1}$$

Before determining the sunken bark samples' mass and volume, we removed excess water from their surface using a moist paper towel. The average time of water absorption by non-silicone samples of fir and spruce bark from the bottom, middle, or top part of trees was calculated as the arithmetic means of the water absorption time achieved by all samples from a given part of trees per individual species.

The bark absorbability BWA (mm) and rate of water absorption RWA (mm h^{-1}) by non-silicone bark samples were calculated according to the equations:

$$BWA = \frac{M - m}{v} \cdot 10 \tag{2}$$

$$RWA = BWA/t \quad (3)$$

where M is the mass of bark sample at the moment it reached a density >1 g cm^{-3} (g), m is the dry mass of bark sample (g) (M-m corresponds to the volume of water stored by bark, assuming a water density of 1 g cm^{-3}), v is the volume of bark sample (cm^3), 10 is a factor of conversion into mm of water in bark with a thickness of 1 cm, and t is the time after which the sample reached a density >1 g cm^{-3} (h).

We used the pycnometer method and 99.8% ethyl alcohol to determine the specific density of bark (Ilek et al., 2017b, 2021). Based on specific density ρ_s and bulk density ρ_d, we calculated the total porosity of bark (Φ) according to the equation:

$$\Phi = \frac{\rho_s - \rho_d}{\rho_s} \quad (4)$$

After determining the average time of water absorption, bark absorbability, and water absorption rate by the non-silicone bark samples, we determined the bark water storage capacity, bark absorbability, and water absorption rate by bark samples sealed with silicone with an area ranging from 20 to 100 cm^2. In determining these parameters, we assumed that: (1) water is absorbed only by the bark's outer layer under simulated rainfall conditions, and (2) during a rainfall event, water can flow freely (gravitationally) down the bark surface.

Rainfall simulations took place in a closed tunnel, 70 cm high, 160 cm long, and 60 cm wide, made of PVC plates with a steel gutter-shaped bottom draining excess water from the tunnel (**Figure 1C**). There was a PVC pipe with 20 spraying nozzles in the upper part of the tunnel, connected to a pump that pumped water from a tank. The rainfall rate was 10 ± 1 mm h^{-1}. During rainfall simulation experiments, the bark samples were positioned vertically, which allowed gravitational drainage of water from the bark surface during a rainfall event. The bark samples were sprinkled for 10 h day^{-1}, and in the intervals between rainfall, they were stored in desiccators partially filled with water, in which the relative air humidity was 100%. The spraying time needed to determine the bark absorbability by silicone bark samples, according to Eq. 2, depended on the average time of water absorption obtained for non-silicone bark from individual parts and tree species (**Table 1**). The water absorption rate of silicone samples was calculated analogously to Eq. 3, where the t-value was constant for each part of the given tree species and corresponded to the average time of water absorption non-silicone samples (**Table 1**).

Bark water storage capacity was determined assuming the same time of sprinkling over the silicone bark samples with water, amounting to 7 days (Ilek et al., 2017b, 2021). Therefore, a 10-h rainfall was simulated for 7 days (170 h). After the last rainfall simulation event, bark samples were also left in a vertical position in the desiccator until the next day, and then samples were weighed, dried at 105°C, and weighed again. The bark water storage capacity $BWSC$ (mm) was calculated according to the equation:

$$BWSC = \frac{M - m}{m/\rho_d} \cdot 10 \quad (5)$$

TABLE 1 | Average time of water absorption by non-silicone bark samples (days) where letters denote difference among parts and tree species based on the Kruskal–Wallis test ($p < 0.05$).

Species	Part of tree	Mean ± SE	Median	Min	Max
Norway spruce	Bottom	7.4 ± 0.1	7.0^a	1.7	15.0
	Middle	5.6 ± 0.2	5.7^b	1.7	13.0
	Top	3.5 ± 0.3	2.7^{cd}	1.0	8.6
Silver fir	Bottom	7.8 ± 0.4	6.9^{ab}	0.9	19.7
	Middle	4.5 ± 0.4	2.2^c	0.9	17.9
	Top	2.3 ± 0.2	1.9^d	0.9	7.8

where M is the mass of bark sample after 170 h of rainfall simulation (g), m is the dry mass of bark sample (g), ρ_d is the average bulk density of spruce or fir bark calculated according to Eq. 1 (g cm^{-3}), and 10 is a conversion factor to result in mm of water in bark with a thickness of 1 cm.

To determine the variation in the bark hygroscopicity along stems of individual tree species, we used silicone-secured bark samples with an area of about 5 cm^2 (56 and 63 samples of fir and spruce bark, respectively). Dried at 35°C bark samples were weighed and put into a desiccator partially filled with water, where a relative air humidity was 100% (Ilek et al., 2017b, 2021). The bark samples were weighed every day until the further storage of bark samples in the desiccator no longer increased their mass, and then the samples were dried at 105°C. The bark hygroscopicity S_H was determined analogously to Eq. 5. Based on S_H and $BWSC$, we calculated the percentage proportion of bark hygroscopicity in bark water storage capacity (C_{SH}).

Statistical Analysis

The statistical analysis and associated graphics were performed in Statistica 13.3 PL (StatSoft Inc.). We used the Mann–Whitney U test to compare the physical and hydrological properties of bark (regardless of tree part) between tree species. Significant differences in bark properties between the bottom, middle, and top parts of trees were tested by non-parametric Kruskal–Wallis test and one-way ANOVA (with *post hoc* Tukey test) after the previous checking of normality by the Shapiro–Wilk test and equality of variance by the Levene's test. We adopted a general linear model (GLM) to investigate the effect of the part of tree and the effect of tree species on bark properties and hydrology. All tests were performed at a significance level of 0.05.

RESULTS

Interspecific Differences in Hydro-Physical Properties of Bark

The physical and hydrological properties of bark samples differed between Norway spruce and silver fir (**Figure 2**). The thickness and bulk density of spruce bark were 32.4 and 25.9% lower than fir bark, while total porosity was significantly higher ($p < 0.001$, **Figure 2**). The ratio of spruce outer-to-total bark thickness was 0.44, on average, while the ratio of outer to total bark thickness in silver fir bark was 0.23 on average. No significant differences were

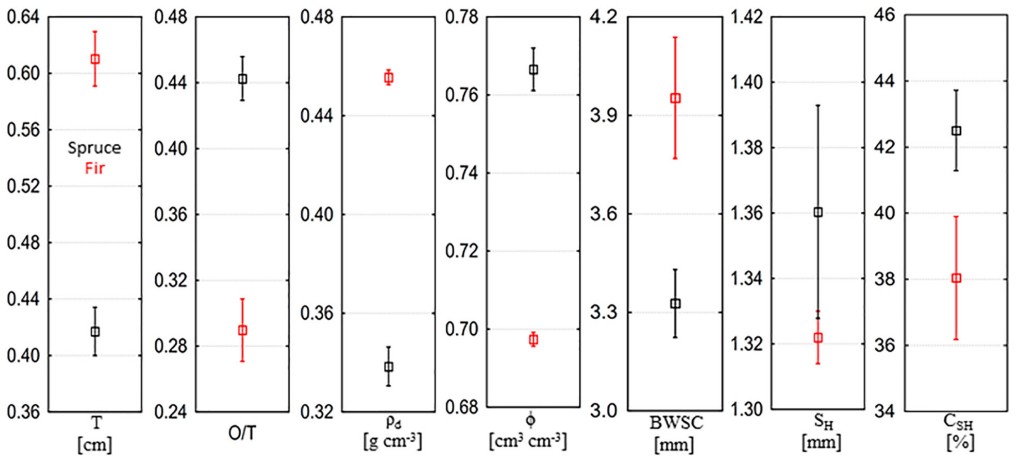

FIGURE 2 | Physical and hydrological properties of Norway spruce and silver fir bark, where *T* is the thickness of total bark, *O/T* is the outer to total bark thickness ratio, ρ_d is the bulk density, ϕ is the total porosity, *BWSC* is the bark water storage capacity, S_H is the bark hygroscopicity, and C_{SH} is the proportion of bark water storage capacity occupied by bark hygroscopicity (mean ± SE).

observed in bark hygroscopicity between species ($p = 0.284$). The water storage capacity of spruce bark was significantly lower than the water storage capacity of fir bark ($p = 0.018$), on average by 15.8% (**Figure 2**). The proportion of bark water storage capacity occupied by bark hygroscopic water ranged from 17.8 to 69.5% and was significantly higher in spruce bark than in fir bark ($p = 0.033$).

Vertical Variation in Bark Properties and Hydrology

The average time of water absorption by non-silicone bark samples decreased along the stem, and in the top part of trees, it was by 52.7 and 70.5% lower compared to the bottom part of Norway spruce and silver fir trees, respectively (**Table 1**). The absorbability of non-silicone spruce bark ranged from 4.8 to 8.4 mm and was significantly higher than the absorbability of non-silicone fir bark ($p < 0.001$), on average by 17.5% (**Figure 3A**). In both species, the bark secured with silicone, which absorbed water only through the outer layer, achieved lower absorbability than the non-silicone bark. These differences were more significant in spruce than in fir (**Figure 3A**). During the absorption of water only by the outer bark layer, the vast majority of samples could not exceed the density of 1 g cm^{-3} (**Figure 3C**). Wet bulk density achieved by silicone fir bark samples was significantly higher than the density achieved by silicone spruce bark samples ($p = 0.002$), on average by 11.9%. In both species, the rate of water absorption differed significantly between the individual tree parts ($p < 0.001$) and increased from bottom to top, in the case of both non-silicone and silicone bark (**Figure 3B**). We found the smallest differences in the average water absorption rate between non-silicone and silicone bark in the bottom and middle parts of the spruce trees, while the greatest differences were in the middle part of the fir trees (**Figure 3B**). Interestingly, the rate of water absorption by non-silicone fir bark was on average 40.6% higher than that of non-silicone spruce bark; that difference in the case of silicone bark was only 4.8%.

The water storage capacity of the spruce bark in the top part was significantly higher than the bark water storage capacity from the bottom ($p = 0.001$) and middle part of trees ($p < 0.001$), on average by 22.8 and 30.3%, respectively (**Figure 4A**). We did not find such differences between the bottom and middle parts ($p = 0.612$). In silver fir, the bark water storage capacity in the top part was on average 12.8% higher than in the middle part and as much as 50.2% higher than in the bottom part of trees.

The spruce and fir bark's hygroscopicity ranged from 1.0 to 1.9 mm and 1.2 to 1.5 mm. The hygroscopicity of the spruce bark from the bottom part was significantly higher than that of the middle part of trees ($p = 0.020$) (**Figure 4A**). In turn, the hygroscopicity of fir bark from the top part of trees was 5.1 and 4.4% lower than the hygroscopicity of the bark from the middle and bottom parts, respectively. The contribution of bark hygroscopicity in the bark water storage capacity varied between species (**Figure 4B**). This contribution ranged from 17.8 to 62.0% in spruce bark and differed significantly between individual tree parts ($p < 0.001$), assuming the highest values in the middle part and the lowest in the top part. In turn, in the case of fir, the contribution of hygroscopicity in the bark water storage capacity differed significantly between the bottom and middle part ($p < 0.001$) and the bottom and top part ($p < 0.001$), decreasing toward the top of the trees. The smallest differences in the contribution of bark hygroscopicity between the spruce and fir bark were observed in the bottom part and the largest in the middle part of trees (**Figure 4B**).

In both species, the thickness of the total bark decreased from bottom to top of trees (**Figure 5**). The thickness of spruce bark in the top part was on average 28.9% lower than the thickness in the bottom part, and in the case of fir, this difference amounted to 48.8%. The thickness of fir bark in the bottom and middle parts was significantly higher than the thickness of spruce bark ($p < 0.001$ and $p = 0.007$, respectively). We found no significant

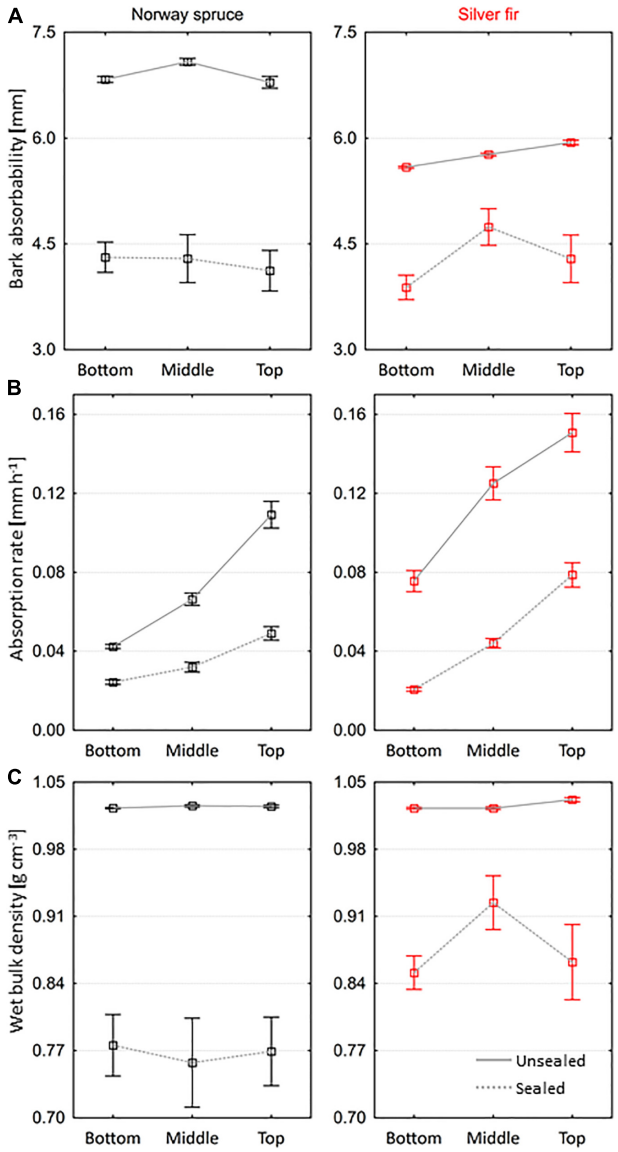

FIGURE 3 | Variation in **(A)** bark absorbability, **(B)** rate of water absorption, and **(C)** wet bulk density of saturated non-silicon and silicone bark samples along stems of Norway spruce and silver fir trees (mean ± SE).

differences in bark thickness in the top part between species. We observed changes in the outer to total bark thickness ratio along tree stems in both tree species (**Figure 5**). In the top part of spruce and fir trees, bark contained 54.5 and 74.8% less outer bark than in the bottom. Fir bark contained less outer bark than spruce in all parts of trees, on average by 48.2% in the bottom, 53.5% in the middle, and 71.3% in the top part. We found no significant differences in bulk density and total porosity between parts of trees, both in spruce and fir trees (**Figure 5**). The bulk density of fir bark from the bottom, middle, and top parts was significantly higher than spruce bark, on average by 25.5, 24.2, and 24.5%, respectively. In the bottom and middle parts, the total porosity of fir bark was significantly lower than spruce bark ($p < 0.001$). No differences were observed in the total porosity of bark in the top part between both species.

The GLM analysis confirmed the influence of tree parts and tree species on some hydro-physical properties of bark (**Table 2**).

DISCUSSION

For the species in this study, vertical variability in BWSC was significant (**Figure 4A**), rejecting hypothesis 1. Moreover, vertical trends in BWSC differed between the species and total BWSC was greater for fir than for spruce (**Figure 2**). Per the measured physical traits, the interspecific differences in water storage may be driven by the thicker bark; after all, for fir bark compared to spruce, overall Φ and ρ_d were lower and higher (**Figure 2**), respectively, and O:T was smaller at all heights (**Figure 5**). Interspecific variability in total BWSC has been ascribed to differences in bark thickness in past comparative studies of tree species across climates and natural forest types (Herwitz, 1985; Levia and Herwitz, 2005; Van Stan et al., 2016; Ilek et al., 2017b, 2021; Campellone, 2018). Few studies have considered bark physical traits (beyond thickness) in assessing the drivers of BWSC variability across species (Van Stan et al., 2016; Ilek et al., 2017b, 2021). The only other study known to the authors that examined BWSC in tandem with bark Φ and ρ_d (Ilek et al., 2021) did not also find a statistically significant influence over interspecific BWSC despite a wide range in Φ (∼0.50–0.80 cm^3 cm^{-3}) for five different broadleaved tree species in the southeastern United States. It may be that, so long as bark pore space is not markedly different between species – note the difference between these species Φ was < 0.10 cm^3 cm^{-3} – the greater thickness of bark results in greater water storage space. The other physical traits examined in past studies for their potential to drive variability in BWSC include surface structural metrics (Van Stan et al., 2016; Ilek et al., 2017a). The studies reported that a bark with greater surface area (Ilek et al., 2017a), roughness (Van Stan et al., 2016), or microrelief (Van Stan and Levia, 2010), enabled greater retention of external (surface) water. A strong linear relationship was reported between BWSC and the bark mean ridge-to-furrow amplitude for individual trees in central Germany (Van Stan et al., 2016). A significant increase in a tree's BWSC was observed for greater bark surface areas (Ilek et al., 2017a) and for larger microrelief (Van Stan and Levia, 2010). Vertical variation in total bark thickness (**Figures 4**, **5**) – which decreased from the bottom to the top of sampled trees – has been well documented in literature (Eberhardt, 2013; Liepiņš and Liepiņš, 2015; Rosell, 2019), also for silver fir and Norway spruce (Stängle et al., 2016; Stängle and Dormann, 2018). The higher BWSC of fir bark than spruce bark (especially in the middle and the top part of trees) is probably associated with a much smaller share of the outer bark in total fir bark thickness, as fir bark contained ∼ 50% less outer bark in the bottom and in the middle parts and over 70% in the top part (**Figure 5**). Interestingly, the bark Φ and ρ_d were relatively constant along the stems; only slight changes (decrease in density and increase in porosity) can be observed in the top part of trees both species (**Figure 5**), characterized by the highest BWSC than other

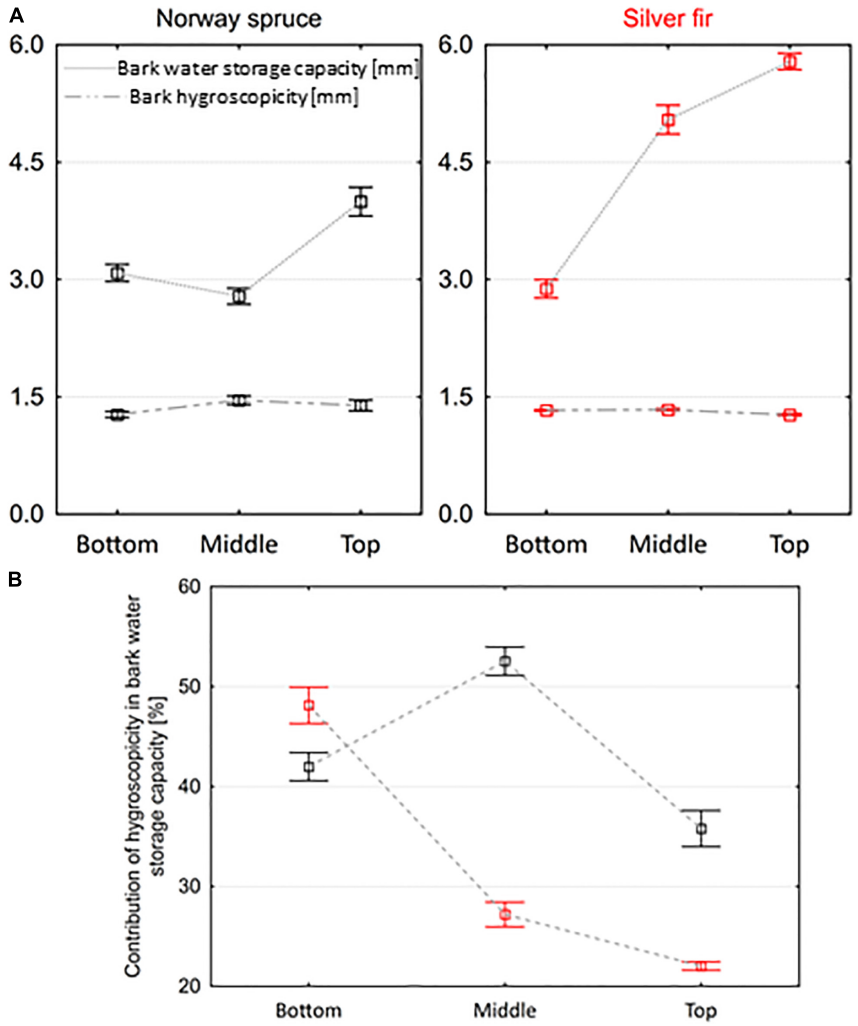

FIGURE 4 | Variation in **(A)** bark water storage capacity and hygroscopicity and **(B)** the proportion of bark water storage capacity occupied by bark hygroscopicity along stems of Norway spruce and silver fir trees (mean ± SE).

parts of trees. Thus, our results show that bark physical traits influence hydrological traits, rejecting hypothesis 3. Quilhó and Pereira (2001) for *Eucalyptus globulus* trees also observed a slight decrease in bark density along stems. Alternatively, Bhat (1982) found a slight increasing trend in bark density from the bottom to the top of trees for two birch species (*Betula pendula* and *Betula pubescens*). Some studies indicate a significant variation in the bark density between individual species (Miles and Smith, 2009) and differences between the density of inner and outer bark, i.e., the density of inner bark is usually less than outer bark (Meyer et al., 1981). The higher density of outer bark may be caused by the expanding periderm which rupture the outer bark cells and, second, the loss of moisture from the outermost bark tissue may result in shrinkage and cell collapse (Martin and Crist, 1970; Meyer et al., 1981; Ugulino et al., 2020). The less-dense inner bark usually has more moisture content than the more-dense outer bark (Kain et al., 2020; Ugulino et al., 2020). Graves et al. (2014) observed that although the density did not differ between inner and outer bark of oaks, the moisture contents were higher in inner than outer bark. Bhat (1982) found the relationship between bark density and bark thickness of two birch species, i.e., density is positively correlated with inner and total bark thickness (probably because the sclerenchyma content of the secondary phloem substantially contributes to the density of the bark), while outer bark thickness is correlated negatively with density because thin-walled periderm cells contribute more to the increase in bark volume rather than bark weight. This agreed with our results, which found thicker and denser fir bark had an average of 73% of the inner bark which stored more water than the thinner and less dense spruce bark, which averaged 43% of the outer bark (**Figure 5**). The chemical composition of bark varies with tree species, tree parts, tree stress, geographic location, climate, and soil conditions (Feng et al., 2013). Legrand et al. (1996) found that bark conductivity of Norway spruce and silver fir trees and bark pH increased with height of trees, i.e., bark was less acid at the top than at the bottom part

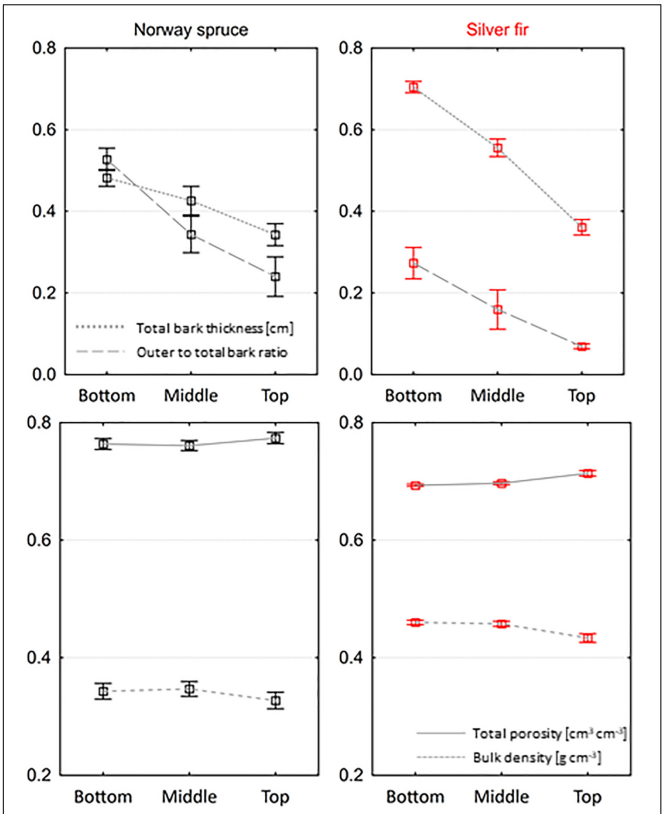

FIGURE 5 | Variation in bark physical properties along stems of Norway spruce and silver fir trees (mean ± SE).

TABLE 2 | General linear model analysis for bark characteristics.

Bark properties	Tree species		Part of tree		Tree species × part of tree	
	F	*p*	*F*	*p*	*F*	*p*
Bark water storage capacity	95.94	**0.000**	74.53	**0.000**	43.24	**0.000**
Bark hygroscopicity	2.66	0.106	2.72	0.070	2.98	0.055
Contribution of hygroscopicity in bark water storage capacity	50.58	**0.000**	36.41	**0.000**	45.97	**0.000**
Bark thickness	35.21	**0.000**	45.57	**0.000**	8.29	**0.000**
Outer to total bark thickness ratio	138.22	**0.000**	41.58	**0.000**	6.04	**0.003**
Bulk density	132.44	**0.000**	1.84	0.163	0.12	0.890
Total porosity	96.91	**0.000**	2.00	0.140	0.24	0.789

The significance effect ($p < 0.05$) is shown in bold.

of trees. Tomczuk (1975) showed that the lignin content in Norway spruce and silver fir bark increased from the bottom to the top of trees (especially within the crown), from 23.8 at the bottom to 25.3% at the top (spruce) and 24.3 to 26.0% (fir). The higher lignin content in fir bark could also have resulted in its higher BWSC – although recent work on bark lignin content, wettability, and stemflow generation suggests that lignin's relationship to water storage capacity may depend on various other bark structural factors (Tonello et al., 2021). Lignin content can also vary between the different layers of the bark: where lignin in the inner bark is similar to the corresponding wood, while the outer bark lignin differs from the inner bark lignin (Sjostrom, 1993).

The lower density of spruce bark and the higher total porosity indicate that spruce may absorb (potentially) more water than the more dense and less porous fir bark. Indeed, it is confirmed by the bark absorbability of non-silicone bark samples (**Figure 3A**), which is significantly higher in spruce than in fir. The differences in bark absorbability by non-silicon and silicone bark samples indicate that the water absorption process is mainly determined by the physical and chemical properties of the outer bark. Significant differences between silicone and non-silicone bark (greater in spruce than in fir) may be caused by the share of outer bark, which was higher in spruce than in fir bark, effectively limited the water absorption by silicone bark samples. On the other hand, the smaller differences in water absorption between silicone and non-silicone bark samples of fir are probably related to the greater density of the inner bark (compared to the inner bark of spruce) and a much lower share of outer bark. In turn, the increasing rate of water absorption along stems is related to the decreasing share of outer bark as well as the age of the bark and chemical composition. Because of the suberization of bark cells, the outer bark slows down the water absorption process. Differences in bark absorbability and absorption rate between non-silicone and silicone bark samples (**Figure 3**) indicate that sealing these bark surfaces not typically in contact with water should be obligatory in laboratory tests. In future investigations of bark–water relations should be distinguished and concerned mainly on outer bark, especially that outer bark is the outermost layer of trees, and as we have shown in our research, its thickness, density, and other properties (which were not examined here) have probably a direct effect on the amount of water absorbed. Furthermore, the inner bark is usually connected with wood, has a high moisture content (Reifsnyder et al., 1967; Kain et al., 2020), and its role in rainwater absorption is probably much smaller than the role of outer bark in this process. These results also reveal difficulties in comparing past research results on bark–water relations due to the lack of uniform methodology, i.e., determination of bark water storage capacity is usually by entirely submerged of bark samples in water for variable amounts of time, from 3 days (Levia and Herwitz, 2005; Valovà and Bieleszovà, 2008), 4 days (Levia and Wubbena, 2006), 7 days (Ilek et al., 2017b, 2021), 1 month (Harmon and Sexton, 1995), or until the bark sample mass remained steady for three consecutive measurements, and further immersion does not increase the bark mass by more than 5% (Van Stan et al., 2016). The last method seems most objective, but according to Ilek et al. (2017a), the time of bark saturation until constant mass is very long and ranges from 24 to 35 days depending on tree species, and does not reflect the natural conditions. The long and unnatural bark wetting process causes that estimation of bark water storage capacity in the laboratory could differ from bark water storage capacities in the field (Levia and Herwitz, 2005). We recommend that the methods reported here (which consider sealing bark surfaces not typically in contact with

water, place samples at their typical orientation, and simulate rainfall rather than submerge) be applied in future research on bark-rainfall interactions to improve inter-study (and inter-species) comparisons.

Vertically, we did not observe a significant change in bark hygroscopicity (i.e., hypothesis 2 was not rejected). Past research, however, has shown that there is a linear relationship between the bark hygroscopicity and the bulk density and porosity: i.e., with increasing ρ_d and decreasing Φ, bark hygroscopicity increases (Ilek et al., 2017b, 2021). This relationship is also well documented for wood (Glass and Zelinka, 2010). In this study, the lack of vertical variation in bark hygroscopicity appears to result from the low variation in ρ_d and Φ along the stems of both species (**Figure 5**). On the other hand, the lack of differences in the bark hygroscopicity between species indicates that the differences in the density and porosity between species amounting to an average of 0.12 g cm^{-3} and 0.07 cm^3 cm^{-3} do not significantly affect changes in hygroscopicity. On the other hand, vertical variability in bark water storage capacity is different between the species (increasing linearly with fir vs. a non-linear trend with spruce). This results in interspecific differences in the vertical variability of the fraction of water storage capacity occupied by hygroscopic water – being lower for the upper fir canopy compared to the stem base, but, for spruce, being higher in the mid-stem than top or bottom. As much of stemflow is generated by upper canopy, e.g., Hutchinson and Roberts (1981) found over half of stemflow is generated by the upper canopy of Douglas fir (*Pseudotsuga menziesii*), this higher upper-canopy water storage availability may impede stemflow generation for fir. Indeed, *Abies* species are reported to have low stemflow fractions: 0.7–0.8% for *Abies balsamea* (Plamondon et al., 1984; Courchesne and Hendershot, 1988), 0.1–0.8% for *Abies grandis* (Ovington, 1954; Aussenac, 1968), and 0.01% for *Abies pindrow* (Negi et al., 1998). On the other hand, for spruce, stemflow generation must overcome a smaller fraction of a lower BWSC in the upper canopy. If this is overcome, the mid-canopy water storage fraction may already be 50% saturated (hygroscopically), enhancing the possibility of upper-canopy branchflows draining down to the surface as stemflow. This builds on previous work that suggests the role additional branch biomass plays on stemflow generation depends on the bark hydrological properties covering those branches (Levia et al., 2015; Sadeghi et al., 2017; Van Stan et al., 2020). Depending on bark hydrological properties and patterns in the canopy, additional branch area may increase drainage as stemflow – as Levia et al. (2015) observed for saplings and Sadeghi et al. (2017) observed for a smooth-barked invasive tree – or, this additional branch area may impede stemflow generation (as reviewed in Van Stan et al., 2020). However, to parameterize hydrologic models that may predict stemflow based on bark properties, further studies on the relationship between bark internal structure, hygroscopic properties, bark water storage capacity, and stemflow production are needed.

Besides being a part of the canopy water balance, bark is a habitat for many microbes (Magyar, 2008; Lambais et al., 2014), meiofauna (Ptatscheck et al., 2015, 2018), and epiphytic vegetation (Zarate-García et al., 2020; Porada and Giordani, 2021) – all of which will, at least in part, depend on moisture availability. Bark water storage may support epiphytic vegetation, yet little work exists that explicitly tests the relationship between epiphytic vegetation and bark–water interactions. A process-based model application for a site with detailed non-vascular epiphyte data (Sardinia, Italy) suggests that "switching off" BWSC may reduce epiphyte net primary productivity by 21%, and reduce physiological diversity of the epiphyte community by 23% (Porada and Giordani, 2021). For vascular epiphytic vegetation, a recent study found a preference by orchids for host trees with larger BWSC (and bark Φ) – even at the expense of bark structures previously believed to be beneficial for orchid attachment (Zarate-García et al., 2020). Micro-habitats in the bark have been described by Magyar (2008) that appear to be linked to precipitation and hygroscopic moisture (Magyar et al., 2021), and may shape the bark fungal and micro-faunal communities. Hygroscopic fractions may be especially important to the formation/sustenance of bark microhabitats (even more so than rainwater storage), because it is present and potentially available during dry periods and may be meaningful during drought. Hygroscopicity may also be complementary to bark water vapor conductance – something recently linked to drought resistance for the plant itself (Wolfe, 2020).

CONCLUSION

This study evaluated vertical changes in bark properties and hydrology along the stems of two coniferous tree species (Norway spruce and silver fir) in southern Poland. Results revealed the following:

(1) The physical and hydrological properties of bark differed between species, i.e., spruce bark was ∼32% thinner than fir bark, contained ∼45% more external than internal bark, also had ∼26% less density, 9% greater porosity, and ∼16% lower water capacity, and the proportion of bark water storage capacity occupied by bark hygroscopicity was ∼28% higher in spruce than fir bark. The interspecific variation in hydro-physical properties of bark was also found between individual tree parts (except for bark hygroscopicity).

(2) In both species, only some hydro-physical properties changed along the stems, i.e., the thickness and the ratio of outer-to-total bark thickness decreased with height, accompanied by an increase in the bark water storage capacity. In contrast, the bark's density, porosity, and hygroscopicity remained relatively constant along stems. These results indicate that bark water storage capacity may primarily be influenced by its thickness and the share of the outer bark, while the bulk density and porosity influence mainly the bark hygroscopicity; thus, all examined physical properties of bark affected the contribution of hygroscopicity in bark water storage capacity.

(3) Differences in bark absorbability and absorption rate between bark samples where the cuts were sealed vs. not sealed (with silicon) indicate that the properties of outer bark mainly determine the water absorption process.

Thus, future investigation of bark–water relations should be focused primarily on the outer bark.

DATA AVAILABILITY STATEMENT

The original contributions presented in the study are included in the article/supplementary material, further inquiries can be directed to the corresponding author.

AUTHOR CONTRIBUTIONS

AI, KM, and JK: conceptualization. AI and KM: sample collection, preparation for analysis, and laboratory research. AI and JK: methodology. AI and JV: analysis and interpretation of data and writing – original draft preparation, review, and editing. AI: resources. JV: writing – language review and editing. All authors contributed to manuscript revision, read, and approved the submitted version.

REFERENCES

Anosike, J. C., Nwoke, B. E., Okere, A. N., Oku, E. E., Asor, J. E., Emmy-Egbe, I. O., et al. (2007). Epidemiology of tree-hole breeding mosquitoes in the tropical rainforest of Imo State, south-east Nigeria. *Ann. Agric. Environ. Med.* 14, 31–38.

Aubrey, D. P. (2020). "Relevance of precipitation partitioning to the tree water and nutrient balance," in *Precipitation Partitioning by Vegetation: A Global Synthesis*, eds J. Van Stan II, E. Gutmann, and J. Friesen (Switzerland: Springer), 147–162.

Aussenac, G. (1968). Interception des précipitations par le couvert forestier. *Ann. Sci. For.* 25, 135–156.

Berry, Z. C., Emery, N. C., Gotsch, S. G., and Goldsmith, G. R. (2019). Foliar water uptake: processes, pathways, and integration into plant water budgets. *Plant Cell Environ.* 42, 410–423. doi: 10.1111/pce.13439

Bhat, K. M. (1982). Anatomy, basic density and shrinkage of birch bark. *IAWA J.* 3, 207–213. doi: 10.1163/22941932-90000841

Campellone, S. V. (2018). *An Investigation into the Factors Affecting Street Tree Rainfall Interception*. Masters Thesis. Philadelphia, PA: Drexel University.

Carmichael, M. J., White, J. C., Cory, S. T., Berry, Z. C., and Smith, W. K. (2020). Foliar water uptake of fog confers ecophysiological benefits to four common tree species of southeastern freshwater forested wetlands. *Ecohydrology* 13:e2240. doi: 10.1002/eco.2240

Courchesne, F., and Hendershot, W. H. (1988). Apport en sulfate et en eau à la surface du sol sous quatre espèces arborescentes. *Nat. Can.* 115, 57–63.

Davies-Barnard, T., Valdes, P. J., Jones, C. D., and Singarayer, J. S. (2014). Sensitivity of a coupled climate model to canopy interception capacity. *Clim. Dyn.* 42, 1715–1732. doi: 10.1007/s00382-014-2100-1

DeBary, H. A. (1853). *Untersuchungen Über die Brandpilze und die Durch sie Verursachten Krankheiten der Pflanzen mit Rücksicht auf das Getreide und Andere Nutzpflanzen. Habilitation*. Muller, Berlin.

Eberhardt, T. L. (2013). Longleaf pine inner bark and outer bark thicknesses: measurement and relevance. *South. J. Appl. For.* 37, 177–180. doi: 10.5849/sjaf.12-023

Feng, S., Cheng, S., Yuan, Z., Leitch, M., and Xu, C. C. (2013). Valorization of bark for chemicals and materials: a review. *Renew. Sustain. Energy Rev.* 26, 560–578. doi: 10.1016/j.rser.2013.06.024

Glass, S. V., and Zelinka, S. L. (2010). *Moisture Relations and Physical Properties of Wood. Wood Handbook: Wood as an Engineering Material: Chapter 4. Centennial ed. General Technical Report FPL; GTR-190*. Madison, WI: US Dept. of Agriculture,

Graves, S. J., Rifai, S. W., and Putz, F. E. (2014). Outer bark thickness decreases more with height on stems of fire-resistant than fire-sensitive Floridian oaks (*Quercus* spp.; Fagaceae). *Am. J. Bot.* 101, 2183–2188. doi: 10.3732/ajb.1400412

Harmon, M. E., and Sexton, J. (1995). Water balance of conifer logs in early stages of decomposition. *Plant Soil* 172, 141–152. doi: 10.1007/BF00020868

Herwitz, S. R. (1985). Interception storage capacities of tropical rainforest canopy trees. *J. Hydrol.* 77, 237–252. doi: 10.1016/0022-1694(85)90209-4

Herwitz, S. R. (1987). Raindrop impact and water flow on the vegetative surfaces of trees and the effects on stemflow and throughfall generation. *Earth Surf. Process. Landf.* 12, 425–432. doi: 10.1002/esp.3290120408

Hutchinson, I., and Roberts, M. C. (1981). Vertical variation in stemflow generation. *J. Appl. Ecol.* 18, 521–527. doi: 10.2307/2402413

Ilek, A., Kucza, J., and Morkisz, K. (2017b). Hygroscopicity of the bark of selected forest tree species. *iForest* 10, 220–226. doi: 10.3832/ifor1979-009

Ilek, A., Kucza, J., and Morkisz, K. (2017a). Hydrological properties of bark of selected forest tree species. Part 2: interspecific variability of bark water storage capacity. *Folia For. Pol. Ser. A. For.* 59, 110–122. doi: 10.1515/ffp-2017-0011

Ilek, A., Siegert, C. M., and Wade, A. (2021). Hygroscopic contributions to bark water storage and controls exerted by internal bark structure over water vapor absorption. *Trees* 35, 831–843. doi: 10.1007/s00468-021-02084-0

Ilek, A., Szostek, M., Kucza, J., Stanek-Tarkowska, J., and Witek, W. (2019). The water absorbability of beech (*Fagus sylvatica* l.) and fir (*Abies alba mill.*) organic matter in the forest floor. *Ann. For. Res.* 62, 21–32. doi: 10.15287/afr.2018.1161

Kain, G., Morandini, M., Barbu, M.-C., Petutschnigg, A., and Tippner, J. (2020). Specific gravity of inner and outer larch bark. *Forests* 11:1132. doi: 10.3390/f11111132

Klamerus-Iwan, A., Link, T. E., Klein, R. F., and Van Stan, J. II (2020). "Storage and routing of precipitation through canopies," in *Precipitation Partitioning by Vegetation: A Global Synthesis*, eds J. Van Stan II, E. Gutmann, and J. Friesen (Switzerland: Springer), 17–34.

Kucza, J., and Urbaś, J. (2005). Water absorption of organic matter taken from horizons of ectohumus of forest soils under Norway spruce stands. *EJPAU For.* 8, 50–58.

Lambais, M. R., Lucheta, A. R., and Crowley, D. E. (2014). Bacterial community assemblages associated with the phyllosphere, dermosphere, and rhizosphere of tree species of the Atlantic forest are host taxon dependent. *Microb. Ecol.* 68, 567–574. doi: 10.1007/s00248-014-0433-2

Legrand, I., Asta, J., and Goudard, Y. (1996). Variations in bark acidity and conductivity over the trunk length of silver fir and Norway spruce. *Trees* 11, 54–58. doi: 10.1007/s004680050058

Levia, D. F., and Herwitz, S. R. (2005). Interspecific variation of bark water storage capacity of three deciduous tree species in relation to stemflow yield and solute flux to forest soils. *Catena* 64, 117–137. doi: 10.1016/j.catena.2005.08.001

Levia, D. F., Michalzik, B., Näthe, K., Bischoff, S., Richter, S., and Legates, D. R. (2015). Differential stemflow yield from European beech saplings: the role of individual canopy structure metrics. *Hydrol. Process.* 29, 43–51. doi: 10.1002/hyp.10124

Levia, D. F., and Wubbena, N. P. (2006). . Vertical variation of bark water storage capacity of *Pinus strobus* L.(Eastern white pine) in southern Illinois. *Northeast. Nat.* 13, 131–137.

Liepiņš, J., and Liepiņš, K. (2015). Evaluation of bark volume of four tree species in Latvia. *Res. Rural Dev.* 2, 22–28.

Liu, S. (1998). Estimation of rainfall storage capacity in the canopies of cypress wetlands and slash pine uplands in North-Central Florida. *J. Hydrol.* 207, 32–41. doi: 10.1016/S0022-1694(98)00115-2

Llorens, P., and Gallart, F. (2000). A simplified method for forest water storage capacity measurement. *J. Hydrol.* 240, 131–144. doi: 10.1016/S0022-1694(00)00339-5

Loram-Lourenco, L., Farnese, F. D. S., Sousa, L. F. D., Alves, R. D. F. B., Andrade, M. C. P. D., Almeida, S. E. D. S., et al. (2020). A structure shaped by fire, but also water: ecological consequences of the variability in bark properties across 31 species from the brazilian cerrado. *Front. Plant Sci.* 10:1718. doi: 10.3389/fpls.2019.01718

Magyar, D. (2008). The tree bark: a natural spore trap. *ASP Appl. Biol.* 89, 7–16.

Magyar, D., Van Stan, J. T., and Sridhar, K. R. (2021). Hypothesis and theory: fungal spores in stemflow and potential bark sources. *Front. For. Global Change* 4:19.

Maguire, B. (1971). Phytotelmata: biota and community structure determination in plant-held waters. *Annu. Rev. Ecol. Syst.* 2, 439–464.

Martin, R. E., and Crist, J. B. (1970). Elements of bark structure and terminology. *Wood Fiber Sci.* 2, 269–279.

Meyer, R. W., Kellogg, R. M., and Warren, W. G. (1981). Relative density, equilibrium moisture content, and dimensional stability of western hemlock bark. *Wood Fiber Sci.* 13, 86–96.

Miles, P. D., and Smith, W. B. (2009). *Specific Gravity and Other Properties of Wood and Bark for 156 Tree Species Found in North America (Vol. 38)*. Washington, DC: US Department of Agriculture, Forest Service, Northern Research Station.

Miller, G., Hartzell, S., and Porporato, A. (2021). Ecohydrology of epiphytes: modeling water balance, CAM photosynthesis, and their climate impacts. *Ecohydrology* 14:e2275. doi: 10.1002/eco.2275

Negi, G. C. S., Rikhari, H. C., and Garkoti, S. C. (1998). The hydrology of three high-altitude forests in Central Himalaya, India: a reconnaissance study. *Hydrol. Process.* 12, 343–350.

Nowak, D. J., Coville, R., Endreny, T., Abdi, R., and Van Stan, J. T. II (2020). "Valuing urban tree impacts on precipitation partitioning," in *Precipitation Partitioning by Vegetation: A Global Synthesis*, eds J. Van Stan II, E. Gutmann, and J. Friesen (Switzerland: Springer), 253–268.

Ovington, J. D. (1954). A comparison of rainfall in different woodlands. *Forestry* 27, 41–53. doi: 10.1093/forestry/27.1.41

Plamondon, A. P., Prévost, M., and Naud, R. C. (1984). Interception de la pluie dans la sapinière à bouleau blanc, Forêt Montmorency. *Can. J. For. Res.* 14, 722–730. doi: 10.1139/x84-129

Porada, P., and Giordani, P. (2021). Bark water storage plays key role for growth of Mediterranean epiphytic lichens. *Front. For. Glob. Change* 4:668682. doi: 10.3389/ffgc.2021.668682

Porada, P., Van Stan, J. T., and Kleidon, A. (2018). Significant contribution of non-vascular vegetation to global rainfall interception. *Nat. Geosci.* 11, 563–567. doi: 10.1038/s41561-018-0176-7

Ptatscheck, C., Dümmer, B., and Traunspurger, W. (2015). Nematode colonisation of artificial water-filled tree holes. *Nematology* 17, 911–921. doi: 10.1163/15685411-00002913

Ptatscheck, C., Milne, P. C., and Traunspurger, W. (2018). Is stemflow a vector for the transport of small metazoans from tree surfaces down to soil? *BMC Ecol.* 18:43. doi: 10.1186/s12898-018-0198-4

Quilhó, T., and Pereira, H. (2001). Within and between-tree variation of bark content and wood density of *Eucalyptus globulus* in commercial plantations. *IAWA J.* 22, 255–265. doi: 10.1163/22941932-90000283

Reifsnyder, W. E., Harrington, L. P., and Spalt, K. W. (1967). *Thermophysical Properties of Bark of Shortleaf, Longleaf, and Red Pine. Yale University Forestry Bulletin Number 70*. New Haven, CT: Yale University School of Forestry.

Rosell, J. A. (2019). Bark in woody plants: understanding the diversity of a multifunctional structure. *Integr. Comp. Biol.* 59, 535–547. doi: 10.1093/icb/icz057

Rosell, J. A., Castorena, M., Laws, C. A., and Westoby, M. (2015). Bark ecology of twigs vs. main stems: functional traits across eighty-five species of angiosperms. *Oecologia* 178, 1033–1043. doi: 10.1007/s00442-015-3307-5

Rowlandson, T., Gleason, M., Sentelhas, P., Gillespie, T., Thomas, C., and Hornbuckle, B. (2015). Reconsidering leaf wetness duration determination for plant disease management. *Plant Dis.* 99, 310–319. doi: 10.1094/PDIS-05-14-0529-FE

Sadeghi, S. M. M., Van Stan, J. T. II, Pypker, T. G., and Friesen, J. (2017). Canopy hydrometeorological dynamics across a chronosequence of a globally invasive species, *Ailanthus altissima* (Mill., tree of heaven). *Agric. For. Meteorol.* 240, 10–17. doi: 10.1016/j.agrformet.2017.03.017

Sjostrom, E. (1993). *Wood chemistry. Fundamentals and Applications*, 2nd Edn. Cambridge, MA: Academic Press, 293.

Stängle, S. M., and Dormann, C. F. (2018). Modelling the variation of bark thickness within and between European silver fir (*Abies alba* Mill.) trees in southwest Germany. *For. Int. J. For. Res.* 91, 283–294. doi: 10.1093/forestry/cpx047

Stängle, S. M., Weiskittel, A. R., Dormann, C. F., and Brüchert, F. (2016). Measurement and prediction of bark thickness in *Picea abies*: assessment of accuracy, precision, and sample size requirements. *Can. J. For. Res.* 46, 39–47. doi: 10.1139/cjfr-2015-0263

Tomczuk, R. I. (1975). Skład chemiczny drzew. *Folia For. Pol. Ser. B* 12, 5–14.

Tonello, K. C., Campos, S. D., de Menezes, A. J., Bramorski, J., Mathias, S. L., and Lima, M. T. (2021). How is bark absorbability and wettability related to stemflow yield? Observations from isolated trees in the Brazilian cerrado. *Front. For. Global Change* 4:650665. doi: 10.3389/ffgc.2021.650665

Ugulino, B., Cáceres, C. B., Hernández, R. E., and Blais, C. (2020). Influence of temperature and moisture content on bark/wood shear strength of black spruce and balsam fir logs. *Wood Sci. Technol.* 54, 963–979. doi: 10.1007/s00226-020-01198-x

Valovà, M., and Bieleszovà, S. (2008). Interspecific variations of bark's water storage capacity of chosen types of trees and the dependence on occurrence of epiphytic mosses. *GeoSci. Eng.* 2008, 45–51.

Van Stan, J. T., Hildebrandt, A., Friesen, J., Metzger, J. C., and Yankine, S. A. (2020). "Spatial Variability and temporal stability of local net precipitation patterns," in *Precipitation Partitioning by Vegetation: A Global Synthesis*, eds J. Van Stan II, E. Gutmann, and J. Friesen (Switzerland: Springer), 89–104.

Van Stan, J. T., and Levia, D. F. Jr. (2010). Inter-and intraspecific variation of stemflow production from *Fagus grandifolia* Ehrh.(American beech) and *Liriodendron tulipifera* L.(yellow poplar) in relation to bark microrelief in the eastern United States. *Ecohydrology* 3, 11–19. doi: 10.1002/eco.83

Van Stan, J. T., Lewis, E. S., Hildebrandt, A., Rebmann, C., and Friesen, J. (2016). Impact of interacting bark structure and rainfall conditions on stemflow variability in a temperate beech-oak forest, central Germany. *Hydrol. Sci. J.* 61, 2071–2083. doi: 10.1080/02626667.2015.1083104

Van Stan, J. T., Ponette-Gonzalez, A. G., Swanson, T., and Weathers, K. C. (2021). Concepts and Questions: throughfall and stemflow are major hydrologic highways for particulate traffic through tree canopies. *Front. Ecol. Environ.* 19, 404–410.

Wolfe, B. T. (2020). Bark water vapour conductance is associated with drought performance in tropical trees. *Biol. Lett.* 16:20200263. doi: 10.1098/rsbl.2020.0263

Wolfe, B. T., and Kursar, T. A. (2015). Diverse patterns of stored water use among saplings in seasonally dry tropical forests. *Oecologia* 179, 925–936. doi: 10.1007/s00442-015-3329-z)

Zarate-García, A. M., Noguera-Savelli, E., Andrade-Canto, S. B., Zavaleta-Mancera, H. A., Gauthier, A., and Alatorre-Cobos, F. (2020). Bark water storage capacity influences epiphytic orchid preference for host trees. *Am. J. Bot.* 107, 726–734. doi: 10.1002/ajb2.1470

Zhang, H., Fu, C., Liao, A., Zhang, C., Liu, J., Wang, N., et al. (2021). Exploring the stemflow dynamics and driving factors at both inter-and intra-event scales in a typical subtropical deciduous forest. *Hydrol. Process.* 35:e14091. doi: 10.1002/hyp.14091

Conflict of Interest: The authors declare that the research was conducted in the absence of any commercial or financial relationships that could be construed as a potential conflict of interest.

Advantages of publishing in Frontiers

OPEN ACCESS
Articles are free to read for greatest visibility and readership

FAST PUBLICATION
Around 90 days from submission to decision

HIGH QUALITY PEER-REVIEW
Rigorous, collaborative, and constructive peer-review

TRANSPARENT PEER-REVIEW
Editors and reviewers acknowledged by name on published articles

Frontiers
Avenue du Tribunal-Fédéral 34
1005 Lausanne | Switzerland

Visit us: www.frontiersin.org
Contact us: frontiersin.org/about/contact

REPRODUCIBILITY OF RESEARCH
Support open data and methods to enhance research reproducibility

DIGITAL PUBLISHING
Articles designed for optimal readership across devices

FOLLOW US
@frontiersin

IMPACT METRICS
Advanced article metrics track visibility across digital media

EXTENSIVE PROMOTION
Marketing and promotion of impactful research

LOOP RESEARCH NETWORK
Our network increases your article's readership